University of Washington
Department of Civil and Environmental Engineering

EVALUATION OF THE EFFECTS OF FOREST ROADS ON STREAMFLOW IN HARD AND WARE CREEKS, WASHINGTON

Laura C. Bowling
Dennis P. Lettenmaier

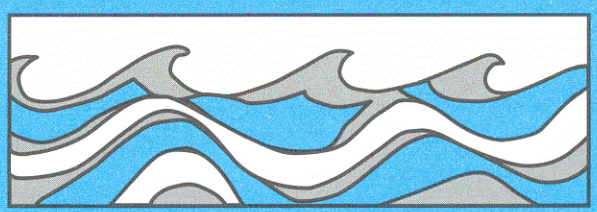

Water Resources Series
Technical Report No.155
October 2002

Seattle, Washington
98195

Department of Civil Engineering
University of Washington
Box 352700
Seattle, Washington 98195-2700

EVALUATION OF THE EFFECTS OF FOREST ROADS ON STREAMFLOW IN HARD AND WARE CREEKS, WASHINGTON

by

LAURA C. BOWLING
and
DENNIS P. LETTENMAIER

Water Resources Series
Technical Report No. 155

September 1997

ABSTRACT

Road networks in mountainous forest catchments may increase peak streamflow by replacing subsurface flow paths with surface flow paths. Forest roads affect runoff generation via two mechanisms: capture of subsurface water by road incisions, and generation of infiltration excess runoff from road surfaces. The quantity of runoff intercepted by the road network was monitored in two small Western Washington catchments, Hard and Ware Creeks (drainage areas 2.3 and 2.8 square km, respectively). Road densities in both catchments are approximately 5.0 and 3.8 km/square km, respectively. Observations indicate that the highest peak culvert discharges in Hard and Ware Creeks are associated with subsurface flow interception rather than road surface runoff. A total of 111 culverts in the two catchments were located using GPS. For each of the road segments defined by the culverts, road widths, slopes and the fraction of the road surface draining to the culvert were measured, and each of the culvert outlets was field checked to determine whether the culvert was hydraulically connected to the channel system. Based on the field study, the effective channel network density was found to have increased by 64% in Hard Creek and 52 % in Ware Creek due to road construction.

The Distributed Hydrology-Soil-Vegetation Model (DHSVM) is an explicitly distributed hydrological model that simulates the land surface water and energy balance at the scale of a digital elevation model (DEM). DHSVM represents water movement through the unsaturated zone and the vegetation canopy in one dimension, as well as subsurface and surface lateral flow. It accounts for interception of precipitation as both rain and snowfall in the forest canopy. A new scheme represents the effects of forest roads on runoff generation in DHSVM via two mechanisms: capture of subsurface water by road incisions, and generation of infiltration excess runoff from road surfaces. Runoff produced by both mechanisms is routed through an expanded (roads plus pre-existing channels) channel network using a Muskingum-Cunge scheme. DHSVM-simulated flows with and without roads were compared to continuous recording gauges at the outlets of each of the basins, and to crest-recording gauges installed on 12 culverts for selected storms during the winter of 1995-96. Simulated basin conditions indicate that the roads redistribute soil moisture throughout the basin, resulting in drier areas beneath the road right-of-way relative to the simulation without roads. Based on retrospective simulations using eleven years of data, the mean annual floods in Hard and Ware Creeks were predicted to have increased by 11%, and the mean of 4 peaks over threshold were predicted to have increased by 8 and 9%, respectively.

TABLE OF CONTENTS

LIST OF FIGURES

LIST OF TABLES

ACKNOWLEDGEMENTS

The research described in this report is based on the Masters thesis of the first author. Funding was provided by a Valle Scholarship to the first author, and by the Washington State Department of Natural Resources. In addition, the National Council for Air and Stream Improvement (NCASI) provided financial support for technical consultation and equipment repair. The advice of University of Washington Professors Stephen Burges, David Montgomery and Ron Nece and Dr. Terrance Cundy (Resource Hydrologist, Potlatch Corporation), who served on the first author's thesis committee, is greatly appreciated.

Thanks also go to the many people who provided support for this project. The Weyerhaeuser Company provided access to the Hard and Ware Creek research basins on their Vail Tree Farm. In particular, Mr. John Heffner and Dr. Jami Nettles (Weyerhaeuser Co.) were very helpful in providing meteorological and vegetation data in support of the modeling effort. Dr. Walt Megahan (NCASI) has provided assistance with the experimental design and the review of this report. The channel routing algorithm was developed by Dr. Mark Wigmosta and Mr. Bill Perkins (Battelle Pacific Northwest Laboratory). Bart Nijssen and Pascal Storck (University of Washington) also made recent improvements to the snow algorithm used in this research, and provided modeling support. Finally, several students within the University of Washington Environmental Engineering and Science program have volunteered their time and energy to the field experiment. For this reason, special thanks go to Keith Cherkauer, Jonathan La Marche, Dag Lohman, Bart Nijssen, William Rowden and Pascal Storck.

CHAPTER 1: INTRODUCTION

1.1: OVERVIEW

What amounts to a wide-spread land-use change experiment has taken place in the Pacific Northwest over the past half-century through forest management. Flood damage associated with several extreme weather events in recent years has focused public attention on the possible contribution of forest harvest and road construction to flood flows and their associated damage. In November 1990, a warm front following an extended period of cool, wet weather caused extreme flooding in many western Washington rivers when as much as 15 inches of rain fell within a 48 hour period, combined with rapid snow melt. The estimated flood damage in King County, which encompasses Seattle, exceeded $ 20 million (Storck et al. 1995).

Another storm in February 1996 was concentrated in southwestern Washington and western Oregon. Portland, OR barely avoided major flood damage as the Willamette River came dangerously close to overflowing its containing dykes. Repair costs of forest roads in the national forests of Oregon and Washington are estimated to exceed $ 40 million (Barnard 1996, Bernton 1996). From an environmental standpoint, storm damage was extensive. Hundreds of landslides occurred in the western Cascades, many associated with clearcut forests and logging roads, sparking a debate in local newspapers regarding the extent to which clearcut logging and the construction of forest roads were to blame for the high flows and the associated damage (Robertson 1996). Headlines such as "The legacy of clear-cutting and road-building: Swollen streams tied to logging (The Oregonian, 2/8/96)" and "Clear-cuts blamed for recent landslides (The Register-Guard 2/14/96)" sparked responses in the form of: "Flooding? Don't blame logging ". Some example articles are included in Appendix A.

As these headlines indicate, the debate centers around two main mechanisms by which forest management might affect hydrology. These include:

- Vegetation effects, primarily Rain-on-Snow (ROS) enhancement of floods; and
- Forest road network effects.

Along with flood enhancement, slope instability is a potential side effect of these two mechanisms. This research will focus primarily on the effect of forest road networks on flood enhancement.

The transient snow zone includes the range of elevations which accumulate and melt snow several times throughout the winter. It is usually assumed to lie between 350 and 1100 m in the Pacific Northwest (Berris and Harr 1987). Because of the frequent accumulation and ablation of snow, the transient snow zone is most affected by ROS enhancement. Forest harvest may influence the magnitude of response to ROS events through two mechanisms:

- Increased snow accumulation in clearings; and
- Increased snowmelt rates in clearings during ROS events.

During accumulation, lack of snow interception results in greater deposition in open sites (Kattelmann 1990, Berris and Harr 1987). The high exposure of snow in the canopy paired with a higher surface-to-volume ratio results in relatively quick melt of snow in the canopy, which can result in significant increases in snow water equivalent (SWE) for open plots relative to forested plots (Berris and Harr 1987).

The convective transfer of sensible and latent heat to the snow is the dominant source of energy for melt during rainfall (Harr 1986). ROS is the predominant means of melt on the western slopes of the Cascade range in Washington and Oregon. Snowpacks in western Oregon and Washington are 'warm', with internal temperatures remaining near $0\ ^{o}C$ for much of the winter which means they can yield water

quickly during periods of high temperature (Harr 1981). Removal of vegetation can increase turbulent transfer of energy and water vapor to the snow surface, thus increasing the rate of snow melt (Harr 1981).

Road corridors in forested catchments act as a permanent clearcut, and as such, they are also a non-trivial source of increased snow accumulation and melt. In addition, roads built in forested catchments may affect both the timing and magnitude of basin response by redistributing runoff through the road drainage network. Roads built into the hillside can capture and re-route runoff through two mechanisms:

- Interception of subsurface flow by the road cutslope; and
- Direct runoff from the compacted road surface which drains to the roadside ditch.

Runoff intercepted by either of these mechanisms is routed through the ditch drainage system where it either enters a natural stream at a stream crossing culvert, or is diverted under the road through a ditch relief culvert. Runoff which is diverted through a ditch relief culvert either infiltrates downslope of the culvert outfall, or continues to follow a surface flow path, in many cases entering the natural drainage system quickly as overland flow.

In addition, runoff flowing in roadside ditches, on road cut and fill slopes and on undisturbed slopes below the road can cause surface erosion (Megahan 1972). Sediment production by forest roads is predominantly finer than 2 mm, with large portions of silt and clay sized particles (Bilby et al. 1989, Duncan et al. 1987, Fahey and Coker 1989). This fine-grained material is most detrimental to fish through increased turbidity and damage to in-stream habitat. Increased sediment in stream bottoms can clog interstitial pore spaces in salmonid redds and suffocate the eggs or emerging fry (Cederholm et al. 1981).

Much of the debate concerning forest roads in the popular press has centered around the contribution of roads and clear-cuts to slope instability. The aftermath of the February 1996 storm emphasizes the

interactions between forest harvest, road construction, and slope stability. A preliminary aerial survey in the USFS Mapleton, OR Ranger District immediately following the February 1996 storm revealed 114 landslides associated with clear-cut areas, 68 slides associated with forest road right-of-ways and 3 in undisturbed forested areas (Robertson 1996b). Although some of the slides in forested areas may go undetected in areal surveys, similar studies support these results (Lyons and Beschta 1983, Swanson and Dyrness 1975). Landslides occurring in clear-cut areas may also be larger than those occurring in forested areas. Swanson and Dyrness (1975) found that the total volume of slide erosion from a zone of unstable soil in the H.J. Andrews Experimental Forest in Western Oregon was 2.8 times greater in clear-cut areas than in comparable forested areas. The size and distance traveled by a landslide will determine the effect on local streams due to the increased sediment load. High flows, supplemented by slides entering streams can scour stream bottoms. This is clearly illustrated in Figure 1-1, which shows Mine Creek, a headwater catchment in the Deschutes River of Western Washington following the February 1996 storm. A debris flow initiated on Mine Creek washed out the road in this location and destroyed a bridge further downstream.

Damage such as that shown in Figure 1-1 has focused wide-spread attention on the role that forest roads may play in increasing streamflow response during extreme storm events, and the resulting damage that might be expected from future events. This research examines, through field investigation and modeling, the mechanisms that interact to increase streamflow following road construction and forest harvest.

1.2: OBJECTIVES

The purpose of this research is to evaluate, through field investigation, the ability of a spatially distributed hydrological model to predict the influence of forest roads on the magnitude and distribution of catchment runoff response. It is based on the central hypothesis that avenues exist through which road networks in mountainous forest catchments can increase streamflow by replacing subsurface flow

FIGURE 1-1: MINE CREEK FOLLOWING A DEBRIS FLOW IN FEBRUARY 1996

paths with surface flow paths, and that these avenues can be represented by a spatially distributed hydrological model. The specific objectives of this project are to:

- Assess the overall connectivity of road drainage to the stream network;
- Examine through field investigation the relative contribution of subsurface flow interception by, and infiltration excess runoff from forest roads to peak streamflow events;
- Determine, through field investigation, causal factors associated with subsurface flow interception by forest roads; and
- Use the resulting field data to test the applicability of a road-routing algorithm in a distributed hydrology model.

1.3: ANALYTICAL APPROACH

Extensive field experiments have been conducted to determine the localized effects of vegetation changes and road construction, at the plot or sub-basin scale (e.g., Bosch and Hewlett 1982, Berris and Harr 1987, Megahan 1972, Rothacher 1965, 1970). These experiments are important for understanding the physical processes that interact in natural and disturbed landscapes. However, it is difficult to extrapolate the effects found from small field experiments to river basins at the scale of concern during large flood events (e.g. 10^2 - 10^3 km^2 and up), where a combination of management practices interact (in a manner sometimes termed "cumulative effects"). At larger scales, it is difficult if not impossible to collect enough field data to understand the complex interactions of surface conditions and catchment runoff response. In these cases, a model (either statistical or physical) is needed to integrate point observations over the landscape.

A related issue is retrospective evaluation of the effects of land management over a range of temporal scales. This requires separating the effects of land use changes from natural climate variability. The classical approach is statistical analysis of paired watersheds (e.g., Jones and Grant 1996). If similar watersheds can be identified with different land use histories, statistical analysis of the discharge difference series will filter out systematic climate variations. An important limitation of the paired catchment approach is that the catchments must have minimal geographic separation in order to have nearly coincident meteorological records since it is essentially to difference flood events which were not caused by the same storm. Identification of paired catchments with long, coincident discharge records, and significantly different land use histories can be problematic.

An alternate approach is to simulate the natural system using a deterministic, spatially distributed hydrologic model. Since the model and the natural system are driven by the same sequence of climatic

variables, the residual time series (for instance modeled discharge versus observed streamflow) should effectively filter out the effect of climate variability.

There are two problems to be addressed by model application: both the production of an output variable (e.g. streamflow) and detection of a change in response to changing land use scenarios. Both of these problems rely on the accuracy of the deterministic model. Therefore, it is critical to have field data to evaluate the mechanisms represented by the model. Extensive analysis has been done for some of the mechanisms involved in basin response to forest harvest and road construction. For example, snow melt response during ROS events has been investigated with detailed data on snow accumulation and ablation for both foreseted and cleared sites (Berris and Harr 1987, Kattelman 1990, Storck 1997). However, field investigation of road/channel network effects on hydrology has been limited.

For this study, a distributed hydrology-soil-vegetation model (DHSVM) was used in conjunction with field studies of two headwater creeks in the Deschutes River basin of the western Cascades of Washington to examine the effects of forest roads on streamflow. An explicit road network runoff algorithm was tested by comparing simulated runoff for selected storms to observations of road runoff from thirteen road segments made during the winter of 1995 and 1996. Basin discharge was then simulated for the period 1985 - 1996 with and without the road runoff algorithm. In addition, the overall connectivity of the road network to the drainage network was assessed based on field observations and GIS.

The remainder of this thesis is organized as follows: Chapter 2 reviews background research related to this study. The physical hydrology of the study region and the field data collection program are described in Chapter 3. A spatial analysis of potential road contribution to the drainage system of the study basins is described in Chapter 4. Chapter 5 describes the model used as well as the data pre-processing needed to drive the model. The results of model calibration versus point observations and continuous basin discharge are discussed in Chapter 6. In Chapter 7 the model is used to compare

observed discharge for a ten year period which includes the effects of extensive harvesting and road construction with simulated discharge which does not include these effects. Conclusions and recommendations are presented in Chapter 8.

CHAPTER 2: BACKGROUND

The role of forest roads in basin storm response depends upon the physical and temporal scale of interest, in addition to the interacting hydrological mechanisms described in Chapter 1. The effects of forest harvest and road construction on streamflow have been investigated at a variety of spatial scales. For the purpose of this study, hillslope scale will refer to areas generally less than 2 ha which are dominated by subsurface processes, i.e. below the scale of stream formation. Catchment scale will refer to the area drained by a first or second order stream, approximately 100 - 300 ha in area. Basin scale will be used to refer to areas where the cumulative effects of several catchments interact, generally between 100 - 1000 km in area. The relationship of the different scales is illustrated in Figure 2-1.

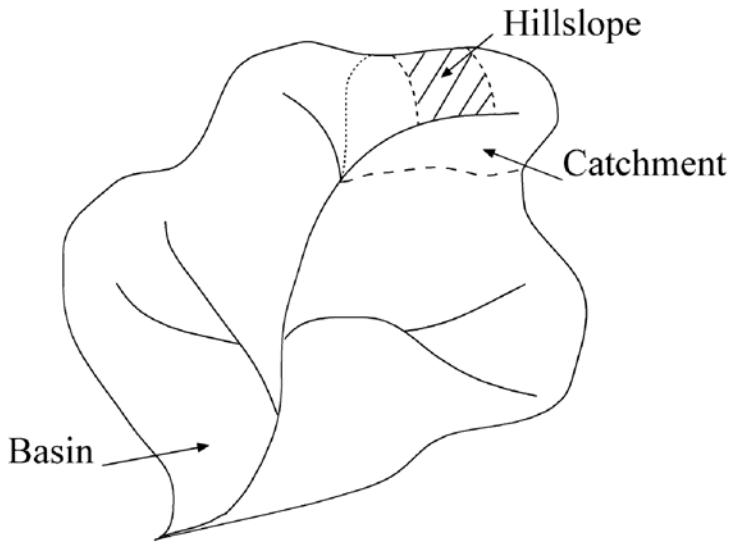

FIGURE 2-1: DESCRIPTION OF SPATIAL SCALES

This chapter will first review research that addresses the individual mechanisms of road network contribution to runoff response at the hillslope scale. Secondly, it describes catchment and basin-scale statistical studies aimed at detecting the cumulative effects of road construction and forest harvest. Finally, it touches on other physically-based models which relate to modeling of forest roads.

2.1: HILLSLOPE PROCESSES AND ROAD INTERACTION

The hydrological impact of roads in a forested catchment will depend primarily on four factors: vegetation, subsurface flow interception, surface runoff generation, and the overall network connectivity. By changing soil moisture content, removal of vegetation can influence the quantity and distribution of water available for interception by the road network. As illustrated in Figure 2-2, runoff traveling as subsurface flow may be intercepted by a road cut and diverted through the roadside ditch. In addition, precipitation falling on the compacted road surface is either diverted into the roadside ditch or over the side of the road. Diverted runoff travels as open channel flow in the roadside ditch until it reaches either a stream crossing or ditch-relief culvert. The connectivity of the road network to the natural drainage system will control the timing of discharge response at the basin outlet following redistribution of runoff by the road network. Each of these mechanisms is explored further below.

2.1.1: VEGETATION EFFECTS

The removal of vegetation for forest harvest or road construction affects the water balance of a catchment in several ways. The contribution of precipitation to streamflow will vary depending on the quantity, distribution, rooting depth and health of the vegetative cover through its control on evapotranspiration (Keppeler and Ziemer 1990). Reduced evapotranspiration means higher soil moisture storage at the end of the growing season, which can cause a significant increase in the volume of small autumn storms (Ziemer 1981).

Reduction in evapotranspiration primarily influences annual water yield. In a review of 94 catchment experiments world-wide, Bosch and Hewlett (1982) found no instances where removal of cover caused a reduction in water yield. Coniferous forests in higher rainfall areas show the largest yield changes, with an average increase of 40 mm per year per 10% of cover removed. Mean annual precipitation for the sites examined varied between 800 and 2500 mm with an increasing trend in annual water yield increase across the entire range. The review is based primarily on studies in the Pacific Northwest, supplemented

with a few studies of mixed conifer stands in Japan. Yield changes tend to be least persistent in high rainfall areas, due to faster regrowth (Bosch and Hewlett 1982). The influence of vegetation on soil moisture distribution and quantity may enhance the effect of forest roads. By increasing soil moisture upslope of the road cut, clearcuts will contribute greater subsurface flow for interception by the road network. In contrast, removal of vegetation downslope of the road will create a local increase in soil moisture relative to the unharvested basin during the growing season. This increase in soil moisture will counteract the loss of moisture from runoff which is diverted by the road network during storms, thus diminishing the consequences of this redistribution.

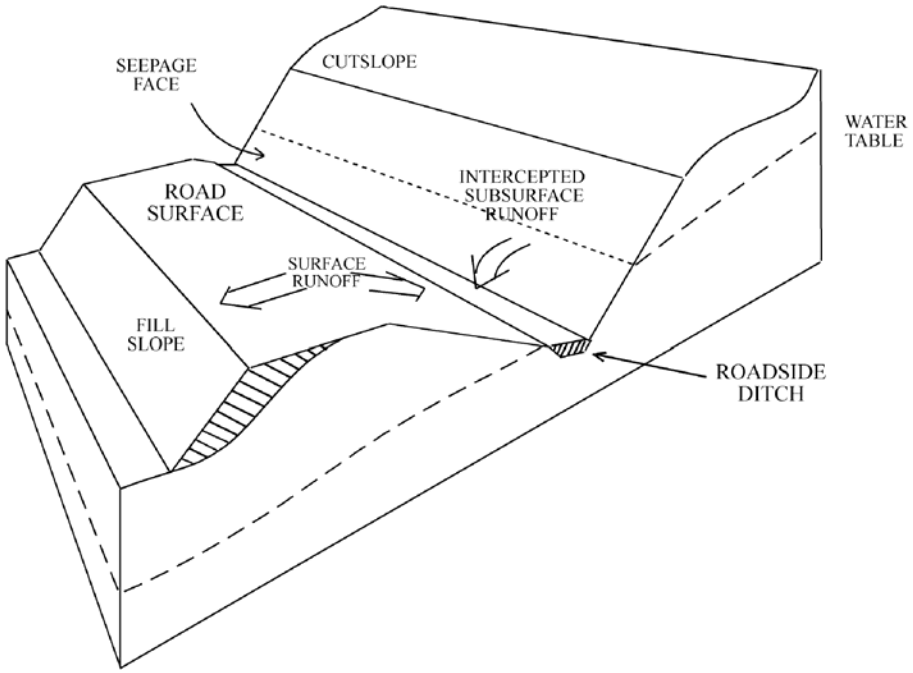

FIGURE 2-2: MECHANISMS OF RUNOFF INTERCEPTION BY THE ROAD NETWORK

Within the transient snow zone of the Pacific Northwest increased rates of snow accumulation and melt in clearcuts can increase ROS storm peaks and decrease the time to peak. Kattelmann (1990) found 20 cm (98 cm vs. 78 cm) greater peak accumulation of SWE in a cleared area in the Sierra Nevada relative to a forested area. The differences are increased if snowfall is separated by a period of slightly warmer

temperatures, so that intercepted snow melts from the forest canopy, and therefore increases available interception storage prior to the next storm (Berris and Harr 1987). In a paired watershed study in central Idaho, Megahan (1983) found a statistically significant increase in annual peak snow water equivalent after one basin was clearcut, with an average increase of 41 %. He found little difference in accumulation in the unlogged watershed after a wild fire removed all leaves in that basin, which suggests that aerodynamic effects, such as increased deposition in clear cuts caused by discontinuities in the airflow across the forest canopy may be as important as interception losses (Megahan 1983).

Snowmelt caused by both direct solar radiation and rain-on-snow (ROS) events is influenced by deforestation. Snow melt in the Sierra Nevada is dominated by direct solar radiation. Kattelmann (1990) found that the decreased shading in a clearing resulted in melt rates 75 % greater on average than in the forest near Soda Springs, CA. Snow in the clearing disappeared between 10 and 30 days faster than under the forest cover, depending on the peak snow accumulation (Kattelmann 1990).

In western Oregon, Berris and Harr (1987) found that a forested plot at 900 m elevation consistently had lower air and dew-point temperatures, and lower wind speeds than an adjacent clear-cut plot. This resulted in 40% greater melt in the clear-cut plot for the common period of melt during ROS events (Berris and Harr 1987). They also detected less shortwave radiation in the forested plot relative to the clearing, but there is some question regarding the accuracy of these shortwave measurements.

The increased rate of snow accumulation and melt associated with clear cuts can result in larger pulses of meltwater supply to the subsurface. Although the smallest relative snowmelt contribution to runoff will occur during high rainfall events, this volume would most likely increase storm runoff volume and size of instantaneous peaks from already swollen streams (Harr 1981). On average, ROS peak flows were higher than rain-only peak flows for a small catchment in western Oregon (Harr 1981). In addition, all but two of the largest 23 annual peaks from 163 years of reconstructed historical data for the Willamette River were associated with snowmelt during rainfall (Harr 1981). This is not suprising since in the

Pacific Northwest the largest storms occur in the winter when snow is present. Megahan (1972) found that subsurface flow rates were driven by the rate of snowmelt. As a result, the magnitude of streamflow increase resulting from faster snowmelt will depend on the position of the clear cut relative to the road system.

2.1.2: SUBSURFACE FLOW

As illustrated in Figure 2-2, one component of the effect of forest roads on streamflow is the interception of subsurface flow through the road cut and subsequent routing as surface flow. Conversion of subsurface runoff to surface runoff may substantially decrease catchment response time. Dunne and Black (1970a) observed that the velocity of water emerging from the soil surface as return flow increased by a factor of 100 to 500 relative to the rate of subsurface flow in a study near Danville, Vermont. Many factors seem to influence the degree to which roads will intercept subsurface flow. Megahan (1972) found that the total volume of subsurface flow intercepted by a road cut in an Idaho catchment was over 7 times greater than the estimated direct runoff from the road surface. In contrast, Reid and Dunne (1984) found no significant subsurface contribution to ditch runoff in the Clearwater basin on the Olympic Peninsula. Ditches carried no baseflow between events and cutbank seepage was not observed, despite the fact that road cuts intercepted the entire soil column. These studies indicate that the quantity, velocity and distribution of water traveling in the shallow subsurface will therefore control the magnitude of forest road influence on basin hydrology.

In simplified terms, subsurface flow can be classified as either subsurface storm flow or deep groundwater flow, as illustrated in Figure 2-3. Subsurface storm flow refers to the water which infiltrates the surface and moves laterally through the upper soil layers as unsaturated flow or as shallow, perched saturated flow above the main groundwater table, during and shortly after a storm. Groundwater flow is derived from deep percolation of infiltrated water that enters the saturated groundwater flow system (Freeze 1974). This represents a simplification because macropore and

pipeflow can result in linkages of the pathways shown in Figure 2-3, e.g. by bypassing the soil matrix to quickly recharge the groundwater table (Anderson and Burt 1990). Runoff generation occurs by different mechanisms depending on location. In areas with shallow groundwater tables, runoff may originate from small source areas which generate overland flow during rain events (Freeze 1974, Dunne and Black 1970a, 1970b). Forested basins in the Pacific Northwest have large infiltration capacities and relatively low rainfall rates. As a result, overland flow is a rare occurrence and in many forested areas subsurface stormflow is the primary source of streamflow (Freeze 1974, Hewett and Hibbert 1967, Montgomery et al. 1997, Whipkey 1969). The primary mechanism of runoff generation will depend on the rainfall intensity, infiltration rate, soil permeability and local slope (Montgomery et al. 1997).

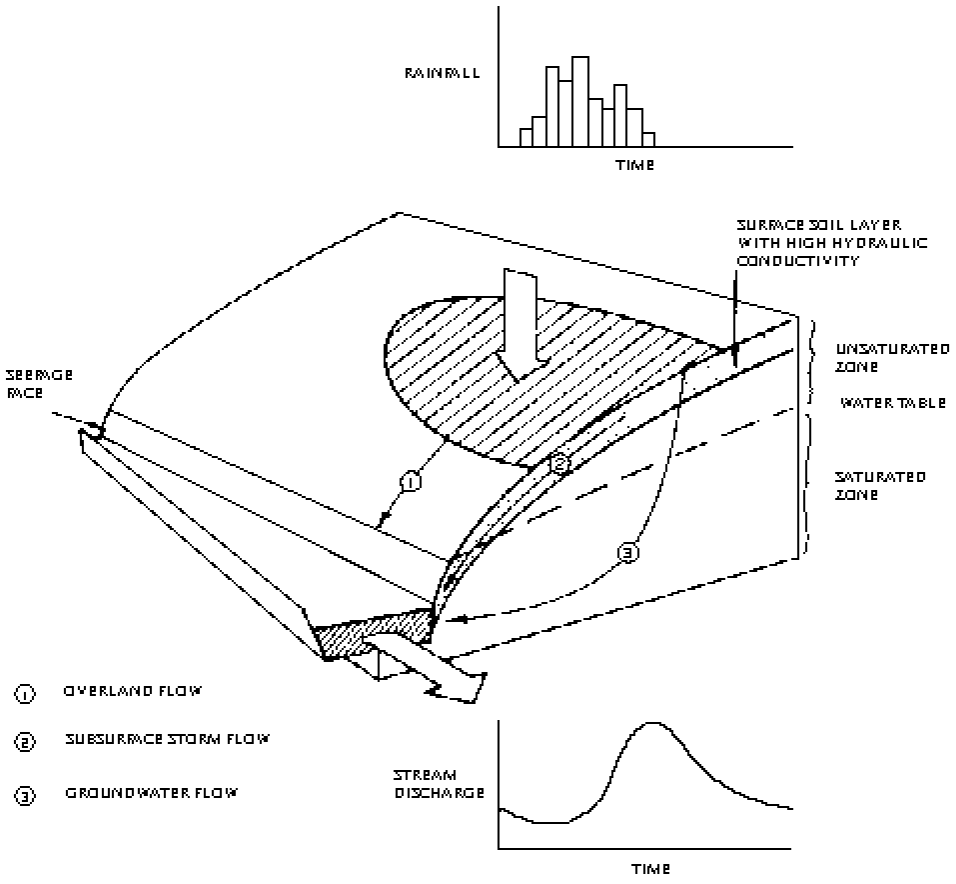

FIGURE 2-3: SCHEMATIC OF HILLSLOPE RUNOFF RESPONSE (FROM FREEZE 1974)

The volume and velocity of water traveling as subsurface flow will control the influence of forest roads on peak storm flow. If streamflow in a basin without roads originates largely from variable source areas, it implies that subsurface flow response must be slower. Therefore, subsurface flow may not reach the road network quickly enough during a storm to contribute to the hydrograph peak. However, this situation would cause the largest change in runoff velocity as the slow moving groundwater flow is eventually intercepted by the road network and converted to surface flow. Runoff traveling as subsurface stormflow, including pipeflow, will reach the road network in time to contribute to the stream hydrograph. However, in this case the difference in the runoff velocity may not be as great. In either case, the interception of subsurface flow will still have an indirect effect on the storm hydrograph through redistribution of soil moisture and through direct runoff from saturated seepage faces.

Field monitoring programs have yielded contradictory results on the ability of subsurface stormflow to contribute significant volume to the storm hydrograph (Dunne and Black 1970a, 1970b, Hewlett and Hibbert 1967, Montgomery et al. 1997, Whipkey 1969). Montgomery et al. (1997) found that all runoff generation was due to subsurface stormflow during three years of observation in a zero order basin near Coos Bay, Oregon. Also at the hillslope scale (13.7 m by 81 m), Whipkey (1969) found that subsurface stormflow, rather than overland flow, was the major contributor to the storm hydrograph in the Allegheny-Cumberland plateau of eastern Kentucky. In silt loam and loam soils, subsurface stormflow began responding 20 to 60 minutes from the beginning of storms and peaked shortly after rainfall subsided. The rate of water flux was approximately 3 m/hr. In contrast, a relatively course textured sandy loam soil at the same site did not respond until nearly 30 hours after the storm, and provided a steady baseflow as a function of the matrix hydraulic conductivity (Whipkey 1969).

Megahan (1972) monitored subsurface flow intercepted by roads in two small Idaho watersheds. Subsurface flow peaks were found to lag behind snowmelt peaks (measured using a snow lysimeter) by 1.5 days with an average travel distance of 200 feet, which yields an approximate flux rate of 1.7 m/hr.

However, average saturated hydraulic conductivity measured from undisturbed core samples was approximately 19 feet/day (0.24 m/hr). Subsurface stormflow can be either Darcian, traveling through the soil matrix, or non-Darcian, bypassing the soil matrix through macropores or pipes (Anderson and Burt 1990). The average flux rate observed by Megahan (1972) to be greater than the matrix hydraulic conductivity suggests that some of the subsurface runoff may bypass the soil matrix.

Macropore flow, through capillary size pores, is likely to occur where root holes and other biopores exist in abundance. Pipes are usually considered larger versions of macropores, however, they generally exhibit a greater degree of connectivity (Anderson and Burt 1990). Pipes in the Caspar Creek Experimental Watershed in Northwestern California have been observed at depths up to 2 meters, with diameters range from 1 to 100 cm (Ziemer and Albright 1987). Research in a variety of landscapes has shown that pipeflow may account for a substantial portion of subsurface stormflow. Ziemer (1992) found that pipeflow accounted for virtually all of the stormflow from three monitored hollows in the Caspar Creek Experimental Watershed in Northwestern California. A small percentage of seepage through the soil matrix was observed during storms, and baseflow was sustained in the pipe network between storm events (Ziemer and Albright 1987). Tsukamoto et al. (1982) found that pipeflow was responsible for 95 % of the runoff from a small granitic catchment in Japan. Jones and Crane (1984) estimated that 46 % of streamflow in an upland basin in mid-Wales originated as pipeflow.

Pipes are generally fed through saturation-excess overland flow or by drainage of saturated soil. Therefore they will only respond with sufficient moisture input (Anderson and Burt 1990). Wilson and Smart (1984) observed that water was diverted into the pipeflow system only after the surface seepage capacity was exceeded in a catchment in Brecon Beacons, Wales. Pipeflow in this basin was ephemeral in nature, with flow occurring for a limited duration during storms. Under dry antecedent conditions runoff infiltrates through the floor of the pipe network and contributes to throughflow (Smart and Wilson

1984). Pipe discharge in Caspar Creek does not begin until a threshold of soil moisture is reached, at which point additional rainfall is quickly reflected in pipeflow hydrographs (Ziemer and Albright 1987). Similarly, Tsukamoto et al. (1982) found that pipeflow did not begin until groundwater saturation reached the pipe level.

Once inititated, flow through macropores and pipes can greatly increase the rates of subsurface drainage. Ziemer and Albright (1987) measured discharges up to 8.5 l/s during storms through pipes between 15 and 45 cm in diameter. Smart and Wilson (1984) calculated an average pipe flow velocity of 0.9 m/s was found for a sample of 212 m of pipe, by timing measured volumes and dye travel times. These velocities are similar in magnitude to that of overland flow observed in the study area. However, depending on the connectivity of the network the pipes may not extend to an outlet. Smart and Wilson (1984) demonstrated that the general structure of a pipe network in a South Wales basin was stable over a five year period, although microscale changes occur within individual storm events. Through observing that the quantity of pipe discharge decreased downslope, they concluded that the pipes serve to recharge the soil moisture at the slope base. In this way the pipe network could enhance both saturated overland flow by concentrating water quickly in topographic hollows or subsurface storm flow by increasing the depth of the saturated zone and therefore the lateral hydraulic conductivity.

In contrast, Dunne and Black (1970a) found that the timing and quantity of observed subsurface stormflow could not explain the storm hydrograph in a field study near Danville, Vermont. They found that there was very little response to summer storms within the root zone and that base flow in the deep sub-root zone did not respond to individual rainstorms. Subsurface flow during a large autumn storm with very wet antecedent conditions lagged the beginning of rainfall by 2.25 to 2.5 hours. Flow from the sub-root zone lagged rainfall by 1.33 to 3.33 hours. However, the volume was not sufficient to explain the storm hydrograph. They concluded that the major contribution to stormflow was direct precipitation on saturated areas located near the stream in accordance with the partial area concept of runoff production (Dunne and Black 1970b).

In a study of a watershed in the H.J. Andrew's Experimental Forest in western Oregon, Harr (1977) found that subsurface flow accounted for 97% of stormflow, with only 3% attributable to channel interception of rainfall. The maximum rate of water movement in the top soil layer was 3 - 4.5 mm/hr. Subsurface flow was concentrated in well-defined seeps which appeared to reflect the micro-topography of unweathered bedrock near the stream. A monitored seep of subsurface flow began to increase 5.5 hours after rainfall began, which is when streamflow also began to rise. The maximum flux from the deeper sub-soil layer was 0.5 mm/hr. This, coupled with the fact that during storm events the vertical and downslope components of flux in the upper most soil layer were equal, means that a unit of rainfall contributes less to quick flow and more to soil moisture storage and baseflow as one moves upslope from a stream in an undisturbed basin. As the density of the stream or road channel network increases, the upslope flow path will decrease and a decreasing percentage of rainfall will contribute to soil moisture storage and base flow.

It follows that the spatial distribution of subsurface routing relative to road location will control the magnitude of forest road interception. By making comparisons of intercepted subsurface flow to perennial stream discharge in neighboring catchments, Megahan (1972) concluded that approximately 35% of subsurface flow was captured by the road cut for a site in the Pine Creek catchment near Crouch, Idaho. The remaining 65% was assumed to pass beneath the level of the road cut at the measurement site. As another measure, Megahan compared the upslope contributing area per unit length of road draining the area for two watersheds and found that one watershed could be expected to yield over 3 times more water per unit length of road, assuming equal yields per area of drainage, due to the topography above the road cut..

Topographic controls on the distribution of subsurface water include saturation of regions of reduced storage due to thinner soils, as well as locations where lateral subsurface flow contributes to soil water storage. Such locations include topographic hollows and low gradient slopes where the rate of subsurface drainage is reduced by the low hydraulic gradient (Anderson and Burt 1978). Anderson and

Burt (1978) have shown that topographic hollows (convergent hillslopes) are a major source of subsurface runoff. A convergent hillslope includes a hollow in which flow from a wide contributing area is concentrated into a narrower outlet downslope (see Figure 2-4). A divergent hillslope includes a local peak where runoff can disperse into many directions. In the Slapton Wood catchment in South Devon, Anderson and Burt (1978) found that convergence of water into a subsurface hollow is responsible for a delayed peak in stream discharge which occurs one to two days after the primary streamflow peak. The secondary peak accounts for the majority of catchment runoff. Woods and Rowe (1996) investigated the spatial variability of subsurface flows in a New Zealand catchment by dividing flow from sections of a hillside into a series of collection troughs. They found that the relative proportion of flow between convergent, divergent and straight hillslopes was not constant over time. Flows tended to be concentrated in troughs draining the largest convergent area. However, two troughs draining divergent areas occasionally had high percentage contributions following extended dry periods, due to shallow soils (lower soil moisture deficit) and short average flow distance (shorter response time). Similarly, in the Slapton Wood catchment lateral subsurface flow does not occur when soil moisture deficits are high. In these cases, flow convergence does not occur and only a primary hydrograph peak is observed (Anderson and Burt 1978, Burt et al. 1983). Woods and Rowe (1996) also found that several troughs carried approximately equal volumes during high flow events although their contributing areas seemed to be much different. One explanation suggested by the authors is that the flow within the drainage leading to the most convergent trough becomes so large that it 'overflows' laterally into the drainage for neighboring troughs. Similarly, Harr (1977) observed that saturated zones at the base of the slope would expand upslope and laterally as rainfall progressed. This was also observed by Montgomery et al. (1997) in a zero-order catchment near Coos Bay, Oregon.

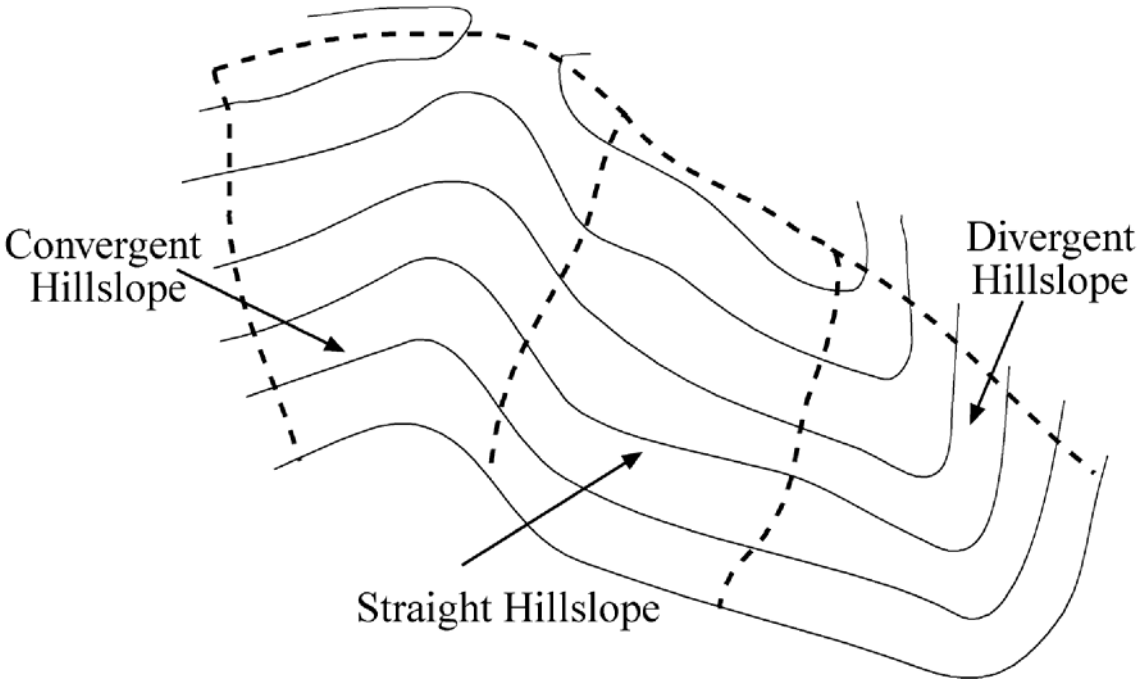

FIGURE 2-4: DEFINITION OF HILLSLOPE TYPE

In addition, Woods and Rowe (1996) found that topographic shape exerts little influence under wet antecedent conditions in which soil moisture deficits are uniform. Dunne and Black (1970a) found that the importance of hillslope shape depended primarily on the ability of a given hillslope to generate overland flow through return flow. Even during extreme events, no subsurface stormflow was produced from a straight hillside. Subsurface flow from the convergent hillslope was larger for the root zones, but smaller and slower for the sub-soil layer (Dunne and Black 1970a).

As described above, field research done at the hillslope scale is useful for examining the connection between precipitation input, subsurface flux rate, hillslope topography and soil depth to the quantity of subsurface flow which can be intercepted by the road cut. Megahan (1983) showed that the rate of subsurface flow interception by a road cut in the Pine Creek catchment in Idaho was well predicted by the volume of water stored in the subsurface flow water table. The rate of subsurface depends on local geology, with response times ranging from 20 minutes to 5.5 hours after the beginning of rainfall for

typical hillslope lengths between 40 and 100 m (Whipkey 1969, Megahan 1972, Dunne and Black 1970a, Harr 1977). The natural timing of subsurface response will influence the degree of change in catchment response time due to roads. The depth and position of the road cut relative to soil depth and topography will control the quantity of subsurface flow captured by the road network (Megahan 1972, Reid and Dunne 1984, Harr 1977, Anderson and Burt 1978). These factors together will control the fraction of subsurface water intercepted by the road cut and ultimately, the degree of change in hydrograph response due to roads.

2.1.3: RUNOFF FROM ROAD SURFACES

The compacted surfaces of forest roads have decreased infiltration capacity relative to the undisturbed forest floor (Megahan 1972, Folz and Burroughs 1990, Reid and Dunne 1984, Luce and Cundy 1994). If the rate of rainfall plus snowmelt over the road surface exceeds the rate of infiltration, Horton runoff over the road surface will occur. Depending on road surface conditions, this flow may become concentrated in road ruts or other surface channels, before being diverted either over the side of the fill slope or into the roadside ditch at the base of the cutslope (see Figure 2-5). The quantity and timing of infiltration excess runoff from the road surface will depend on the infiltration capacity of the road surface and drainage ditch, the area and gradient of the road segment and the topography and roughness of the road surface.

Quantifying the reduced infiltration capacity from road surfaces is difficult, and much of the information available is based on qualitative observations. Some infiltration does occur. Fahey and Coker (1989) found that in only 46 of 133 storms greater than 5 mm did total precipitation produce measurable runoff in South Nelson, New Zealand. The road surface was freshly graded and surfaced with local river gravel. In this case, 'depression' storage may play an important role in preventing runoff of low intensity rainfall before infiltration can occur.

The ratio of runoff to rainfall for forest roads in the Caribou National Forest near Idaho Falls, Idaho was found to vary from 0.55 to 0.99 for artificial storms depending on antecedent conditions and the presence or absence of an imposed wheel rut (Foltz and Burroughs 1990). The same experiment was conducted on forest roads in the Routt National Forest near Steamboat Springs, Colorado, yielding ratios between 0.8 and 0.91. The roads were freshly graded for both sets of experiments. After grading, artificial wheel ruts were imposed on one plot at both sites. Total infiltration was highest for dry antecedent conditions and road segments with no wheel ruts. Based on rainfall intensity and total runoff depth published by Foltz and Burroughs, average areal infiltration rates for the two experiments ranged between 0 and 21.5 mm/hr

FIGURE 2-5: ROAD SURFACE RUNOFF IN HARD CREEK, WA

for the Idaho sites and between 4.2 and 9.6 mm/hr for the Colorado site. As a basis of comparison, the approximate one year return period one hour precipitation for the Idaho site is 8.3 mm/hr (Hershfield 1961). Typical rainfall intensity would be somewhat less than this, but it is clear that in many cases the

rainfall rate would exceed the derived infiltration rates. One hour precipitation for the Colorado sites is approximately 12.7 mm/hr with a one year return period (Hershfield 1961), which is well above the observed infiltration rates. An average infiltration rate of 0.5 mm/hr was found for frequently traveled gravel surfaced roads in western Washington (Reid and Dunne 1984). The one hour precipitation with an occurrence frequency of one year is also about 12.7 mm/hr for this area. These values indicate that a significant, though variable, portion of rainfall may runoff directly from the road surface.

Road gradient and surface area directly influence the timing and volume of surface runoff from forest roads. Drainage area is the main determinant of the size of runoff peaks. Slightly higher discharge per unit area, shorter time to peak and shorter flow duration are associated with steep road segments (Bilby et al. 1989). Many studies that have related road area to catchment response have been unclear if the width of road right-of-way was included in the calculation. Assumed and measured road surface widths in the literature range from 3.5 meters to 5.6 meters in Oregon, Washington and New Zealand (Piehl et al. 1988; Fahey and Coker 1989; Reid and Dunne 1984; Montgomery 1994). The total width of disturbed area due to road construction includes the cut and fill slopes as well. This total width is often the only road width reported. Piehl et al. (1988) found an average sub-grade width of 6.6 meters for roads in United States Forest Service (USFS) land in the Oregon coast range. Other reported values for road right-of-way range from 16 to 28 meters in the H.J. Andrews Experimental Forest, Western Oregon and Caspar Creek watershed in Northern California (; Swanson and Dyrness 1975, Wemple et al. 1996, Wright et al. 1990). The cut and fill slopes are generally not compacted, although they may have reduced infiltration after being wetted. Therefore, it may not be appropriate to assume the same reduced infiltration capacity for the entire right-of-way.

In addition to infiltration rate, area and gradient, road surface conditions will also control road surface runoff hydrographs. Reid (1981) found that well-used gravel and paved roads in western Washington produce unit hydrographs that were similar in both size and shape. This suggests that the difference in surface roughness between the road types does not control the hydrograph, probably because of the short

distance traveled as surface flow before runoff is concentrated in ruts or ditches (Reid 1981). Hydrographs from abandoned forest roads were found to be more attenuated, probably due to increased roughness and the absence of wheel ruts (Reid 1981). Flow response for the gravel and paved roads was found to last for 50 - 55 minutes in response to a 15 minute storm. In contrast, Sullivan and Duncan (1981) found flow durations between 8 and 17 hours in response to storms from 1 to 2 hours in duration. (The longer responses are most likely due to the contribution of subsurface stormflow which was observed for at least some of the sites.) Once surface runoff reaches the roadside ditches the speed of delivery is controlled by roughness elements in the ditches. Foltz (1996) found that roughness coefficients are generally higher for ditch flow than for similar stream channels since the water is not deep enough under normal conditions to cover the roughness elements completely.

The above studies indicate that forest road surfaces generate runoff when precipitation rates exceed the rate of infiltration through the road surface. The compacted surface width of roads in the Pacific Northwest averages around 4.5 meters. Infiltration rates through the road surface vary between 0.0 to 21.5 mm/hr during a storm, based on antecedent wetness, surfacing material and the degree of compaction. The average of all measured infiltration rates reported here is 5 mm/hr. Using this average rate, a typical storm in the Pacific Northwest of 10 mm/hr will generate 22.5 m^3 of runoff per km of forest road for a one hour storm. The downstream effect of this surface runoff will depend on how it travels from the road surface.

2.1.4: DRAINAGE NETWORK CONNECTIVITY

The ultimate effect of surface or subsurface runoff intercepted by forest roads on hydrograph timing and peaks depends on the flow paths followed after being intercepted by the road network. For example, Rothacher (1973) observed that localized surface runoff generated from truck and skid roads in a newly harvested catchment usually travels to less compacted areas where infiltration can occur. If infiltration occurs soon after runoff interception there will be no detectable influence due to roads. However, if the

road drainage network directs intercepted runoff to a natural stream channel through a shortened surface flow path, a significant reduction in response time may occur, as discussed in Section 2.1.2. Basin response will depend on the number and location of road drainage points in relation to the natural drainage network. Possible flow paths for intercepted runoff are illustrated in Figure 2-6, taken from Wemple (1994).

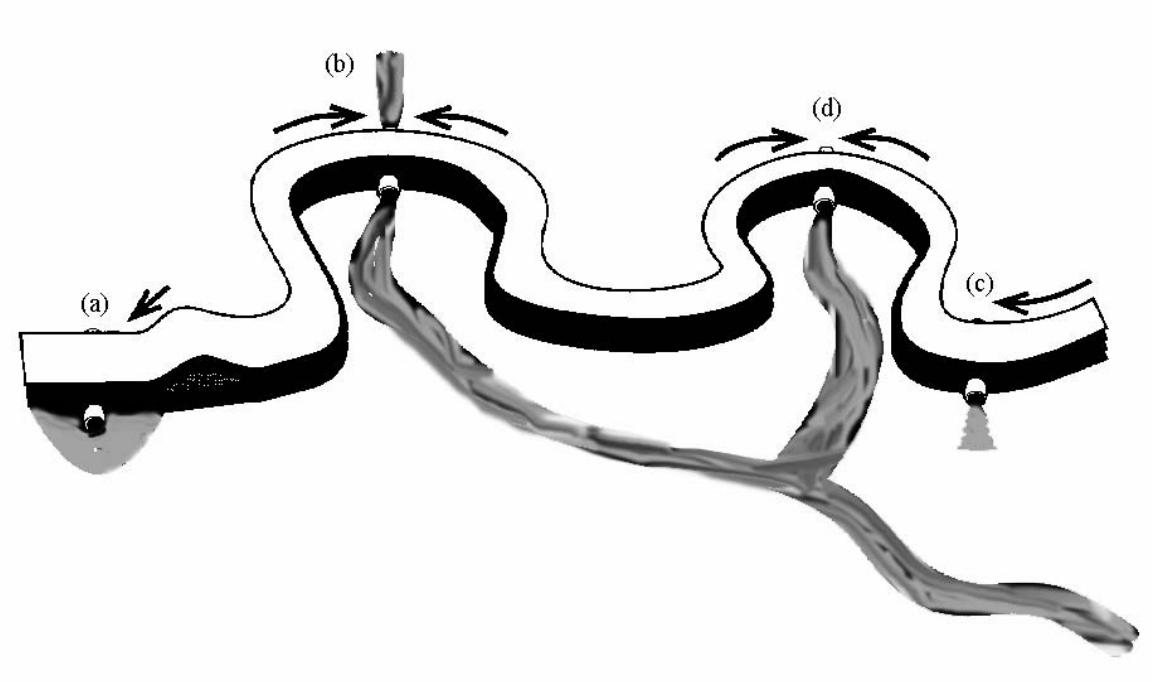

FIGURE 2-6: ROAD DRAINAGE AND INTEGRATION OF ROADS AND STREAMS
Road runoff may discharge a) to a ditch-relief culvert and infiltrate below outlet, b) to a stream crossing culvert, c) to a gully that extends some distance downslope or d) to a gully that connects to a stream channel or saturated zone near the channel (Wemple 1994).

Bilby et al. (1989) found that 34 % of road runoff points surveyed in three large watersheds in western Washington drain to a stream. For their study, a defined channel below the discharge point or some evidence of intermittent surface flow between the discharge point and the channel was taken to indicate drainage into streams. About 70 % of the sites enter first-order channels (Bilby et al. 1989). Based on topographic surveys, Reid and Dunne (1984) found that 16 % of road runoff generated is diverted off the outer side of the road where it infiltrates. For the runoff that enters the ditch, 75 % of the ditch relief

points are connected to streams. Wemple (1996) found that 56 % percent of culverts surveyed network in two western Oregon basins in the H.J. Andrews Experimental Forest divert water directly to the stream. Of the culverts which divert water directly to the stream, 59 % were stream crossings. The remaining 41 % of the culverts were connected to the stream through incised gullies (Wemple et al. 1996).

The concentration of road drainage to points where it can follow a surface pathway to a stream increases the effective length of the channel network by decreasing the length of subsurface flow. Integration of the road and channel networks was found to increase the effective drainage density by 57 % in a 1.2 square km basin in the Sierra Nevada without taking into account the length of any new channels incised between culverts and channel heads (Montgomery 1994). Drainage density was increased by 23 % in three basins on Mettman Ridge, Oregon (Montgomery 1994). Based on a sample of 20 % of the road network in two basins in the H.J. Andrews Experimental Forest, the road network was found to increase drainage density by 21 to 50 %, as summarized in Table 2-1 (Wemple et al. 1996). The studies described above indicate that between 34 and 68 % of road runoff points discharge runoff directly to streams as surface flow. The subsequent increase in drainage density and decrease in the effective hillslope length may have a significant effect on hydrograph timing from individual catchments.

Runoff routing through the road drainage network may actually cause a decrease in flow response from other parts of the catchment by concentrating subsurface water below culvert outfalls rather than over the entire hillslope. Removing subsurface water by road interception decreases water available downslope for vegetation growth and could affect species health and composition, although this has never been established. In addition, if culverts are spaced too far apart, they may rob one basin of water at the expense of another (Megahan 1972). Montgomery (1994) found that culvert locations in a southern Sierra Nevada catchment divert water from four headwater hollows and subsequently concentrate flow in another three. The ridge top road is paved so runoff from the road surface is maximized. Channels began immediately downslope of culverts in the hollows with additional drainage. Channels began

significantly further downslope for the other four hollows. Redistribution of drainage by roads did not alter the dominant channel initiation process, although less drainage area was required to initiate a channel for hollows receiving diverted road drainage (Montgomery 1994). Wemple et al. (1996) found that the occurrence of gullying within 10 m of the culvert outfall increased with increasing culvert spacing and hillslope gradient. Piehl et al. (1988) also observed outlet erosion at 38% of ditch relief culverts surveyed in the Oregon coast range. The volume of eroded material below culverts increased in response to a larger distance between culverts. Erosion at the culvert outlet alone does not represent an extension of the channel head unless it extends all the way to a natural stream channel. Gullying is indicative of excess energy at the culvert outlet and the potential extension of channel heads.

TABLE 2-1: ESTIMATED CHANGES IN DRAINAGE DENSITY IN LOOKOUT CREEK AND BLUE RIVER (FROM WEMPLE ET AL. 1996)

	PERCENT CHANGE IN DRAINAGE DENSITY	
ASSUMPTIONS	LOOKOUT CREEK	BLUE RIVER
Only road ditches draining to stream-crossing culverts are connected to the natural drainage network	21 %	23 %
Road ditches draining to stream-crossing culverts and ditch-relief culverts with gullies are connected	36 %	39 %
Road ditches draining to stream-crossing culverts or ditch-relief culverts with gullies and the gullies themselves are connected	40 %	41 %
Road ditches draining to stream-crossing culverts or ditch-relief culverts with gullies and the gullies themselves are connected but the stream network is 25 % shorter than estimated using a 2 ha source area.	48 %	50 %

2.1.5: WATERSHED SCALE EFFECTS

Watershed size and the cumulative effects of forest management in headwater catchments affect the observed hydrograph response. Most studies involving land use change have focused on runoff changes for small first and second order catchments (Bosch and Hewlett 1982). Of the 94 catchment experiments reviewed by Bosch and Hewlett (1982), only 10% of the catchments were larger than 10 km^2, 79% of

the catchments were smaller than 2 km^2. Observed changes in runoff depth and peak runoff rate in small headwater catchments will be attenuated as runoff accumulates downstream. Spatial variability in total runoff depth is reduced in the downstream direction and is less responsive to individual subwatersheds. Accumulation of runoff forces the runoff depth to converge to a representative value for the entire watershed as drainage area increases, see Figure 2-7 (Garbrecht 1991). The magnitude of peak runoff rate per unit area decreases in the downstream direction (Figure 2-7). This is because the upstream drainage area increases faster than the accumulated peak runoff rate. Since the hydrographs from downstream watersheds reach the downstream location earlier than the accumulated hydrograph, they contribute relatively less to the peak runoff rate. The end effect is that spatial runoff accumulation tends to integrate upstream conditions into one representative downstream value, diminishing the importance of spatial variability of catchment runoff (Garbrecht 1991).

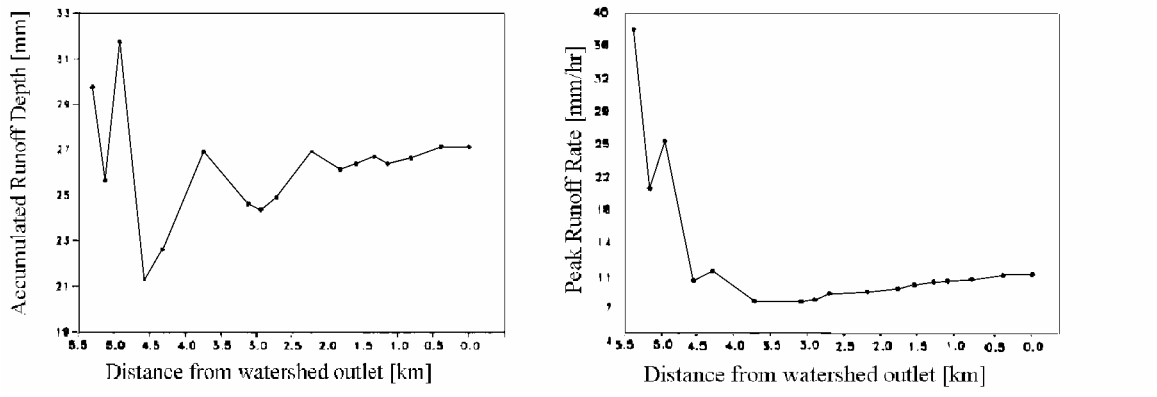

FIGURE 2-7: VARIATION OF PEAK RUNOFF RATE AND RUNOFF DEPTH AS A FUNCTION OF DISTANCE DOWN THE DRAINAGE NETWORK
(from Garbrecht 1991)

The relationship between the spatial distribution of subcatchments and the timing of hydrographs at a downstream location is depicted in Figure 2-8 taken from Garbrecht (1991). Figure 2-8 also illustrates how the downstream hydrograph may respond to road construction in a headwater catchment (Catchment 1 in the figure), using a theoretical hydrograph response due to roads adapted from Wemple

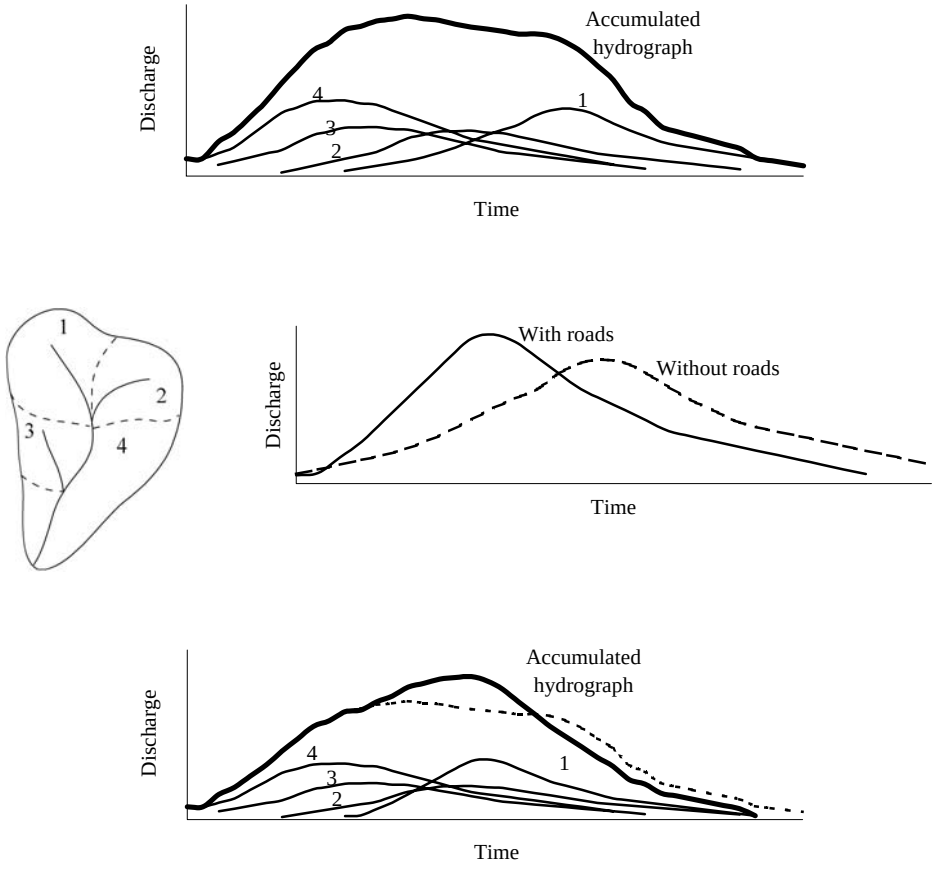

FIGURE 2-8: SCHEMATIC ILLUSTRATION OF THE INTERPLAY BETWEEN SPATIAL DISTRIBUTION OF SUBWATERSHEDS, HYDROGRAPH TIMING AND ACCUMULATED HYDROGRAPHS
(Adapted from Garbrecht 1991 and Wemple et al. 1996)

et al. (1996). In addition, by changing the timing of flood hydrographs, changes in vegetation may desynchronize hydrographs and actually reduce peak flows downstream (Harr 1981). The lag between subcatchment hydrographs places more weight on the hydrographs whose timing coincide with the accumulated hydrograph, generally those near the centroid of the basin (Garbrecht 1991). Therefore, by advancing time to peak, road construction and forest harvest in catchments near the basin centroid are more likely to desynchronize hydrographs, while forest management activities upstream of the centroid may be more likely to coincide with the accumulated hydrograph and increase peaks downstream.

2.2: RETROSPECTIVE STUDIES

The previous section focused on the existing mechanisms which interact within a basin with roads to alter the natural basin response. Vegetation, subsurface flow, surface runoff generation and the road network connectivity all interact to affect hydrographs at the basin outlet after road construction. Because of the hillslope interactions and spatial accumulation of runoff it is not straightforward to predict the effects of forest management at catchment and basin scales. The following sections describe retrospective studies designed to detect changes in watershed response following forest management activities. Since the effect of forest roads often cannot be separated from vegetation changes for more than a few years, changes due to forest harvest will be investigated first. These studies may provide insight into the studies which review the simultaneous effects of road construction and forest harvest.

2.2.1: FOREST HARVEST EFFECTS ON STREAMFLOW

Many researchers have found a range of watershed responses to timber harvest using statistical, paired catchment techniques. The most consistent response detected is an increase in summer and annual water yield due to a decrease in evapotranspiration losses. For instance, Keppeler and Ziemer (1990) found a significant increase in both annual water yield and summer low flows following removal of 67% of the timber volume from the 424 ha Caspar Creek watershed in Northwestern California. Relative increases in seasonal water yield were greater during the summer, however increases in annual water yield were more persistent in time. The summer flow increases generally disappeared within five years. Similar to the Caspar Creek study, summer low flows increased 12-28% for a 25% patch-cut basin in the H.J. Andrews Experimental Forest relative to a control basin for the six years of record (Rothacher 1965). A statistically significant increase in annual water yield was found for several years after road construction and cutting, although none was observed for roads alone. The percentage increase in summer low flows each year for a third basin which was 100% clear cut over a period of years mirrored the percentage of the basin cut. There was also a statistically significant increase in annual water yield, with much of the increase due to increased runoff volume during fall storms (Rothacher 1965; 1970). In another paired

catchment study in the H.J. Andrews Experimental Forest, one watershed was clearcut and another had 60% of the total basal area removed in a shelterwood cut. Annual water yields increased by 30% for the clearcut treatment relative to an undisturbed catchment and by 22% for the shelterwood cut (Harr et al. 1982). The number of summer low flow days also decreased for both watersheds. Although no significant post-logging increase was detected, an increasing trend in annual minima following logging was observed in a paired catchment study in the Oregon Coast Range (Harris 1977). A significant increase in annual yield (26%) was also detected after one basin was 100% clearcut.

The effect of evapotranspiration decrease on peak flows is less pronounced. In the Caspar Creek watershed, Ziemer (1981) found increases in the first streamflow peaks in the Autmun of almost 300%. However, these early fall storms were generally small and had little hydraulic consequence. There was no significant increase in the larger winter storm peak flows once the basin was wetted (Ziemer 1981). Wright et al. (1990) found statistically significant increases in total storm volume, quick flow volume and peak flow of small storms following logging. Quick flow was separated by projecting the line from the initial rise until it intersected the hydrograph falling limb, after Hewlett and Hibbert (1967). A statistically significant increase of the volume of three day high flows after clear-cutting was also found in the Alsea River basin in western Oregon (Harris 1977). Increases in peak flow observed in three sub-watersheds in the Oregon coast range following clear-cutting were higly statistically significant. Non-significant increases in total volume were also observed. However, interpretation of these results is problematic because no peak during the post cutting period exceeded the mean annual peak (Harr et al. 1975).

Rothacher (1965) found no measured increase in peak flows in a basin in the H.J. Andrews Experimental Forest with 8% of the basin area occupied by roads and an additional 25% patch cut. The size and timing of peak flows was not altered significantly by clear cut or shelterwood logging two basins in the H.J. Andrews Experimental Forest (Harr et al. 1982). In a paired catchment study in western Oregon, Jones and Grant (1996) observed increased average peak discharges of 50% in small

basins (0.6 - 1.0 km^2) and up to 100% in large basins (60 - 600 km^2) over the past 50 years. The peak discharge record included on average 10 storms per year for small basins and 3 to 5 storms per year for large basins. They found a significant number of storms to produce higher peak discharge, higher volume, advanced hydrograph rise times and delayed peak times following 100% clearcutting of a small watershed, with greater changes for small rainfall depths.

At a larger scale, Rosencrantz et al. (1995) found statistically significant increases in the instantaneous annual peak discharge (annual maxima) for four catchments of the Snoqualmie River basin in western Washington from 1961 - 1993. The catchments have been harvested during this period and the percent of basin area with trees younger than 20 years averages between 8 and 15 % for the 30 year history. A statistically significant increasing trend was also detected in the peaks-over-threshold (POT) series for the most heavily harvested catchment. The threshold was selected to include on average three events per year, based on the mean daily discharge. No statistically significant trends were detected in the difference series for two subcatchments with contrasting harvest histories.

Storck et al. (1995) controlled for climatological changes by analyzing the difference series between observed streamflow and discharge simulated using DHSVM (Storck et al. 1995, Wigmosta 1994), a distributed hydrology model, for the main stem Snoqualmie River. Since the model is driven with observed meteorological data and vegetation is fixed in the simulation, any trends in the residual series should be due to vegetation changes alone. No statistically significant trends were detected in the annual maxima peak flood flow series for the main stem Snoqualmie, the POT series which included on average one storm per year, based on mean daily discharge, or the POT series which included on average two to three storms per year. A statistically significant increase was detected in the smaller floods of the POT series which included approximately the 2^{nd} and 3^{rd} largest storms per year (Storck et al. 1995).

In an attempt to account for the influence of accumulated snow on hydrograph response, Harr (1986) reanalyzed Rothacher's 1973 data from the H. J. Andrews Experimental Forest. He found that peak

flows associated with snowmelt appeared to be higher following logging, with the greatest change in moderate-sized flows. In looking at data first presented by Harr and McCorison (1979), Harr found considerable variation in the relationship between peak flows in the pre-logged basins, which seemed to relate to antecedent snow conditions. The original analysis of two paired catchments in the H.J. Andrews Experimental Forest suggested a 36 % reduction and delayed response for annual peak flows caused by rain on snow following clear-cutting. No significant changes were detected in flows resulting from rainfall alone (Harr and McCorison 1979). No clear conclusions could be drawn from the reanalysis, but it is clear that not separating data according to antecedent snow conditions can skew the results when comparing pre- and post-logging peak flows (Harr 1986).

Rosencrantz et al. (1995) partitioned the POT series for the main stem Snoqualmie River and four subcatchments based on snowmelt contribution as a percentage of rainfall. The total water available for runoff (WAR) was obtained using DHSVM. A statistically significant increase was detected in the POT series from 1961 - 1993 for the main stem Snoqualmie and the most heavily harvested subcatchment for those events in which snowmelt was less than 5% of precipitation. Storck et al. (1995) found that the largest changes due to vegetation harvest in the Snoqualmie basin occurred for spring peak flows, rather than Autumn ROS events. However, the Spring peak flow rate for this wes- slope Cascade Mountains basin are smaller than bankfull capacity.

The effects of timber harvest on streamflow are varied at the catchment and basin scale. Many studies have demonstrated an increase in annual water yield following forest harvest (Keppeler and Ziemer 1990, Rothacher 1965;1970, Harr et al. 1982). Statistically significant increases in peak flows have also been demonstrated (Wright et al. 1990, Jones and Grant 1996, Rosencrantz et al. 1995, Storck et al. 1995, Harr 1986). In many cases the change in peak flow response depends on antecedent snow conditions (Harr 1986, Rosencrantz et al. 1995). By effecting the volume and variability of subsurface water, forest harvest will influence the degree of subsurface flow interception by forest roads.

2.2.2: INFLUENCE OF CONSTRUCTED ROADS ON STREAMFLOW

Many of the paired watersheds used in the studies described above include the effects of forest roads, but it is difficult to segregate the effects of roads at the catchment scale. Furthermore, even in the small number of controlled experiments that do segregate road effects the period with roads alone often lasts only a few years for the obvious reason that road construction usually accompanies logging. Jones and Grant (1996) analyzed a four year period with roads alone in a small Western Oregon watershed. They found that the time to onset of storm runoff was reduced and peak flows were higher for the largest winter events in the study period. They concluded that the observed changes in peak flow found throughout the record were largely attributable to changes in flow paths due to roads (Jones and Grant 1996). Duncan (1986) examined the combined effect of harvesting and roads for the Deschutes watershed in western Washington in comparison to the relatively unlogged Naselle basin, on the southwestern Wasington coast. The Deschutes basin is approximately 429 km^2 and the Naselle basin is approximately 142 km^2. Using a linear regression of peak flow versus total storm rainfall depth, he found no time trend in the residuals for either the Deschutes or the Naselle. However, the variance in the residuals was much larger for the Deschutes, and less than half of the variance in peak flows could be accounted for by storm rainfall.

King and Tennyson (1984) monitored the effect of road construction on six forested headwater catchments in north central Idaho, ranging in area from 28 to 148 ha. Roads constituted between 1.8 to 4.3 % of the catchment areas. The annual flow variables included in the analysis were peak flow rate, instantaneous minimum flow rate, annual water yield (in mm) and the flow rate equaled or exceeded 5%, 25% and 75% of the time. A statistically significant increase in the "streamflow exceeded 25% of the time" was found in one watershed following road construction. The road in this watershed was located mid-slope with a potential for intecepting subsurface flow from a 0.5 km^2 upslope area. Intercepted subsurface flow was diverted to the stream as surface flow. A statistically significant decrease was observed in "flows exceeded only 5% of the time" in the watershed which had the highest fraction of

road area. In this case the road was located on the upper slopes of the catchment, with only 24% of the catchment area above the road. Desyncronization of the subsurface and surface water flow from different units of the watershed may have caused this decrease in flow rates (King and Tennyson 1984). For example, a decrease in soil moisture downslope of the road resulting from subsurface interception may decrease basin response at the initiation of a subsequent storm (King and Tennyson 1984).

Harr et al. (1975) found a statistically significant increase in peak flows for the Autumn and Winter period following road construction in four Oregon Coast Range watersheds. Significant increases in peak flow (20%) were observed in the basin with the highest fraction (12%) road area. Roads were separated as a treatment effect for only one season prior to forest harvest. Hydrographs were separated into quick and delayed flow following Hewlett and Hibbert (1967). The average quick flow volume decreased following road construction, with a subsequent increase in delayed flow. However, this may have been due to errors in determining runoff initiation. No consistent change in time to peak was observed.

In Ziemer's (1981) Caspar Creek study, in which approximately 5% of basin area was in roads and 10% in skid trails and landings, the percent of the treated watershed compacted by roads, landings and skid trails was the most significant independent variable for predicting annual flow volume differences between the treated and control watersheds. In contrast, Rothacher (1965) found no significant increase in annual yield after road construction alone in the H.J. Andrew's Experimental Forest. The continued persistence of the increase in annual flow volume over that of Summer low flows found by Keppeler and Ziemer was attributed to a reduction in interception losses from roads, landings and skid trails, which would not grow back, accompanied by a minimal reduction in soil moisture (Keppeler and Ziemer 1990). In the same paired catchment study, Wright et al. (1990) concluded that roads alone did not significantly affect total storm or quick flow volumes, peak flows or lag times.

Although roads alone did not significantly affect the timing of basin response, lag time was decreased approximately 1.5 hours following both road building and logging (Wright et al. 1990). The results of the Caspar Creek study suggest an enhanced contribution due to roads following logging (Ziemer 1981, Keppeler and Ziemer 1990, Wright et al. 1990). Jones and Grant (1996) also detected a synergism between forest harvest and road construction effects for two paired catchments in the H.J. Andrews Experimental Forest. This seems logical since an increase in water input to the soil following timber harvest will result in more intercepted subsurface flow. Megahan (1983) found that the volume of subsurface flow intercepted by a road cut increased by 2.5 times following clearcutting in the Pine Creek catchment in central Idaho. An increase in the quantity of intercepted subsurface flow may result in a more detectable road effect.

2.3: PREVIOUS MODELING APPROACHES

To date, studies of the effect of forest roads on streamflow have focused primarily on identification of mechanisms and detection of effects, rather than prediction. Prediction of the effects of vegetation changes through physically-based modeling has generally neglected road network effects (Storck et al. 1995, Rosencrantz. et al. 1995). Storck et al. (1995) found that observed changes in the POT series for the Snoqualmie River basin were much larger than those predicted using DHSVM. They concluded that land use effects not represented by DHSVM, such as forest roads, may be the cause.

Some modeling has been done which addresses the individual components of road network interception of subsurface flow and rainfall excess. Dunn and Mackay (1996) incorporated the effect of open ditch drainage into a physically based hydrologic model (SHETRAN). The model was first applied with a grid resolution of 100 m by 1000 m and then parameterized to run at a resolution of 1 km by 1 km. Ditches running parallel to the slope were explicitly added to the model as channel grid elements for the case of a simple hillslope. The model was forced using data from Northumberland, UK, an area of poor soil drainage and very high water tables. For these simulations an increase in ditch drainage resulted in

higher peak flows, increased water table depth and increased subsurface flow, although there was no detectable change in total runoff. The time to peak was also decreased.

The SHETRAN model was adapted to the basin scale by parameterizng the two major features of the ditch drainage: increased subsurface flow caused by head differences and increased speed of surface runoff by changes in path length and surface roughness (Dunn and Mackay 1996). Application to a 114 sq. kilometer catchment in northeast England indicated an improvement over previous model simulations.

Luce and Cundy (1994) modeled hydrographs from forest road segments with a physically based model of Horton overland flow, depression storage and routing. Infiltration parameters were fit using two different linear programming algorithms. Simulated hydrographs were compared to 92 hydrographs observed from 11 field sites in Idaho, Montana and Colorado. The two lp formulations both converged to the same set of physically reasonable parameters and were able to reasonably replicate hydrographs for other antecedent conditions and plot sizes (Luce and Cundy 1994).

Open channel ditch drainage and road surface runoff are two examples of the relatively unexplored model components which must be accommodated in a physically based hydrology model to account for road network effects. The modeling approach taken in this study is further explored in Chapter 4.

CHAPTER 3: FIELD DATA COLLECTION

3.1: BASIN CHARACTERISTICS

Field investigation of the mechanisms associated with forest road interception and routing of surface runoff was conducted in Hard and Ware Creeks, two headwater catchments of the Deschutes River in western Washington (Figure 3-1). These two adjacent catchments are separated by a steep southeasterly trending ridge and drain to the southwest. Ware Creek is 2.84 km^2 in area; Hard Creek area is 2.31 km^2. The basins are characterized by steep, v-shaped valleys, as illustrated in Figure 3-2. Elevations range between 463 - 1220 meters in Hard Creek, with slopes between 60-100%. Ware Creek is slightly lower in elevation, ranging between 457 - 1180 meters, with slopes between 40-60% (Sullivan et al. 1987). Slopes are underlain by resistant and weathered andesite, basalt and breccia bedrock. Soils are stony and shallow, averaging 0.6 meters depth in Hard Creek and 1.0 meter depth in Ware Creek. Ware Creek soils are finer textured, derived from softer, more highly weathered bedrock (Sullivan et al. 1987).

3.1.1: PRECIPITATION

Average annual precipitation measured at the lowest elevation in the basins, just upstream of the confluence of Ware Creek and the Deschutes River is 2600 mm/year. This average is relatively high for an elevation of 460 m. Comparison of Ware Creek precipitation with four regional precipitation gauges indicates that Ware Creek precipitation is much higher than other gauges in the same elevation range (see Figure 3-3). The predominant storm path across the basins is from the southwest although there is significant variability. This is evident from the frequency of the estimated 850 millibar wind direction interpolated to a point in the basins, illustrated in Figure 3-4. The high annual precipitation and predominant storm direction suggests that air masses traveling inland from the Pacific Coast have already undergone some orographic lifting to pass over previous ridges, causing relatively high

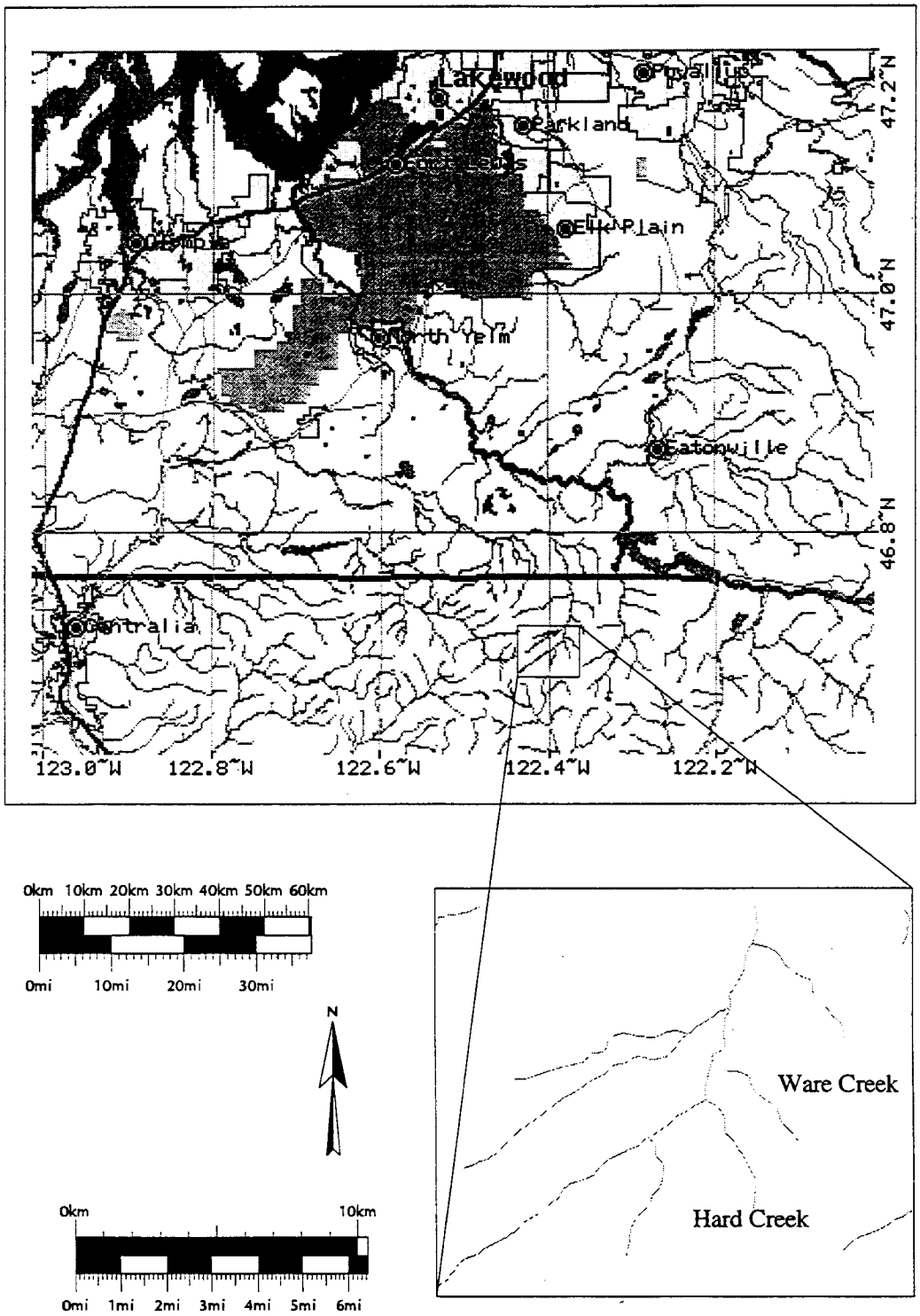

FIGURE 3-1: DESCHUTES RIVER LOCATION MAP

FIGURE 3-2: PHOTO OF HARD AND WARE CREEK WATERSHEDS
(taken from Hard Creek looking north east)

precipitation at the Ware Creek precipitation gauge. This reduces the orographic effect observed within Ware Creek itself. To investigate the effect of orographic lifting on precipitation a second precipitation gauge was installed within Ware Creek at an elevation of approximately 855 m for three months in 1996. The second gauge shows that there is some increase in precipitation with elevation, averaging 3789 mm/yr/km over the period of record. This variation within the basin can cause significant differences in storm totals. Figure 3-5 illustrates the differences in rainfall hyetographs recorded for an extreme event in February 1996. Total storm precipitation differed by 61 mm for the four day event.

The basins have a Mediterranean climate, with the greatest quantity of precipitation falling in the autumn and winter. On average, based on data from 1974 through 1993, November is the wettest month and July is the dryest month. Average precipitation by month is shown in Figure 3-6. The basins lie almost

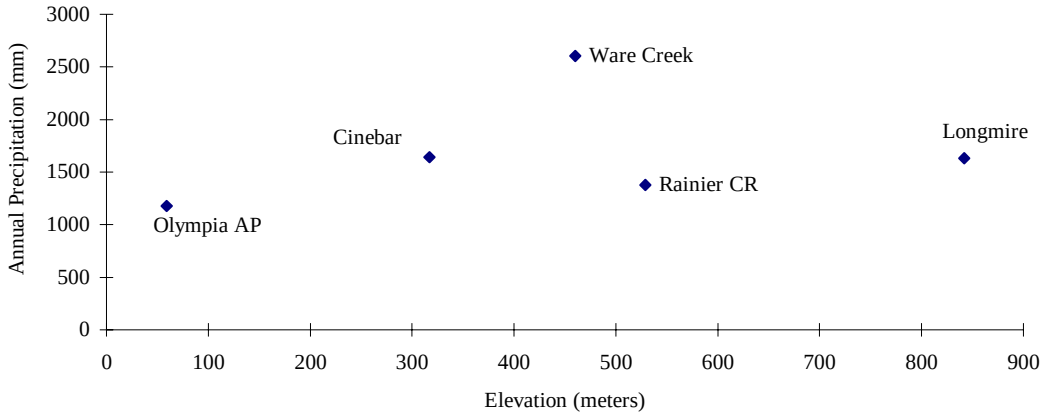

FIGURE 3-3: AVERAGE ANNUAL PRECIPITATION AT REGIONAL STATIONS

entirely within the transient snow zone, which is usually taken to be between 350-1100 meters in elevation in Western Washington. Thin snowpacks develop and melt several times throughout the winter. Snow accumulation at the basin outlet usually only amounts to a few centimeters and melts very quickly. The highest basin elevations are generally snow covered between December and March. Intermediate elevations may develop a 0.5 meter snowpack 2 to 3 times throughout the winter.

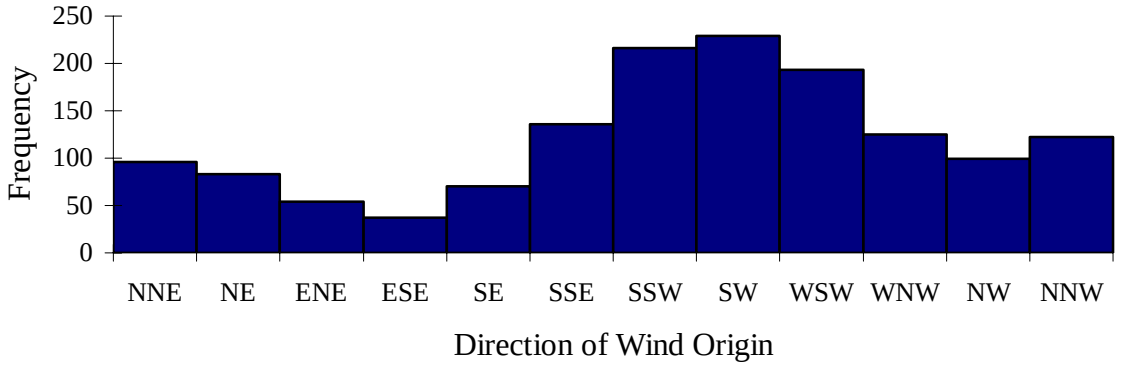

FIGURE 3-4: FREQUENCY OF 850 MBAR WIND DIRECTION FOR 1995

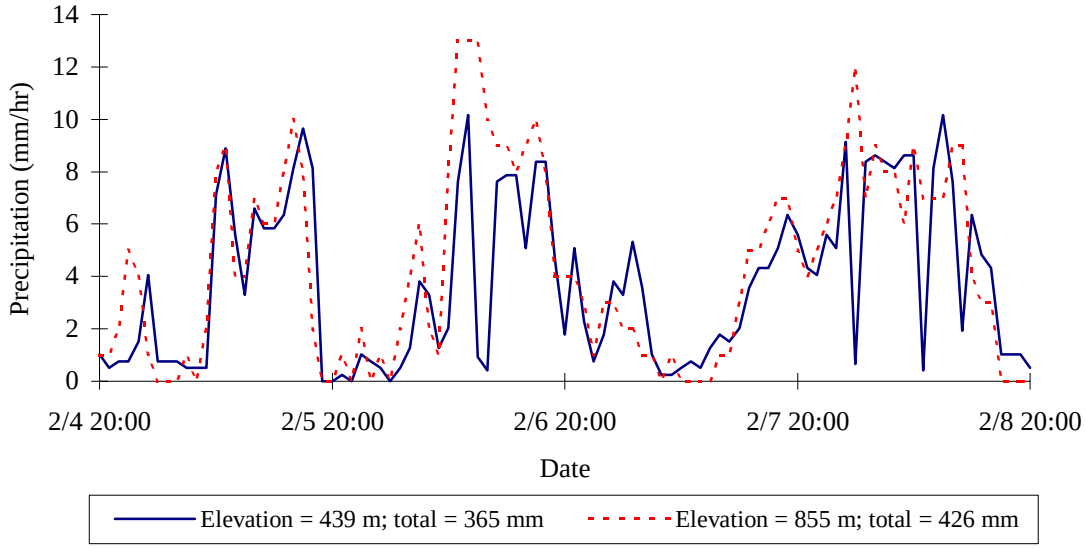

FIGURE 3-5: DESCHUTES BASIN PRECIPITATION
FEBRUARY 4 - 8, 1996

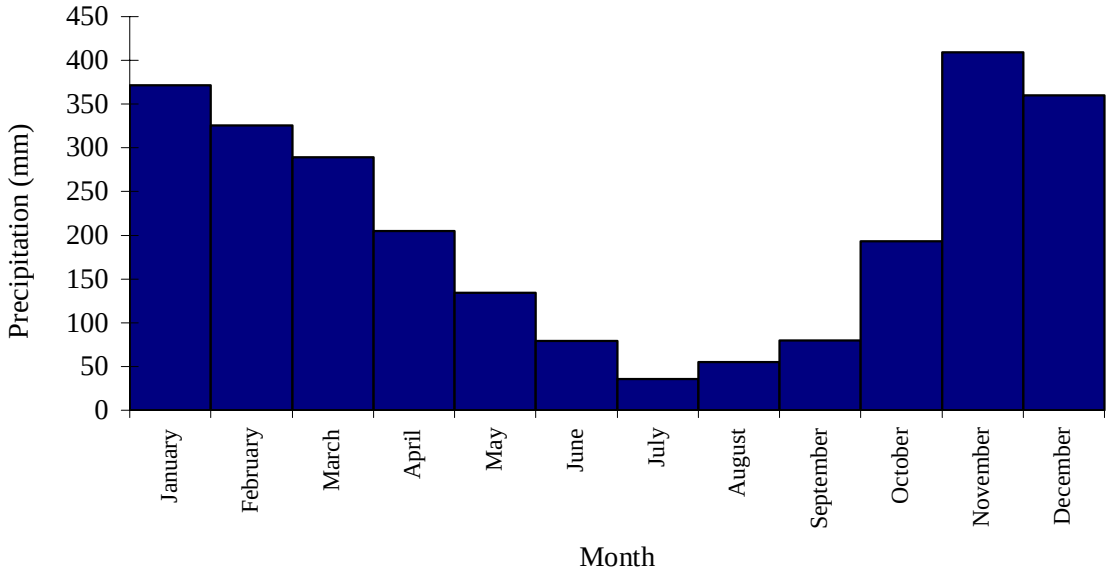

FIGURE 3-6: AVERAGE MONTHLY PRECIPITATION 1974 - 1993
WARE CREEK, WASHINGTON

3.1.2: TEMPERATURE

Average annual temperature is 2.6 ^{o}C at the base of Ware Creek and 3.0 ^{o}C at the base of Hard Creek. Air temperature measurements for 1995 are available at both the outlet of Ware Creek and the top of Cougar Mountain, the highest point in the Deschutes watershed. The data were used to investigate the change in temperature with elevation within the basins.

Air temperature in the near surface layers usually decreases with elevation. Under appropriate meteorological conditions, temperature inversions can form, causing temperature to increase with elevation. Temperature inversions are most likely to form during early morning hours under the following combination of conditions (Bras 1990):

- Clear, cloudless skies and dry air;
- Calm, stable air;
- Long nights; and
- Snow-covered ground.

Steep lapse rates generated by high air temperatures near the ground usually destroy a surface inversion before noon. As the day progresses temperature lapse rates may reach the dry adiabatic lapse rate of 10 ^{o}C/km (Linsley et al. 1982).

Inversions occur quite frequently between Ware Creek and Cougar Mountain. The frequency of inversion occurrence by month and time is summarized in Table 3-1. Temperature comparisons were made at 6-hour time intervals. Causal factors were investigated using a surrogate for cloudiness, precipitation and wind speed to predict inversion occurrence. This is described further in Chapter 5.

The observed temperature lapse rate behaves differently depending on the time of year, as indicated in Figure 3-7. During the summer months, the temperature lapse rate reaches a maximum (negative) value

of 7-8 ^{o}C/km at 6 pm. The daily Ware Creek temperature has a much larger range than the Cougar Mountain temperature. Over night, the lapse rate becomes more positive as the Ware Creek temperature deviates further below its daily mean. If the Ware Creek temperature drops far enough, a temperature inversion occurs. It is not clear why the Ware Creek temperature should vary more than Cougar Mountain. The gauge is more shielded due to both the valley location and the presence of mature forest.

TABLE 3-1: FREQUENCY OF TEMPERATURE INVERSIONS BY MONTH FOR 1995

MONTH	% OF MONTH W/ INVERSION LAYER	% OF INVERSIONS OCCURING FOR EACH TIME			
		MIDNIGHT - 6 AM	6 AM - NOON	NOON - 6 PM	6 PM - MIDNIGHT
January	20	25	25	31	19
February	39	25	30	23	23
March	31	29	29	16	26
April	18	41	32	0	27
May	29	47	42	0	11
June	23	44	37	4	15
July	21	35	35	0	30
September	35	23	23	31	23
October	31	26	29	21	24
November	23	29	29	18	25
December	31	26	26	24	24

Note:
No Cougar Mountain temperature data was available for August.

The lapse rate does not depend on the diurnal cycle during the winter months. As shown for December 1995 in Figure 3-7b, there is significantly more variability of each station relative to the other. In addition, inversions appear to be equally likely anytime of day. This seems to be because inversions may last for several days once stable conditions prevail.

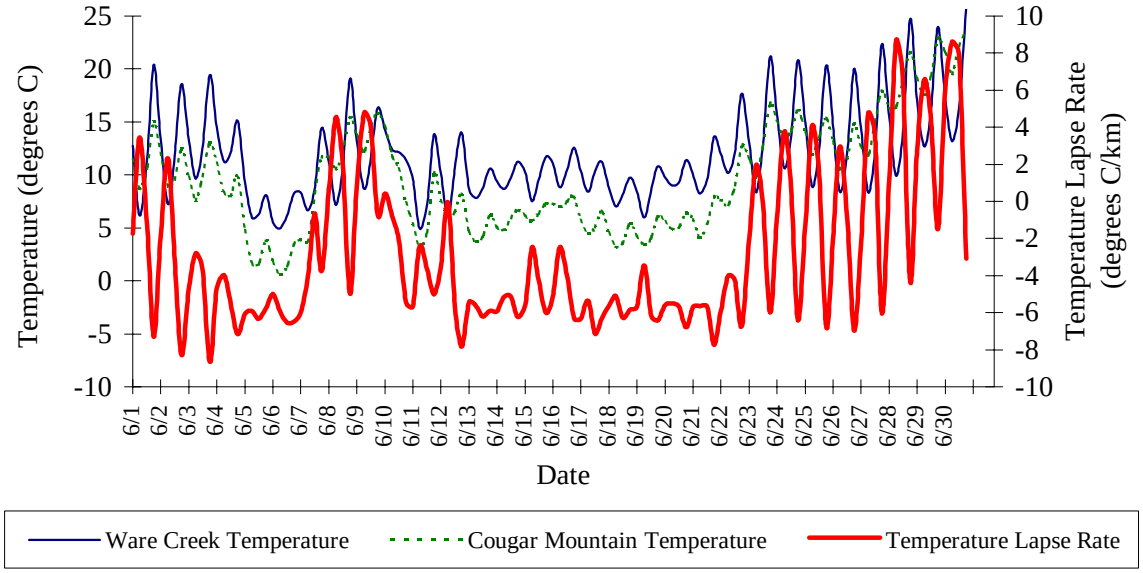

A) TEMPERATURE COMPARISON FOR JUNE 1995

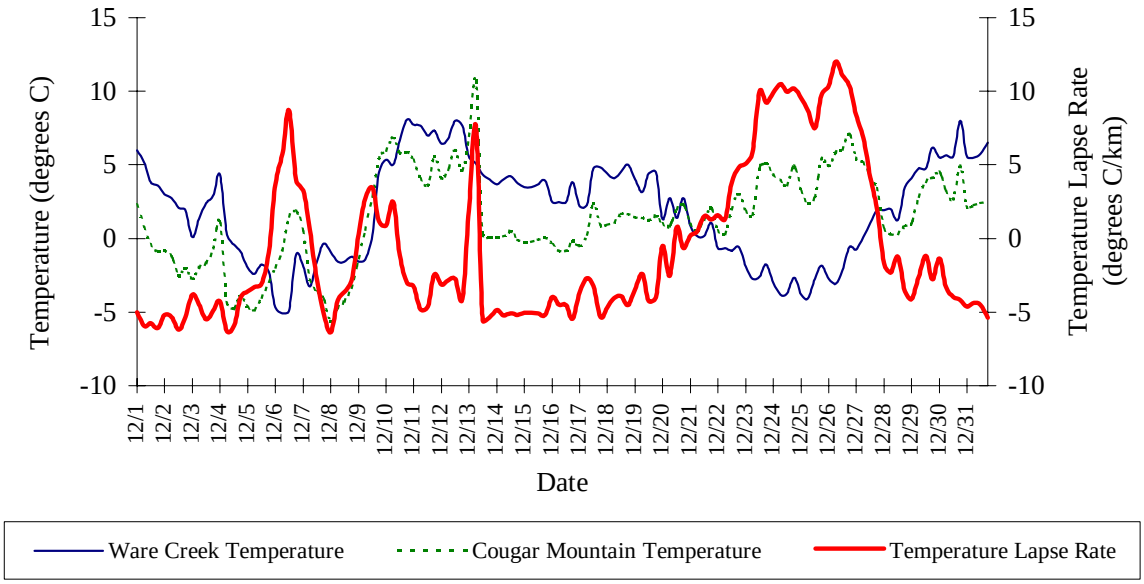

B) TEMPERATURE COMPARISON FOR DECEMBER 1995

FIGURE 3-7: TEMPERATURE LAPSE RATE COMPARISON

3.1.3: DISCHARGE

Mean annual flow is 0.19 m^3/s (0.066 $m^3/s/km^2$) for Ware Creek and 0.13 m^3/s (0.056 $m^3/s/ km^2$) for Hard Creek. The greatest quantity of runoff usually occurs in December and January for Ware Creek, in response to heavy rains coupled with snowmelt. On average, the greatest runoff in Hard Creek occurs in December. However, both basins usually have several runoff peaks throughout the rainy season. Average discharge by month for both basins for the period 1974 - 1993 is shown in Figure 3-8. For intermediate events in the fall and spring the basin responds quickly to rainfall, depending on antecedent conditions. Basin response to a typical storm occurring in October 1995 is shown in Figure 3-9a. This was the first significant storm of the season and soil moisture would have been near the seasonal low. Total precipitation between October 8th and 16th was 127 mm. Total discharge for this period was 110,000 m^3 for Hard Creek and 117,000 m^3 for Ware Creek. Time to peak for the first 16 hour burst of

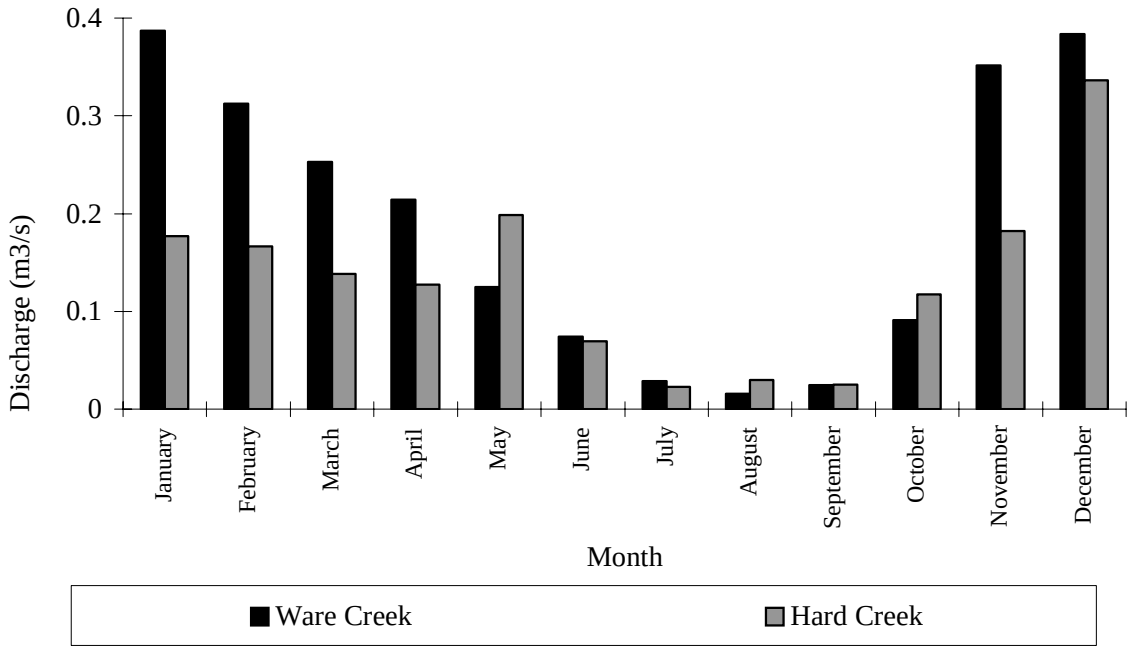

FIGURE 3-8: MONTHLY MEAN DISCHARGE, 1974-1993

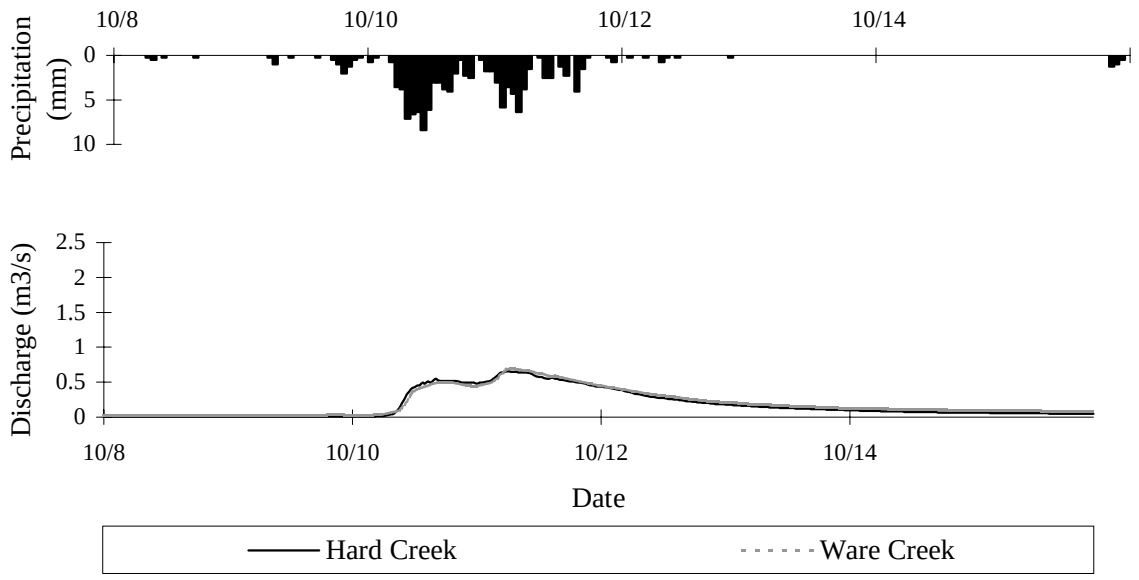

a) October 1995 Storm: Dry Antecedent Conditions

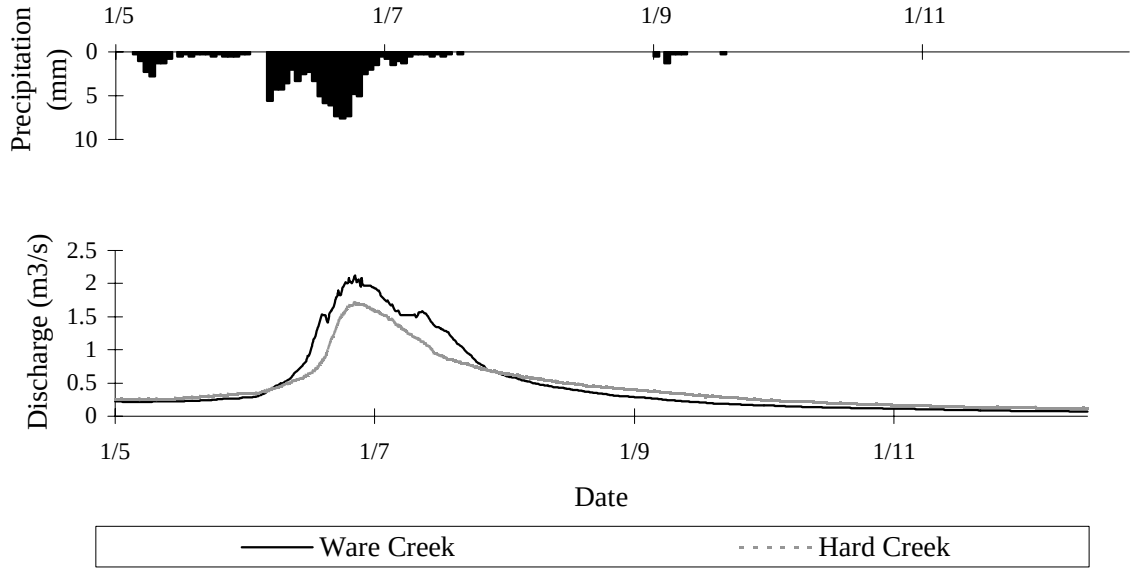

b) January 1996 Storm: Wet Antecedent Conditions

FIGURE 3-9: BASIN RESPONSE TO TWO RAIN EVENTS

rainfall was approximately 4 hours. Basin response to a similar storm occurring in January 1996 with wet antecedent conditions is shown in Figure 3-9b. Total precipitation between January 5th and January 12th was slightly lower at 112 mm. However total discharge for this period was 314,000 m^3 for Hard Creek and 306,000 m^3 for Ware Creek. Time to peak for the entire rain storm was less than one hour. It is also interesting to note that although Hard Creek is smaller in area, it has a higher discharge for the January storm. This may result from higher precipitation in Hard Creek due to its slightly higher elevation.

3.1.4: FOREST MANAGEMENT

Hard and Ware Creeks lie entirely within the Weyerhaeuser Compay's Vail Tree Farm where extensive harvesting and road construction have taken place, beginning in the 1950's. The road construction and harvest history for Hard and Ware Creeks is summarized in Table 3-2. Logging began in 1974 and continues to the present. Vegetation consists primarily of Douglas-fir (Pseudotsuga menziessii), western hemlock (Tsuga heterophylla) and Pacific silver fir (Abies amabilis). Harvested areas have been replanted with Douglas-fir, but regrowth has been limited in many areas. A rich understory of meadow grass and bushes has developed in these areas (see Figure 3-10).

TABLE 3-2: HARD AND WARE CREEKS LAND USE HISTORY

	WARE CREEK	HARD CREEK
Basin area	2.8 km^2	2.3 km^2
Road construction	1975 - ??	1977 - 1980
Total road length	10.7 km	11.4 km
Harvesting	1979 - present	1984 - present
Harvested area (estimated)	66 %	35 %

The majority of road construction in Ware Creek was conducted between 1975 and 1984 (Sullivan et al. 1987). However, an additional 2.3 km of road were constructed at an unknown time between 1987 and 1995. The length of roads constructed over time is illustrated in Figure 3-11. Roads were constructed

by cut and fill. Excavated material from the road cut is used as the foundation for part of the road bed. Construction of roads in such steep terrain requires considerable excavation to produce a road surface of required width, and cutslopes are therefore quite high in some places. Cutslopes range in height from 0 meters on the ridgetop roads to over 10 meters for midslope roads, as shown in Figure 3-12. In many cases the cut intercepts the entire soil column, and vertical bedrock forms the roadcut in many places.

FIGURE 3-10: PHOTO OF REGENERATING CLEAR-CUT IN WARE CREEK
(looking west, showing a hillslope across the Descutes valley in the background)

Continuous seepage of subsurface flow is visible in many parts of the basin. Unweathered bedrock outcrops often have a moist face with seepage visible between cracks. Based on observation alone, a larger volume of subsurface flow seems to be intercepted in zones of locally deep soil. Macropores appear to be the main mechanism for transport of this subsurface water and several different points of exfiltration can be observed on exposed sandy banks.

Ditches are lined with either very coarse rock fragments or vegetation. Infiltration rates are very high in the crushed rock and intercepted subsurface flow often infiltrates into the ditch between storms. As in most forested catchments in the Pacific Northwest, surface overland flow is limited on the hillslopes. However, it is common for flow to concentrate in the top few inches of soil just below the root mass in clearcut areas. Runoff travels in this surface zone and accumulates in small topographic depressions. The subsurface stream is typically audible beneath the tangle of roots and surface vegetation, but it is not visible from the surface. These subsurface streams of water emerge from the cutslope just below the vegetation layer and are subsequently routed through the ditch drainage network. This phenomenon was only witnessed in clear cut areas.

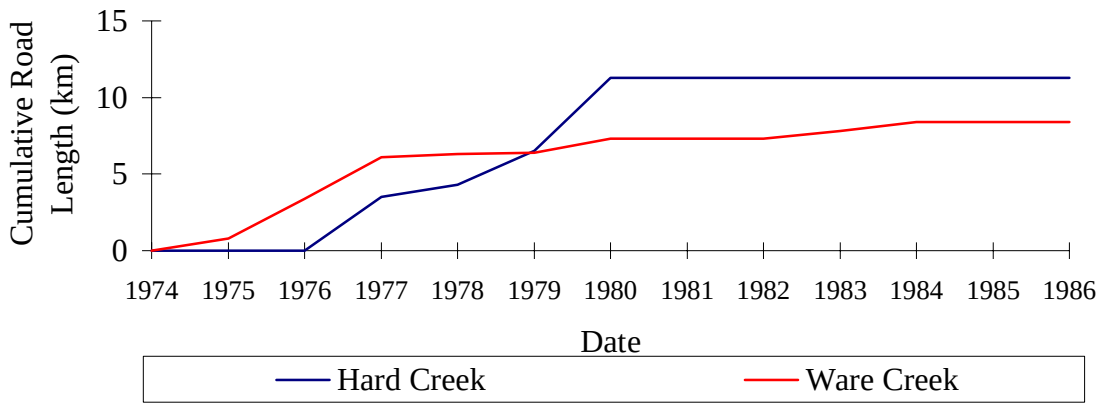

FIGURE 3-11: CUMULATIVE ROAD LENGTH CONSTRUCTED IN EACH BASIN, BY YEAR

3.2: STUDY SITE SELECTION

Peak culvert discharge was measured for thirteen road segments within the Hard and Ware Creek basins. Road segments were selected based on characteristics considered most influential to generating a road segment response, including:

- Hillslope position and elevation;

FIGURE 3-12: TWO EXAMPLES OF EXPOSED CUT SLOPES

- Soil depth and bedrock condition; and
- Vegetation treatment above the road segment.

The cross-section of characteristics of the chosen locations are summarized in Table 3-3. The location of monitored culverts and the area contributing to each are shown in Figure 3-13. Contributing areas were calculated by delineating the upslope portion of land draining to each monitored road segment. Delineations were performed by hand in Arc/Info (Geographic Information System software produced by the Environmental Systems Research Inc.) using elevations from a 30 meter resolution digital elevation model (DEM). Using this technique the boundary of the contributing area is most likely placed within the correct 30 m pixel. Therefore, the most error in this technique comes from placement of the boundary of the contributing area within the pixel. The placement of the boundary within the pixel may be off by up to one half the pixel width. Assuming that the boundary was placed in the correct pixel, this could result in an error in the contributing area by up to one-quarter the pixel area or 225 m^2 for each border pixel. The contributing area and the road length draining to each culvert are summarized in Table 3-4. An estimate of the range in error associated with the contributing area calculation is also included in Table 3-4.

Crest recording gauges were constructed at the entrance to twelve culverts. The gauges consisted of a 4" (10.2 cm) diameter stilling well and inlet pipe, as shown in Figure 3-14. Peak stages were measured using floating cork and were recorded periodically from January - May 1996. Stage was measured as the distance from the top of the gauge to the uppermost cork line. These values were later transformed to stage above the culvert lip by subtracting them from a measured base distance between the culvert lip to the top of that gauge. The discharge rate was measured in triplicate for different stages by timing and capturing the discharge from the culvert outfall in a five gallon bucket. The stage-discharge curve for each culvert type was derived using a combination of field measurements and experimental results from

TABLE 3-3: CHARACTERISTICS OF ROAD SEGMENTS SELECTED FOR MONITORING

	HILLSLOPE POSITION			UPSLOPE VEGETATION		SOIL CHARACTERISTICS			PREDOMINANT RUNOFF MECHANISM			CUT SLOPE HEIGHT		
	BASE	MID	TOP	IMM.	MATURE	SOIL	SOIL/BED	BED.	ROAD	SUB	BOTH	< 10 FT	10-20 FT	> 20 FT
H007	X			X				X	X					X
H010			X		X	X			X					X
H018	X				X	X					X		X	
H023		X		X		X				X				X
H028		X			X			X			X		X	
H042	X				X		X			X			X	
H046		X			X		X				X		X	
W014		X		X			X				X		X	
W018		X		X			X			X		X		
W029		X		X		X			X				X	
W032	X			X				X			X			X
W038			X	X		X				X		X		
W053			X	X			X			X			X	

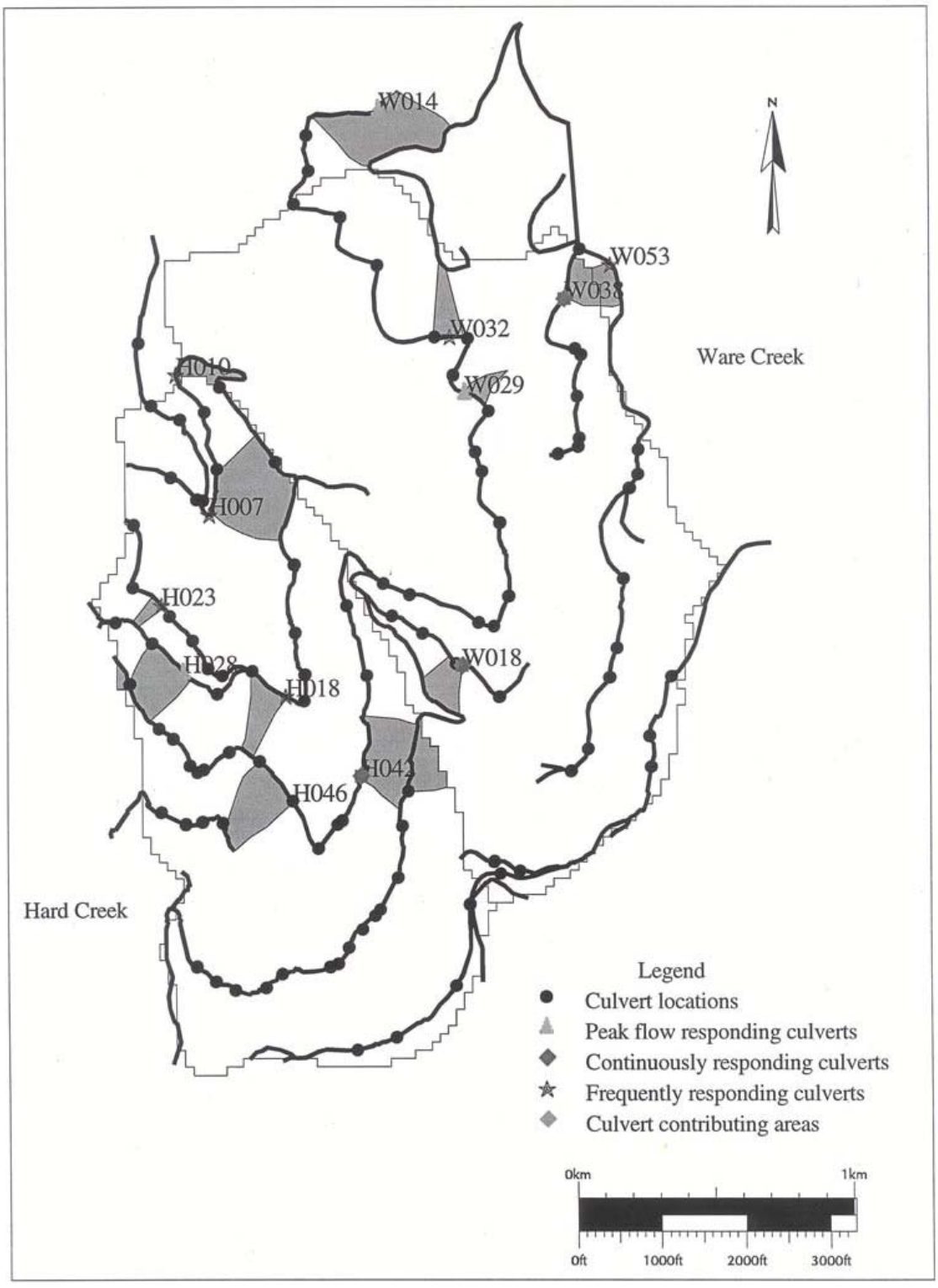

FIGURE 3-13: CULVERT LOCATIONS AND CONTRIBUTING AREAS

TABLE 3-4: CULVERT CONTRIBUTING AREAS AND ROAD LENGTHS

CULVERT ID	CONTRIBUTING AREA		CONTRIBUTING ROAD LENGTH (M)			
	AREA (HA)	ERROR (HA)	TOTAL	INSLOPED	OUTSLOPED	CROWN
H007	7.67	0.60	164.4	85.9	78.5	0.0
H010	1.17	0.22	344.3	165.5	50.3	128.5
H018	2.27	0.72	160.9	93.5	10.1	57.3
H023	0.49	0.22	16.1	16.1	0.0	46.9
H028	3.89	0.54	202.8	77.4	59.8	65.6
H042	6.93	1.04	260.5	82.5	104.6	73.4
H046	4.22	0.68	189.4	98.3	0.0	91.1
W014	7.27	0.72	147.8	115.8	0.0	32.0
W018	1.99	0.40	347.3	-	-	-
W029	0.75	0.40	92.0	23.8	14.9	53.3
W032	1.77	0.76	111.6	38.4	52.1	21.1
W038	1.54	0.40	150.0	0.0	78.7	71.3
W053	1.09	0.40	191.6	0.0	0.0	191.6

the Federal Highway Administration (FHA) (Normann et al. 1985). Ditch relief culverts in Hard and Ware Creeks are corrugated metal. They generally have a pool of water at the upstream end and a free fall at the culvert outlet, so there is no backwater influence on the water surface profile within the culvert. Culvert slopes are hydraulically steep, ranging between 0.02 and 0.14 for the monitored road segments. These conditions create an inlet-controlled situation, so discharge can be estimated from the head at the culvert inlet. For each of the monitored road segments, the pool in front of the culvert was enlarged and deepened when the crest gauge was installed. Sediment was removed from the pool periodically, after large storms. Nevertheless, the pools did tend to fill again rapidly. For the range of stages measured in Hard and Ware Creeks, velocities in the roadside ditch were generally low and were further damped by the pool at the inlet to each culvert. Therefore, the velocity head of the pool can be neglected, and the headwater depth at the culvert inlet, *HW*, is equal to the stage above the lip of the culvert pipe.

FIGURE 3-14: EXAMPLE CREST-RECORDING GAUGE

The FHA has developed guidelines for the hydraulic design of highway culverts based on laboratory experiments to determine culvert diameter and entrance type based on design discharges (Normann et al. 1985). Culvert entrance types include headwall, projecting or mitered to conform to slope. For a known entrance type and culvert diameter, the normalized headwater depth over diameter can be used to determine the discharge in cfs from the design table for a corrugated metal pipe with inlet control (see Figure 3-15). However, since this table was derived for design considerations, it is concerned with maximum discharges and does not extend low enough for most of the field observations in Hard and Ware Creeks. It was therefore necessary to extrapolate below the end of the discharge and HW/D lines shown in Figure 3-15.

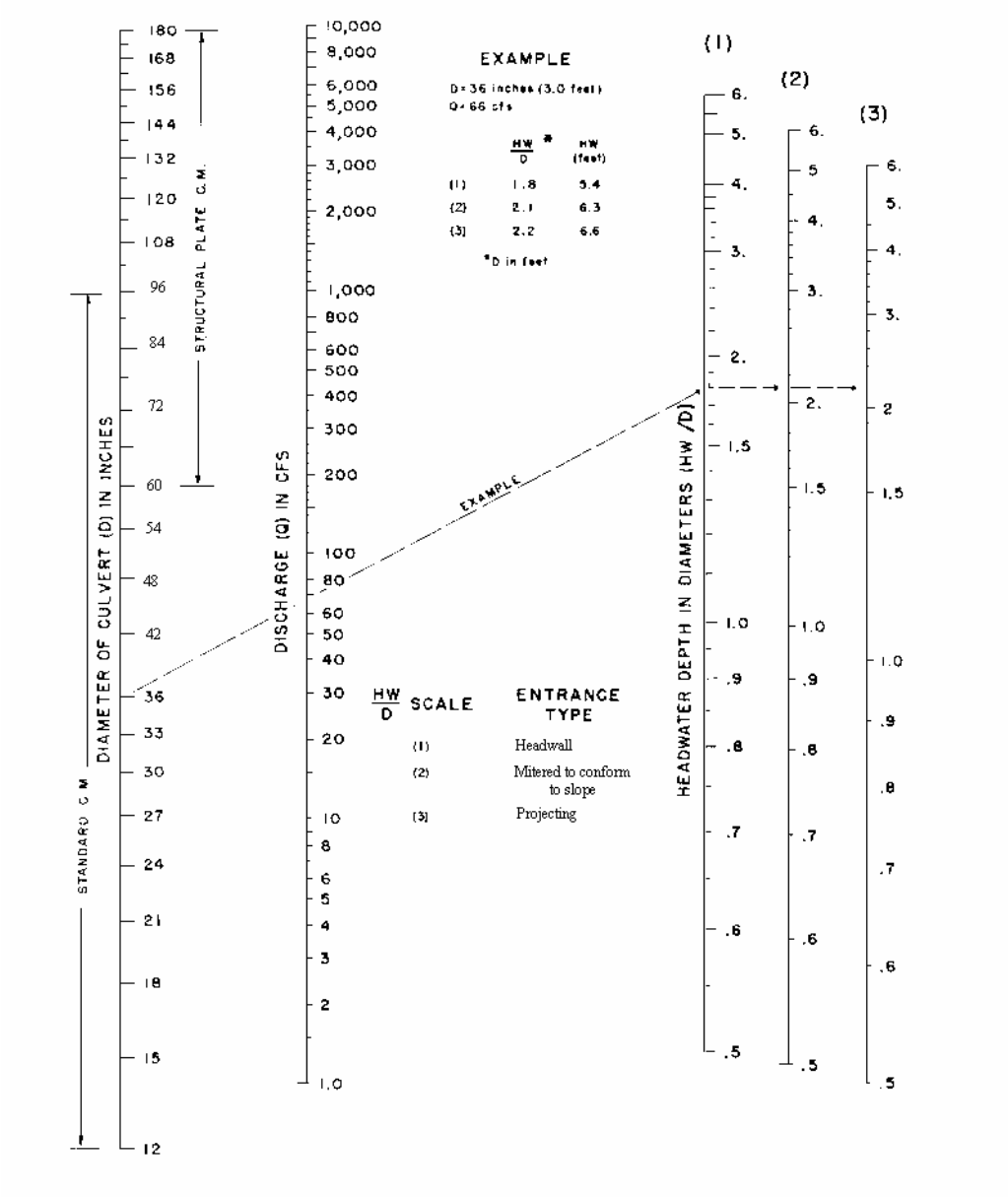

FIGURE 3-15: HEADWATER DEPTH FOR CORRUGATED METAL PIPE CULVERTS WITH INLET CONTROL

(from Normann et al. 1985)

The space between each 0.5 increment on the HW/D line in Figure 3-15 was found to follow a exponential profile, of the form:

$$y = ce^{bx} \quad \textbf{3-1}$$

An exponential profile was fit to the incremental distances (in mm) between values of headwater depth over diameter for the headwall and projecting entrance types, as shown in Figure 3-16. The parameters of the derived curves, *c* and *b*, are given in Table 3-5. The incremental distance in mm between each 0.5 cfs on the discharge line was found to fit a power curve, according to:

$$y = cx^{b} \quad \textbf{3-2}$$

The fitted profile is shown in Figure 3-17 and the parameters are given in Table 3-5.

TABLE 3-5: CURVE-FITTING PARAMETERS

DESCRIPTION	PROFILE	C	B
Headwall HW/D	Exponential	32.78	-2.009
Projecting HW/D	Exponential	26.52	-1.729
Discharge	Power	11.71	-1.098

The 12 monitored ditch relief culverts were grouped into one of four categories:

- 18” projecting entrance;
- 18” headwall entrance;
- 15” projecting entrance; and
- 15” headwall entrance.

The characteristics of each of the monitored culverts are summarized in Table 3-6. In some cases, the culvert entrance has been damaged and is no longer round. The original pipe diameter was used in these cases, but the entrance conditions will impose some error on the observed discharge. The fitted profiles of incremental distance were used to extrapolate discharge from Figure 3-15 down to HW/D values of

0.2. Discharge values from the expanded chart were plotted in conjunction with observed values of stage and discharge for each of the four culvert categories. A polynomial was fitted to each of these values to obtain a stage discharge curve for each culvert class. The fitted stage-discharge curves are shown in Figure 3-18. Discharge for recorded peak stages was obtained by reading from the derived stage-discharge curves. No observations of peak stage exceeded the height of the culvert.

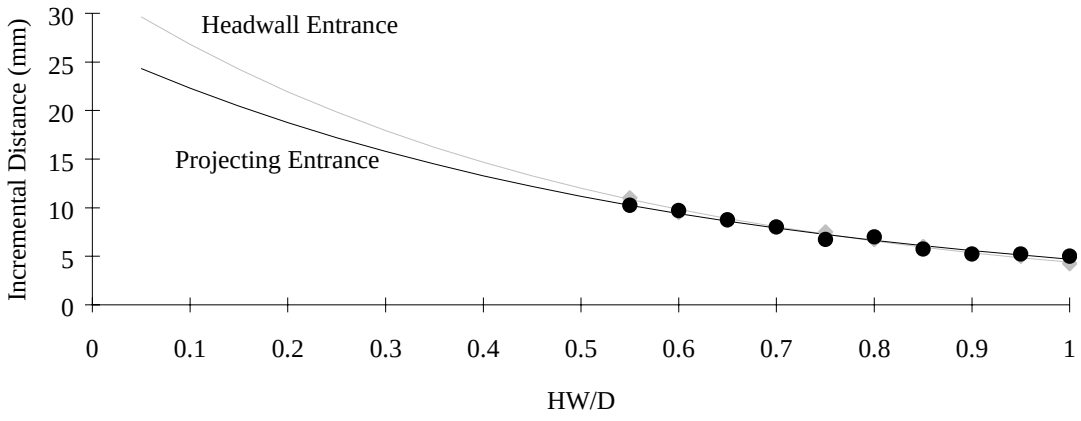

FIGURE 3-16: EXPONENTIAL PROFILE OF INCREMENTAL DISTANCE BETWEEN MEASUREMENTS OF HW/D

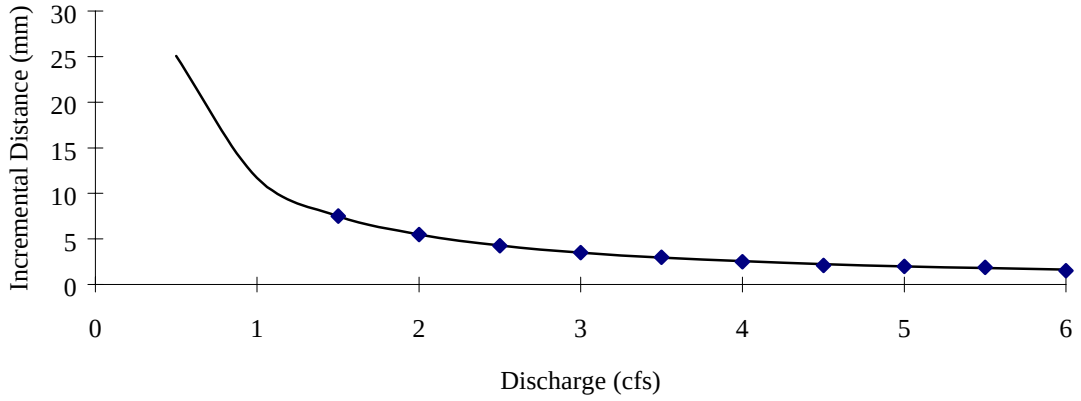

FIGURE 3-17: POWER PROFILE OF INCREMENTAL DISTANCE BETWEEN MEASUREMENTS OF DISCHARGE

TABLE 3-6: DISCHARGE CALCULATION PARAMETERS

CULVERT ID	ENTRANCE TYPE	SLOPE	PIPE DIAMETER (INCHES)	BASE DISTANCE (INCHES)
H010	Headwall	0.02	15	21.13
H018	Headwall	0.02	15	22.50
H023	Projecting	0.14	18	22.60
H028	Projecting	0.07	18	21.69
H042	Headwall	0.07	15	24.56
H046	Headwall	0.02	18	23.13
W014	Projecting	0.05	15	16.81
W018	Headwall	0.04	18	19.88
W029	Headwall	0.02	18	22.88
W032	Projecting	0.02	18	24.88
W038	Projecting	0.05	15	20.40
W053	Headwall	0.06	18	21.06

Notes:

Base distance is the distance from the top of the crest-recording gauge to the culvert lip. It is used to adjust the measurements of stage (measured from the top of the gauge to the cork line) to height above the culvert lip.

Sharp-crested V-notch box weirs were constructed on either side of a thirteenth road segment to segregate subsurface and road surface runoff. One weir captured runoff generated by the road surface. The other captured primarily subsurface flow captured by the roadside ditch.

Discharge through a weir can be calculated according to:

$$Q = C_d \tan\left(\theta/2\right)\sqrt{g}H^{5/2} \qquad \textbf{3-3}$$

Where θ is the notch angle and H is the head above the crest of the v-notch. C_d is the discharge coefficient, taken to be 0.44 for a v-notch weir meeting prescribed geometry guidelines (Leupold and Stevens 1978). These guidelines specify that the width on either side of the notch should exceed twice the maximum head above the weir crest. In addition, the height of the weir crest above the bottom

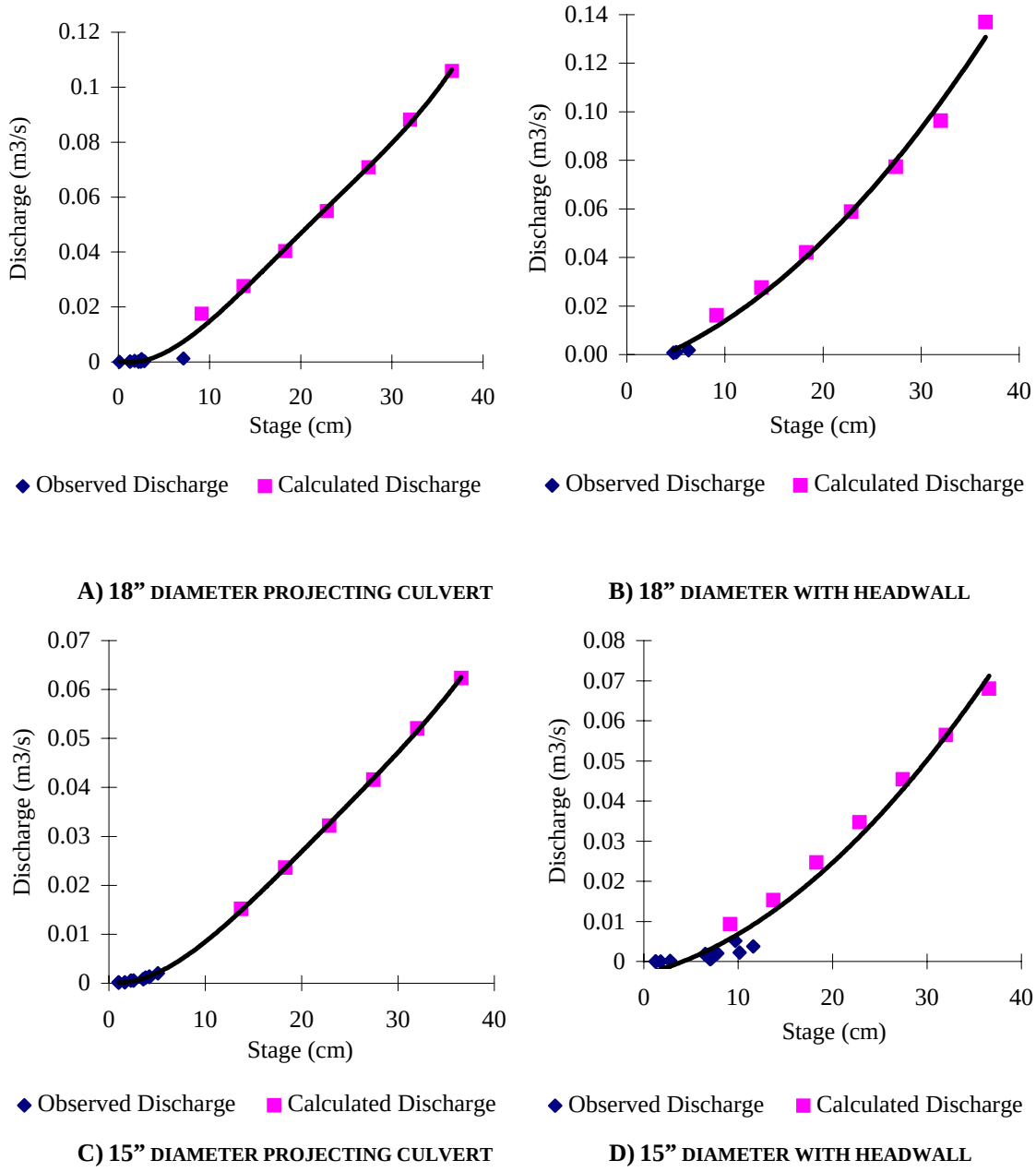

FIGURE 3-18: STAGE DISCHARGE CURVES

Note: Observed discharge measured on field visits by timing discharge captured at the culvert outfall in a five-gallon bucket. Measurements were made in triplicate and averaged.

should exceed twice the maximum head above the weir crest, as illustrated in Figure 3-19. The completed weir dimensions are also given in Figure 3-19. As can be seen from this figure, the weir height does not exceed twice the head for the highest observed flows. This may result in a departure from the theoretical equation for these flows. No values for observed discharge are available for comparison. Due to the low velocity of the observed flows, the departure should be small, and the theoretical equation was used for calculations of weir discharge.

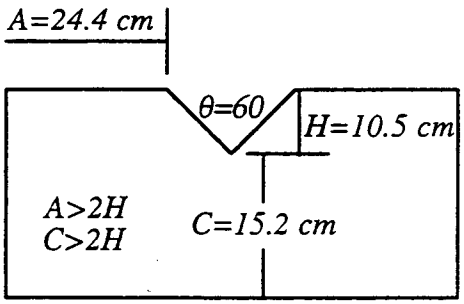

FIGURE 3-19: WEIR CROSS-SECTION

3.3: ROAD MONITORING RESULTS

Crest recording gauges were installed in early January 1996. Peak stage during the interval from the previous observation and stage at the time of observation were recorded approximately once per week from January - June, weather permitting. All sites were inaccessible for much of January due to snow. Sites were also inaccessible the second week of February due to numerous road failures following a large storm February 5-8, 1996.

Based on these observations the 13 monitored road segments can be divided into the following three categories:

- Class 1: Peak flow responding culverts: Segments W014, W029 and H028;
- Class 2: Continuosly responding culverts: Segments H042, W018 and W038; and
- Class 3: Frequently responding culverts: Segments W032, W053, H010, H018, H023 and H007 (weir location).

Culvert H046 never registered a response. In addition, the weir designed to capture subsurface flow never registered a response above the weir crest. This was most likely due to infiltration losses from the bottom of the gauge. The peak flow responding segments only registered stages above zero for the 2 or 3 largest storms over the period of record. Frequently responding road segments registered discharge for most rainfall events, but would dry out after a period with no precipitation. Continuously responding road segments received continuous subsurface flow throughout the summer after long periods with no precipitation. Each of these categories is explored further below.

3.3.1: PEAK FLOW RESPONDING CULVERTS

The characteristics of the three culverts which only respond to extreme rain events do not lead to a simple explanation. Culvert W014 has the second largest contributing area, W029 has the smallest and H028 has an average contributing area. The recorded peak flow responses normalized by contributing area for culverts W014, W029 and H028 are shown in Figure 3-20. As shown in Table 3-4, the error associated with delineation of the contributing areas is high. Recorded peak stages were assumed to occur on the date of maximum daily rainfall since the last recorded stage. Significant peak stages were recorded for these culverts for the two largest storms over the period. The first storm occurred from February 5-8. Total precipitation for the four day event was 365 mm. Less than one-third of the total precipitation of the February storm, 148 mm, fell during the second storm between April 22-24.

Culvert W014 is located in a small topographic hollow covered in mature forest. In addition, the ditch leading to the culvert receives some runoff from the road surface. There is a large depression directly in

front of the culvert mouth that is often damp. This depression is overgrown with skunk cabbage (Lysichitum americanum) during the spring and summer. It appears that this area must allow any surface runoff to infiltrate and travel as subsurface flow under the road surface for moderate rain storms. For extreme events, the soil matrix becomes sufficiently saturated that surface runoff can no longer infiltrate and is forced to travel through the road culvert.

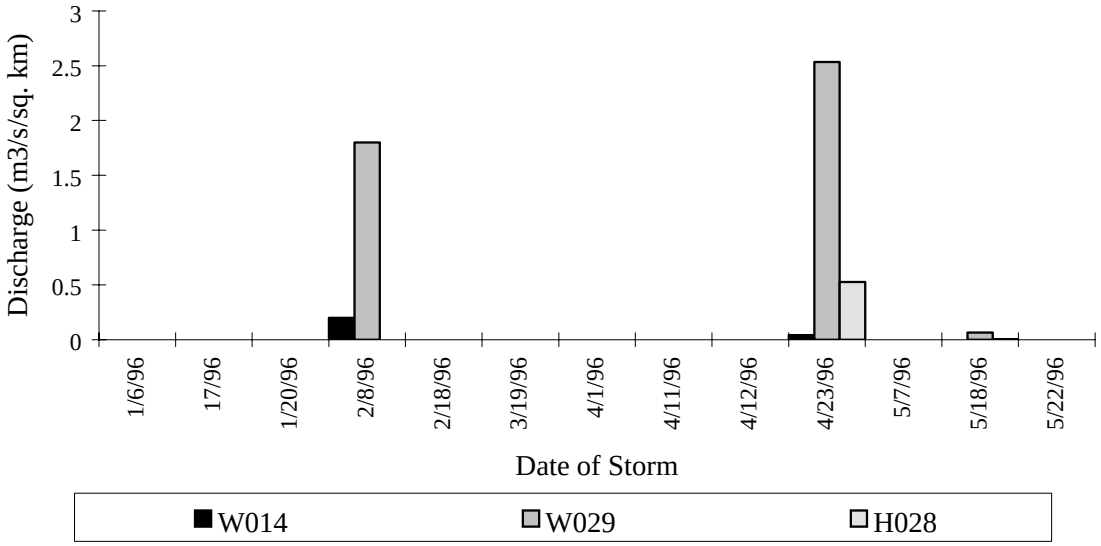

FIGURE 3-20: PEAK DISCHARGE FOR PEAK FLOW RESPONDING CULVERTS

In contrast, Culvert W029 is located on a straight hillslope with an exposed, loose sand cutslope approximately 3 meters tall. Seepage was never observed from this slope. The road segment adjacent to this culvert is part of a long straight stretch with very little lateral slope. Surface runoff is routed along the road surface which is evident from surface erosion and gullies. Many prominent new gullies were formed following the February storm which directed much of the surface runoff over the side of the road onto the fillslope. The location of the surface channels was observed to change over the season, possibly increasing the fraction of surface runoff diverted to the roadside ditch. Thus, the increase in response for this culvert for the April storm may be a result of changing surface runoff patterns. In addition, the cork line from which peak stage is read was scattered and unclear following the February storm. This may be

due to several fluctuations in the peak flow over a period of hours. In any case, the peak discharge recorded for the February storm may be inaccurate.

The gauge at Culvert H028 was not operating correctly for much of the season, including the February storm, so it is not clear if this segment will only respond to peak flows. Culvert H028 also showed a low response for a much smaller rain event on May 18th (37 mm total precipitation). The roadside ditch draining to this culvert does not receive significant road surface runoff. Subsurface seepage was observed emerging from a fractured bedrock outcrop directly above the culvert mouth. This small seepage stream flows to a large rock-lined area in front of the culvert and often infiltrates. Therefore, the response could be controlled by the same mechanism as Culvert W014.

3.3.2: CONTINUOUSLY RESPONDING CULVERTS

Culverts H042, W018 and W038 showed a peak response for almost every observation period and discharge frequently continued over extended dry periods. Figure 3-21 illustrates observed and peak discharge over time for each of these culverts. Although the general pattern of response is similar, there are several important differences in how these road segments respond to rainfall events.

Culvert H042 is located in an area of mature forest just below a slight topographic hollow. The cutbank varies from 3 to 6 meters in height and is composed of a mixture of bedrock, exposed soil and vegetation. It has a large upslope contributing area, but receives negligible road surface runoff. A steady flow of water was first observed to be seeping from a fractured bedrock outcrop just above the culvert. The observed seepage was later traced to a small stream that begins approximately 100 meters up the hillslope and flows over the exposed bedrock of the cutslope. There is no clearly defined incised channel for this surface flow. The discharge from this culvert appears to be consistent with the rainfall record and was never observed to be completely dry.

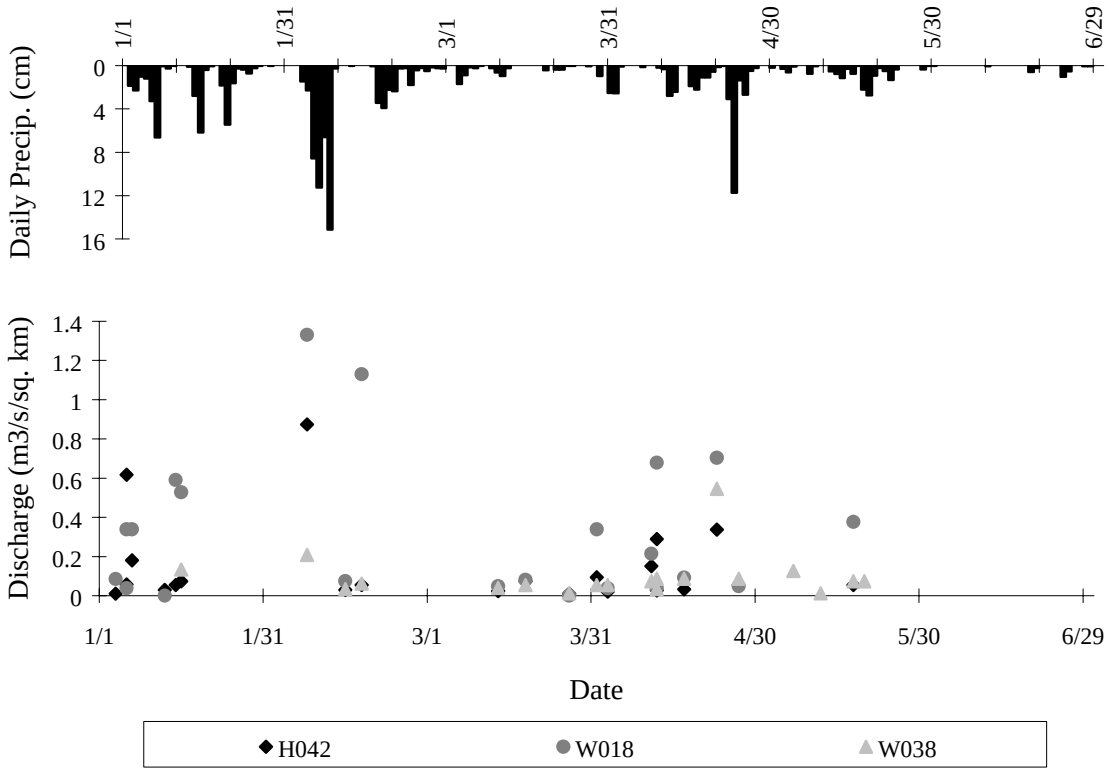

FIGURE 3-21: DISCHARGE VS. TIME FOR CONTINUOUSLY RESPONDING CULVERTS

Culvert W018 is located on the opposite side of the ridge from Culvert H042. It is clearcut upslope with very little overstory regrowth. The cutbank is composed of unvegetated loose, sandy soil, approximately 5 meters deep. Several macropores are visible which seep constantly. Subsurface flow is captured by the roadside ditch all along the exposed face. The road segment is fairly flat with many holes and depressions and no clearly defined lateral flow direction. It appears that precipitation from most moderate events pools on the road surface and eventually infiltrates. The contributing area for this culvert is approximately 2 ha. This is the constant area threshold which was found to be appropriate for stream initiation when concentrated at a point in the Hard and Ware Creek watersheds, as described in Chapter 4. Given this information it is not surprising that a roadside ditch which is able to capture the distributed flow from this subsurface area is found to contain discharge most of the time.

Culvert W038 is located at a similar elevation to Culvert W018 on the opposite side of the Ware Creek basin. However, this segment is closer to the ridgetop and in a much more exposed location. The aspect of the road segment is almost due west and it always seems much windier at this site. The contributing area is clearcut although smaller than the contributing area for W018. As would be expected, Culvert W038 had a consistent but somewhat smaller response than Culverts H042 and W018 up until the April 22nd storm. Following that event, it responds significantly more for the April storm and two subsequent peaks than Culvert H042.

3.3.3: FREQUENTLY RESPONDING CULVERTS

The remaining group of respond frequently to moderate rainfall events to channel runoff efficiently from the road and ditch. However, they do not continue to flow for a significant time following precipitation events.

To investigate the role of physical factors on the effect of roads on watershed function, the flow response from these culverts was analyzed according to hillslope position, soil depth, age of upslope vegetation and predominant runoff mechanism. Normalized peak flow response according to hillslope position is shown in Figure 3-22(a). From this figure it appears that the largest peaks are often associated with culverts located at the bottom and middle of the hillslope, although there is not a consistent trend. It is logical that the trend is insignificant since the discharge data are already normalized by the contributing area.

Figure 3-22(b) shows the flow response according to upslope vegetation age. In this case, all of the largest peaks were recorded for road segments below immature forests. This reflects the importance of antecedent conditions on subsurface flow generation. Increased soil moisture for the clear-cut plots may have made these segments more responsive to precipitation events.

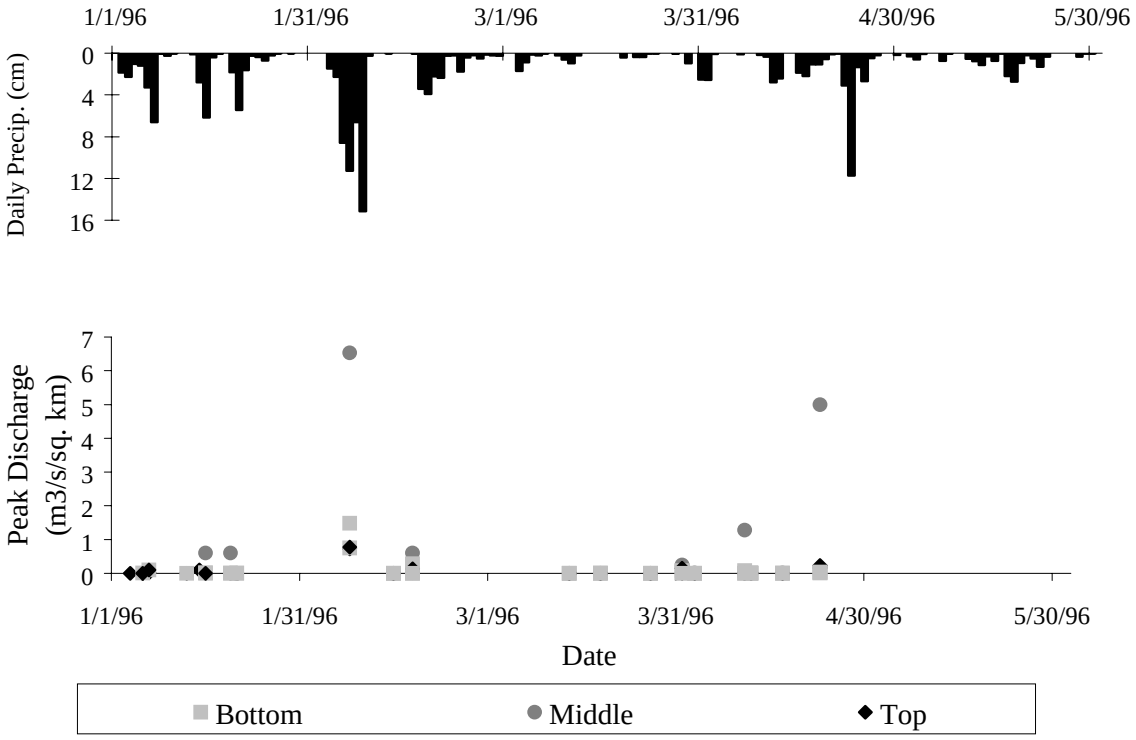

A) PARTITIONED BY HILLSLOPE POSITION

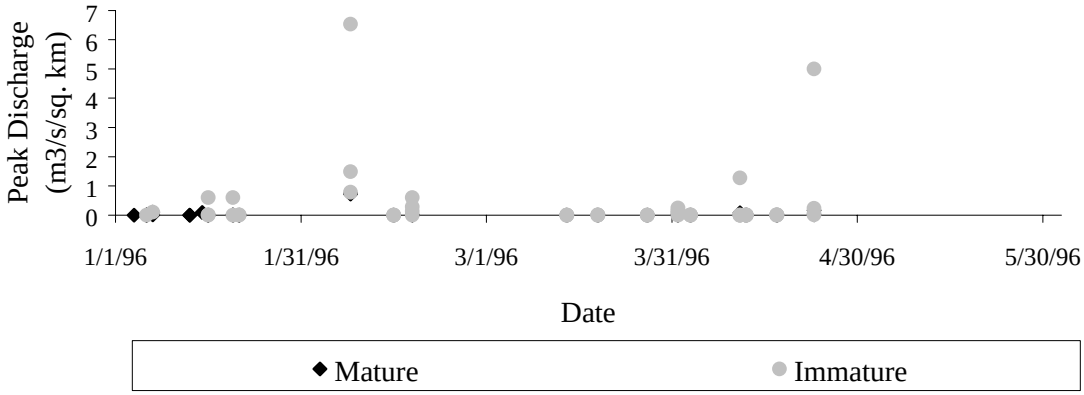

B) PARTITIONED BY UPSLOPE VEGETATION

FIGURE 3-22: PEAK FLOW RESPONSE FOR FREQUENTLY RESPONDING CULVERTS

Figure 3-23(a) shows the relationship between soil type and segment flow response. This figure indicates that the largest observed discharges are associated with regions of deep soil. This seems consistent with observations. The exposed soil slopes appear loose and porous, with many visible macropores. In many locations the bedrock appears fairly dense, with large spaces between fractures. There is one large discharge value associated with dense bedrock. This culvert drains two rock outcrops divided by a slight depression and tallus slope. There is evidence of a past slope failure in the tallus region. The high peak discharges associated with this site may indicate the development of surface flow in this region under saturated conditions.

Finally, the relationship between road runoff mechanism and peak discharge is illustrated in Figure 3-23(b). For only one rain event is the largest observed discharge associated with road runoff alone. The magnitude of the response from the road surface is limited by the contributing length of road. Since the roads in Hard and Ware Creeks are steep and curvy, the lateral road slope changes frequently. Surface road runoff is often directed over the side of the road, decreasing the peak concentrated flow observed at the culvert. The mechanism for the highest flows is split fairly evenly between road segments with subsurface contribution alone and segments with both subsurface and surface runoff components. This is likely dependent on the timing and magnitude of the precipitation event. For extended storms such as the February event, several days of rain created saturated conditions and initiated subsurface flow. When the highest intensity rain fell on February 8th the nearly instantaneous runoff from the road surface coincided with the subsurface response, creating a larger peak flow. For shorter events, the subsurface and surface responses may be offset, creating responses of similar magnitude among culverts receiving subsurface flow alone and culverts receiving both subsurface and surface flow.

3.3.4: EXTREME STORM EVENTS

Two significant storm events occurred during the study period which merit closer examination. The February 1996 event caused flooding in Oregon and the southern third of Washington State. The

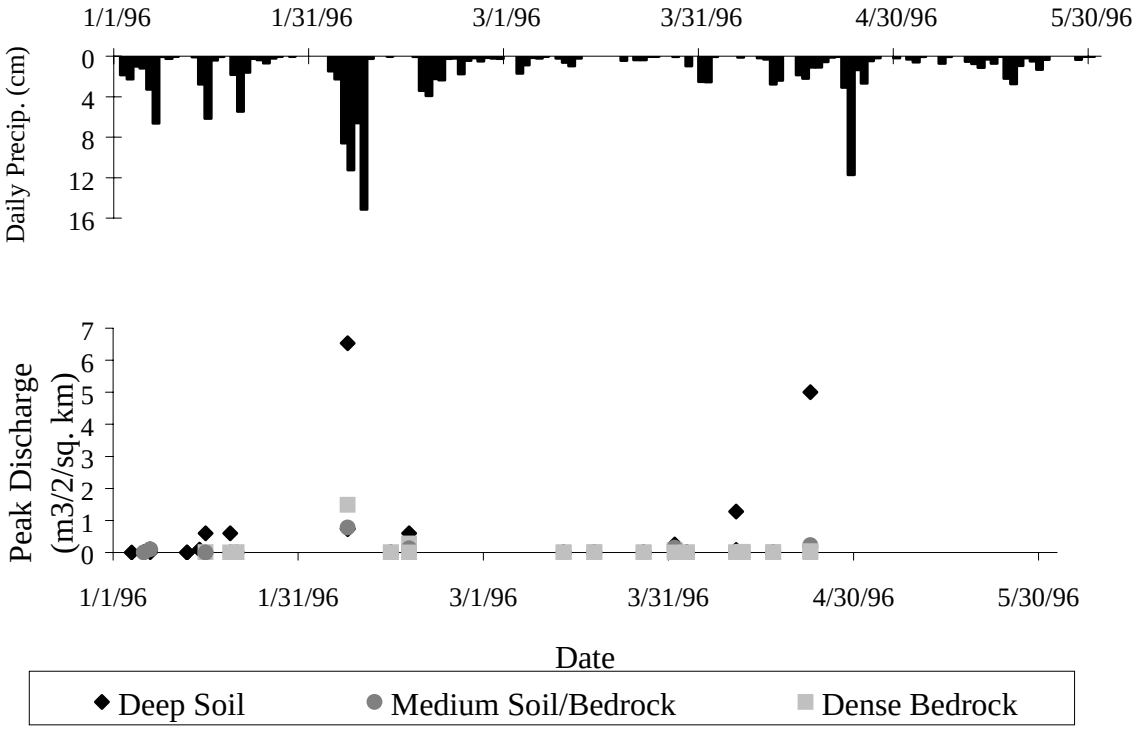

A) PARTITIONED BY SOIL TYPE

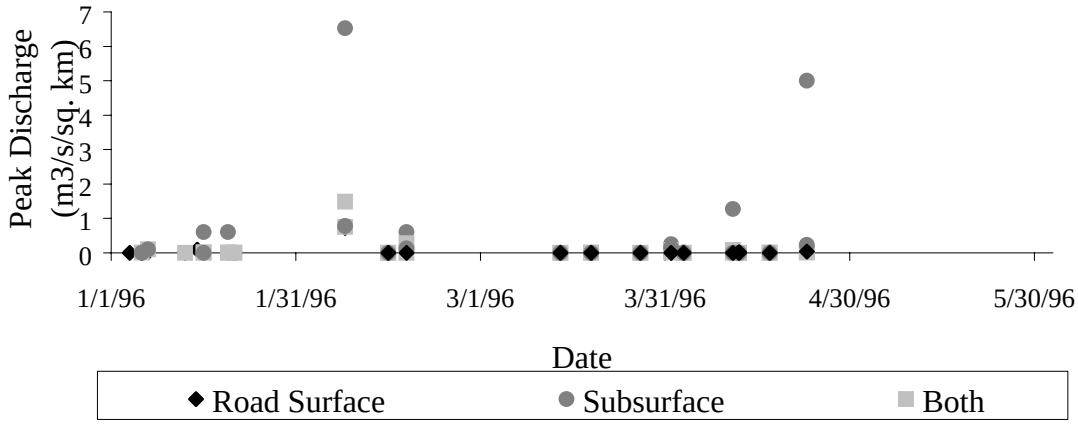

B) PARTITIONED BY RUNOFF MECHANISM VEGETATION

FIGURE 3-23: PEAK FLOW RESPONSE FOR FREQUENTLY RESPONDING CULVERTS (CONT.)

precipitation measured at Ware Creek between February 5 - 8, 1996 is shown in Figure 3-24. A neighboring river, the Chehalis River near Doty, WA tied a 57 year flow record of 27,500 cfs during this event. In addition, the Chehalis River exceeded all records at gauge locations further downstream. The Nisqually River, near National, WA peaked at 20,000 cfs, exceeding the previous flood of record for a 53 year record. The previous flood of record was 17,100 cfs which occurred on December 2, 1977. In the Deschutes basin itself, storm damage included several slope failures along the road network as well as a debris flow initiated in Mine Creek, a tributary adjacent to Hard Creek. The debris flow washed out the road above a culvert crossing in the headwaters as well as a bridge farther downstream (Figure 1-1).

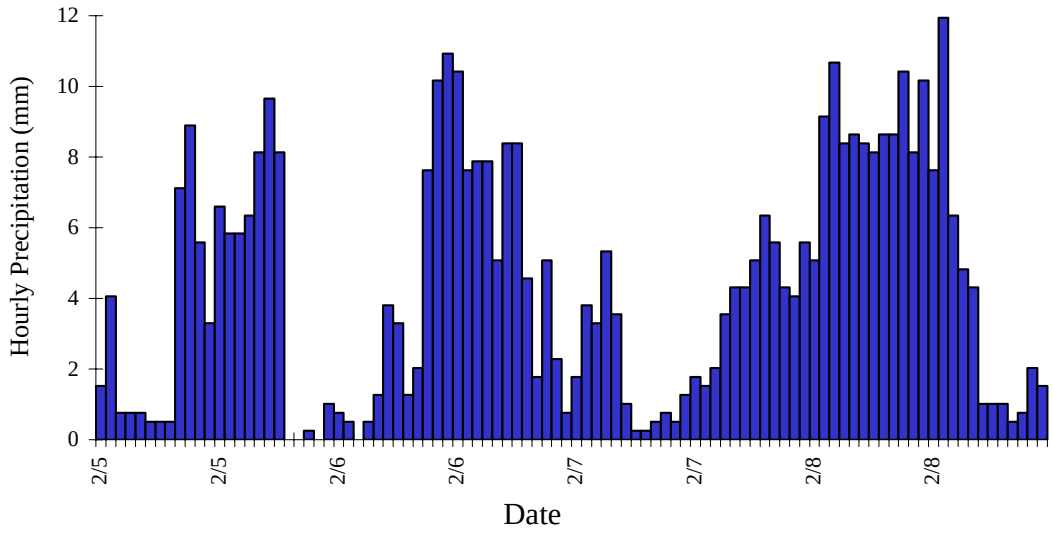

FIGURE 3-24: HOURLY PRECIPITATION 2/5/96 - 2/8/96
TOTAL PRECIPITATION = 417 MM
PEAK INTENSITY = 174 MM/DAY

For a second storm in April 1996, roughly one third of the total precipitation of the February storm fell, but at similar intensity for the two day event. The recorded precipitation for this event is shown in Figure 3-25 The recorded discharge for the February and April storms normalized by the culvert contributing area is shown in Figure 3-26 for eleven of the culvert locations and Hard and Ware Creeks. Several features stand out in this figure. The gauges for road segments H028 and H007 were not

functioning during the February storm. Culvert H018 shows a negligible response for the April event. When this culvert was checked on April 27th it was no longer reading the correct current stage due to about 15 cm of accumulated sediments which blocked the inlet hose. Therefore, the recorded peak may not be accurate. Culvert W032 also shows a much lower response for the April event. As discussed in Section 3.3.3, this may be a result of overland flow during the February storm. The response for culvert W029 in April exceeds the response for the February storm. The difference may be due to alteration of surface runoff flow paths over time, or inaccuracy of the February peak measurement.

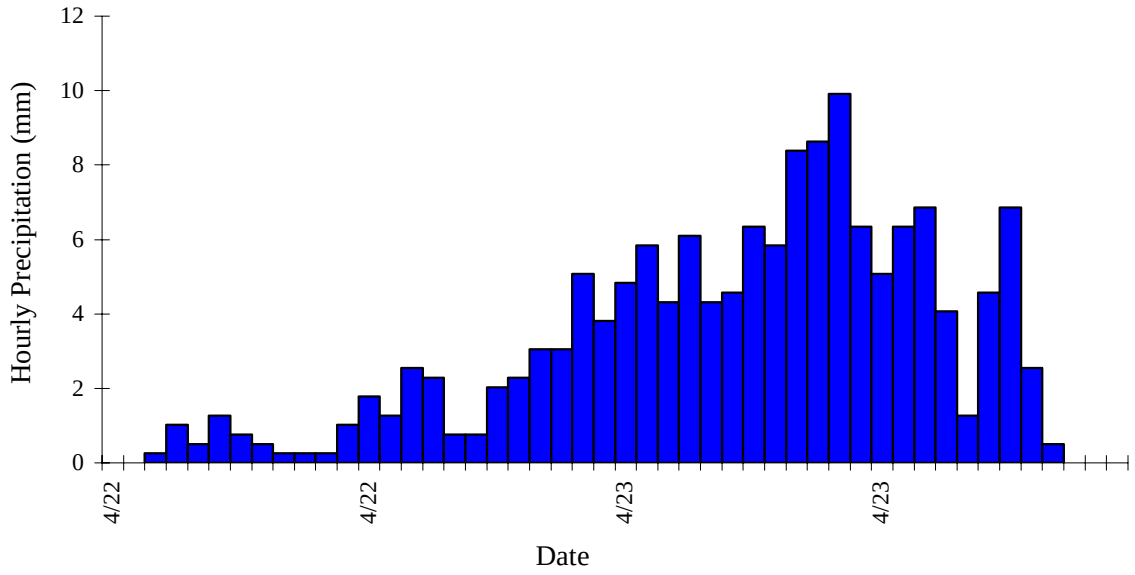

FIGURE 3-25: HOURLY PRECIPITATION 4/22/96 - 4/23/96
TOTAL PRECIPITATION = 148 MM
PEAK INTENSITY = 128 MM/DAY

For both peak events Hard Creek shows a larger response per unit area than Ware Creek. Although the Ware Creek basin has been clear cut significantly more, the Hard Creek basin has a greater road and drainage density. In addition, the Hard Creek basin is slightly higher in elevation and therefore may receive greater precipitation. Average summer runoff (April through September) is consistently higher for Hard Creek than Ware Creek for the period 1975 - 1985 (Sullivan et al. 1987). However, for winter flows (October through March), the average normalized runoff for Ware Creek exceeds Hard Creek

flows for 1975, 1976, 1984 and 1985. Road construction began in Hard and Ware Creeks in 1976 and 1974, respectively. Harvest began in 1984 and 1979, respectively. In 1984 and 1985 67 ha were harvested in the Ware Creek basin, compared to only 2 ha in the Hard Creek basin (Sullivan et al. 1987). Therefore, the difference in response for these two basins seems to be tied to both forest harvest and road construction, as well as natural climatological conditions.

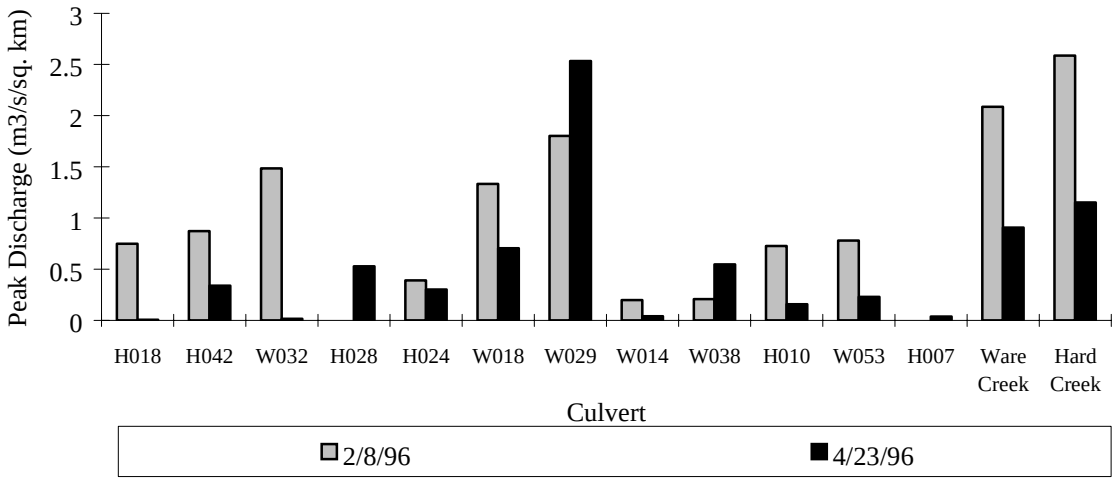

FIGURE 3-26: PEAK ESTIMATED DISCHARGE FOR THE FEBRUARY AND APRIL STORMS

CHAPTER 4: EFFECT OF ROADS ON SURFACE AND SUBSURFACE FLOW PATHS IN HARD AND WARE CREEKS

As described in Chapters 1 and 2, road networks in forested catchments capture water through intercepted subsurface flow and direct runoff from the road surface. Runoff captured by the road network is routed through the roadside ditch until it either intercepts a stream crossing or ditch relief culvert. Road runoff enters the natural drainage network directly at stream crossings. Ditch relief culverts transfer runoff from the roadside ditch to the opposite side of the road where runoff is discharged to the hillslope below the road. Runoff which is diverted to the hillslope can either reinfiltrate at the culvert outfall or travel as surface flow in an incised gully below the culvert outfall (Figure 2-6). Therefore, runoff captured by the road network can travel to the basin outlet entirely as surface flow through two flow paths: by entering a stream crossing culvert or through a ditch relief culvert and eroded gully which extends to the natural drainage network.

The drainage density, taken as the total length of all channels in a basin divided by the basin area, is one of several linear measures used for comparison of the scale of topographic features. Horton (1945) used drainage density to characterize the degree of drainage within a basin . If drainage density is assumed to be constant everywhere in a catchment, the average length of a contributing hillslope is approximately one-half the average distance between streams, or:

$$L_c = 1/2D = A/2L_s \qquad \textbf{4-1}$$

Where D is the drainage density, A is the basin area and L_s is the total length of channels within a basin (Horton 1945). In the Pacific Northwest, very little runoff travels as overland flow, so L_c is a measure of the length of subsurface flow. An increase in the drainage density decreases the length of the subsurface flow path, which will result in changes in travel time to the basin outlet. By converting subsurface

runoff to surface runoff, the road network also decreases the length of the subsurface pathway, as illustrated in Figure 4-1.

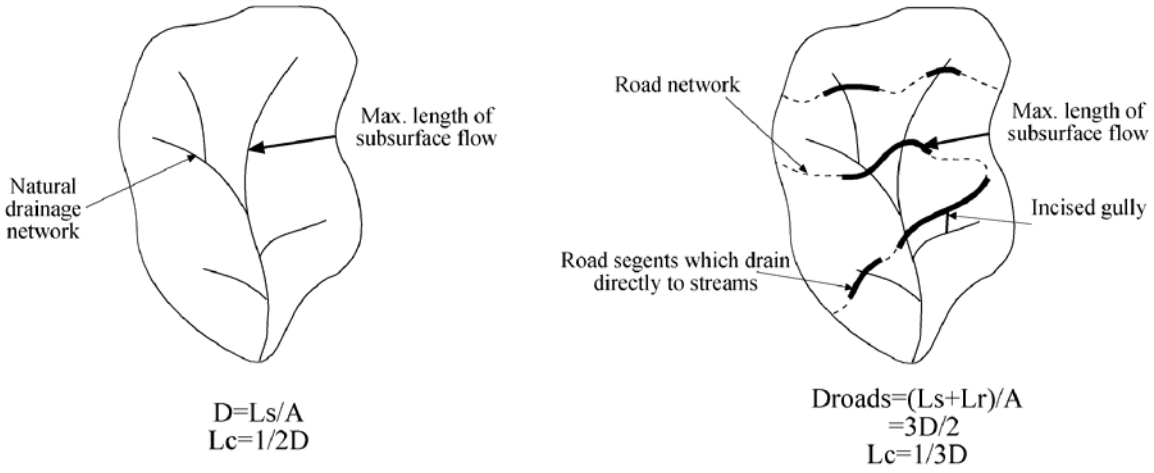

FIGURE 4-1: ILLUSTRATION OF SURFACE FLOW PATHS DUE TO A ROAD NETWORK

The significance of a change from subsurface to surface flow depends on the natural method of runoff generation in a catchment, as discussed in Section 2.1.2. Conversion of Darcian flow through the soil matrix to surface flow can substantially increase the flow velocity (see e.g. Dunne and Black 1970a), whereas localized pipe flow velocities may already approach the velocity of overland flow (Ziemer and Albright 1987, Smart and Wilson 1984). Pipeflow networks have been demonstrated to account for up to 95 % of subsurface flow (Tsukamoto et al. (1982). The proportion of subsurface pipeflow will vary with time, geological setting and antecedent wetness (Smart and Wilson 1984, Tsukamoto et al. 1982, Ziemer and Albright 1987). Therefore, conversion of the flow path will result in different changes for variable regions of the watershed. In some cases, flow emerging from the subsurface will arrive at the basin outlet more quickly. At other times, runoff may travel at comparable speeds over a different flow path. In all cases, runoff captured by the road network will travel a different route to the basin outlet which will most likely change the travel time. Even slight changes in timing will tend to increase or offset the accumulated basin hydrograph, as discussed in Section 2.1.5. The degree of change in natural

flow paths can be related to the length of road 'channels' which supply surface runoff to the natural stream network.

The length of road channels which contribute surface runoff to streams depends on the number of stream crossing culverts and the occurrence of eroded gullies which extend to the drainage network. Culvert spacing, road location and topography will all influence the amount gullying that takes place. Guidelines for the placement of ditch relief culverts on federal lands are specified by the USDA Forest Service in its Road Preconstruction Handbook (USDA Forest Service, 1987). These guidelines include consideration of road gradient, surface material, soil type, runoff characteristics and the expected effects of water concentration below the road. Piehl et al. (1988) observed outlet erosion at 38% of surveyed ditch relief culverts in the Oregon coast range, with an increase in erosion volumes relative to distance between ditch relief culverts. For any contributing road length, Wemple et al. (1996) found that the likelihood of gully occurrence was substantially higher for hill slopes greater than 40% than for hill slopes less than 40 %. In addition, the likelihood of gullying on steep slopes increased with increasing culvert spacing (Wemple et al. 1996).

Culvert location is also important relative to topography. Haupt et al. (1963) noted that the roadside slope is generally more disturbed at the inside of curves, and is therefore less likely to absorb road drainage. Placement of ditch relief culverts at the inside of curves will not only increase the chances of gullying at the culvert outlet, but may increase the likelihood of the gully extending all the way to the surface drainage network, through concentration of subsurface flow in the topographic hollow.

The physical extent of road contribution of surface flow to streams was estimated for Hard and Ware Creeks through field investigation and a Geographical Information System (GIS). The natural drainage density of the catchments was first determined for reference purposes by delineating the stream network and basin area using Arc/Info routines, as described in Section 4.3. For this analysis, a road segment was considered to significantly alter the natural runoff pathway if runoff from the segment followed a

predominately surface flow path to the natural drainage network. Therefore, road segments were classified according to the flow path (surface or subsurface) at the culvert outfall. Once the length of road segments contributing to the drainage network was determined, an extended drainage network, and therefore, the reduction in the length of subsurface flow due to roads, was determined.

4.1: CULVERT CLASSIFICATION

Ditch-relief and stream crossing culverts in the Hard and Ware Creek Watersheds were located using a hand-held portable Global Positioning System (GPS). A Trimble GeoExplorer II was used to record culvert locations. (One hundred twenty positions were averaged to obtain each culvert location to improve the location accuracy.) The dilution of position (DOP) is a dimensionless number which indicates the degree of error associated with the geometry of satellite positions at the time position is calculated. DOP values range from one to infinity, with one being the most accurate. The position DOP (PDOP) is a combination of horizontal, vertical, geometeric and time DOP and is the measure of accuracy available on common GPS receivers. PDOP can increase dramatically as satellites near the horizon (Beadles 1995). For this project, a PDOP threshold of 8.0 was selected. If the PDOP exceeded this threshold, position data were not collected until more favorable satellite conditions returned. Positions were differentially corrected with signal data obtained from the Heritage-CBS Continuous Operating Reference Station (CORS) in Olympia, WA for an estimated position precision of 2-5 m. This range is significantly less (7-17%) than the resolution of the 30 m DEM available for this area. Therefore, culverts were most likely located within the correct DEM pixel. A total of 111 culverts were located: 69 in the Hard Creek basin and 42 in the Ware Creek basin.

Each culvert was classified for its potential connectivity to the drainage network during an extensive field survey using the following categories adapted from Wemple et al. (1996):

- **Directly Connected -**

  - **Stream Crossing:** road segment delivers water directly to a natural stream, identified by a channel both above and below the culvert;
  - **Gully:** road segment delivers water to an eroded gully, evidence of a surface flow path exists which eventually connects to a natural stream channel; and
- **Not Connected:** road segment delivers water to a soil surface or short gully where reinfiltration occurs well before a natural stream.

Road segments were classified in the summer of 1996 by following the flow path below each culvert outlet. A culvert was considered directly connected through a gully if evidence of erosion and overland flow existed from the culvert outlet until the point at which a permanent stream channel was first encountered. If there were no visible signs of an overland flow path leading to a permanent channel, all runoff was assumed to reinfiltrate after exiting the culvert. No precise rules were followed regarding the length of the overland flow path required for culvert classification. Rather, classifications were individually based on the physical characteristics of each hillslope and the presence of a continuous, channelized, surface flow path between the culvert outfall and the stream network.

Culverts which were difficult to classify were flagged for verification following rainstorms in the winter and spring of 1997. A total of 28 culverts (25%) were identified for resurveying. Following the verification survey, 6 of the culverts (5% of total) were reclassified (see Table 4-1). Two of the 28 culverts were not verified due to the presence of snow on the last survey date in May 1997. One additional culvert classification could not be verified since a slope failure destroyed the culvert crossing during the winter of 1997. The final results of the culvert classification are summarized in Table 4-1 and are illustrated in Figure 4-2.

4.2: ROAD SEGMENT CONTRIBUTION

Road locations were surveyed on foot using GPS. Positions were calculated every five seconds as the roads were traveled. Attributes were associated with the road vectors in the field to distinguish between insloped, outsloped and crown road portions. A road segment is considered insloped if greater than one

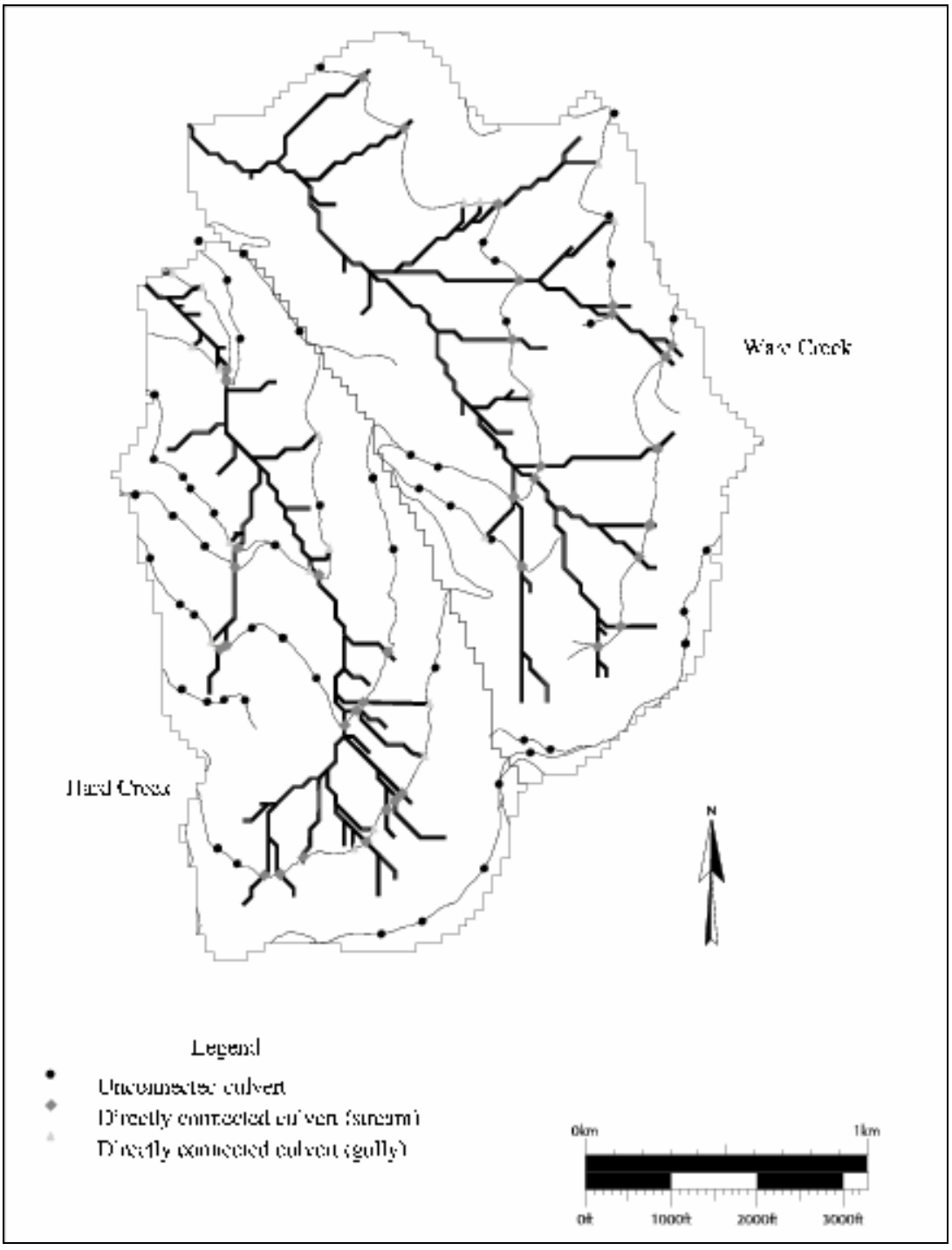

FIGURE 4-2: HARD AND WARE CREEK STREAM NETWORK AND CULVERT CLASSIFICATIONS

TABLE 4-1: CULVERT CLASSIFICATION RESULTS

CULVERT CLASS	WARE CREEK		HARD CREEK	
	NUMBER	PERCENT	NUMBER	PERCENT
Directly Connected (stream)	18	43 %	18	26 %
Directly Connected (gully)	6	14 %	13	19 %
Not Connected	18	43 %	38	55 %
Culverts flagged for resurveying	16	38 %	12	17 %
Culverts resurveyed	14	33 %	11	16 %
Culverts reclassified	2	5 %	4	6 %

half of the road surface drains to the ditch and outsloped if greater than one half of the road surface drains over the hillside. A combination of techniques were used to determine the drainage direction of the road surface. Where possible, channels on the road surface were used to specify the dominant drainage direction. If no surface patterns were visible, a rod and level were used to determine the predominant slope of the road. A total of 22.0 km of roads were located in the two basins, 10.6 km in Ware Creek and 11.4 km in Hard Creek, yielding a road density of 3.7 km/km^2 and 4.9 km/km^2, respectively. Of the 22 km of roads, 21.8 % were insloped, 25.7 % were outsloped and 52.5 % were crowned. As shown in Figure 4-3, the drainage direction of the road surface changes frequently in response to the underlying topography. Therefore, the length of flow paths over the road surface are often much less than the distance between culverts.

4.3: STREAM NETWORK DERIVATION

Total stream channel length was calculated using the grid analysis features of the Arc/Info geographical information system and a 30 meter resolution (approximately 1 arc-second) Digital Elevation Model (DEM). The DEM was obtained from the raw USGS 1 arc-second product and reprojected to the Universal Transverse Mercator (UTM) coordinate system. The DEM was first processed to fill any anomalous depressions. A flow accumulation map was generated based on eight-point pixel flow directions. The extent of the stream network was determined from the flow accumulation map by

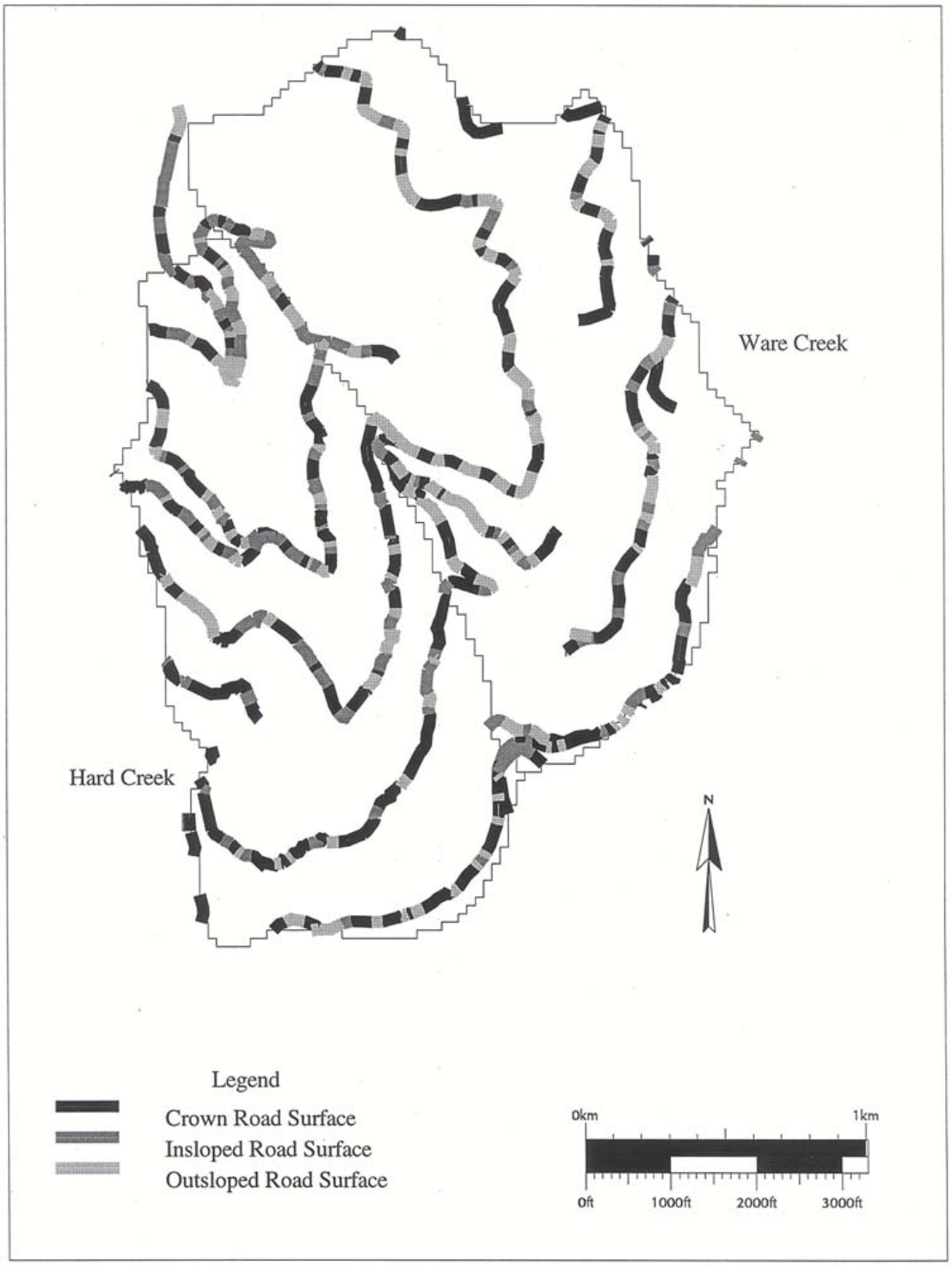

FIGURE 4-3: ROAD SURFACE DRAINAGE DIRECTION

specifying a minimum number of contributing pixels for stream channel initiation. Twenty-two pixels (2 ha) were used as the minimum number of contributing pixels. Therefore, the derived stream network is based on the constant threshold area theory for stream channel initiation.

There are two main methods of channel network extraction from digital terrain data: the constant threshold area method and the slope-dependent critical area method (Montgomery and Foufoula-Georgiou 1993). The most commonly used method is to specify a critical support area that defines the minimum drainage area required to initiate a channel. Use of a threshold area for channel initiation is based on the assumption that channel heads represent a transition from slope-dependent sediment transport on hillslopes to discharge and slope-dependent sediment transport in channels. For a constant-area threshold, the transition point is related to the change in sediment transport rate per change in support area through assumed sediment transport models (Montgomery and Foufoula-Georgiou 1993).

The initial stream locations for Hard and Ware Creeks were determined by specifying a minimum contributing area of 2 ha to represent the approximate stream length during high flow winter runoff events. Stream vectors were derived from the grid of flow accumulation using the Arc/Info Streamline function. This algorithm uses the flow direction from each pixel to aid in vectorizing intersecting and adjacent cells. The derived stream network was compared with field classifications of culvert types for accuracy. The 2 ha stream network was found to most closely match the observed extent of stream channels based on visual examination.

Montgomery and Foufoula-Georgiou (1993) explored problems with the constant support area conceptual model and found that it is more appropriate for estimating the scale of transition between convergent and divergent topography than for estimating channel inititation. They found that a slope-dependent critical support area is both theoretically and empirically more appropriate for defining the extent of channel networks. For tis application, data is not available across the range of slopes required to estimate a slope-dependent model. Since the derived channel network only serves as a base to be

modified using field observations, the constant area threshold was deemed appropriate for identiying runoff producing zones.

The intersection of the derived stream network with the roads did not match exactly with culvert locations, due to the DEM resolution and the accuracy of the stream location within a 30 m pixel. Stream vectors were assigned to the center of each pixel they pass through. Stream crossings were within 30 m of the true culvert location for 25 of the 36 culverts classified as stream crossings. Five of the culverts had DEM-based stream crossings greater than 30 m from the culvert location. The extent of the DEM-based stream network stopped below the road crossing for the remaining six culverts. The positions of all of the stream crossing culverts were adjusted to match the stream positions. This was done rather than adjusting the stream positions in order to keep the streams in the valley axes of the DEM. Stream crossings and stream crossing culverts must be aligned for the model simulation. Although it may seem more reasonable to move the stream locations since these were not located in the field, this would require changing the DEM in a consistent way. Otherwise, the modeled subsurface flow would drain to topographic hollows, but not necessarily to the stream channels. Culverts were moved between 0.6 m and 80.8 m. The average distance moved was 17 m. Five culverts were moved to a new pixel.

The derived streams crossed the roads in nine locations where there either was no culvert within 30 m or the culvert was not classified as a stream crossing. In these cases the streams were adjusted so the channel head was downhill from the road crossing. A total of 1,183 m of streams (6% of the final stream network) were deleted from the derived network on this basis. In cases where the derived streams ended below the observed stream crossing, the streams were extended along the path of the topographic hollow. A total of 1,602 m of streams (or 9% of the final stream network) were added to the derived network. The final stream network included 8,282 m in Hard Creek and 10,460 m in Ware Creek. This yields a natural drainage density of 3.6 km/km^2 and 3.7 km/km^2, respectively. The final stream network is also shown in Figure 4-2.

4.4: EXTENDED DRAINAGE NETWORK

Surface and subsurface runoff intercepted by the road network travel to the stream network by slightly different paths. Intercepted surface runoff, generated by infiltration excess precipitation on the compacted road surface, will drain either into the roadside ditch or over the side of the fill slope depending on the road drainage direction. For outsloped roads, it is assumed that drainage over the fill slope is distributed along the length of the road, and therefore reinfiltration occurs. If roads are insloped or crowned, a portion of the excess precipitation is immediately concentrated in the roadside ditch where it may follow a surface flow path to the natural stream channel or reinfiltrate below the culvert outfall. Therefore, only insloped and crowned roads draining to gullies or streams can contribute intercepted surface runoff to the storm hydrograph.

Most of the roads in the Hard and Ware Creek basins have a drainage ditch between the cutbank and the road surface. Intercepted subsurface water reaches the drainage ditch as surface flow regardless of the road surface slope, if the seepage rate exceeds the infiltration capacity of the drainage ditch. Therefore, the length of road segments contributing surface runoff to streams is different for intercepted surface and subsurface runoff.

The extended drainage network for road surface drainage was calculated by summing the total length of insloped roads and one-half the length of crowned roads, for each road segment which drains to either a stream or gully. Only one-half of the crowned road length is included to represent the fact that these segments contribute half as much water as the insloped segments. This distinction is somewhat qualitative, since the analysis does not take into account contributing area through variable road widths. For road segments draining to gullies, the shortest distance between the culvert outfall and a permanent stream was also included. In many cases the culverts which are connected to the stream network through newly eroded gullies drain into topographic hollows. In these cases the eroded gullies represent the migration of channel heads up the valleys as a result of the concentration of runoff in these hollows. This analysis does not take into account the possible reduction of channel lengths in other hollows due to

the diversion of drainage by the road network. The total length of roads which contribute surface runoff to streams is 2.25 km in Ware Creek and 1.8 km in Hard Creek, as illustrated in Figure 4-4. Bold road segments which appear disconnected in this figure are connected through the road side ditch. The separating road segment is outsloped, therefore it does not contribute to the changes in flow path. The change in drainage characteristics is summarized in Table 4-2.

TABLE 4-2: CONTRIBUTION OF ROADS TO DRAINAGE DENSITY

	Hard Creek	**Ware Creek**
Basin area (km^2)	2.3	2.8
Stream length *(km)*	8.3	10.5
Original drainage density (km/km^2)	3.6	3.7
Original length of subsurface flow, L_c *(km)*	0.14	0.14
Length of roads draining to streams *(km)*	2.2	4.0
Insloped Roads *(km)*	0.6	0.6
Outsloped Roads *(km)*	0.5	1.4
Crown Roads *(km)*	1.1	2.0
Length of roads draining to gullies *(km)*	2.2	0.9
Insloped Roads *(km)*	0.6	0.1
Outsloped Roads *(km)*	0.6	0.5
Crown Roads *(km)*	1.0	0.3
Length of gullies *(km)*	0.9	0.6
Extended network drainage density for intercepted surface flow (km/km^2)[1]	5.0	4.6
Increase in drainage density due to roads for intercepted surface flow (%)	37.9	23.2
Extended network drainage density for intercepted subsurface flow (km/km^2)[2]	5.9	5.6
Increase in drainage density due to roads for intercepted subsurface flow (%)	63.5	52.3
Reduced length of subsurface flow due to roads *(km)*	0.08	0.09
Decrease in length of subsurface flow (%)	42.9	35.7

Notes:
[1]Includes total stream length, gully length, length of insloped roads draining to streams or gullies and one-half the length of crown roads draining to streams or gullies.
[2]Includes total stream length, gully length, and the length of all roads draining to streams or gullies.

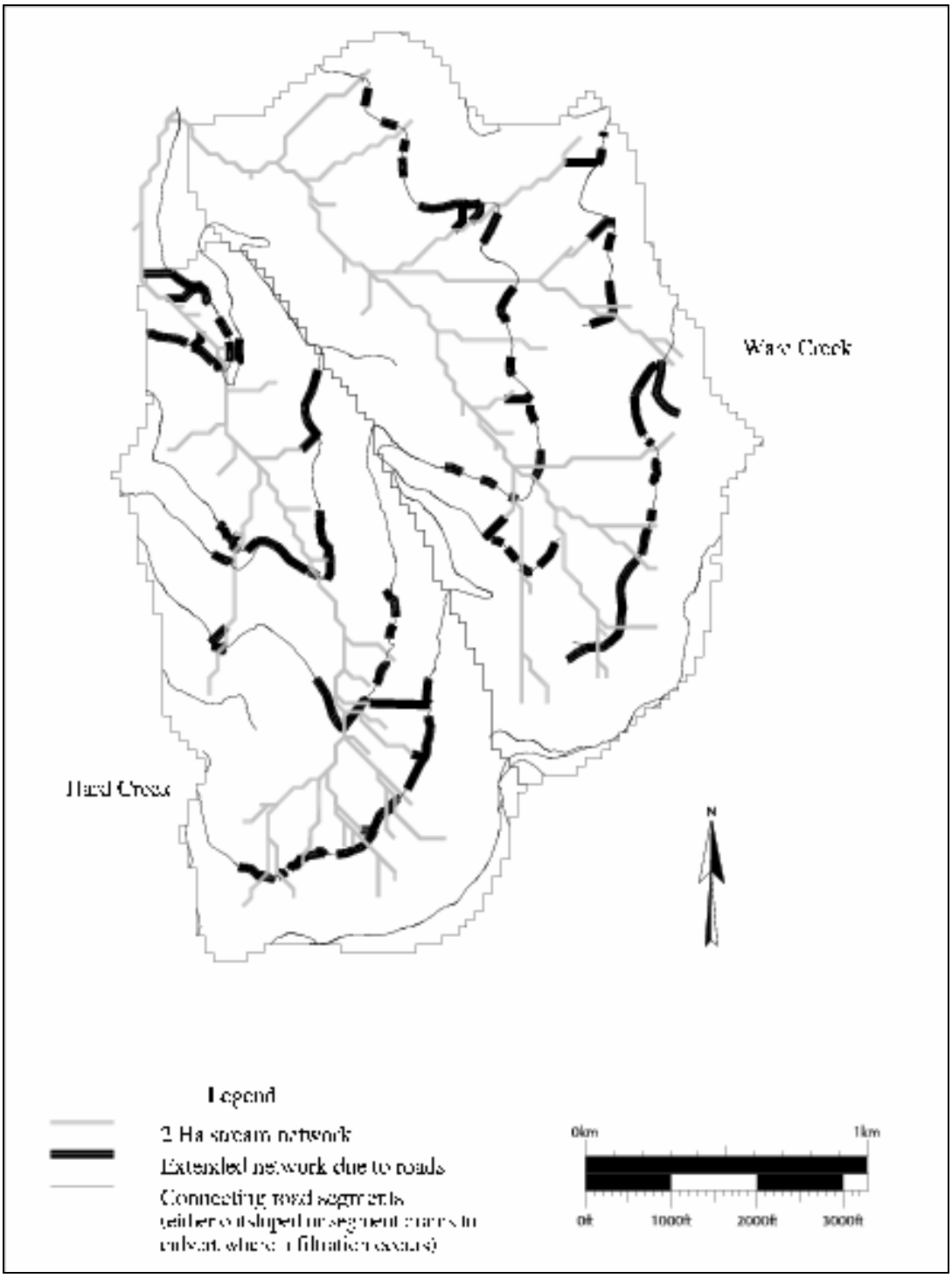

FIGURE 4-4: EXTENDED DRAINAGE NETWORK FOR ROAD SURFACE RUNOFF

For intercepted subsurface flow the entire road length draining to streams or gullies is considered to contribute to the drainage network (see Figure 4-5 and Table 4-2). This represents the maximum extent of flow path conversion due to intercepted subsurface flow. Surface runoff may be generated by all roads when the precipitation rate exceeds the infiltration rate through the road surface. However, not all cutslopes will contribute significant runoff to the roadside ditch. Since it is not clear how to classify contributing cutslopes, the maximum extent of contribution is presented here.

4.5: DISCUSSION

There is a temptation to infer from drainage density how catchment behavior may change in response to forest management. For example, the work with geomorphological instantaneous unit hydrographs (GIUH) calculates hydrological response based on inferred drainage networks (e.g., Gandolfi and Bischetti 1997). However, the change in 'drainage density' due to roads alone may not be a good indicator of catchment response. High drainage densities often occur in areas of highly erodible and relatively impermeable soil such as in the Badlands National Monument, South Dakota (Linsley et al. 1982). These conditions decrease the volume and velocity of runoff needed for channel erosion to begin. In the case of roadside ditches, the channels are artificially imposed on the landscape and so are not related to a threshold of channel initiation. Therefore, although the network may exist for channelized surface flow, there is no guarantee that sufficient discharge exists to fill these channels.

In addition, the artificially imposed drainage network will change the distribution of soil moisture within a basin, thus altering the function of the natural drainage network. In an undeveloped basin, soil moisture is expected to increase more or less progressively downslope from the ridges, with localized exceptions due to soil and vegetation characteristics, creating areas near saturation on either side of the channel. These areas may reach saturation quickly during a storm event and contribute significantly to the storm hydrograph (e.g. Dunne and Black 1970b). In a catchment with roads, hillslopes below roads will likely be drier than the undeveloped equivalent due to the redistribution of subsurface water. This may reduce

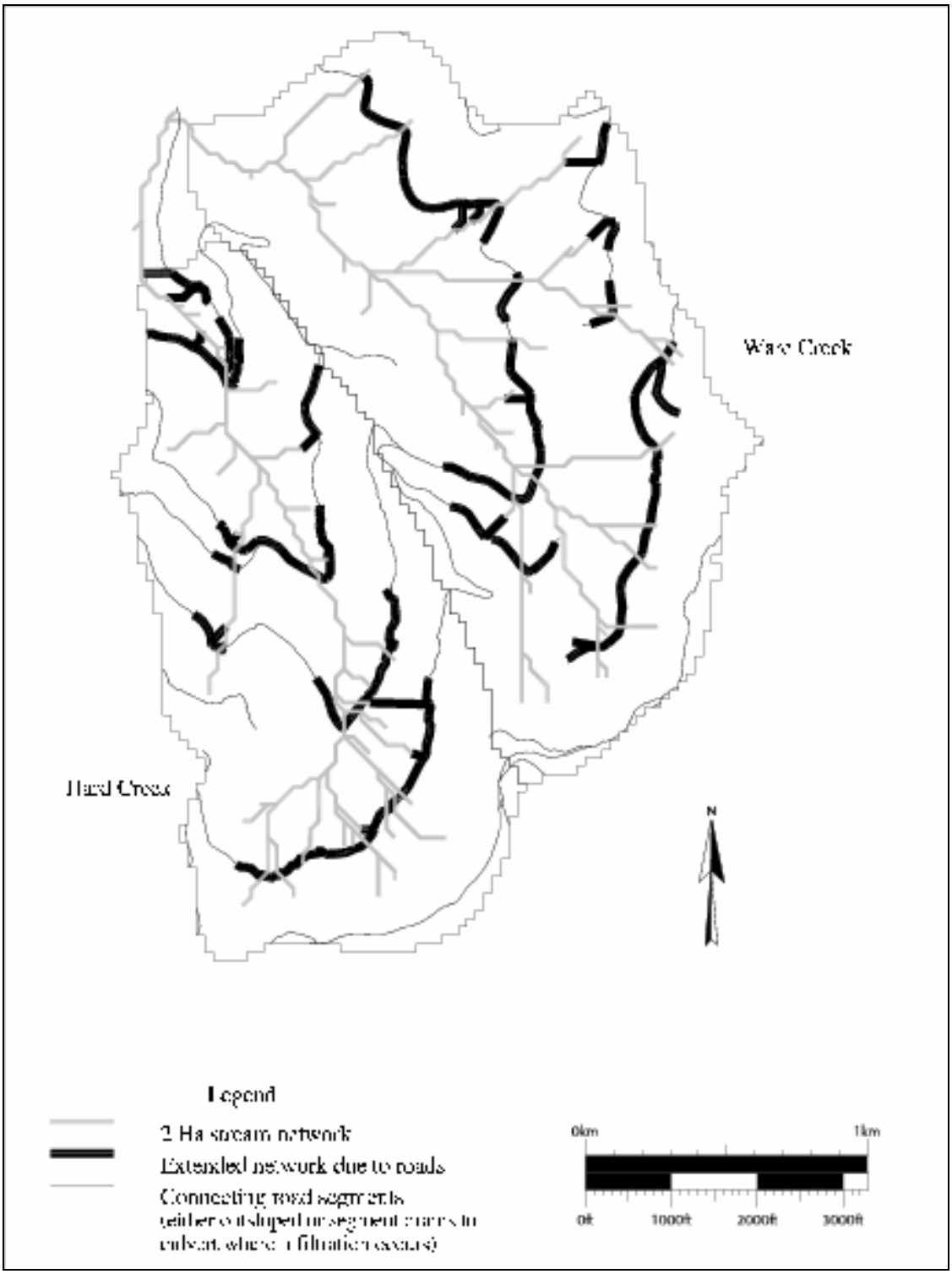

FIGURE 4-5: EXTENDED DRAINAGE NETWORK FOR SUBSURFACE RUNOFF

the component of storm response due to runoff from saturated areas, which would tend to mitigate the effect of increased drainage density. The effect of soil moisture redistribution can be investigated further through distributed modeling.

The importance of this distinction between natural and road-induced drainage density remains to be resolved and may be catchment-specific. The integrated road/channel network may actually change the controlling response mechanism of the catchment from runoff from saturated areas to a system dominated by channel flow. Therefore, the total length of road segments in a basin which convert subsurface flow to surface flow is not an indicator of a proportional increase in peak flow due to roads. It is only an indicator of the degree to which natural drainage pathways have been altered by the road network. Subsurface flow paths, road position, construction technique and culvert spacing will interact to determine the effect of these changed pathways on the accumulated hydrograph. Calculation of the length of contributing road segments serves to verify that flow routes do exist through which roads can interact with the drainage network, as well as allowing spatial analysis of road segments which most influence watershed response. Such analysis will be useful for design and restoration of forest road systems.

CHAPTER 5: DISTRIBUTED HYDROLOGY-SOIL-VEGETATION MODEL

5.1: MODEL DESCRIPTION

DHSVM, originally developed by Wigmosta et al. (1994) and extended for use in maritime mountainous watersheds by Storck et al (1995), is a physically-based hydrologic model which explicitly solves the water and energy balance for each model grid cell. Therefore, DHSVM requires spatial image data which represent the distribution of land surface characteristics of the modeled catchment (vegetation type, elevation and soil type) and meteorological forcings (precipitation, air temperature, wind speed, relative humidity and incoming short- and longwave radiation). Meteorological forcings must be specified for each timestep. Following a brief summary of the model structure, the source and development of the land surface characteristic images and meteorological forcings are described in this chapter.

5.1.1: GENERAL MODEL DESCRIPTION

The governing equations of DHSVM in its original form are described in Wigmosta et al. (1994) and Storck et al. (1995) and summarized briefly here. Recent enhancements to DHSVM are described in detail by Storck et al. (1997). DHSVM consists of a two-layer canopy representation for evapotranspiration, a two-layer energy-balance model for snow accumulation and melt, a one-dimensional unsaturated soil model, and a two-dimensional saturated subsurface flow model. An independent one-dimensional (vertical) water balance is calculated for each pixel. Stomatal resistance is calculated for each vegetation layer based on air temperature, the vapor pressure deficit, soil moisture conditions, and photosynthetically active radiation. Evaporation of intercepted water from the surface of wet vegetation is assumed to occur at the potential rate, while transpiration from dry vegetative surfaces is calculated using a Penman-Monteith approach.

Downward moisture flux in the unsaturated zone is calculated using Darcy's law. Soil moisture is removed from the unsaturated zone via evaporation and transpiration. The soil profile can consist of a variable number of rooting layers and a deep layer. The fraction of both overstory and understory roots in each soil layer is specified. This determines the relative amount of available soil moisture removed from each layer as transpiration. Soil evaporation is calculated from the surface soil layer only when no understory is specified, using a soil physics-based approach (Entekhabi and Eagleson 1989). No soil evaporation or understory transpiration occurs when snow is present. The downward flux of moisture which is not removed through evapotranspiration serves to recharge the grid cell water table. Each DEM grid cell exchanges saturated subsurface flow with its four adjacent neighbors, by assuming that the local hydraulic gradient is equal to the local ground surface. Return flow and saturation overland flow are generated in locations where grid cell water tables intersect the ground surface.

Precipitation occurring below a threshold temperature is assumed to be snow. Snow interception by the overstory is calculated as a function of Leaf Area Index and is adjusted downward for windy or cold conditions (Schmidt and Troendle, 1992). Intercepted snow can be removed from the canopy through snow melt, sublimation, and mass release. Melt of intercepted snow is calculated based on a single layer energy balance approach. Mass release occurs if sufficient melt water is generated during an individual time step such that the snow slides off the canopy (Bunnell et al., 1985; Calder, 1990). Drip from the canopy is added to the ground snowpack (if present) as rain while the cold content of any mass release or unintercepted snow is added directly to the ground snowpack.

Ground snow accumulation and melt are simulated using a two-layer energy-balance model at the snow surface. The model accounts for the energy advected by rain, throughfall or drip, as well as net radiation and sensible and latent heat. Incoming short and long wave radiation and wind speed are attenuated through the canopy. Separate shortwave and longwave radiation budgets are developed for the overstory, understory, and ground surface. If snow is present, it is assumed to cover the understory and

thus affects radiation transfer and the wind profiles via increased albedo and decreased surface roughness. Temperature and relative humidity are not adjusted through the canopy.

5.1.2: ROAD AND CHANNEL ALGORITHM

A recent addition to DHSVM includes a road and channel network algorithm to represent the formation of direct runoff from road surfaces and intercepted subsurface flow and the subsequent routing as open channel flow. The algorithm uses explicit information on the location of stream channels and road networks based on GIS coverages.

The fraction of each pixel covered by a road or stream along with the depth of the road cut and/or channel incision is calculated prior to the model run by mapping GIS coverages of the road and channel network to specific rows and columns in the DEM. At present, each road segment is assumed to be crowned within the model. Subsurface flow is discharged into these networks based on the height of the local water table relative to the bottom of the channel or road. Once in the network, intercepted subsurface flow and directly intercepted precipitation are routed through roadside ditches and stream channels using a Muskingum-Cunge scheme. Open channel flow in the roadside ditches is released to the stream network at specified culvert locations, where the road runoff is added to the stream channel flow. If the specified culvert location does not correspond to a stream crossing, the runoff is added to the soil surface and is then available for reinfiltration. Surface water not in the channel or road networks is modeled as overland flow and can reinfiltrate into neighboring model pixels.

5.2: SPATIAL DATA

5.2.1: DIGITAL ELEVATION DATA

Digital elevation data are required to determine topographic controls on radiation, saturated subsurface flow, air temperature and precipitation, at the scale of the model pixel. Digital elevation data for Hard

and Ware Creeks was obtained from raw USGS 1-arc second DEMs for WA state. The DEMs were merged and converted to the Universal Transverse Mercator (UTM) coordinate system. The DEM was processed within Arc/Info to fill two anomalous depressions. A mask file which defines the basin boundary is also required for input. Hard and Ware Creeks were delineated using the watershed analysis features of Arc/Info, following Jenson and Domingue (1988). The masked DEM is shown in Figure 5-1.

5.2.2: DISTRIBUTED VEGETATION DATA

In each model pixel, the modeled land surface may be composed of overstory vegetation, and/or either understory vegetation or soil. The overstory may cover a variable prescribed fraction of the land surface. The understory, if present, covers the entire ground surface. The model allows land surface representations ranging from a closed two-story forest, to sparse low-lying natural vegetation or bare soil, through the specification of canopy closure, vegetation height and leaf area index (LAI).

Vegetation in Hard and Ware Creek consists of mature and regenerating second growth mixed conifers, including white fir, silver fir and douglas fir. Weyerheauser provided Arc/Info coverages of forest stand boundaries for 1996 with accompanying attributes of LAI, tree height and canopy closure. The attributes were calculated based on literature values of LAI and height provided to Weyerheauser, which were scaled by the 1996 tree height. Stands with similar values were grouped together into vegetation classes and the weighted average LAI, height and canopy closure was computed for each class. Thirteen vegetation classes were used, as illustrated in Figure 5-1. The derived parameters for each vegetation class are listed in Table 5-1. Due to a lack of age and species-specific information, the remaining vegetation parameters were not changed for each vegetation class (Table 5-2). These parameters were taken from Stork et al. (1995) and are based on literature values consistent with Pacific Northwest conifers.

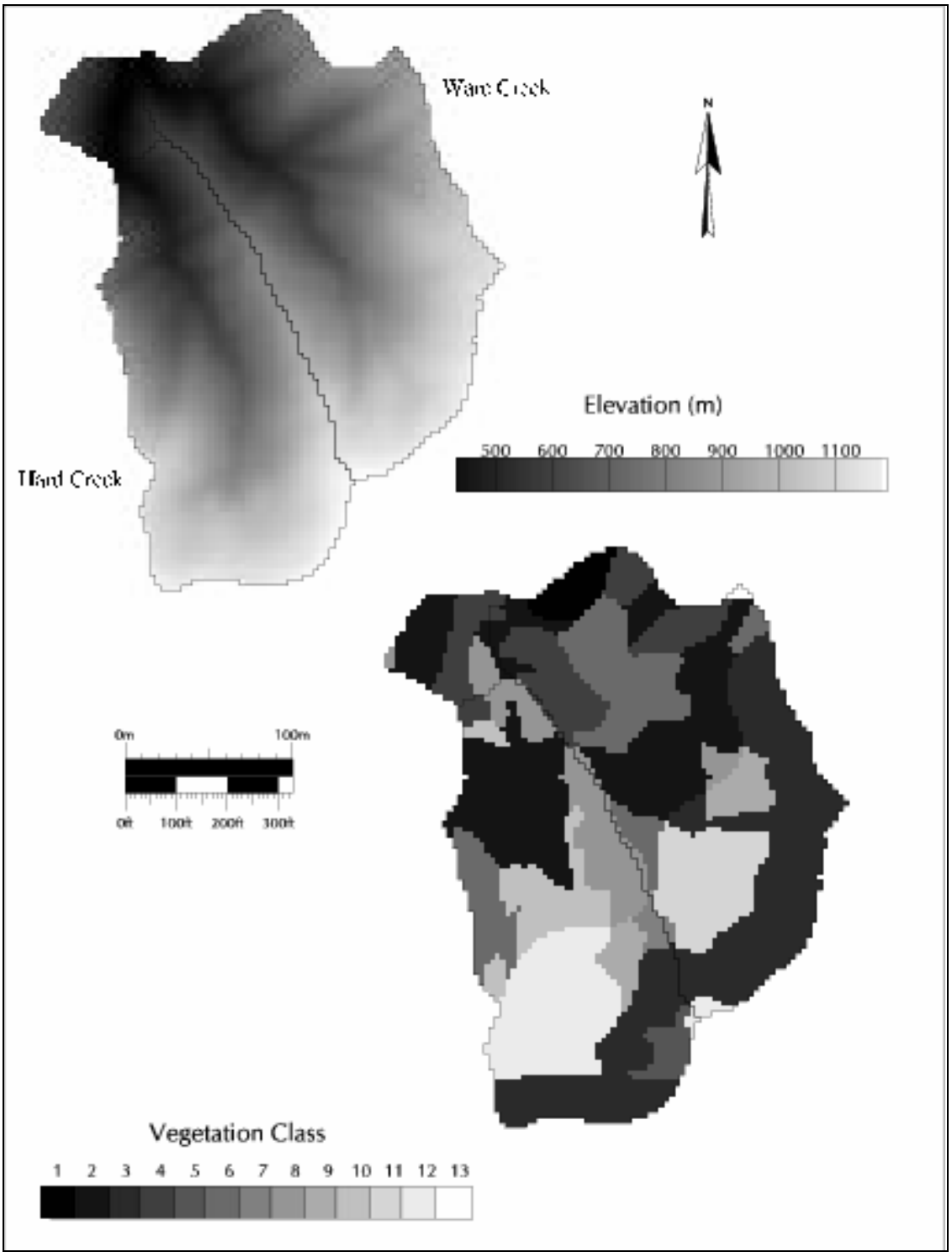

FIGURE 5-1: DHSVM ELEVATION AND VEGETATION IMAGE FILES

TABLE 5-1: VEGETATION CLASS PARAMETERS

	VEGETATION CLASS					
	4[1]	**5**	**6**	**7**	**8**	**9**
Vegetation height (m)	1.2	2.1	4.3	10.4	19.1	19.8
Fractional coverage	0.03	0.05	0.1	0.23	0.69	0.9
Fractional trunk space	0.5	0.5	0.5	0.5	0.5	0.5
LAI	0.68	0.85	1.73	5.85	7.66	14.13
Overstory root fraction in soil layer 1	0.31	0.3	0.31	0.3	0.31	0.3
Overstory root fraction in soil layer 2	0.36	0.5	0.36	0.5	0.36	0.5
Overstory root fraction in soil layer 3	0.23	0.2	0.23	0.2	0.23	0.2
Understory root fraction in soil layer 1	0.62	0.6	0.62	0.6	0.62	0.6
Understory root fraction in soil layer 2	0.29	0.4	0.29	0.4	0.29	0.4
Understory root fraction in soil layer 3	0.09	0.0	0.09	0.0	0.09	0.0
	VEGETATION CLASS					
	10	**11**	**12**	**13**	**UNDERSTORY**	
Vegetation height (m)	22.8	24.4	41.5	42.1	0.3	
Fractional coverage	0.9	0.9	0.9	0.93	1.0	
Fractional trunk space	0.5	0.5	0.5	0.5	-	
LAI	13.6	9.8	23.4	16.8	3.0	
Overstory root fraction in soil layer 1	0.31	0.3	0.3	0.31	-	
Overstory root fraction in soil layer 2	0.36	0.5	0.5	0.36	-	
Overstory root fraction in soil layer 3	0.23	0.2	0.2	0.23	-	
Understory root fraction in soil layer 1	0.62	0.6	0.6	0.62	-	
Understory root fraction in soil layer 2	0.29	0.4	0.4	0.29	-	
Understory root fraction in soil layer 3	0.09	0.0	0.0	0.09	-	

[1] Vegetation classes 1 - 3 do not have an overstory.

TABLE 5-2: CONSTANT VEGETATION PARAMETERS

	OVERSTORY	UNDERSTORY
Max. stomatal resistance	1000	5000
Min. stomatal resistance	333.3	250.0
Soil moisture threshold which restricts transpiration	0.33	0.13
Vapor pressure deficit threshold which causes stomatal closure (Pa)	4000	4000
Radiation attenuation coefficient	0.5	0.5
Albedo	0.18	0.20
Aerodynamic attenuation coefficient for wind through the overstory	3.5	3.5

5.2.3: DISTRIBUTED SOIL DATA

Basin soil data were extracted from the State Soil Geographic (STATSGO) Data Base produced by the United States Department of Agriculture (USDA) Soil Conservation Service (SCS) (USDA 1994). STATSGO units are defined with a minimum area of 1 km^2. Therefore, several soil types are contained within each STATSGO unit. STATSGO data provides a rough characterization of soils within Hard and Ware Creeks. Areal extent, USDA soil texture, depth, and percentage sand, clay and silt for each soil layer are available from the database for each soil type within the STATSGO unit. The physical boundaries are only available for each unit. For this application, soil horizon layers were chosen to be consistent with the majority of the soil types. Percentage sand, clay and silt were computed using a

TABLE 5-3: STATSGO SOIL PARAMETERS

LAYER	DEPTH (M)	USDA TEXTURE	% CLAY	% SAND	% SILT
SOIL TYPE 1					
1	0 - 0.1	gravely silt loam	21.8	29.5	48.7
2	0.1 - 0.4	gravely silt clay loam	30.0	24.6	45.4
3	0.4 - 0.85	gravely clay loam	32.1	29.8	38.1
4	variable	gravely silt loam	13.5	9.0	77.5
SOIL TYPE 2					
1	0 - 0.05	gravely loam	13.9	41.2	44.9
2	0.05 - 0.2	gravely silt loam	17.9	39.8	42.3
3	0.2 - 0.85	very gravely loam silt	16.6	46.0	37.4
4	variable	silt	6.7	6.1	87.2
SOIL TYPE 3					
1	0 - 0.11	gravely silt loam	19.7	32.3	48.0
2	0.11 - 0.41	gravely silt loam	19.7	36.0	44.3
3	0.41 - 0.81	very gravely loam	25.9	36.8	37.3
4	variable	silty clay loam	27.2	21.1	51.7

weighted average of the soil types. The resulting average parameters for the three STATSGO soil units within Hard and Ware Creeks are listed in Table 5-3. The soil parameters required for DHSVM were derived from published empirical relationships using this data. The derived soil parameters are listed in Table 5-4. A complete description of the derivation of these parameters can be found in Appendix B.

TABLE 5-4: DERIVED SOIL PARAMETERS

Parameter Name	Soil Type 1			Soil Type 2			Soil Type 3		
	Layer 1	Layer 2	Layer 3	Layer 1	Layer 2	Layer 3	Layer 1	Layer 2	Layer 3
Porosity (%)	53	49	44	48	53	53	53	53	53
Pore-size index[1]	0.31	0.28	0.27	0.32	0.32	0.32	0.31	0.31	0.29
Air bubbling pressure	0.172	0.292	0.243	0.110	0.120	0.105	0.133	0.13	0.124
Field Capacity	0.330	0.366	0.318	0.270	0.330	0.270	0.330	0.330	0.270
Wilting point	0.133	0.208	0.197	0.117	0.133	0.133	0.133	0.133	0.117
Density (kg/m^3)	1000	1200	1200	840	970	1030	840	940	1030
Vertical saturated hydraulic cond. (m/s)	9.2×10^{-6}	9.2×10^{-6}	9.2×10^{-6}	1.3×10^{-6}	1.8×10^{-6}	2.7×10^{-5}	1.1×10^{-5}	2.1×10^{-5}	3.1×10^{-5}
Rpc[2]	0.108			0.108			0.108		
Lateral saturated hydraulic conductivity (m/day)	0.002			0.002			0.002		
Lateral hydraulic conductivity exponent	2.0			2.0			2.0		
Effective solids thermal conductivity (W/mK)	6.29	6.56	5.74	7.31	6.97	7.24	6.57	6.71	6.36
Maximum infiltration rate (m/s)	1.68×10^{-6}			1.68×10^{-6}			1.68×10^{-6}		
Thermal Capacity (J/m^3K)	1.4×10^{6}			1.4×10^{6}			1.4×10^{6}		

Note:
[1]The pore-size index is a parameter of the Brooks and Corey model for soil water retention.
[2] R_{pc} is the light level where the soil surface resistance to vapor transport, r_s, is equal to two times the minimum soil surface resistance.

The depth to each soil horizon is available from STATSGO, however, the scale is too large to distinguish topographic controls on soil depth. Therefore, a map of soil depth was created by specifying buffer areas around the stream channels and ridgetops. Consistent with field observations, soils adjacent to stream channels were assigned the largest depths and soils adjacent to ridge tops were assigned the shallowest. The primary source of field observations for determining soil depth were road cuts. All exposed road cuts in both basins were classified as having deep, moderate or shallow soil during the field investigation. These classifications were not based on a measured soil depth. Road cuts were classified as having deep soil if the cut was covered in soil and vegetation. Road segments were considered to have shallow soil if the cut consisted primarily of rock outcroppings. The moderate classification represented a mixture of soil and rock visible in the road cut. The assigned buffer widths were adjusted to match the boundaries of these observations. Depths were assigned to each buffer such that the average soil depth for each basin matched the average depth determined by a Weyerheauser Company survey (Sullivan et al. 1989), which reported soil depth averages of 0.6 m in Hard Creek and 1.0 m in Ware Creek. The final variable soil depth map and associated values are illustrated in Figure 5-2. For purposes of sensitivity analyses reported in Chapter 6, a second map of soil depth was created with a constant depth of 0.9 m.

5.3: ROAD AND STREAM NETWORK INPUTS

The road and stream networking algorithm requires information about the spatial distribution of the road and stream channels, as well as their hydraulic characteristics. Required stream characteristics include the channel width, depth and Manning's roughness coefficient. GIS overlays of the stream network were derived as discussed in Chapter 4.0. The stream coverage was processed within Arc/Info to generate DHSVM input files which map the length, slope, aspect and channel characteristics of each stream segment to the appropriate pixel. The local slope of each stream segment within a pixel is found by sampling the DEM at intervals of 1.5 times the DEM spacing, along the stream length. The sampling spacing was chosen arbitrarily to ensure that the same pixel was not sampled twice. The depth and width

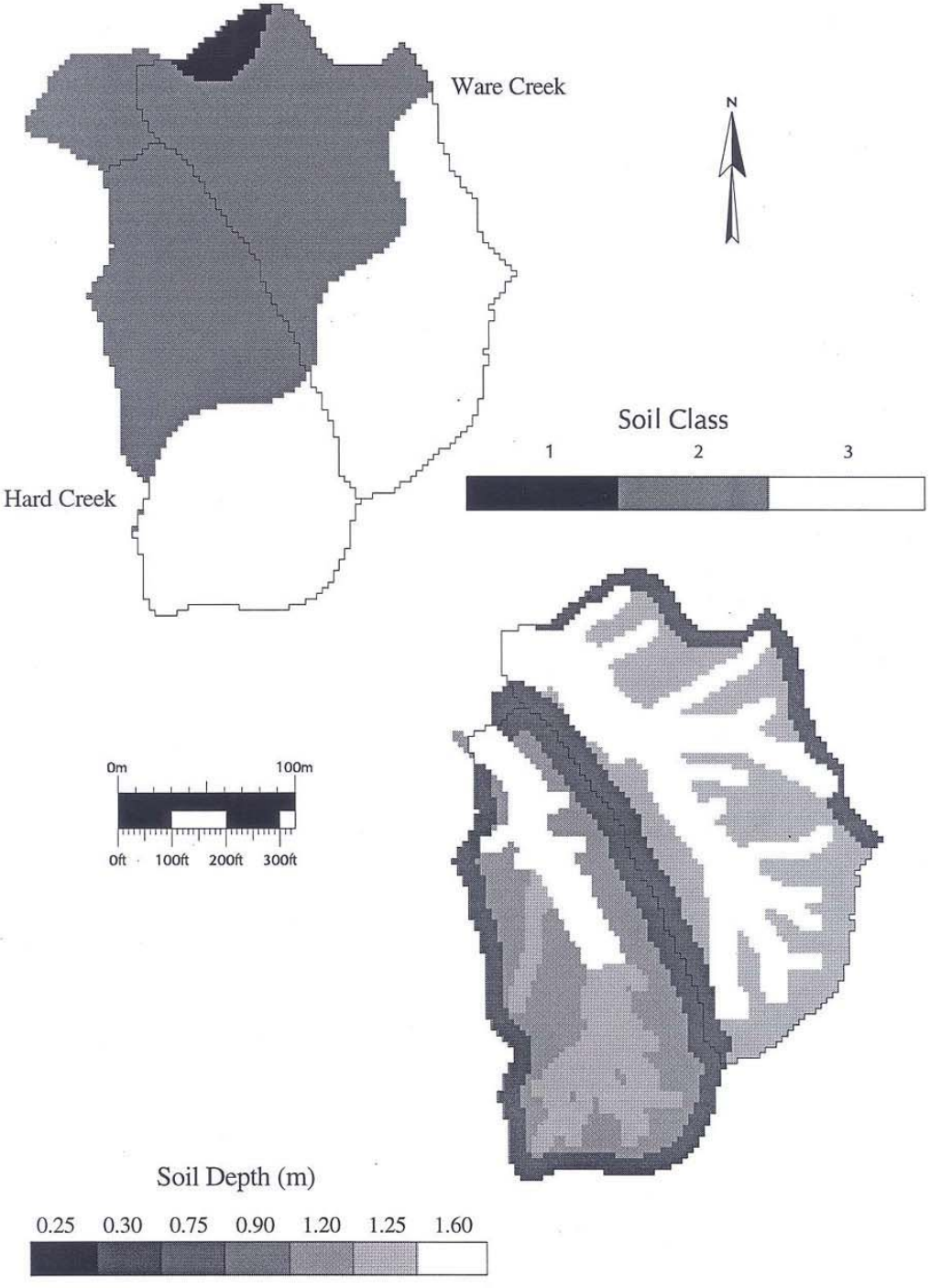

FIGURE 5-2: HARD AND WARE CREEK SOIL IMAGES

of the channel incision into the soil layer is specified for each channel class and were estimated from field observation. Classes were assigned to stream channels based on the Strahler stream order. The stream channel input files also explicitly specified the location of the gullies which connect ditch relief culverts with the natural drainage system. These gullies were assigned a separate channel class. The parameters assigned to each channel class are given in Table 5-5. The Manning's roughness coefficient of 0.015 listed in Table 5-5 is low. Based on literature values for straight, natural channels with weeds and stones a value of 0.035 would be more appropriate for Hard and Ware Creeks (Linsley et al. 1982). The coefficients used were changed experimentally in the early part of model calibration and were inadvertently never changed back. This error will route runoff in the channel network to the basin outlet more quickly. Based on comparison of model results when the coefficient was first altered, the effect on model timing is not large for these small basins.

TABLE 5-5: STREAM CHANNEL PARAMETERS

Channel Order	Width (m)	Depth (m)	Manning's Roughness
Gullies	0.4	0.15	0.015
1	0.5	0.25	0.015
2	1.0	0.35	0.015
3	2.5	0.50	0.015
4	3.5	1.00	0.015
5 (Deschutes)	5.5	2.50	0.015

Specification of the road network requires information regarding cutbank height, cutbank slope, road surface width, roadside ditch depth and width and road surface drainage direction. Determination of road surface drainage was described in Chapter 4. Ditch width and depth were measured at a representative point for each road segment draining to a particular culvert. Cutbank height and slope were visually estimated for the same road segments. Road surface width was estimated (by pacing) for

each road segment defined by a new surface drainage direction. Channel segments with similar physical characteristics were grouped into classes. One hundred and eighteen classes were formed. The full set of parameters associated with each road class are included as Appendix B. Basin average values are given in Table 5-6.

TABLE 5-6: AVERAGE ROAD DIMENSIONS

VARIABLE	MINIMUM	MEAN	MAXIMUM
Road width	2.4 m	5.3 m	10.4 m
Cutbank height	0.0 m	5.3 m	12.2 m
Cutbank slope	0.0 m/m	19.31 m/m	61.4 m/m
Ditch depth	0.05 m	0.21 m	0.48 m
Ditch width	0.25 m	0.04 m	1.98 m

Preparation of the road network is performed within Arc/Info using Arc Macro Language (AML) programs developed by Battelle Pacific Northwest Laboratories specifically for use with DHSVM. The GIS coverage of the road network is first split at known culvert locations, after they have been adjusted to match stream locations. The location of other sinks and divides along the road network is estimated based on the slope direction of each road segment. The local slope of each road segment is found by sampling the DEM at intervals of 1.5 times the DEM spacing. Since this does not take into account the height of the cut slope, there are errors between the predicted and true sink and divide locations. The drainage direction of each road segment was checked and adjusted by hand to make the road drainage consistent with field observation.

5.4 METEOROLOGICAL DATA

Meteorological conditions (precipitation, air temperature, solar radiation, wind speed and vapor pressure) are prescribed at a specified reference height well above the overstory for each model time step at specific station locations. The model allows for a variable number of stations, with a minimum of one

station located within the model boundary. Meteorological conditions were specified at one location within Hard and Ware Creeks, the Ware Creek stream gauge (Figure 5-3). Air temperature has been collected continuously at Ware Creek by the Weyerhaeuser Company since 1989. Precipitation has been collected at Ware Creek since October 1974, but the pre-1985 data have been lost. A two hour model time step was used since this was the minimum frequency at which precipitation data were collected. A two-hour timestep represents a reasonable compromise between the response time of the catchment (approximately 0 to 4 hours) and limitations of computation time.

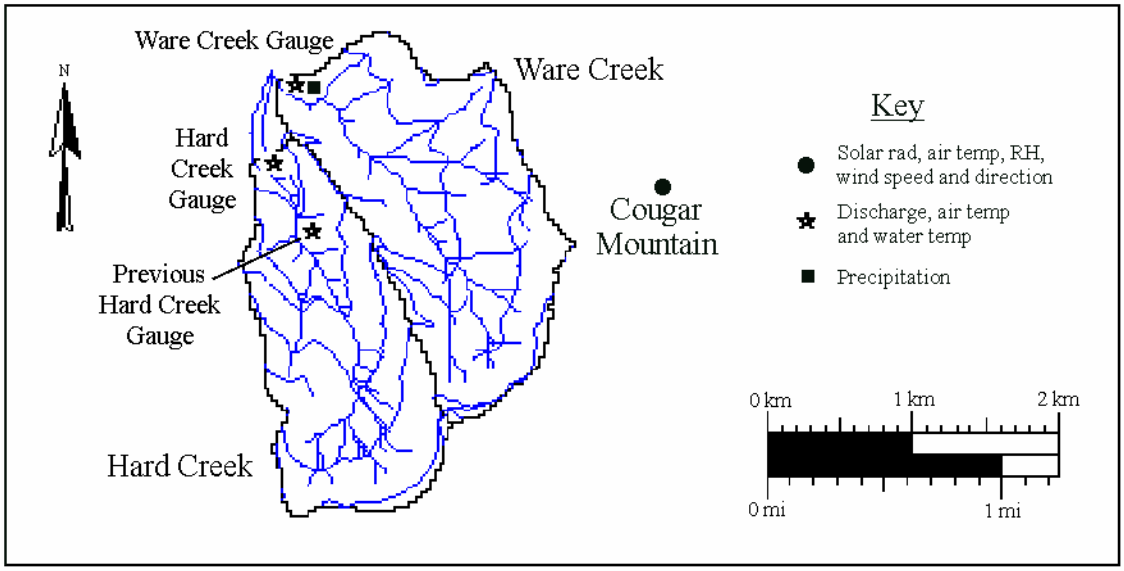

FIGURE 5-3: LOCATION OF THE HARD AND WARE CREEK GAUGES

5.4.1: AIR TEMPERATURE

Hourly air temperature data were collected at the Ware Creek gauge between April and July 1989, and January 1995 through the present. Half-hourly air temperature data were collected between July 1990 and December 1994. A two hourly time series was created for this period by averaging all air temperature measurements collected within each two hour interval. Air temperature prior to 1989 was calculated based on the air temperature at Olympia Airport. Monthly mean temperatures were calculated

for both locations using data from 1989 -1996. On an average annual basis, Olympia Airport is 2.4 ^{o}C warmer than Ware Creek, ranging from 1.5 ^{o}C warmer in January to 4.5 ^{o}C warmer in June. Air temperature from Olympia Airport was adjusted by the difference in monthly means for each month to create the Ware Creek temperature record for 1985-1988.

The temperature lapse rate is also specified for each model time step. As discussed in Chapter 3.1.2, temperature inversions occur frequently in the Ware Creek basin. Higher elevation air temperature at the Cougar Mountain site is only available from January 1995 - June 1996. Therefore, to account for inversions in the specification of temperature lapse rate, a simple algorithm was developed to predict the occurrence of temperature inversions. The occurrence of an inversion within a 6 hour time period was compared to wind speed, cloud cover and time since precipitation. The following factors were tested as predictors of inversion occurrence:

- Wind speed < 7 m/s;
- Cloudiness < 50 %; and
- Dryness (No precipitation for 12 hours before and 6 hours after).

The number of inversions predicted by each of these factors alone for each month of 1995 is summarized in Table 5-7. The number of false predictions for each month is also included in Table 5-7. Dryness appears to be the best predictor of inversion occurrence during the winter months. All three factors can predict the majority of inversion occurrences during the summer months. However, the number of false predictions often exceeds the number of inversions for a month. From a modeling point of view, the development of inversions is more important during winter and most during winter precipitation events, when air temperature will control whether precipitation will fall as rain or snow. The temperature records for Hard and Ware Creek indicate that temperature inversions generally do not occur during precipitation events. Given that, it becomes most important to correctly estimate the

occurrence of inversions during winter months, when the temperature lapse rate will effect the rate of ablation at higher elevations.

TABLE 5-7: COMPARISON OF INVERSION OCCURRENCE WITH WIND SPEED, PRECIPITATION AND CLOUDINESS

	No. of	Wind < 7 m/s[2]		Cloudiness < 50%[3]		Dryness[4]	
	Inversions[1]	No. Predicted	No. False Predicted	No. Predicted	No. False Predicted	No. Predicted	No. False Predicted
January	16	1	14	1	3	13	17
February	44	20	25	8	16	37	15
March	38	26	23	24	8	35	8
April	22	22	67	19	25	20	21
May	36	26	55	34	34	35	52
June	27	26	79	27	33	27	78
July	20	14	64	17	27	16	64
September[5]	13	8	13	13	0	13	1
October	38	27	44	5	7	35	24
November	28	13	8	2	6	21	4
December	38	29	11	0	8	27	13

Notes:

[1] The number of 6 hour time periods within the month for which the Cougar Mountain temperature exceeded the Ware Creek temperature.
[2] Based on NCEP/NCAR reanalysis data interpolated to Cougar Mountain, as explained in Section 5.5.1.
[3] Calculated from equation 5-3 in Section 5.4.2.
[4] Precipitation at Ware Creek is used as a surrogate for dryness. If no precipitation occurred at Ware Creek for the six hours prior to, after and during the current time step, the air is considered dry.
[5] No data available August 1995.

To reduce the number of false predictions, the two joint sets of inversion occurrence predicted by wind/dryness and cloudiness/dryness were also examined, as summarized in Table 5-8. For summer months, including cloudiness significantly reduces the number of false predictions with little decrease in the number of true predictions. For winter months, dryness alone still seems to be the best predictor of inversions. Using this information, a lapse rate time series was created. The lapse rate was assumed equal to -5.5 ^{o}C/km for time steps without an inversion and equal to 5.5 ^{o}C/km for timesteps with an inversion. For October - March, inversions are assumed to occur in a given time step if no precipitation was recorded at Ware Creek for the 12 hours before and 6 hours following the given time step.

Inversions are assumed to occur between April and September if there is no precipitation and the cloud cover is less than 50%.

TABLE 5-8: COMPARISON OF INVERSION OCCURRENCE WITH COMBINED PREDICTORS

Month	No. of Inversions	Wind < 7 m/s and Dryness			Cloudiness < 50% and Dryness			Dryness		
		Predicted		No. False Predicted	Predicted		No. False Predicted	Predicted		No. False Predicted
		No.	%		No	%		No	%	
January	16	1	6	4	1	6	3	13	81	17
February	44	17	39	11	7	16	6	37	84	15
March	38	25	66	6	23	61	5	35	92	8
April	22	20	91	20	19	86	15	20	90	21
May	36	23	64	36	32	89	33	35	97	52
June	27	22	81	75	25	93	30	27	100	78
July	20	11	55	51	15	75	26	16	80	64
September[1]	13	8	62	0	13	100	0	13	100	1
October	38	25	66	19	5	13	3	35	92	24
November	28	12	43	1	1	4	0	21	75	4
December	38	27	71	11	0	0	1	27	71	13

Note:

[1] No data available August 1995.

5.4.2: SOLAR RADIATION AND HUMIDITY

Local observations of solar radiation and vapor pressure were not available for the entire length of the model run. Therefore, these inputs were calculated using physically based formulas. Longwave radiation was calculated for each timestep based on observed air temperature, following a method given by Bras (1990):

$$I_l = U_c E_a \sigma T_a^4 \quad \textbf{5-1}$$

Where T_a is the local air temperature (in Kelvin) for each timestep, U_c is the fraction of cloudless sky insolation received on a day with overcast skies, σ is the Stefan-Boltzmann constant, equal to 5.67x10^{-8} W/m^2K^4 and E_a is the atmospheric emissivity:

$$E_a = 0.7 + 0.0000595 \cdot e \cdot \exp(1500/T_a) \quad \textbf{5-2}$$

Where *e* is the vapor pressure at the gauge in millibars. The cloudiness, U_c , is related to the fraction of sky covered by opaque clouds, *N*, by (Bras 1990):

$$U_c = 1 + 0.17N^2 \quad \textbf{5-3}$$

N takes a value of 1 for completely overcast skies.

The amount of sunlight incident on the earth's surface depends on atmospheric conditions. Water vapor, dust, pollutants, ozone and clouds will all attenuate the radiation incident on the outer edge of the earth's atmosphere. The daily transmittance, T_t is the fraction of radiation at the top of the atmosphere which reaches the ground along the zenith path (Gates 1980). Detailed information about cloud cover is not available, so fractional cloud cover can be estimated from measured shortwave radiation, and therefore, the daily transmittance, T_t (Bras 1990, Gates 1980):

$$N = \sqrt{\frac{1.0}{0.65}\left(1 - \frac{T_t}{T_{CS}}\right)} \quad \textbf{5-4}$$

Where T_{CS} is the clear sky transmittance which was assumed to be 0.72. Daily total atmospheric transmittance is calculated according to the method of Bristow and Cambell (1984):

$$T_t = A\left[1 - \exp\left(-B\Delta T^C\right)\right] \quad \textbf{5-5}$$

Where ΔT is the daily range of air temperature, calculated as:

$$\Delta T(j) = T_{\max}(j) - \left(T_{\min}(j) + T_{\min}(j+1)\right)/2 \quad \textbf{5-6}$$

Where *j* is an index of the current julian day. The mean of the two minimum temperatures was used to reduce the effect of large-scale hot or cold air masses which may cross the study area. For example, a warm air mass moving through the area on day *j* may increase $T_{max}(j)$ above the value possible from incoming radiation alone (Bristow and Campbell 1984). Including the minimum temperature on either side of this day will reduce the short term increase in temperature, since it will most likely not be reflected in both daily minimums.

The variables *A*, *B* and *C* in equation 5-5 are empirical coefficients defined by Bristow and Campbell (1984). *A* and *C* were found to equal 0.72 and 2.4 respectively, for Seattle/Tacoma Washington. *B* was calculated from the monthly mean ΔT according to:

$$B = 0.036\exp\left(-0.154\overline{\Delta T}\right) \quad \textbf{5-7}$$

In order to obtain shortwave radiation at the ground surface, the calculated transmittance must be multiplied by the solar radiation above the atmosphere. The instantaneous amount of solar radiation incident on a horizontal surface at the top of the atmosphere can be computed by (Gates 1980):

$$Q_o = S_o\left(\frac{\bar{d}}{d}\right)^2\left(\sin\phi\sin\delta + \cos\phi\cos\delta\cos(h_s)\right) \quad \textbf{5-8}$$

Where S_o is the solar constant (1360 W/m^2), $\bar{d}$ is the mean distance from earth to sun, *d* is the local distance from sun to earth, φ is the local latitude, δ is the solar declination (Bras 1990):

$$\delta = 23.45 \cdot \cos\left(\frac{2\pi}{365}(172 - j)\right) \quad \textbf{5-9}$$

h_s is the half daylength, given by:

$$\cos(h_s) = -\tan\phi \tan\delta \quad \textbf{5-10}$$

All angles are in radians. Gates (1980) noted that $\left(\bar{d}/d\right)^2$ never differed from unity by more than 3.5 %, so it was assumed to be one. In order to compute the average irradiance for each model time step, equation 5-8 is integrated between the corresponding sun angles, as follows:

$$Q_{ij} = \int_{h_i}^{h_j} S_o(\sin\phi\sin\delta + \cos\phi\cos(h))\, dh/\omega \quad \textbf{5-11}$$

$$= \frac{S_o}{(h_j - h_i)}\left[(h_j - h_i)\sin\phi\sin\delta + \cos\phi\cos\delta(\sin(h_j) - \sin(h_i))\right]$$

To get the total irradiance in J/m^2 for each time step, Q_{ij} must be multiplied by 7200 seconds/time step. The average attenuated shortwave radiation for each time period is calculated as the product of the average incident radiation and the daily total transmittance:

$$I_s = T_t \cdot Q_{ij} \quad \textbf{5-12}$$

The saturated vapor pressure, e_s in kPa, is calculated from temperature as follows:

$$e_s = 0.6108\exp\left(\frac{17.27T_{air}}{237.3 + T_{air}}\right) \quad \textbf{5-13}$$

The quantity of direct solar radiation observed by a hillslope depends on slope and aspect, as well as shading effects from surrounding topography. Solar radiation incident on a pixel is composed of direct and diffuse radiation. Direct beam radiation has two components: direct radiation from the sun and

ground-reflected radiation. Direct radiation on the slope is controlled by the angle of illumination between the incident solar rays and the normal to the slope (Gates 1980). Diffuse solar radiation consists of the diffuse skylight and isotropically ground-reflected sunlight and skylight (Gates 1980).

The effect of terrain reflectance and shadowing on the total clear sky shortwave radiation received by each model pixel was calculated independently of DHSVM following the method of Arola (1993) and Dubayah (1990), using the Image Processing Workbench (IPW) developed by Frew (1991). Diffuse and direct beam radiation is calculated monthly for each pixel based on the distribution of solar radiation at the solar midpoint of each month and then discretized into ten equiprobable classes. This method provides clear sky radiation for each pixel in the basin at each model time step. The IPW-derived solar radiation is then scaled based on the radiation time series created using equation 5-11.

Relative humidity was calculated from observed temperature using daily minimum temperature as a surrogate for dew point temperature, as follows:

$$RH = e / e_s = \exp\left(\frac{17.27 T_{\min}}{237.3 + T_{\min}} \right) / e_s \qquad \textbf{5-14}$$

5.4.3: PRECIPITATION

Precipitation data from the Ware Creek gauge were provided by Weyerheauser for the period 1985 - 1995. The collection frequency changed many times during this period with collection intervals as short as 12 minutes and as long as 2 hours. Precipitation collected at shorter time intervals was aggregated up to the two hour time step by summing the observations from the previous two hours. Some of the data collected at two hour intervals were recorded on the odd hour intervals, rather than the even. In these cases, the total precipitation for each two hour interval was split evenly between the surrounding ‘even’ time intervals.

The primary precipitation gauge did not function between February 6, 1992 and March 24, 1992. Data for this time interval was replaced with data from a backup gauge which was temporarily in operation in the basin. Data was also missing for February 12 and 13, 1991. Precipitation for this time period was filled with data from four regional stations using the normal-ratio method. For this method, the amount of precipitation at Ware Creek, P_{wc}, is weighted by the ratios of the normal annual precipitation, as follow:

$$P_{wc} = \frac{1}{4}\left(\frac{N_{wc}}{N_A} \cdot P_A + \frac{N_{wc}}{N_B} \cdot P_B + \frac{N_{wc}}{N_C} \cdot P_C + \frac{N_{wc}}{N_D} \cdot P_D \right) \qquad \textbf{5-14}$$

Where *N* is the station normal annual precipitation and *P* is the station precipitation at each time step. Normal annual precipitation was calculated for the period 1974 - 1994 for Ware Creek and the four regional stations. The stations used and computed precipitation ratios are summarized in Table 5-9.

The completed uniform precipitation record was tested for consistency with the precipitation record at Olympia Airport using a double mass curve (Figure 5-4). The break in slope which occurs around November 1, 1988 indicates that there was a problem with the Ware Creek precipitation record at this time. Subsequent conversations with the Weyerheauser field hydrologist confirmed that the gauge was malfunctioning during this period. Therefore, the Ware Creek precipitation between November 1988 and October1989 was replaced using the normal-ratio method described above. The double mass curve for the corrected record is shown in Figure 5-5.

TABLE 5-9: NORMAL RATIO METHOD PARAMETERS

STATION NAME	ELEVATION	RATIO P_{WC}/P_{STN}
Longmire Rainier NPS	841.9 m	1.595
Olympia Airport	59.4 m	2.210
Rainier Carbon River	528.9 m	1.889
Cinebar	317 m	1.587

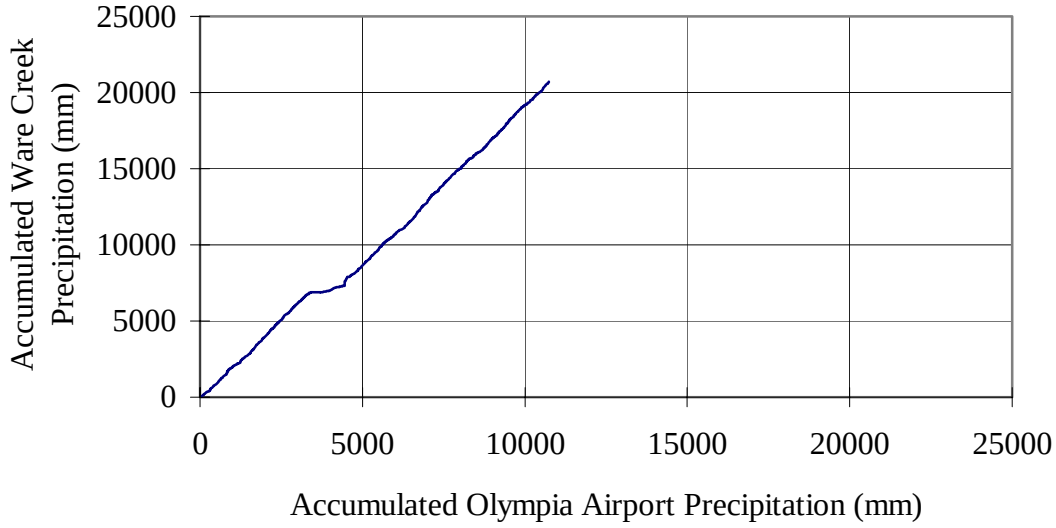

FIGURE 5-4: WARE CREEK PRECIPITATION VERSUS OLYMPIA AIRPORT PRECIPITATION, 1985 - 1994

5.5: WIND DATA

Accurate description of the surface wind field is one of the most difficult model inputs to obtain. Measurements of wind speed are sparse and the extreme influence of topography and other structures makes interpolation from distant stations nearly meaningless. Wind speed is particularly important for quantifying turbulent heat transfer accurately during ROS events. Three different approaches of increasing complexity were used to generate wind inputs for Hard and Ware Creeks. These include:

- Annual average Cougar Mountain wind speed;
- Interpolation of NCEP/NCAR reanalysis fields; and
- Distributed wind modeling.

A recording anemometer was installed 6 meters aove the ground at the top of Cougar Mountain in January 1995. An average annual wind speed of 9.2 m/s was calculated based on the one year of

available data. For the first approach, this average wind speed was used for each model time step. Since it was measured on the top of a ridge, this average is relatively high. It is expected that average wind speeds in the valley bottoms will be much lower. The other two input techniques are described below.

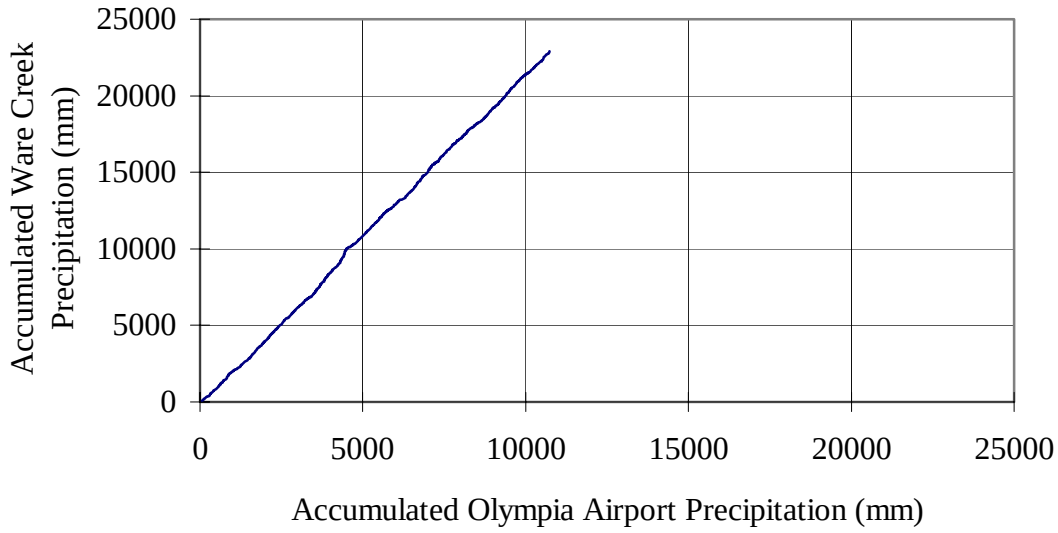

FIGURE 5-5: CORRECTED WARE CREEK PRECIPITATION VERSUS OLYMPIA AIRPORT, 1985 - 1994

5.5.1: NCEP/NCAR REANALYSIS DATA FIELDS

The National Center for Environmental Prediction/National Center for Atmospheric Research NCEP/NCAR Reanalysis Project is an effort to reanalyze historical data using a current and fixed (January 1995) version of the NCEP data assimilation and operational forecast model. The NCEP global spectral model generates many output fields at 2.5^{O} resolution at a 6 hour timestep. U and V winds are available at 17 pressure levels. The geopotential height of each pressure level is also available. Although at coarse resolution, the model does reproduce the general nature of atmospheric circulation including upper air wind speed and direction at 6-hourly intervals.

To supplement the Cougar Mountain record, the 700, 850 and 925 mbar U and V winds were linearly interpolated to Cougar Mountain from the four closest reanalysis fields. These include: -122.5^{O}, 45.0^{O};

-122.5^{O}, 47.5 ^{O}; -120.0^{O}, 45.0 ^{O}; and -120.0^{O}, 47.5 ^{O}. U and V vectors were interpolated separately. Vectors were interpolated in the longitudinal direction before interpolating in the latitudinal direction. After horizontal interpolation, the wind vectors were interpolated in the vertical direction to bring them to the height of Cougar Mountain. The NCAR data reproduce the range and variation of the observed Cougar Mountain wind as illustrated in Figure 5-6. Although the observed wind fields cannot be reproduced, this data set allows us to represent the variability of the natural wind fields.

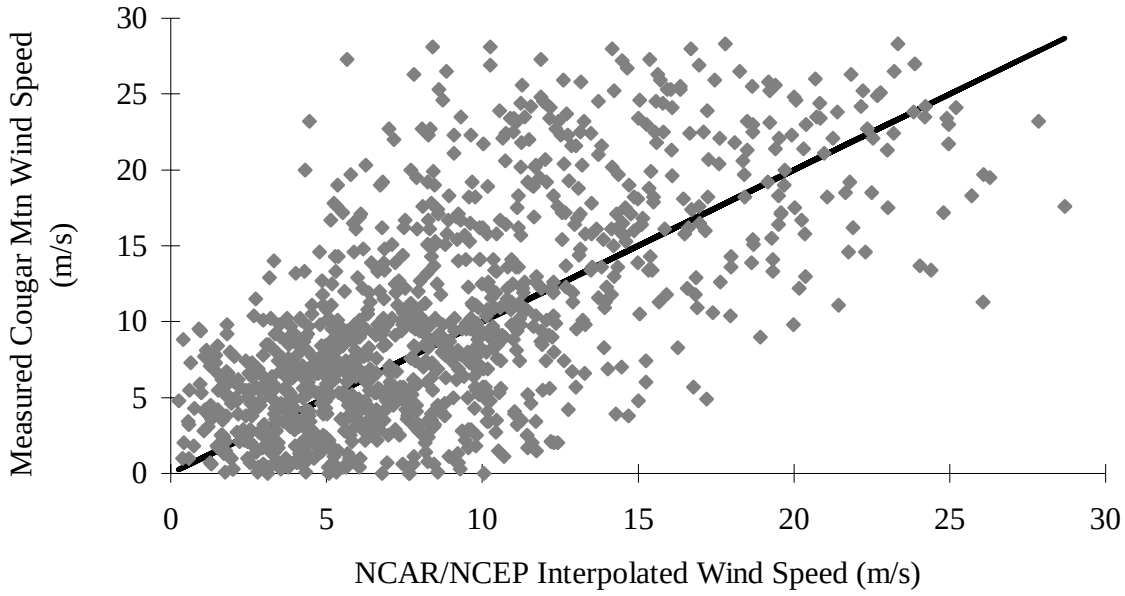

FIGURE 5-6: OBSERVED COUGAR MOUNTAIN WIND SPEED VERSUS NCAR/NCEP MODELED WIND SPEED

5.5.2: NUATMOS DISTRIBUTED WIND MODEL

As noted above, interpolation of station observations to the catchment scale is a meaningless exercise. Wind speed and direction are strongly controlled by topography. During field visits to Hard and Ware Creeks, it became clear that wind speed varies widely within and between the catchments. For instance, even during relatively calm days elsewhere in the basin, one ridge in the northeast corner of Ware Creek always seemed to have higher wind speeds. In addition, during storms individual clouds could be seen

ascending the slope, and their paths indicated a strong topographic influence. For these reasons, DHSVM was modified to include the option of specifying wind maps for each time step and an effort was made to model the distributed wind field.

Two-dimensional wind vectors for each model pixel were obtained using NUATMOS Version 6.0 (Ross et al. 1988, NUATMOS 1992). This model was chosen because it employs terrain following coordinates and variable vertical layers, which are necessary to adequately represent complex mountainous terrain. The structure of vertical layers in the NUATMOS model are illustrated in Figure 5-7. NUATMOS produces wind velocity estimates, averaged over each layer in the vertical, by pushing user-specified wind observations over the topography. This means that for each vertical layer the station wind observations are interpolated while accounting for the varying area of flow. This produces a mass consistent wind field based on interpolation of observations arbitrarily located within the model domain (Ross et al. 1988).

A variational calculus method (Kitada et al. 1983) is used to constrain the flow to be divergence-free using the continuity equation. The method requires minimizing the difference between the initial interpolated wind field and the final wind field, subject to the constraint that the divergence is zero. The constraint equation is incorporated into the minimization integral using lagrange multiplier theory. The choice of lagrange multiplier, $\lambda = 0$, at the free boundaries allows adjustments to be made at the domain boundaries, while $d\lambda/dz$ at the surface ensures that the vertical velocity is preserved at the earth's surface. These boundary conditions are possible due to the selection of terrain following coordinates (sigma layers) in the vertical direction, as follows:

$$\sigma = (z_t - z)/(z_t - z_s) = (z_t - z)/\pi \qquad \textbf{5-15}$$

Where z_t is the top of the solution domain, z_s is surface elevation and z is the elevation above datum. NUATMOS works with a rectangular elevation grid in UTM coordinates oriented with the four cardinal points of the compass. For each time period, wind observations from locations within the grid boundary are required at locations throughout the grid, with observations within each sigma level. A minimum of one upper atmospheric observation is also required for model stability.

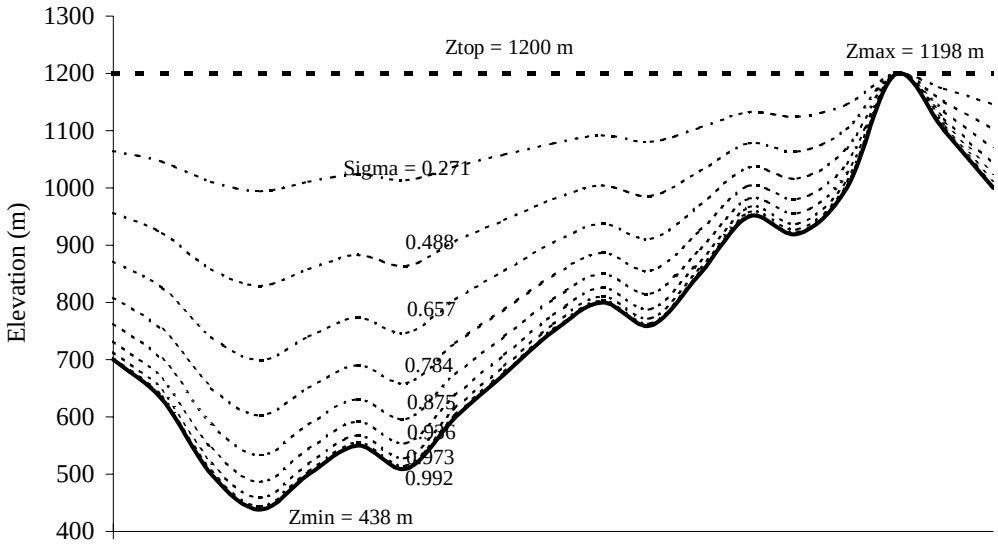

FIGURE 5-7: ILLUSTRATION OF TERRAIN FOLLOWING COORDINATES

There are only limited observations of wind within the DHSVM model domain. Therefore, a nested approach was used to obtain the wind field over Hard and Ware Creeks. The NUATMOS model was first run at a course resolution with 900 m grid cells, to encompass the 2.5^O by 2.5^O area bounded by the NCAR reanalysis data. Wind vectors output for the 900 m model were used as "station" data to drive a fine resolution model over Hard and Ware Creeks. The two model domains are illustrated in Figure 5-8. The fine resolution model was run with 30 m grid cells to correspond to the DHSVM resolution.

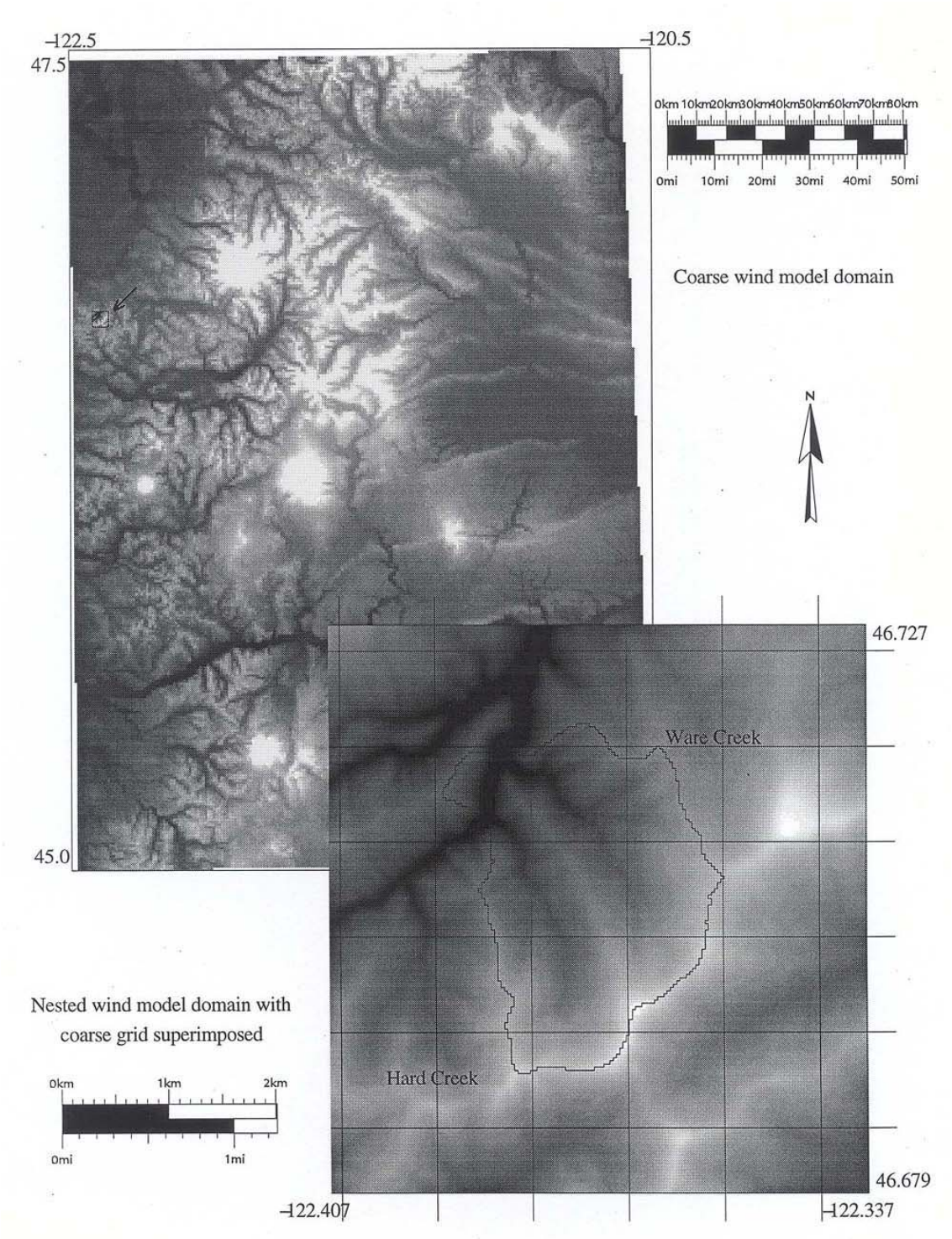

FIGURE 5-8: NUATMOS MODEL DOMAIN

Due to the large data requirements and time required to run the nested models, it is not feasible to solve for a new wind field for each DHSVM model timestep. Therefore, wind maps were developed for the eight primary wind directions (NNE, ENE, ESE, SSE, SSW, WSW, WNW, NNW), based on the reanalysis wind interpolated to Cougar Mountain. For each DHSVM model timestep, the reanalysis wind direction at Cougar Mountain is used to select the appropriate wind map. Each wind map includes the wind speed at each model pixel for the 'design' wind storm. Design wind speeds are based on wind events which generated winds of approximately 10 m/s at Cougar Mountain in 1995. Therefore, for each time step the map wind speed must be scaled according to the 'observed' wind speed at Cougar Mountain. The NCEP/NCAR interpolated reanalysis fields are used as the 'observed' Cougar Mountain time series. The eight completed wind maps are included as Appendix D.

To verify that a linear scaling is applicable, the model was run for a range of wind speeds for winds originating from SSE, SSW, WSW and WNW. Winds at Cougar Mountain originate from the remaining four directions less frequently and reanalysis wind speeds for these directions did not exceed 15 m/s during 1995. Therefore, these directions were not checked for linearity. For each of the wind directions that were checked, wind speed at four points in the two basins was compared to the interpolated reanalysis Cougar Mountain speed, as shown in Figure 5-9 for SSE.

This analysis indicates that a linear scaling factor is applicable, although the difference in slope of the trendlines indicates that the rate of increase is different for different points in the basins. It was also found that the slope of each of the trendlines in Figure 5-8 is not substantially different from the slope between the 10 m/s design storm and zero, as illustrated in Figure 5-9. Therefore, the rate of wind speed increase for each model pixel for an increase in Cougar Mountain wind speed can be approximated by dividing the modeled pixel wind speed by the Cougar Mountain design wind speed. The design storms used for each wind direction are summarized in Table 5-10. Wind speed for each pixel for each time step is then found by multiplying the appropriate rate of increase by the Cougar Mountain wind speed for that time step.

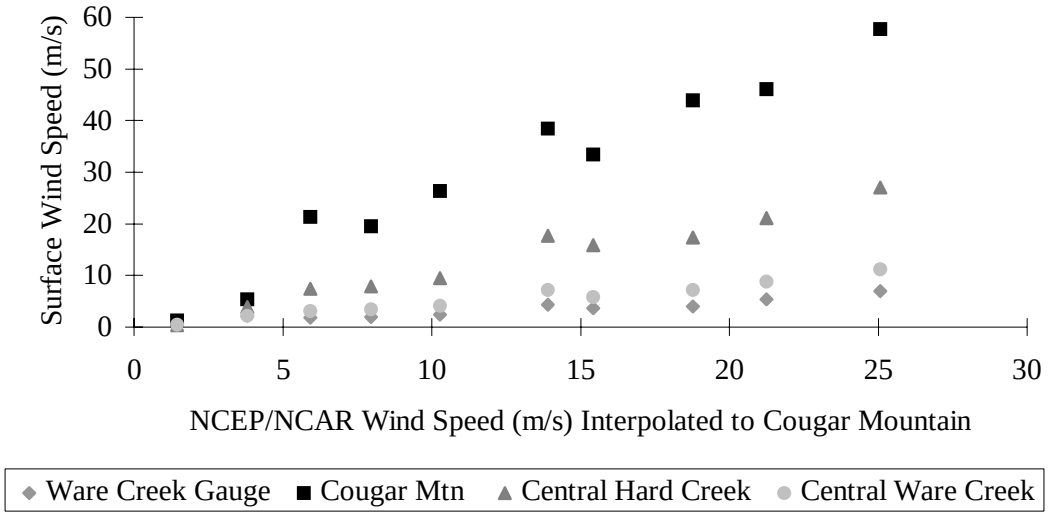

FIGURE 5-9: INCREASE IN WIND SPEED FOR DIFFERENT POINTS IN THE MODELED BASIN

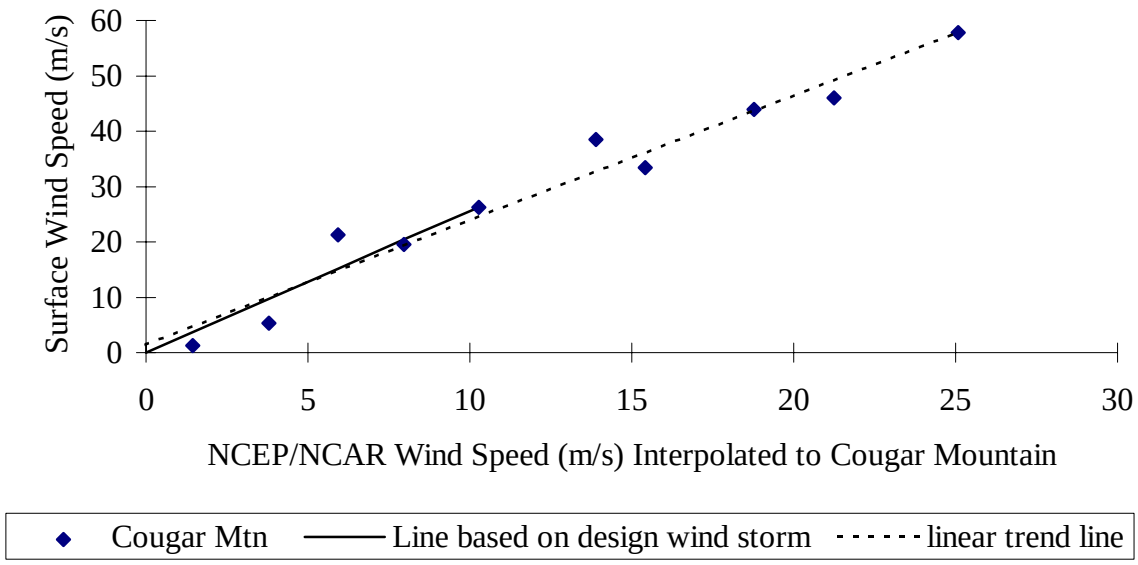

FIGURE 5-10: SLOPE ESTIMATION BASED ON THE DESIGN WIND STORM

In general, use of the NUATMOS model serves to attenuate the higher wind speeds observed on Cougar Mountain within the protected valley bottoms. Depending on wind direction, the wind speeds may be increased relative to the NCAR/NCEP wind speed near ridge tops as air is pushed over the ridges. Wind storms originating parallel to the orientation of the basins (NW and SE) produce the largest wind speeds along the top ridge. The effect of these wind fields, particularly on snow melt, will be explored further in Chapter 6.

TABLE 5-10: DESIGN WIND STORM CHARACTERISTICS

PRIMARY DIRECTION	DATE	INTERPOLATED WIND SPEED (M/S)	WIND DIRECTION (DEGREES)
NNW	7/16/95 18:00	10.17	20.8
ENE	3/2/95 6:00	9.89	82.8
ESE	1/3/95 18:00	10.18	122.8
SSE	1/25/95 18:00	9.55	158.1
SSW	4/20/95 0:00	9.88	200.7
WSW	3/15/95 6:00	10.13	247.6
WNW	11/9/95 18:00	9.94	292.4
NNW	2/11/95 12:00	10.43	334.0

5.6: MODEL CONSTANTS

Several physical constants used in the model are not varied over time or space. Those values which are prescribed at the beginning of the model run are listed in Table 5-11. Some of these values were changed during model calibration, as described in Chapter 6.

TABLE 5-11: CONSTANT MODEL PARAMETERS

PARAMETER DESCRIPTION	VALUE
Roughness of soil surface (m)	0.01
Roughness of snow surface (m)	0.01
Minimum temperature at which rain occurs (C)	-1.5
Maximum temperature at which snow occurs (C)	0.5
Snow liquid water holding capacity (fraction)	0.03
Reference height (m) [1]	90.0
LAI multiplier for rain interception	0.0001
LAI multiplier for snow interception	0.0005
Threshold for intercepted snow which must be melted (m)	0.005
Precipitation lapse rate (m/m/2 hr)	0.00003
Edge length of grid cell (m)	30
Number of rows	115
Number of columns	110

Notes:
[1]The height of surface flux calculations above the overstory. Also the assumed height of the input wind speed.

CHAPTER 6: MODEL CALIBRATION AND SENSITIVITY

DHSVM is a physically-based model, which means that the parameters and inputs described in Chapter 5.0 are meant to be based on physically measurable quantities. For this reason, many parameters were not adjusted during the model calibration process. However, it is not always feasible to make the exhaustive measurements that would be necessary to specify all parameters based on observations. Therefore, some calibration of the less well-defined parameters is required. The time period from July 1, 1993 through June 30, 1996 was selected for model calibration.

Selection of this calibration period includes the period from January 1, 1996 to June 30, 1996 for which field observations of culvert discharge were available. In addition, the calibration period encompasses the large ROS event of February 5-8, 1996, as well as the smaller April 28, 1996 event. The model run was started on October 1, 1992 to allow sufficient time for the model to respond to initial conditions. By going through an entire annual cycle, the fall storms of 1995 reflect the modeled summer dry down period. Initial hydrological conditions on October 1, 1992 specified no snow and no precipitation intercepted in the canopy. Soil moisture was assumed to be at field capacity. These are realistic conditions for early autumn before significant rain has fallen, but nonetheless the first seven months of simulation were ignored during the calibration.

The model was first run with the parameters and inputs described in Chapter 5.0. Since the calibration period represents current conditions, the model representation of both road and channel networks was implemented. In addition, the variable soil depth map and NUATMOS wind model (Section 5.5.2) were used during calibration.

6.1: MODEL CALIBRATION

The first step in model calibration included a general check of snow accumulation and ablation. An estimation of the snow line elevation was made during field visits in 1996. The estimated snow line was compared to the modeled distribution of snow water equivalent (SWE) for the date of each of the field visits, as shown in Figure 6-1. The black line in these figures illustrates the snow line inferred from field observations. The shaded areas represent the modeled SWE. On January 4th and 6th, the modeled SWE appears to be more widespread than was observed. However, the observed snow line was usually estimated as the location where solid snow cover began. The modeled SWE over much of the basin on January 4th and 6th is very thin and most likely would appear as patchy cover in the field. For example, on February 15th, patches of snow were observed down to 670 meters, although the snow line was recorded at 1067 m. This partially explains the higher modeled SWE equivalent relative to observed on February 15 and March 14. The February, 1996 ROS event was characterized by high winds and a high rate of turbulent mixing of the air (Storck, personal communication). This results in fairly homogeneous, hydrostatic conditions with no temperature inversions. The NCEP/NCAR interpolated wind speeds at Cougar Mountain during this storm vary between 16 m/s and 25 m/s. Although these wind speeds are quite high, Cougar Mountain is an exposed site, and the effect of the distributed wind model attenuates the velocities. This effect will be explored further in Section 6.3.

The sequence of images beginning on April 12th indicates that the radiation-dominated melt-out in the spring is well represented. The general comparison presented in Figure 6-1 indicates that the distribution of temperature, precipitation, wind and radiation performed by DHSVM is able to represent snow accumulation and ablation reasonably.

DHSVM was further evaluated by comparison of the observed and modeled catchment water balance. The total precipitation at the Ware Creek gauge during the calibration period was 7.972 m. The total observed discharge during this period was 7.017 m for Hard Creek and 6.137 m for Ware Creek.

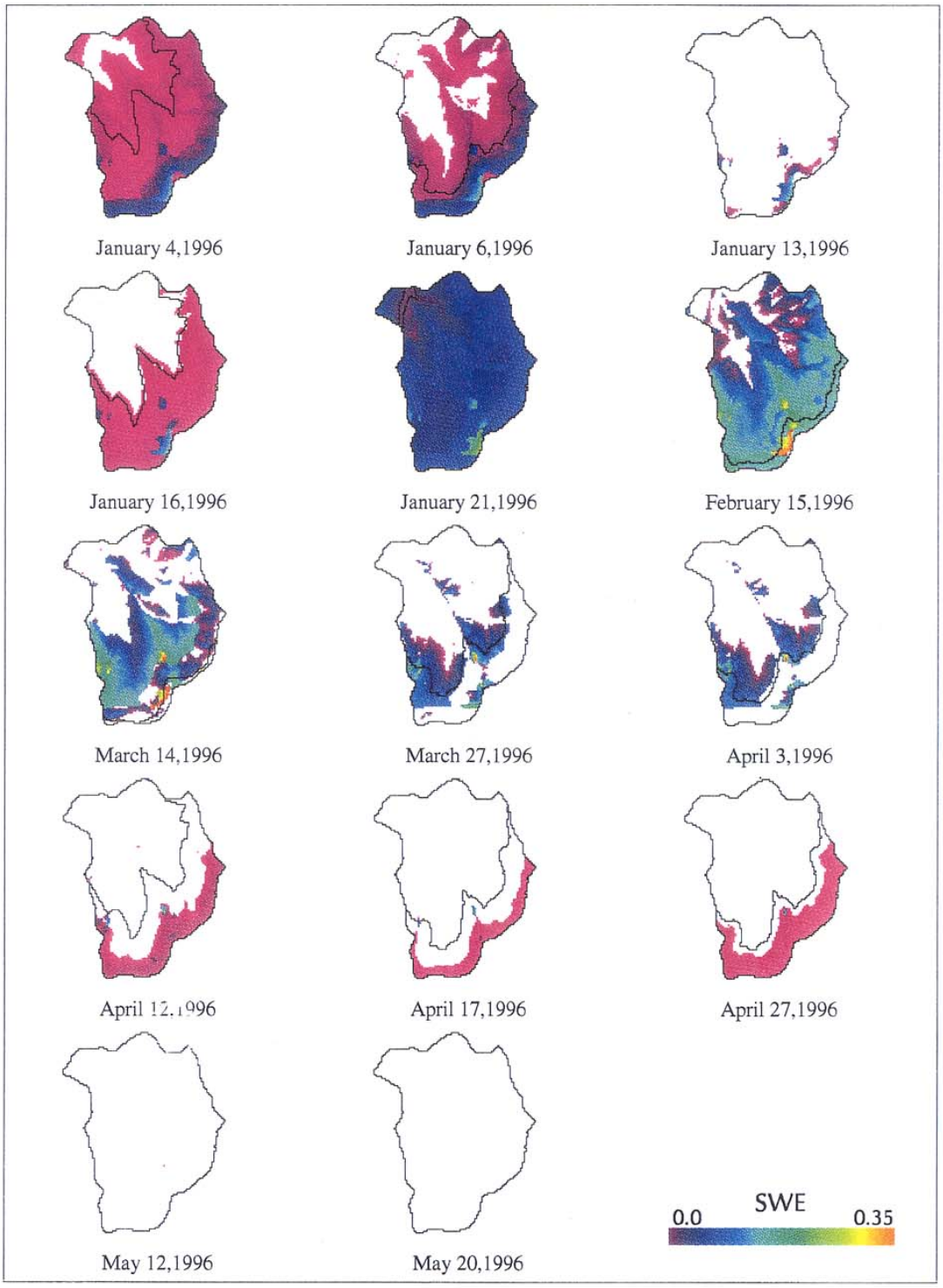

FIGURE 6-1: COMPARISON OF SIMULATED SWE WITH OBSERVED SNOWLINE

Assuming constant precipitation over both basins and that all discharge is captured at the stream gauge, mass balance yields an approximate water loss due to evapotranspiration and snow vapor flux (sublimation from the snow surface) of 1.44 m. Initial model runs did not produce combined evapotranspiration and snow vapor flux of this magnitude. Therefore, the LAI indices for all vegetation classes were increased until evapotranspiration was approximately correct. LAI was increased a total of 45 %. This reflects the uncertainty of the values of LAI used. These LAI values were based on observed values for mature trees. These were scaled downward linearly based on total tree height. As trees do not grow leaves linearly, it is not surprising that these values required adjustment. It is also possible that underflow at one or both of the stream gauges yields overestimation of the annual average evaporation by the mass balance. Neither of the stream gauges is tied into bedrock and the valley material is very coarse textured. DHSVM does not allow loss of water from the basin by deep subsurface seepage, therefore it is assumed that all moisture losses are due to evapotranspiration and snow vapor flux. The possible over-estimation of evaporation rates would contribute to underestimation of peak flows following dry periods. Total evapotranspiration for the final model calibration averaged 1.56 m for the two basins. Estimated evapotranspiration is slightly high when compared to the water balance, which in part reflects the difficulty in matching the water balance for both Hard and Ware Creeks simultaneously.

The observed discharge record for Hard and Ware Creeks from July 1993 through June 1996 was used to further evaluate model performance during the calibration period. The mean predicted Hard Creek discharge for each two hour timestep is compared to the mean observed discharge in Figure 6-2. A similar plot of Ware Creek discharge is given in Figure 6-3. Aside from LAI, the parameters adjusted during this calibration include the lateral hydraulic conductivity, the exponent for decrease in lateral hydraulic conductivity, the deep layer soil depth and the height of the road cuts. The height of the road cuts was adjusted when trying to match observed culvert discharge, as described below. The need to change this value may reflect an inaccurate representation of the road geometry by the model.

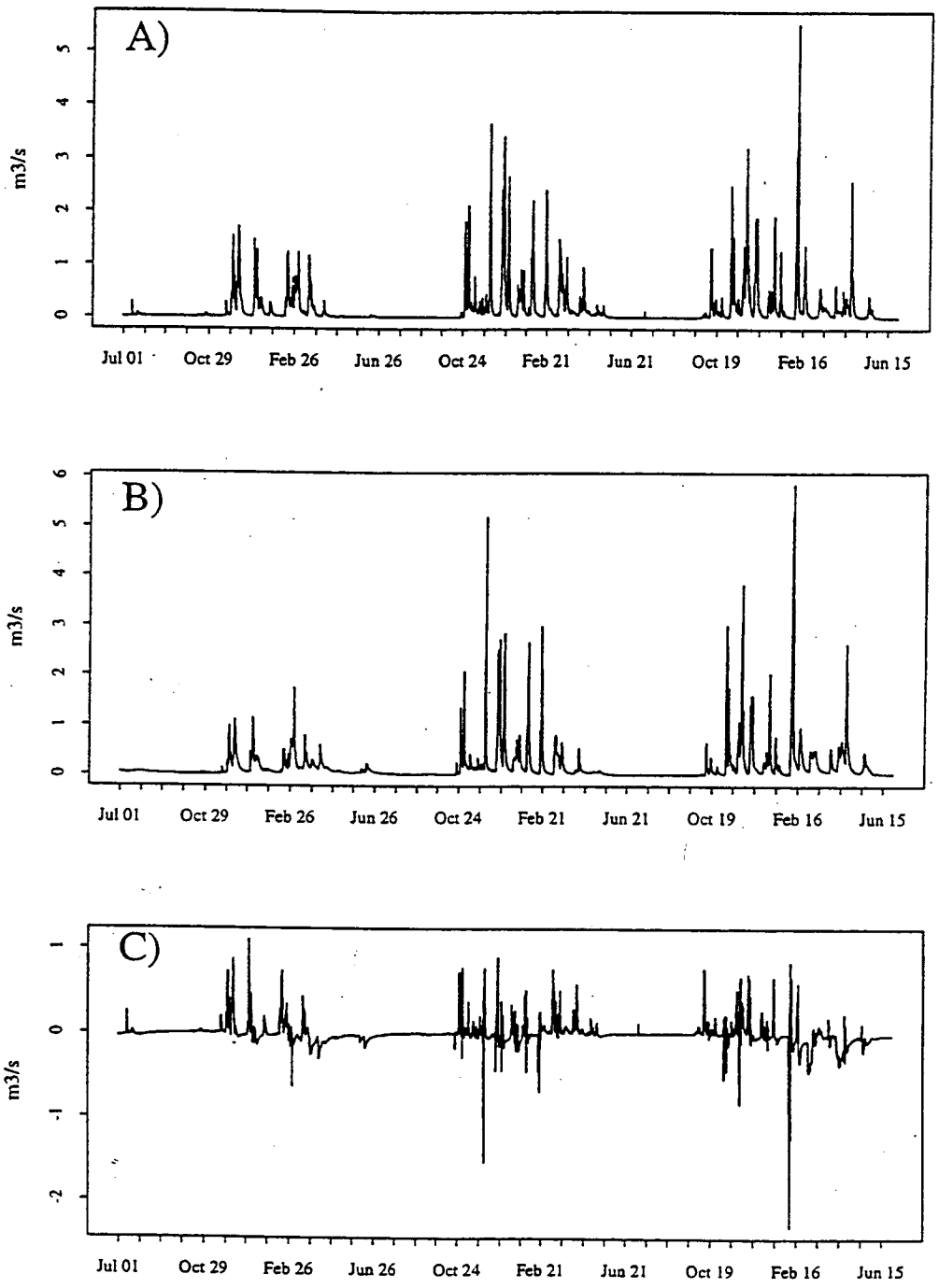

FIGURE 6-2: OBSERVED VS. PREDICTED HARD CREEK DISCHARGE FOR MODEL CALIBRATION, JULY 1, 1993 - JUNE 30, 1996
A) Average 2hr predicted discharge, B) Average 2 hr observed discharge, C) predicted - observed discharge

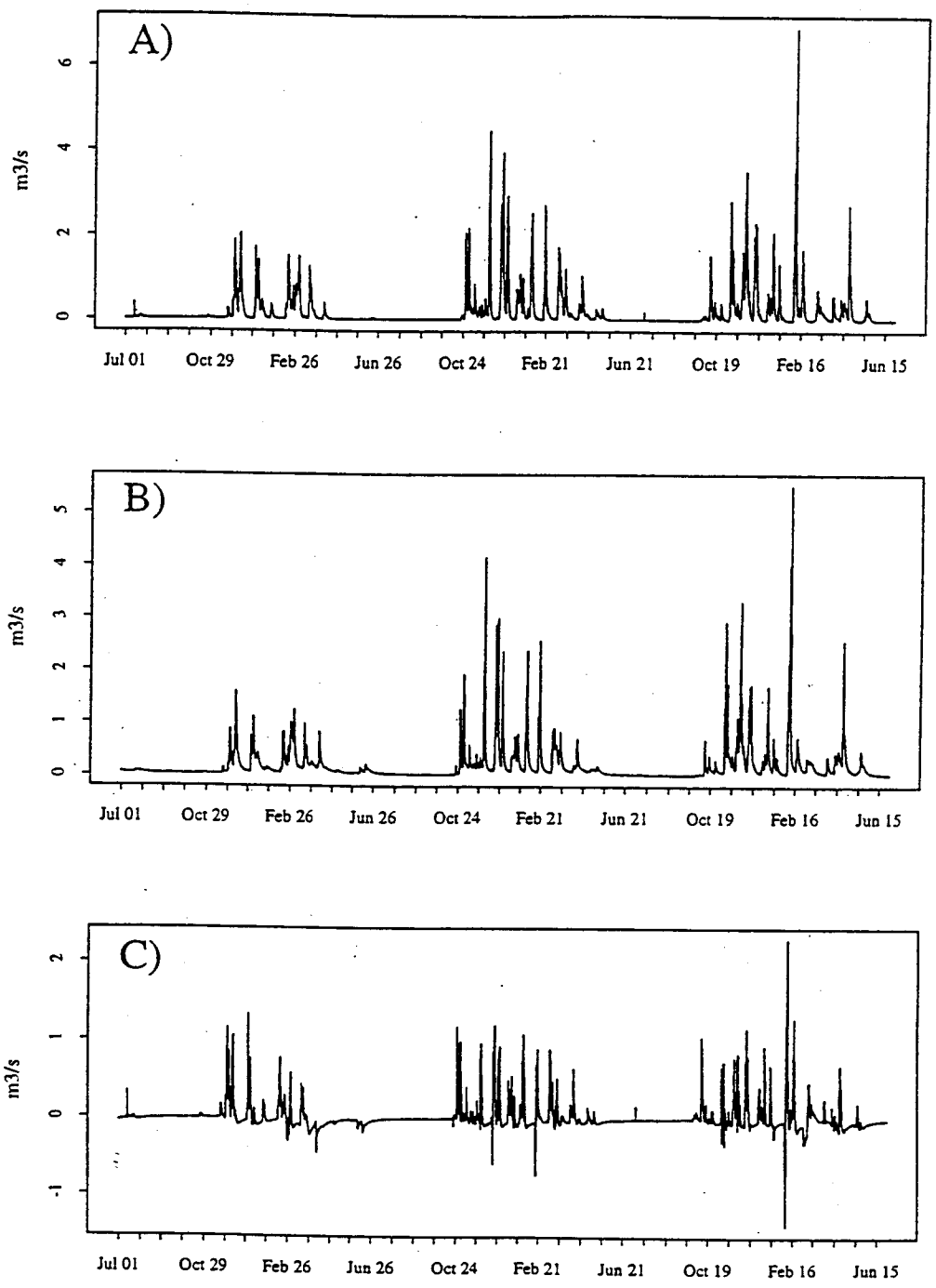

FIGURE 6-3: OBSERVED VS. PREDICTED WARE CREEK DISCHARGE FOR MODEL CALIBRATION, JULY 1, 1993 - JUNE 30, 1996
A) Average 2hr predicted discharge, B) Average 2 hr observed discharge, C) predicted - observed discharge

Most events are fairly well represented. In general, the model underpredicts base flow and overpredicts storm peaks. There is evidence of a slight delay in the model's timing of peak flows which creates a relatively small percentage underprediction, followed by an overprediction. Since the overprediction coincides with the falling limb of the observed hydrograph, the percentage difference can be quite high. In addition, both Figures 6-2 and 6-3 show a very large percentage error in July 1995. This is due to a small summer rainstorm. The observed record shows no streamflow response for this storm. The model discharge produced a sharp pulse, which results in a large percentage error in comparison to the observed low summer discharge.

Total simulated Hard and Ware Creek discharge for the calibration period was 6.62 and 6.37 m, respectively. This represents an overestimation of Ware Creek streamflow and an underestimation of Hard Creek streamflow.

There are two explanations for the difficulty in correctly simulating the water balance in both basins. One is the effect of microclimatology in these steep mountainous basins. As the area elevation curve in Figure 6-4 indicates, the basins have a fairly similar distribution of elevation ranges. Therefore, a simple linear precipitation lapse rate will not result in a significant precipitation difference for the two basins. However, the data record indicates that localized precipitation differences must exist, since there is no consistent trend in catchment response. For example, annual average discharge for the period of record is higher for Ware Creek, however for the calibration period the normalized Hard Creek discharge is higher. The predominant wind direction in these basins is from the southwest. Storms traveling in this direction will cross Hard Creek first and possibly dry out a bit before crossing into Ware Creek. These localized differences in precipitation rate cannot be accounted for within the simulation without an explicit orographic precipitation model.

The final water balance is also very dependent on the total soil depth. Figures 6-2 and 6-3 indicate that base flow is underestimated in both basins. In addition, the model recessions from peak flows tend to be

too steep. This is better observed in a close-up of the hydrograph for the April 23, 1996 event in Figure 6-5. This figure shows that the hydrograph peak is well represented. The timing for the beginning of rise is also fairly well represented, with simulated response slightly lagged in Hard Creek and slightly advanced in Ware Creek. In both cases the difference in timing is approximately two hours and may be due in part to the discretization of stream flow into two hour averages. However, for both hydrographs, the simulated recession is more abrupt than the observed. The length of the recession can be controlled by the deep layer soil depth. Increasing the depth increases the soil moisture storage throughout the basin which can drain more gradually. The final hydrographs presented here represent a compromise between simulated stream flow recessions and the total basin water balance.

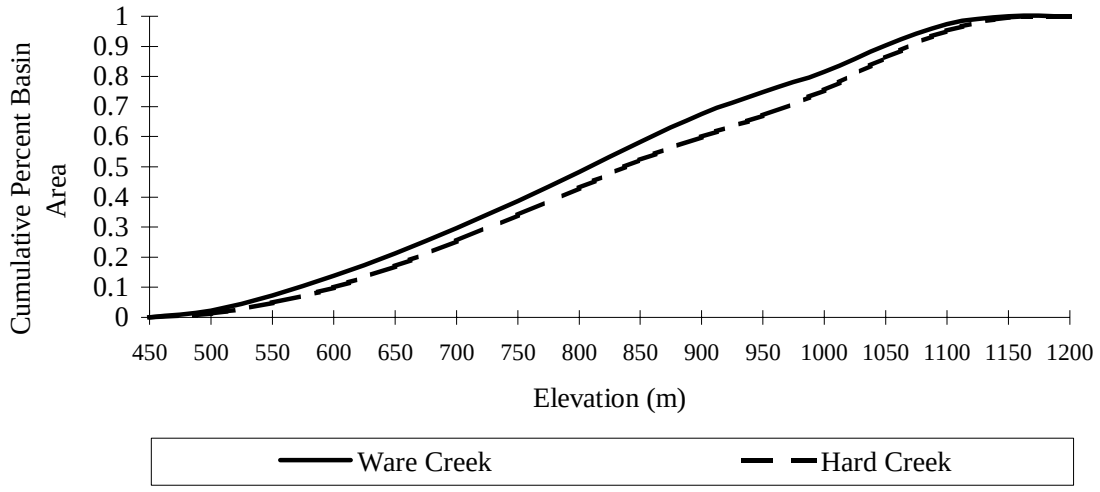

FIGURE 6-4: AREA-ELEVATION CURVES FOR HARD AND WARE CREEKS

The model calibration was further evaluated with comparison to peak culvert discharge measured in the field between January and June 1996. Simulated discharge from ten of the monitored road segments is compared to observed point values in Figures 6-6 and 6-7. The remaining two monitored road segments lie outside the basin and so are not included in the model domain. Square points represent peak stages measured between field visits (via crest stage recorders) and round points represent observed stages on field visit dates. The peak stages were assigned to the day of maximum rainfall, so some offset in timing

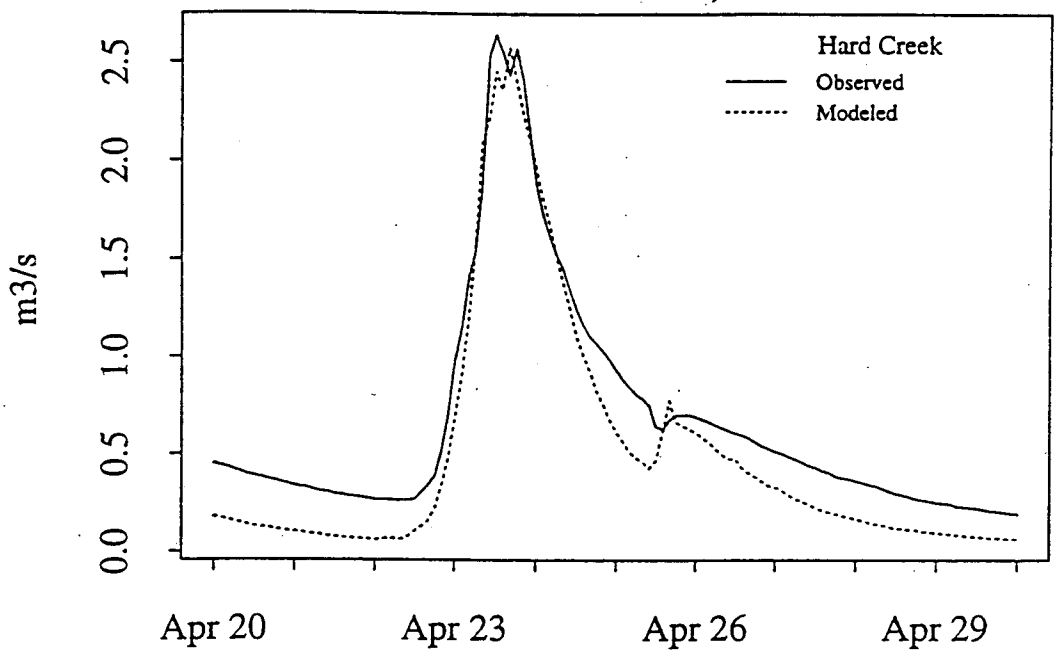

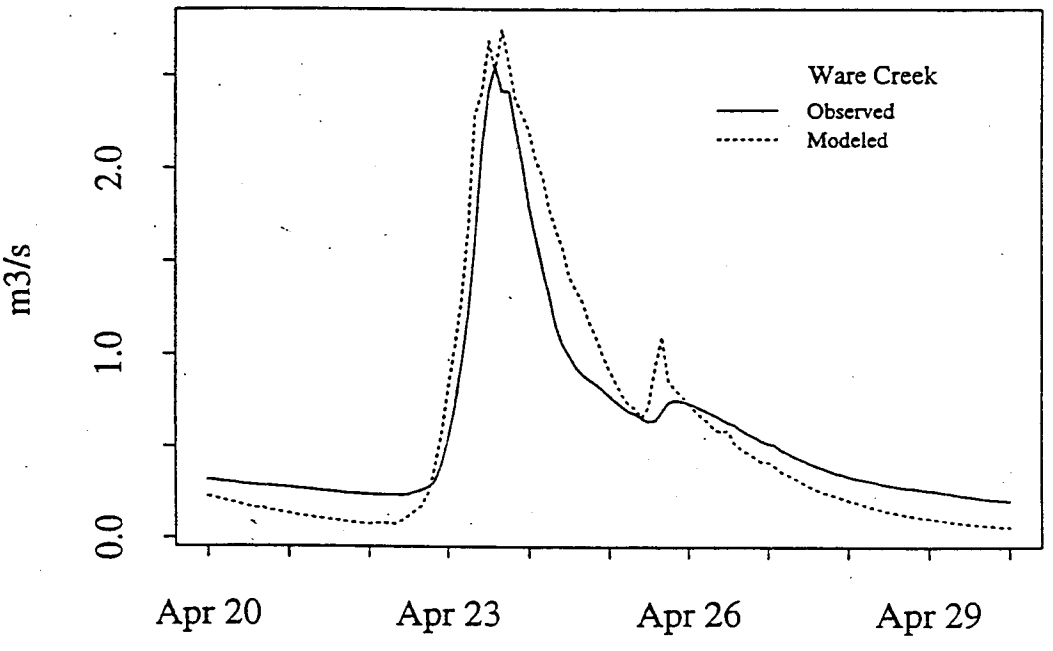

FIGURE 6-5: HARD AND WARE CREEK DISCHARGE, APRIL 20, 1996 - APRIL 30, 1996

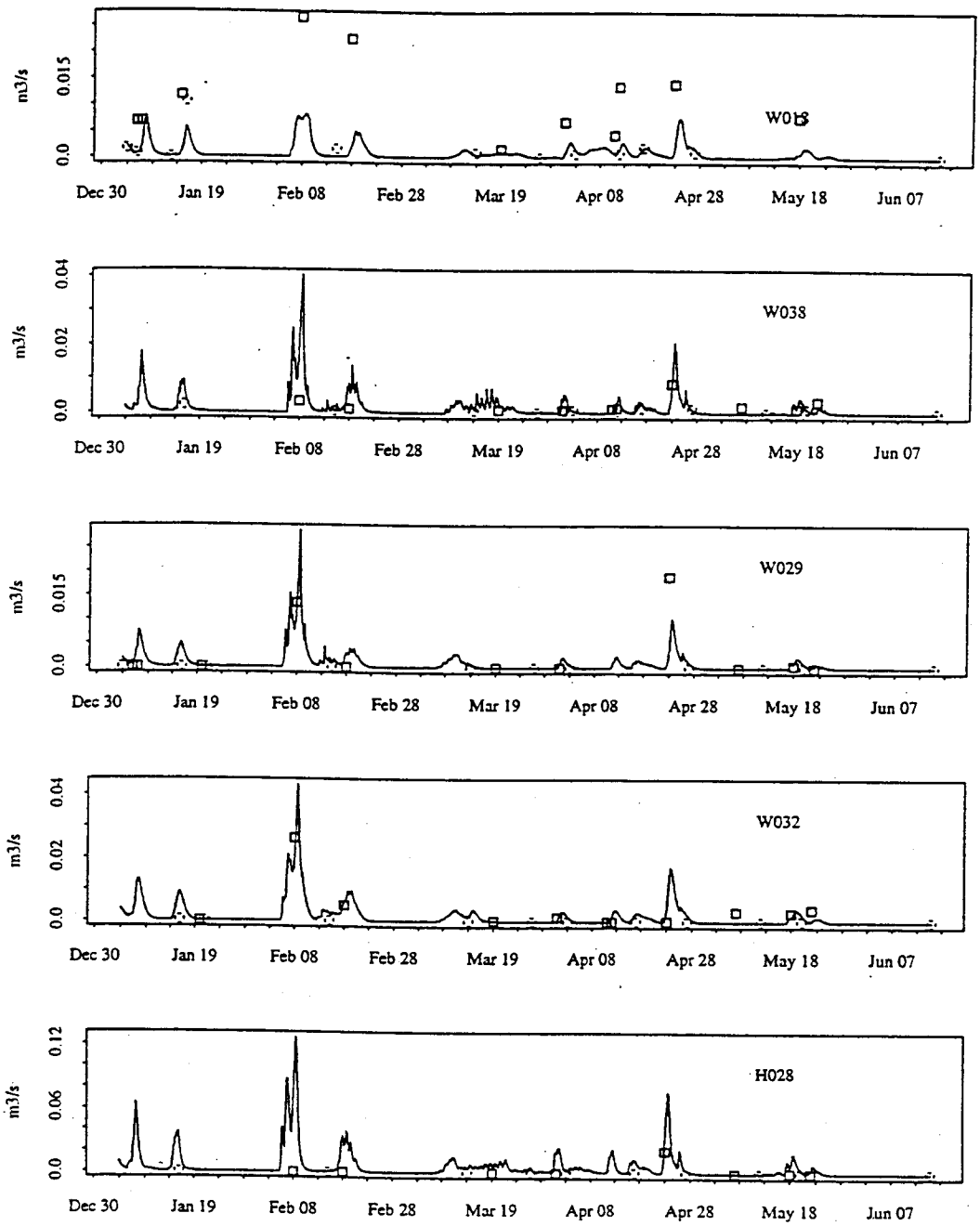

FIGURE 6-6: MONITORED WARE CREEK CULVERT DISCHARGE, JANUARY 4, 1996-JUNE 15, 1996
Squares represent estimated peak discharges, circles are observed discharge and lines are the simulated culvert discharge.

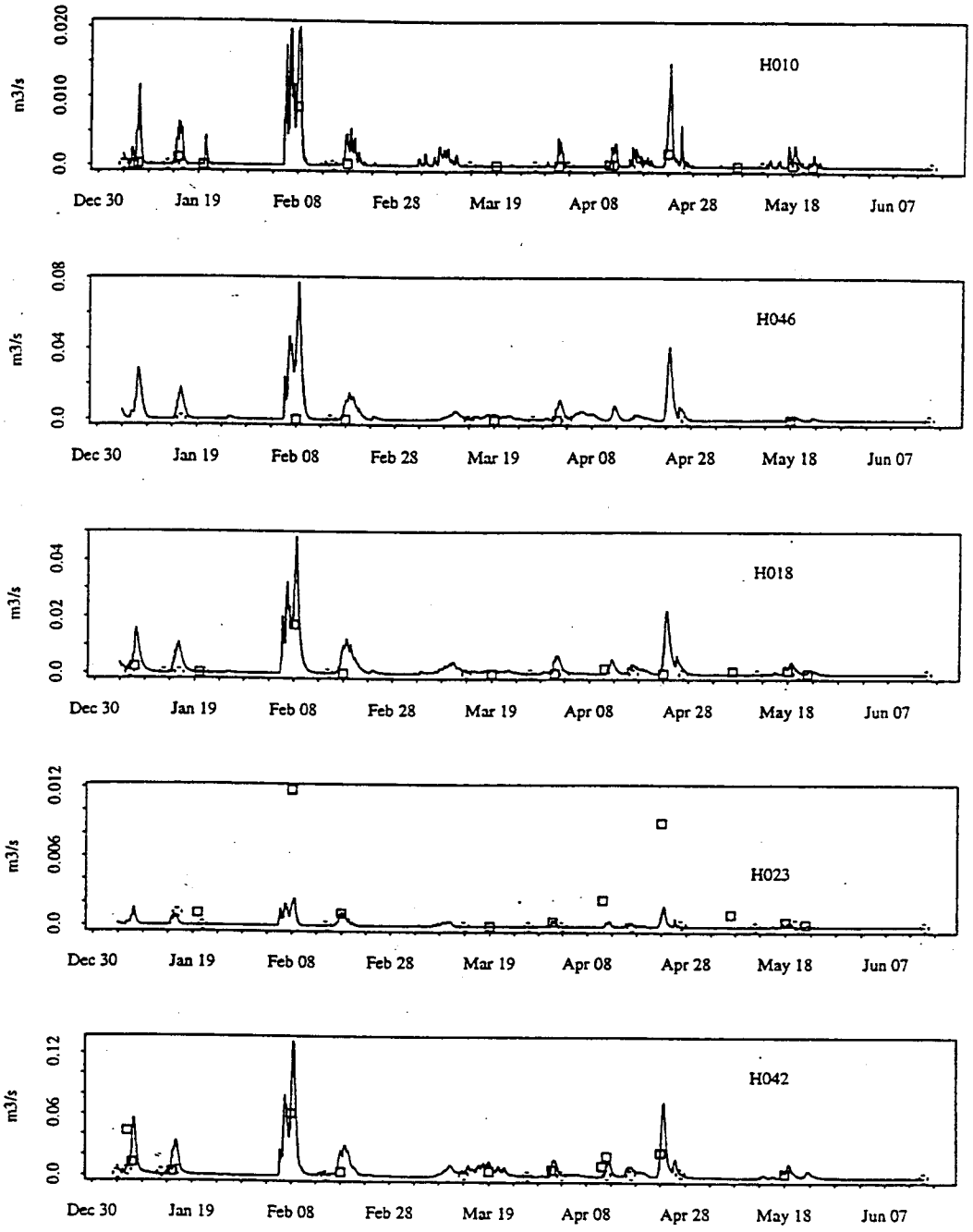

FIGURE 6-7: MONITORED HARD CREEK CULVERT DISCHARGE, JANUARY 4, 1996 - JUNE 15, 1996
Squares represent estimated peak discharges, circles are observed discharge and lines are the simulated culvert discharge.

may occur. The simulated discharge is seen to respond to individual rainfall events throughout the season, with little baseflow between events. This is consistent with field observations. Some of the culverts, such as culvert H042 in Figure 6-7 have flow perennially throughout the year which is also consistent with observations. Two of the culverts, culvert W018 in Figure 6-6 and culvert H023 in Figure 6-7 have much lower simulated responses than observed. Culvert H023 has a relatively small contributing area as delineated from the DEM. It is possible that actual subsurface flow paths do not reflect the surface topography as represented by the DEM. In this case the contributing area may be larger than is reflected in the simulation. In addition, the local soil depth relative to the road cut will effect the amount of water storage in the pixel and therefore how quickly the water table can rise during a storm. It is likely that the under prediction of response from culvert W018 could be corrected by adjusting either the soil depth or cut bank height for this location.

In general the model seems to overpredict road response for the largest storm flows. Figure 6-8 shows a comparison of modeled versus observed discharge for the February and April 1996 events. Figure 6-8 shows a higher than expected number of discharge peaks are overestimated by the model, as indicated by the number and distance of points above the line of equality. However, the simulated values fall within a reasonable range of the observed. Considering the small spatial scale of ditches and hillslope contributing areas, the simulated culvert discharge series seems to be a reasonable representation of reality. It must be expected that with subsurface flow determined based on 30 m pixels, there will be some error associated with subsurface flow being routed to neighboring road segments.

In addition, the overprediction of model peaks may be a result of overcompensating for performance of the current algorithm. To generate subsurface interception in between the two largest storms of the observation period (February and April 1996), it was necessary to increase the cutdepth. The cut depth was originally calculated based on the local hillslope and road surface width, by assuming that one-half of the road surface width intersects the hillside. The road surfaces specified based on field examination only included the width of limited infiltration, therefore, it is likely that the cutdepth was subsequently

underestimated. In addition, the current algorithm for infiltration through the road surface assumes that all rainfall and snow melt infiltrates the road surface unless the water table is above the height of the road cut. Several researchers have shown that the rate of infiltration through forest road surfaces is often less than the precipitation rate (Megahan 1972, Folz and Burroughs 1990, Ried and Dunne 1984, Luce and Cundy 1994). Since the model does not represent infiltration excess surface runoff generation for small intermediate storms, the cutdepth was lowered to generate a response for these events. The lower cutdepth caused a simulated response in excess of that observed for larger storms when road surface runoff was generated.

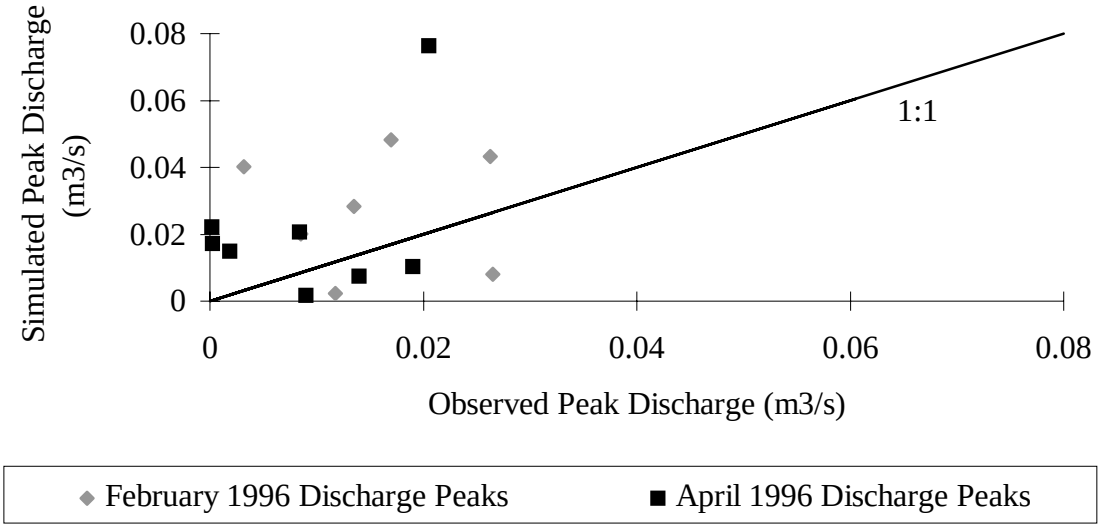

FIGURE 6-8: SIMULATED VS. OBSERVED CULVERT DISCHARGE FOR THE FEBRUARY AND APRIL 1996 STORM EVENT

Finally the basin average values of other variables were checked for plausibility. Figure 6-9 shows the variation of total evapotranspiration, snow water equivalent and soil moisture over time. This figure shows the development of a snow pack each year generally beginning sometime in October and melting completely in early May. The snow pack is much larger in 1996 than in 1994, which is consistent with the above normal precipitation that occurred in 1996. Soil moisture shows a clear annual cycle, usually

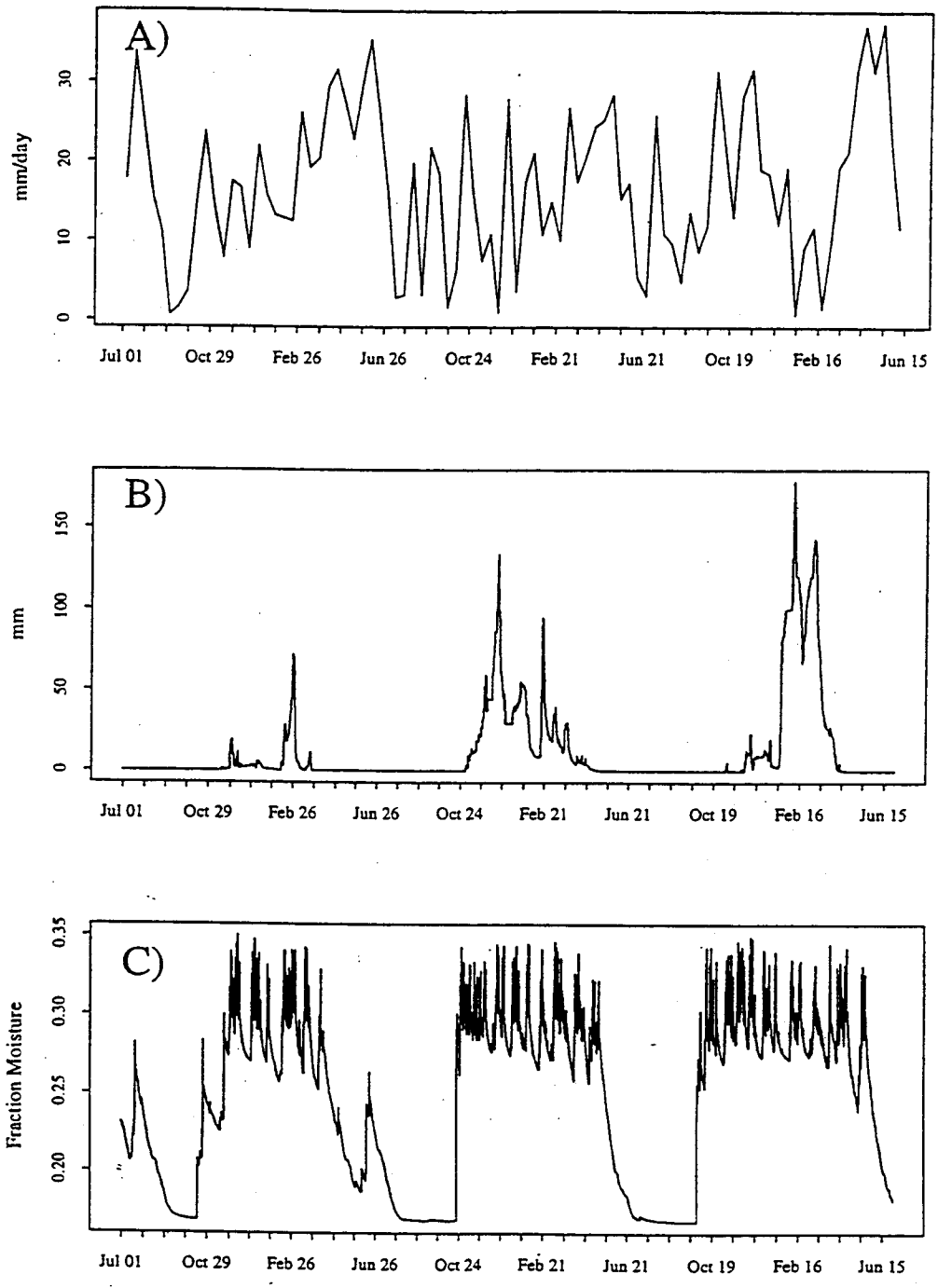

FIGURE 6-9: BASIN AVERAGE VALUES OF SOIL MOISTURE, SWE AND EVAPORATION, JULY 1, 1993 - JUNE 30, 1996
A) Total Evapotranspiration; B) Snow Water Equivalent; and C) Total Soil Moisture

approaching the wilting point in the top two soil layers during the summer. In addition, the soil moisture reflects the anomalously dry conditions of water year 1993.

Following calibration, model performance over time was tested. The model was run from October 1985 through October 1992 for Hard Creek and from October 1989 through October 1992 for Ware Creek. Observed Ware Creek discharge prior to 1989 has been lost. The complete set of evaluation runs is presented in Appendix E. The residuals for this evaluation show no trends which would indicate that the basin either accumulates or loses water over each annual cycle. The results appear consistent with the calibration period.

6.2: MODEL SENSITIVITY TO SOIL DEPTH

The sensitivity of the model to the physical distribution of soil depth was assessed by comparing the calibrated model simulations to simulations using a constant soil depth. The constant value of soil depth chosen was 0.9 m, which is the weighted average of the estimated basin average depths. The effect of soil depth on the distribution of subsurface water for several days following the April 1996 storm is shown in Figure 6-10. The first image shows the depth to water table just after the hydrograph peak. White cells represent completely saturated pixels. The water table is consistently higher in the constant soil depth scenario, as it is restricted by the shallower soil depth. However, it can be seen in the subsequent images that the localized reservoirs of soil moisture storage in the variable soil depth scenario allow the basin to hold onto moisture longer. The actual change in soil moisture due to this effect at the basin scale is actually quite small (Figure 6-11).

As Figure 6-11 indicates the difference rarely exceeds 1% of the average soil moisture for the bottom root layer. However, this results in differences in the simulated culvert discharge, as indicated in Figure 6-12. The decrease in predicted culvert response using the constant soil map followed by an increase of

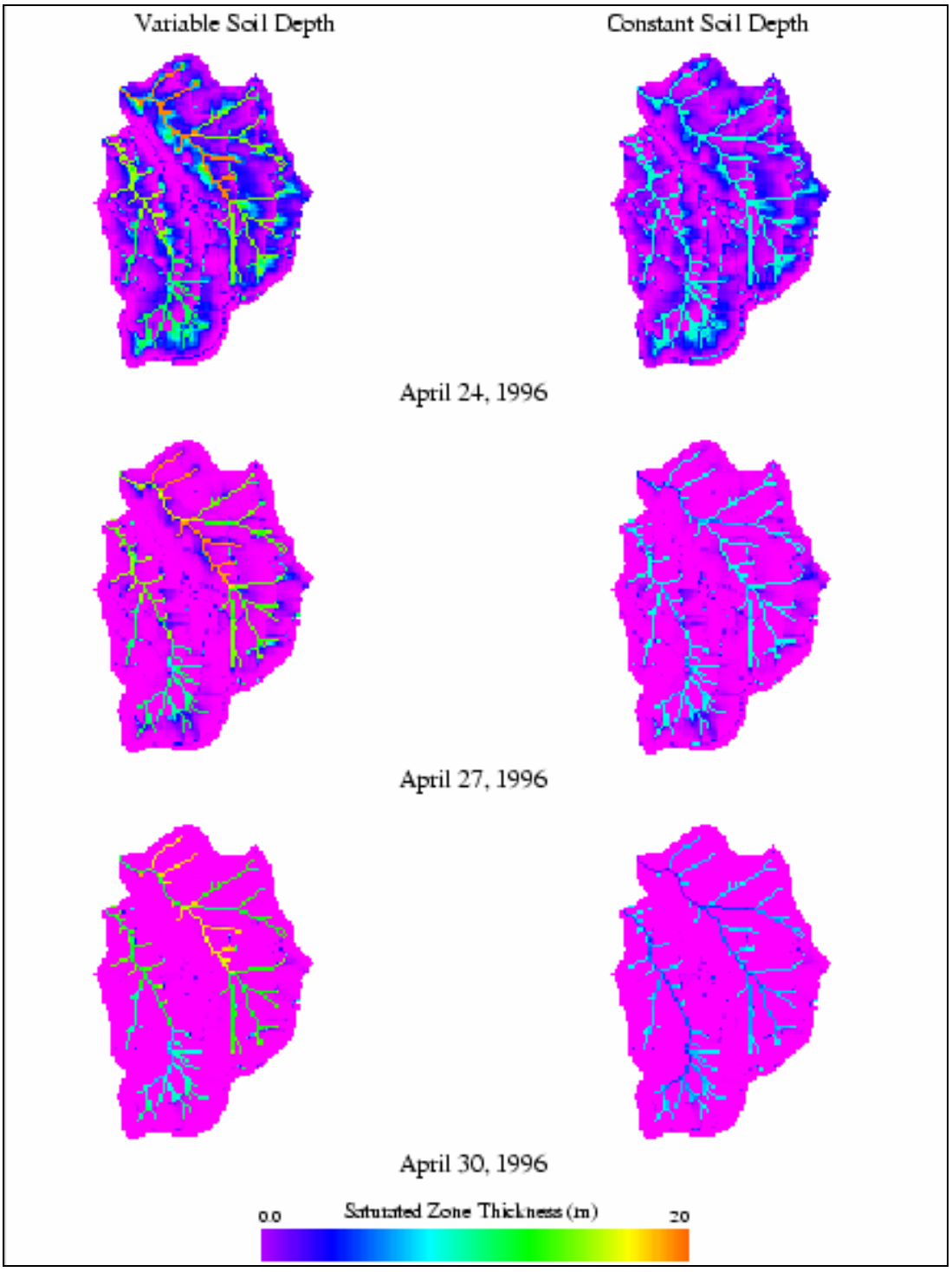

FIGURE 6-10: CHANGE IN WATERTABLE DEPTH DURING THE APRIL 1996 STORM DUE TO SOIL DEPTH

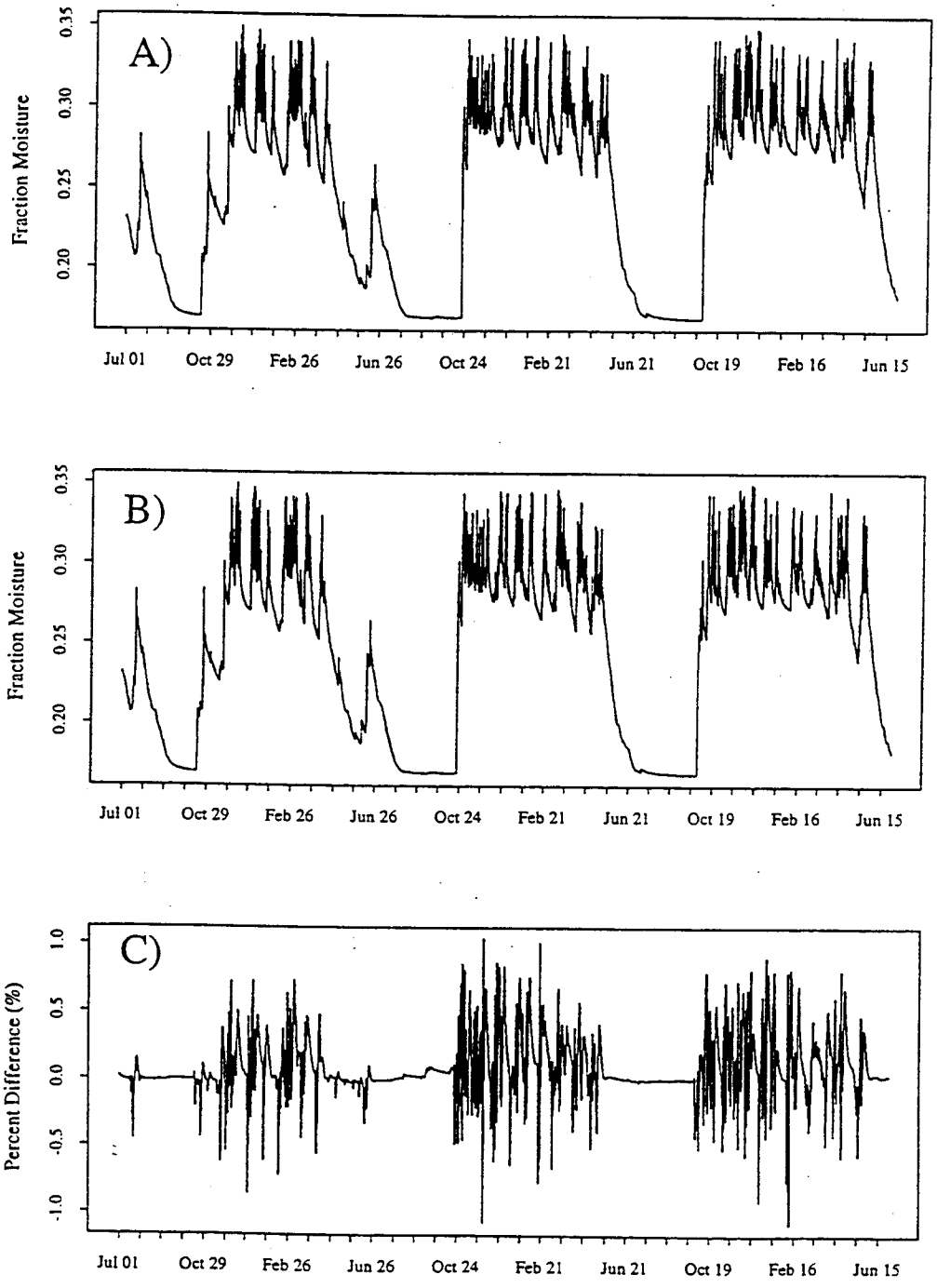

FIGURE 6-11: COMPARISON OF SOIL MOISTURE IN THE BOTTOM ROOT ZONE FOR CONSTANT AND VARIABLE SOIL DEPTHS
A) Soil moisture with variable soil depth; B) Soil moisture with constant soil depth; C) Percent difference in soil moisture with constant soil layer

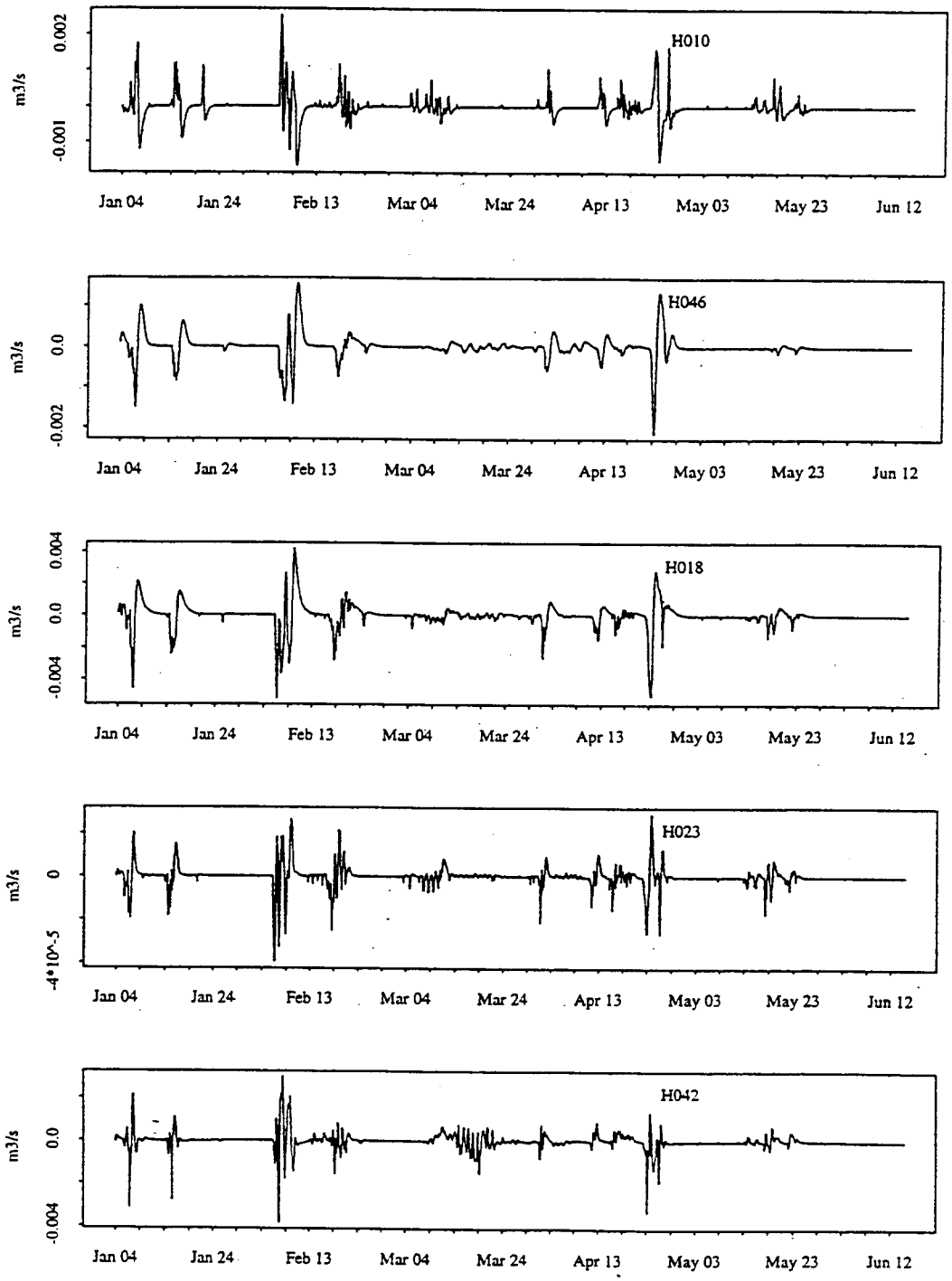

FIGURE 6-12: DIFFERENCE IN SIMULATED CULVERT DISCHARGE BETWEEN CONSTANT AND VARIABLE SOIL DEPTHS, JANUARY 4, 1996 - JUNE 15, 1996

roughly the same magnitude indicates that the constant map of soil depth served to advance the catchment response time. As Figures 6-13 and 6-14 indicate, this effect is not readily apparent in the basin hydrograph; the difference series is very similar for both series. In both cases, the simulated streamflow over predicts the first storms in the fall. Under prediction of fall storms is a frequent problem in the application of distributed models to mediterranean climates due to extreme dry down of soil moisture during the summer. This was the original reason for including a variable soil depth, to increase soil moisture storage over the summer. In this application, the soils seem to be so shallow that the soil moisture deficit is overcome very quickly throughout the basin.

In conclusion, although the variable soil depth map may cause localized differences in soil moisture, these differences do not seem to be enough to effect basin response at the catchment scale. Therefore, there does not seem to be any clear advantage to using a variable soil depth in this case.

6.3: MODEL SENSITIVITY TO WIND SPEED AND DISTRIBUTION

The sensitivity of modeled snowmelt and evapotranspiration to the three sources of wind speed was also analyzed. The three wind speed sources include the annual average Cougar Mountain wind speed, the NCEP/NCAR reanalysis wind speed interpolated to Cougar Mountain and NUATMOS distributed wind modeling. The difference in basin average SWE (both above and below the canopy) during the calibration period for each of the wind sources is shown in Figure 6-15. Although the differences are not large, they indicate that using a constant annual wind speed generally causes greater snow accumulation relative to the base case and using the interpolated wind speed generally causes less snow accumulation. Both of these observations seem consistent. For the majority of the winter, snow is concentrated on the ridgetops. During winter ROS events the average annual wind speed of 9.2 m/s will be much less than both the interpolated winds or the modeled wind field, therefore less snow will be melted. In contrast, the distributed wind model tends to attenuate the interpolated wind speeds at all but the highest

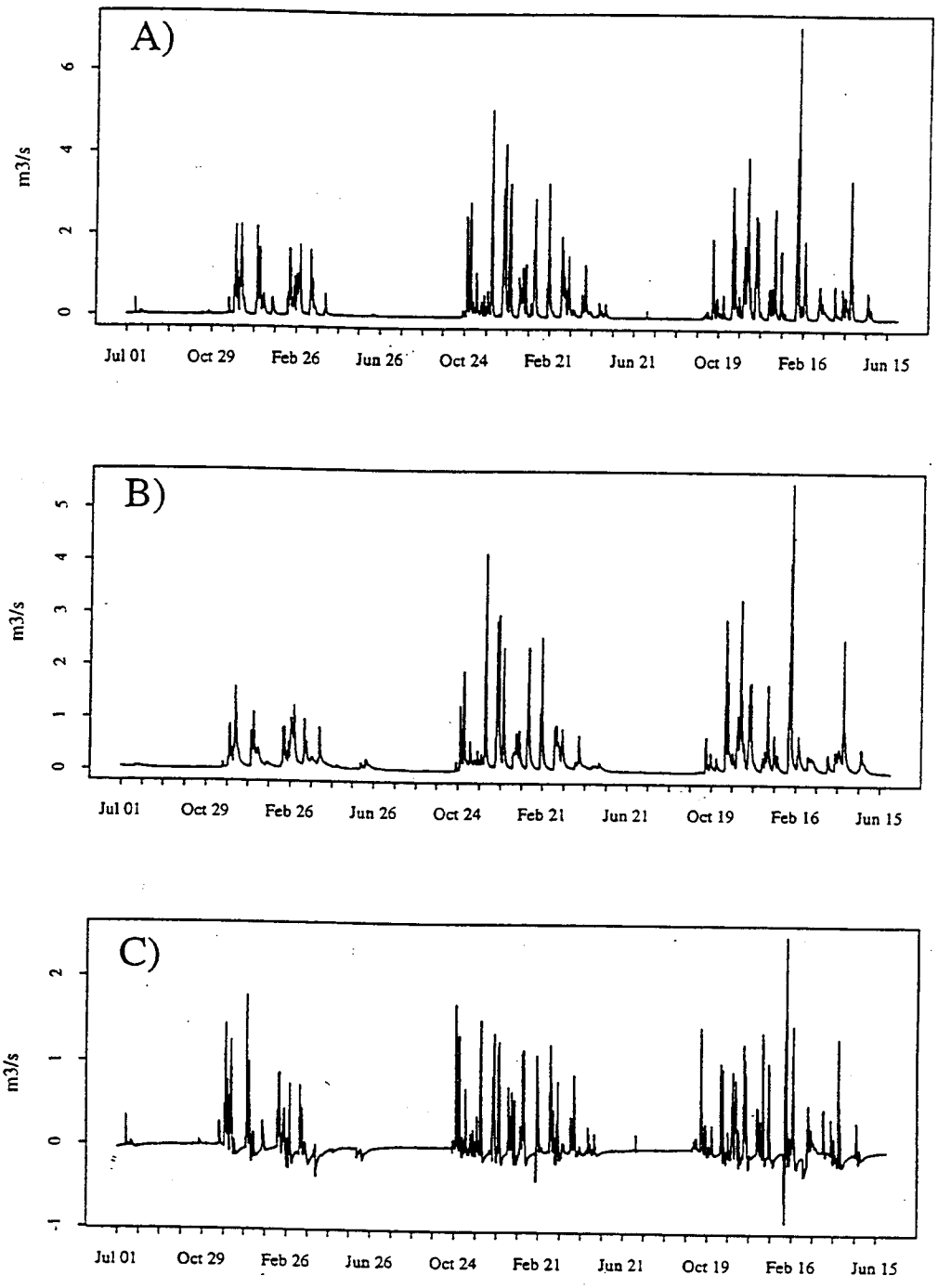

FIGURE 6-13: OBSERVED VS. PREDICTED WARE CREEK DISCHARGE WITH CONSTANT SOIL DEPTH, JULY 1, 1993 - JUNE 30, 1996
A) Average 2hr predicted discharge, B) Average 2 hr observed discharge, C) predicted - observed discharge

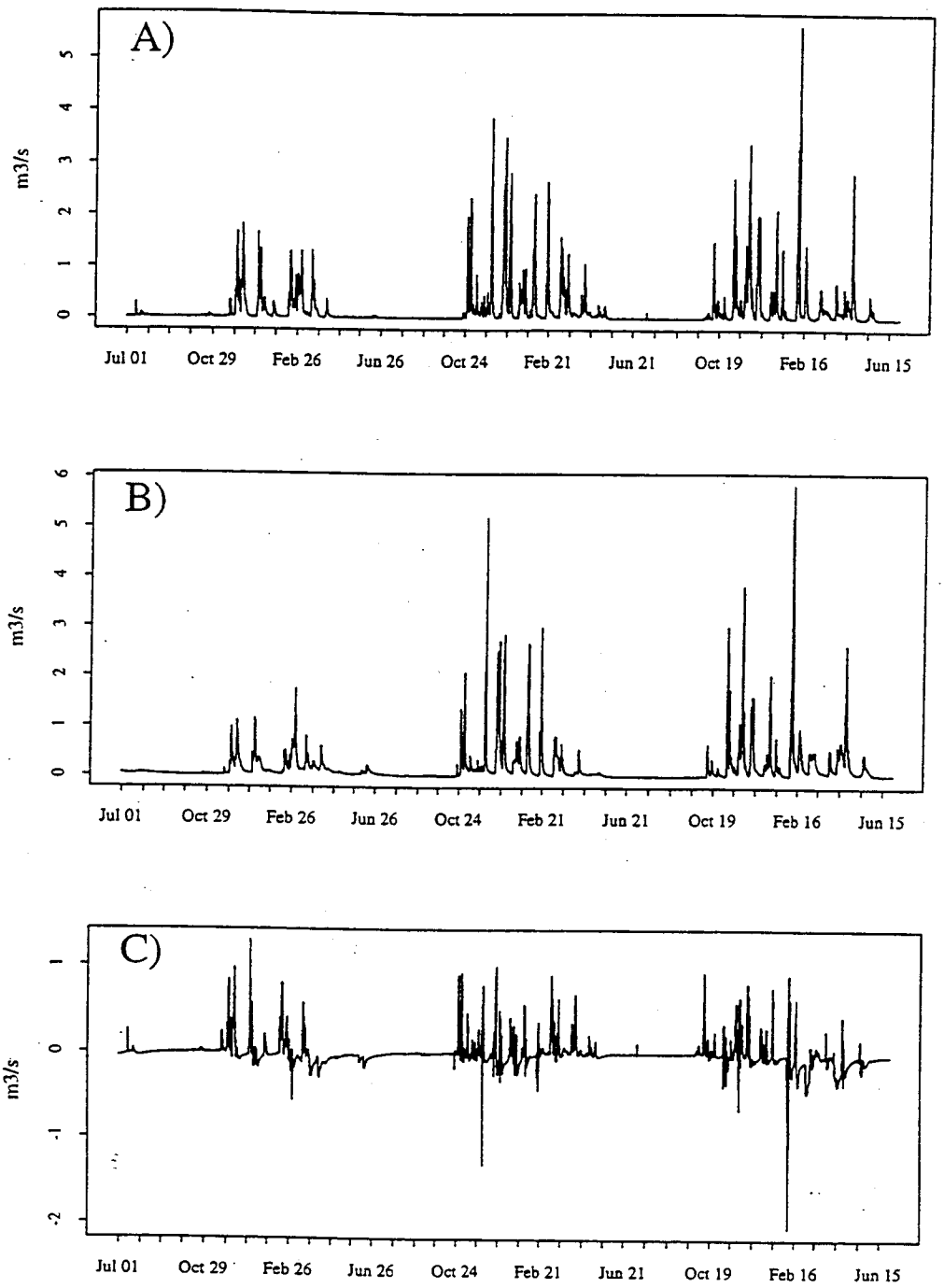

FIGURE 6-14: OBSERVED VS. PREDICTED HARD CREEK DISCHARGE WITH CONSTANT SOIL DEPTH, JULY 1, 1993 - JUNE 30, 1996
A) Average 2hr predicted discharge, B) Average 2 hr observed discharge, C) predicted - observed discharge

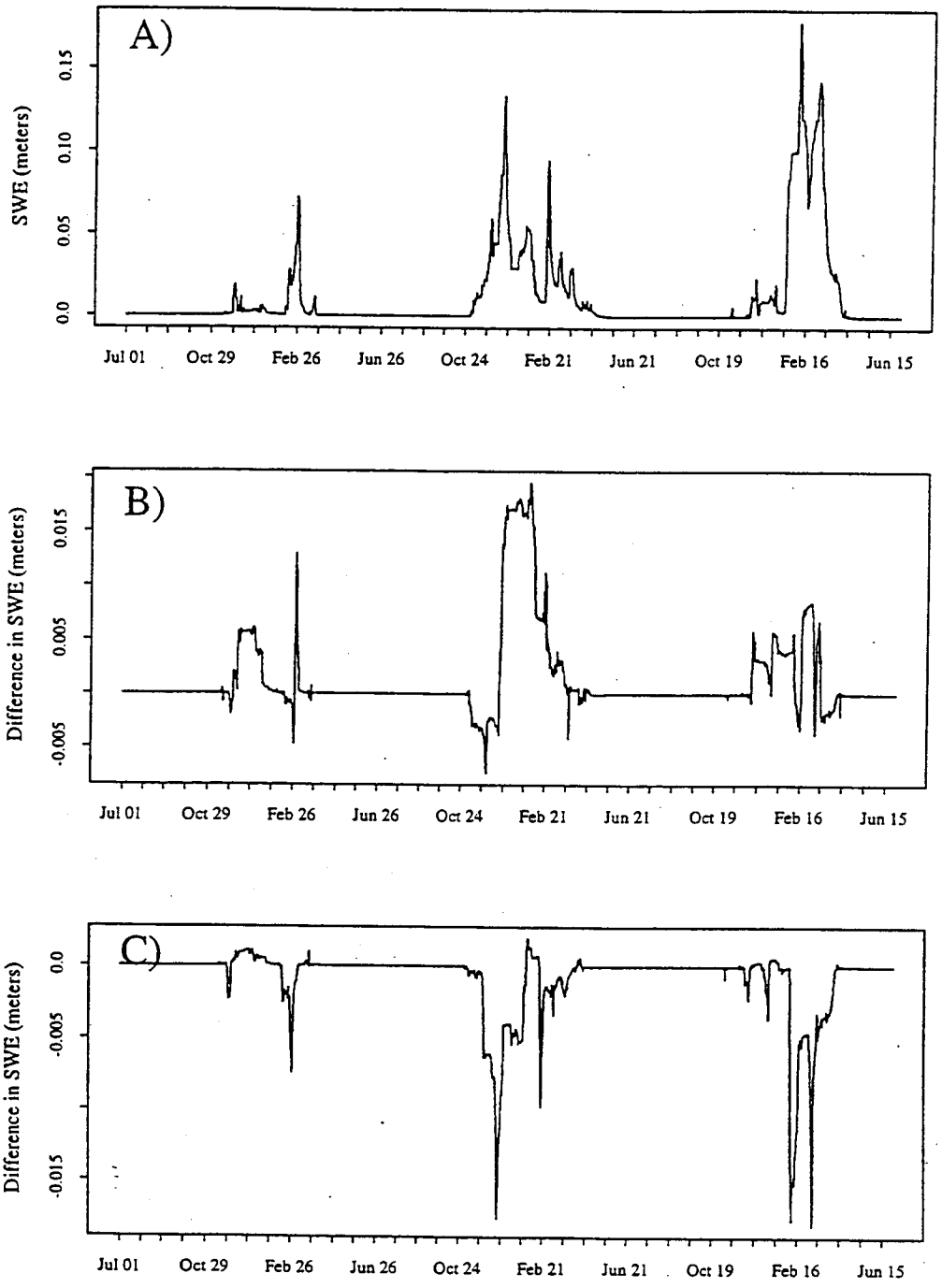

FIGURE 6-15: COMPARISON OF SWE FOR THREE SOURCES OF WIND SPEED, JULY 1, 1993 - JUNE 30, 1996

A) Simulated SWE using NUATMOS wind fields (BASE CASE), B) Difference in SWE relative to base case using constant wind speed, C) Difference in SWE relative to base case using NCEP/NCAR interpolated wind speed

elevations. Therefore, the interpolated wind speed tends to cause greater melt. Figure 6-16 shows the effect this has on melt during the February 1996 event. It appears that more snowmelt occurs in the valleys for both the interpolated and constant wind speeds, since there is no consideration for topography. However, the wind model produces the highest melt rate over the higher elevations.

The effect of wind speed on modeled total evapotranspiration (ET) was also evaluated. As indicated in Figure 6-17, the difference in total evapotranspiration is larger for the constant wind speed than for the interpolated wind speed. However, in both cases the changes oscillate between positive and negative. Total ET for the base case was 1.56 m between July 1, 1993 and June 30, 1996. Total ET for the constant wind scenario was 1.57 m, and 1.63 meters for the interpolated wind. The spatial distribution of evaporation differences is shown in Figure 6-18. This shows evaporation for one time step on July 23, 1995 which had extremely high summer wind speeds. The interpolated NCEP/NCAR wind speed at Cougar Mountain for this time period was 20 m/s. White areas represent areas of no evaporation. All three of the maps show no evaporation on the ridge tops, most likely due to soil moisture below the wilting point in these locations which would restrict transpiration. The lowest evaporation rates result from the distributed wind model. The other two scenarios most likely overestimate evaporation in the valley bottoms. The resulting effect of wind source on Ware Creek discharge is shown in Figure 6-19 and 6-20.

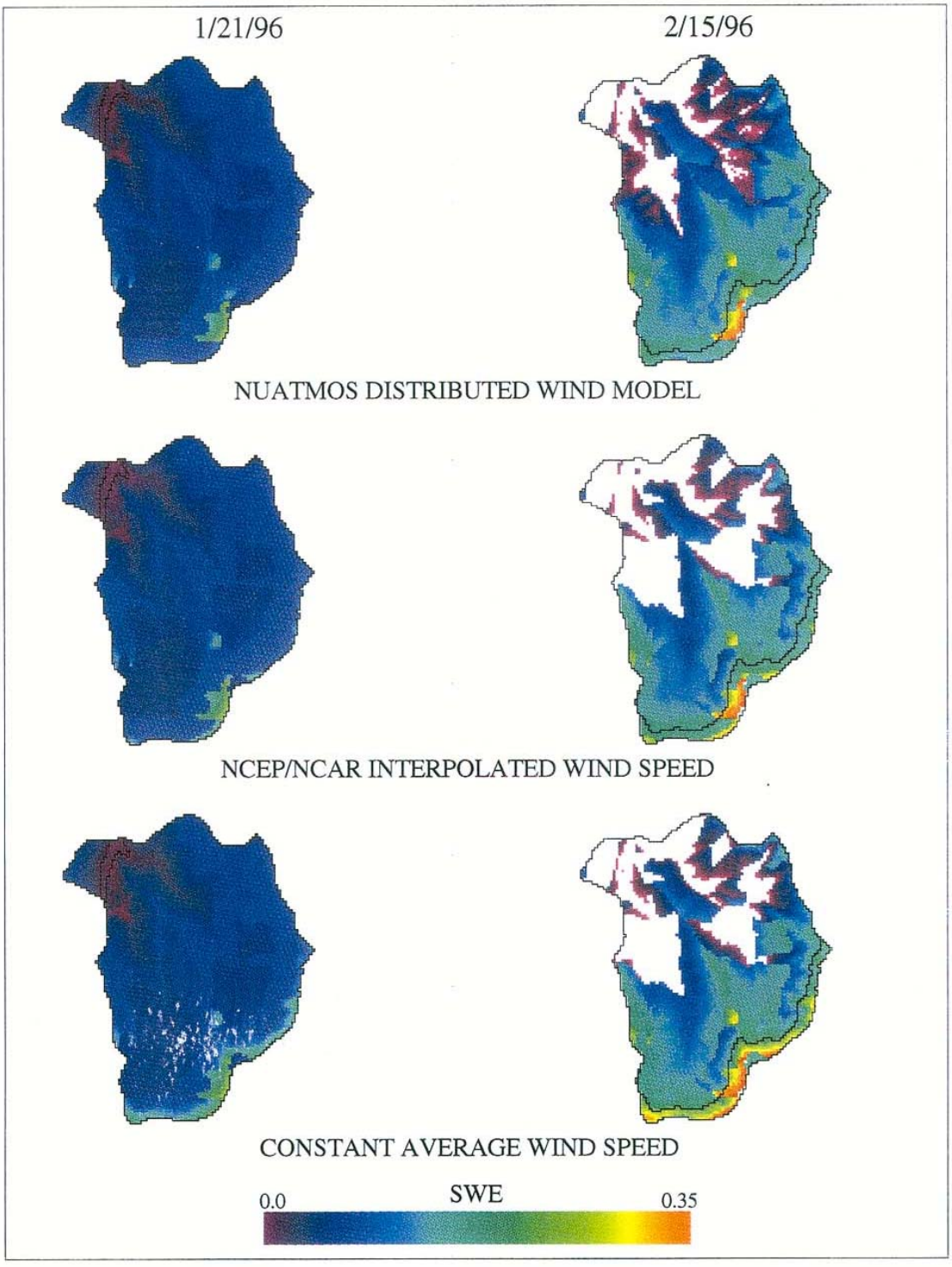

FIGURE 6-16: CHANGE IN SNOWMELT DURING THE FEBRUARY 1996 STORM DUE TO WIND SPEED

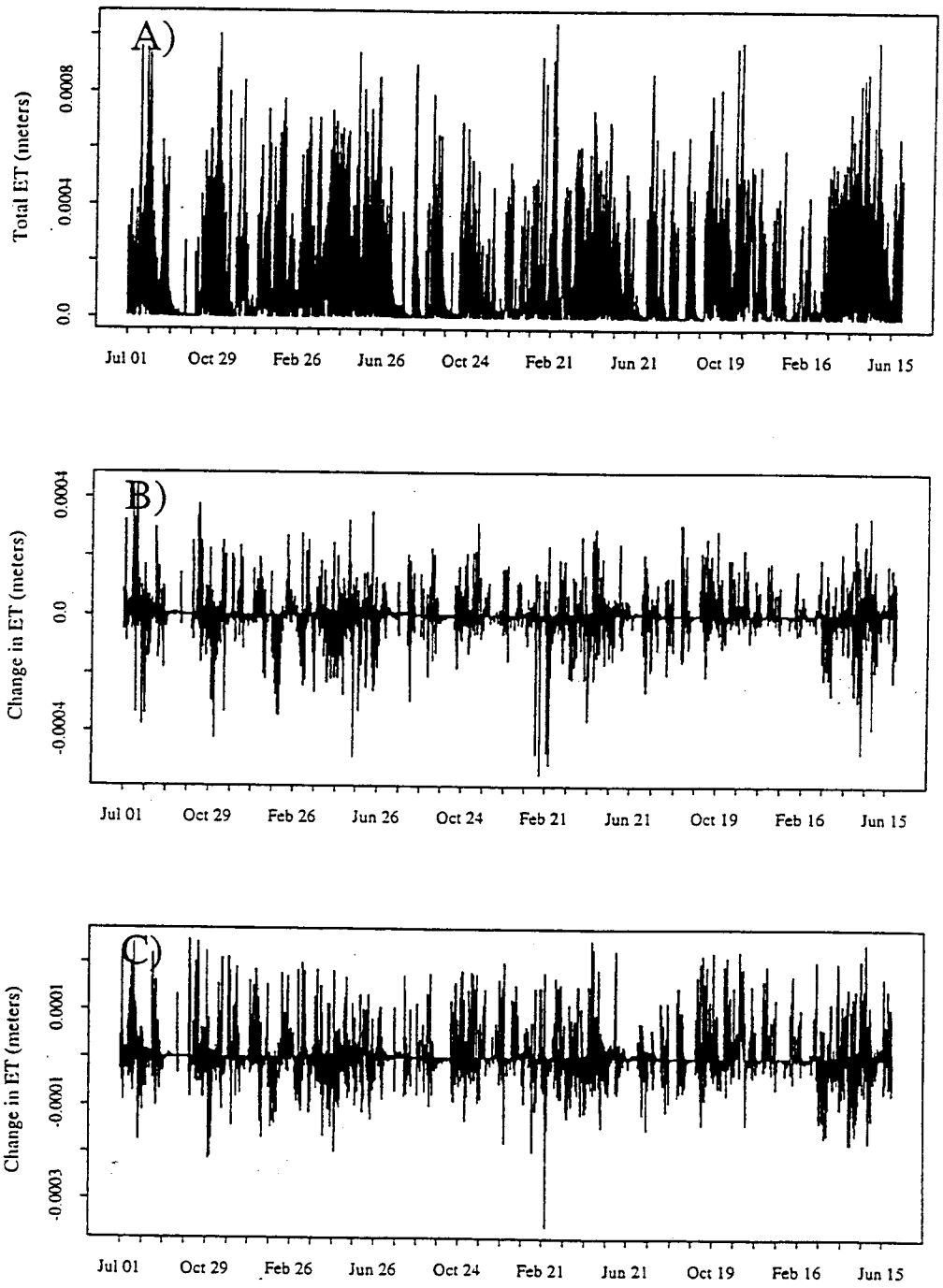

FIGURE 6-17: COMPARISON OF TOTAL EVAPOTRANSPIRATION FOR THREE SOURCES OF WIND SPEED, JULY 1, 1993 - JUNE 30, 1996

A) Total ET using NUATMOS wind fields (BASE CASE), B) Difference in Total ET relative to base case using constant wind speed, C) Difference in Total ET relative to base case using NCEP/NCAR wind speed

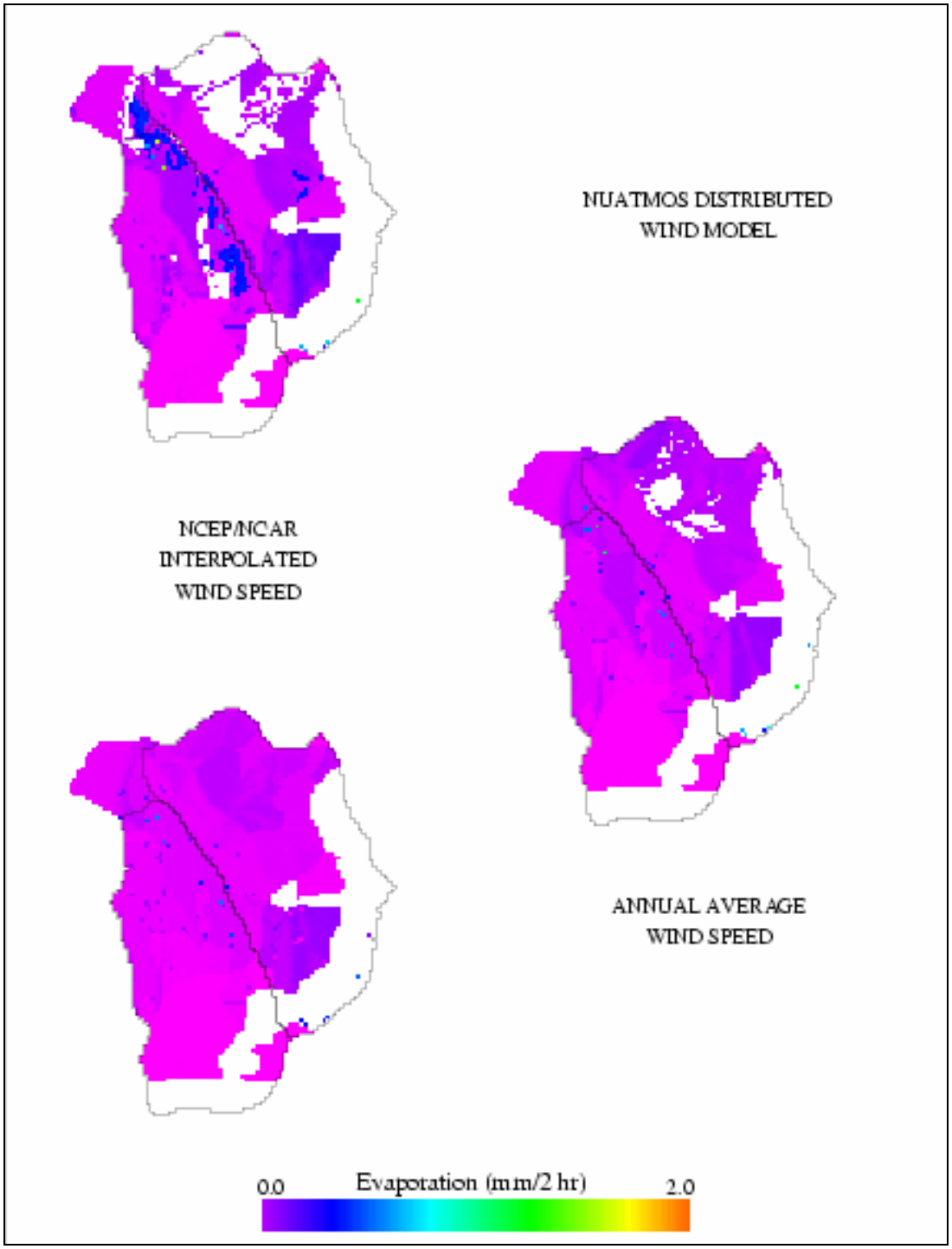

FIGURE 6-18: DISTRIBUTION OF EVAPORATION FOR THREE WIND SOURCES

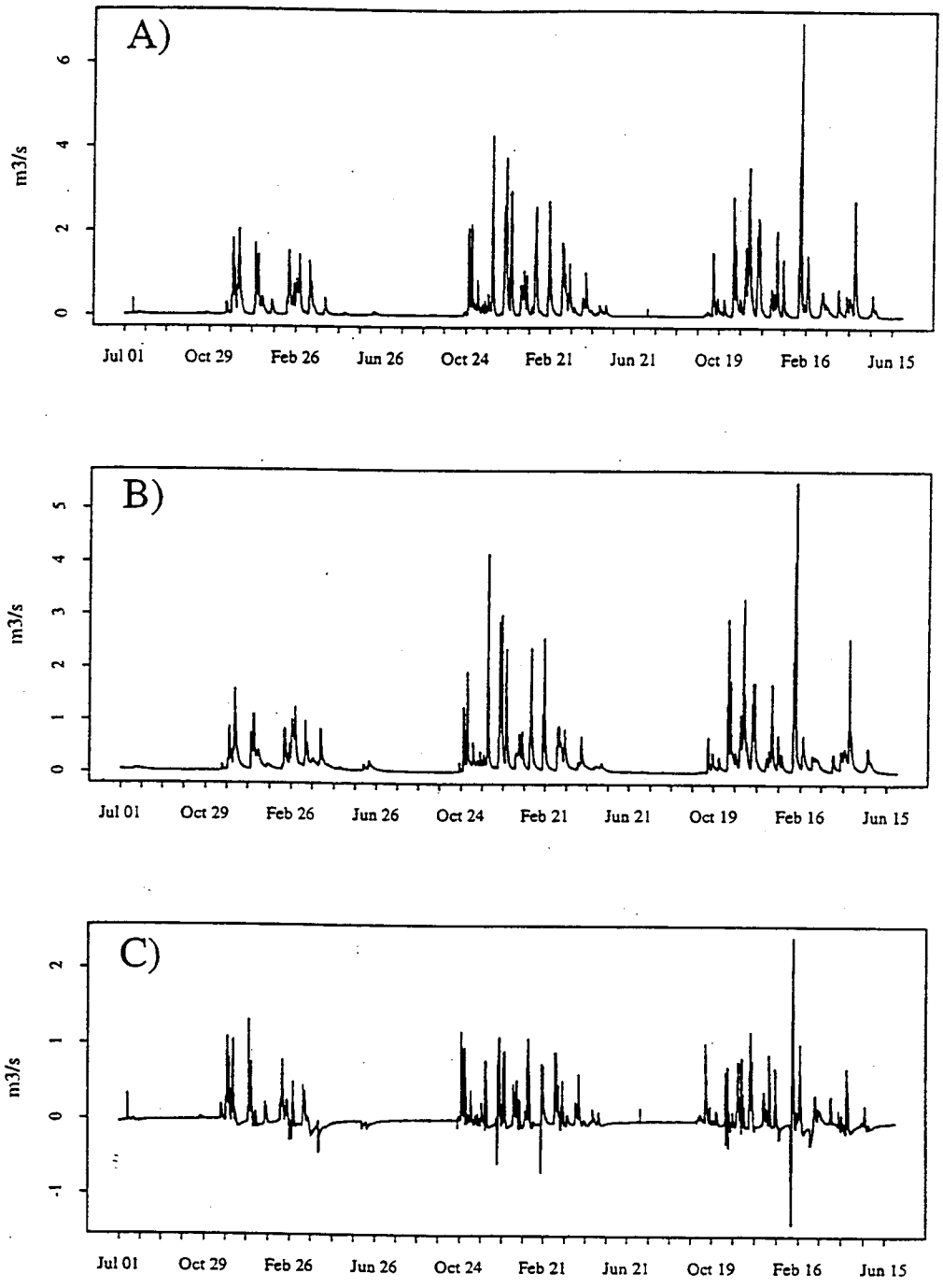

FIGURE 6-19: OBSERVED VS. PREDICTED WARE CREEK DISCHARGE WITH CONSTANT WIND SPEED, JULY 1, 1993 - JUNE 30, 1996
A) Average 2hr predicted discharge, B) Average 2 hr observed discharge, C) predicted - observed discharge

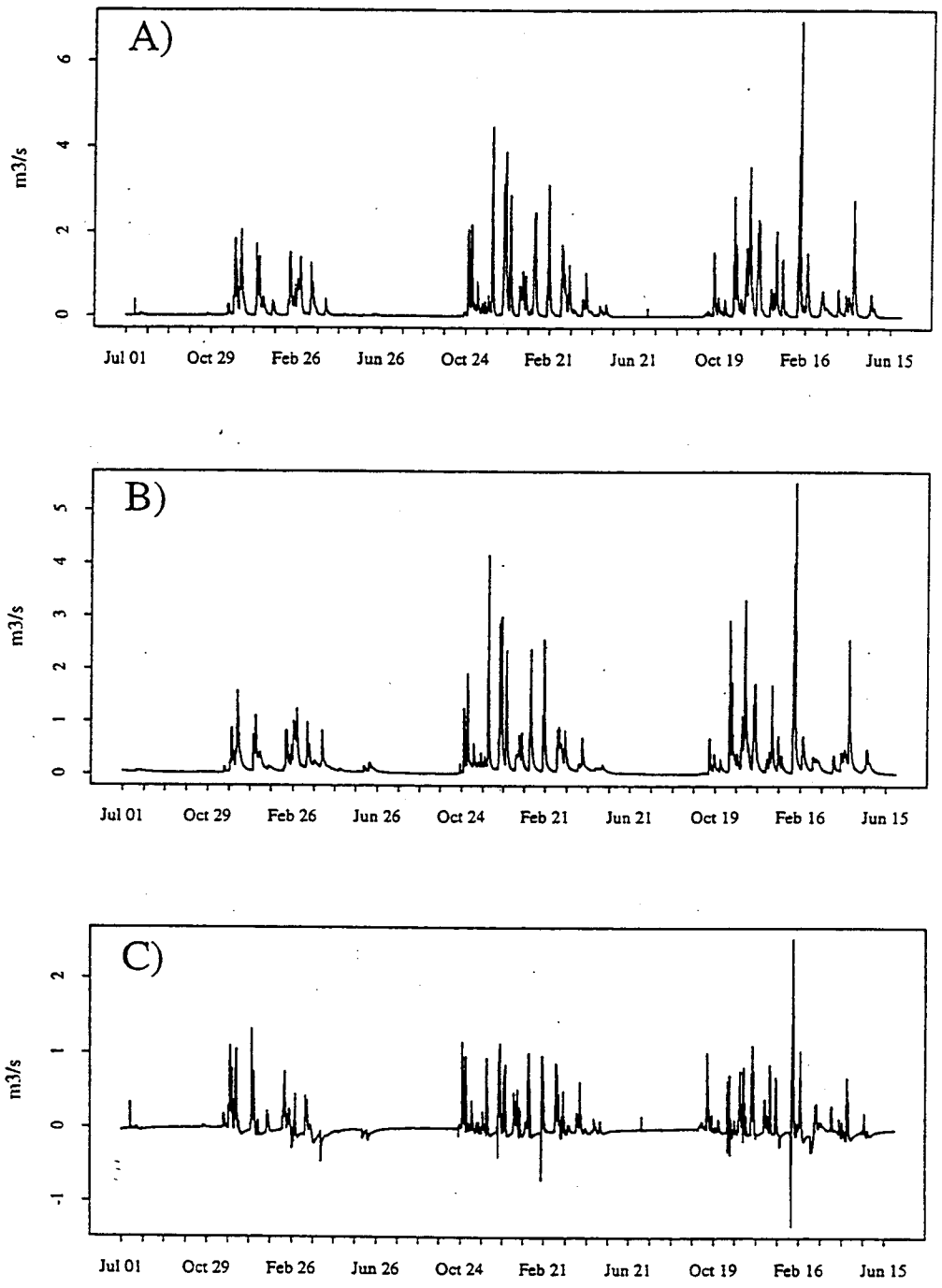

FIGURE 6-20: OBSERVED VS. PREDICTED WARE CREEK DISCHARGE WITH NCEP/NCAR WIND SPEED, JULY 1, 1993 - JUNE 30, 1996
A) Average 2hr predicted discharge, B) Average 2 hr observed discharge, C) predicted - observed discharge

CHAPTER 7: SENSITIVITY OF STREAMFLOW TO ROAD CONSTRUCTION AND FOREST HARVEST

Following model calibration DHSVM was used to simulate Hard and Ware Creek streamflow both with and without roads for the period 1985 through 1996. The modeled discharge was first used to evaluate the effect of roads on catchment water balance and individual storm hydrographs. The ability of forest road networks to increase peak streamflow was then analyzed with respect to the peaks-over-threshold (POT) series and discharge return intervals. A sensitivity analysis was performed to assess the influence of calibration quality on predicted streamflow increases. Finally, DHSVM is used to assess the possible synergism between forest harvest and road construction effects on streamflow.

7.1: ROAD EFFECTS ON BASIN HYDROLOGY

The model-predicted effect of roads on the distribution of soil moisture during the April 1996 storm event is shown in Figure 7-1. This figure shows the water table thickness, both with and without roads as the basin drains following the storm. The first image shows conditions immediately following the storm when much of the catchment was saturated. No known landslides occurred during this storm. The influence of the road network is reflected in drier (more purple) areas beneath the roads. The points of culvert discharge also show up as localized areas of higher water table.

The differences in soil moisture observed in Figure 7-1 appear to decrease as the basin dries out. As described in Chapter 2, the development of drier areas below the roads is likely to counteract the effect of the road network on streamflow, by decreasing runoff from these hillslopes during storms. The diminishing differences in soil moisture between the roaded and non-roaded scenarios for drier conditions indicates that there would be a larger change in the timing and magnitude of peak flow due to roads for storms with dry antecedent conditions since the effect will not be diminished by slower responding areas

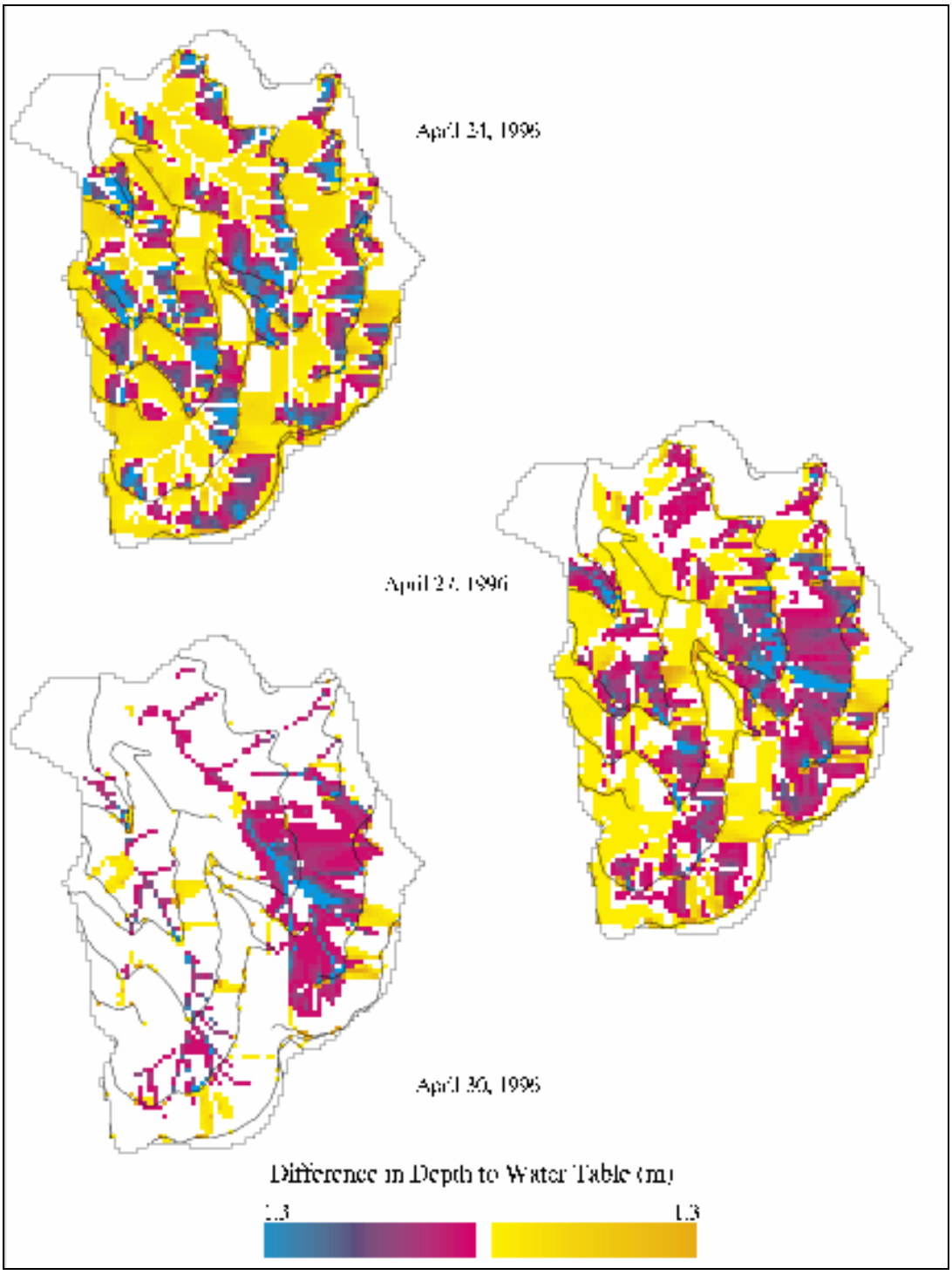

FIGURE 7-1: ROAD NETWORK EFFECTS ON WATER TABLE THICKNESS

below roads. Figure 7-2 shows hydrographs for simulations both with and without the road network for a moderate Autumn storm between September 23, 1992 and October 13, 1992 under dry antecedent conditions. Comparison of the storm hydrographs shows a steeper ascent in the rising limb due to roads and an increase in peak discharge. The increase in discharge is approximately 17% for Hard Creek and 14% for Ware Creek. The recession curve is steeper for the roaded scenario, reflecting the faster drainage of subsurface areas by conversion to surface flow.

For contrast, Figure 7-3 shows the hydrographs for a storm between March 16, 1994 and March 26, 1994 which generated a response of similar size to the September 1992 event. The increase in magnitude of the peak is only slightly smaller for this event, 14 % and 13 % in Hard and Ware Creeks, respectively. This could be a reflection of the antecedent soil moisture, or the fact that the peak streamflow for the March storm is approximately 9% greater than the September 1992 peak. However, Figure 7-3 does indicate that the hydrograph rising limb is not substantially steeper due to roads under wet antecedent conditions.

There is no change in the time to peak due to roads for either wet or dry antecedent conditions reflected in the model results. Changes in timing less than two hours cannot be resolved in the simulated results since discharge is averaged over the two hour model timestep. As indicated in Figure 3-9, the peak discharge in Hard and Ware Creeks responds to rainfall within one to four hours. Therefore, it seems likely that changes in timing due to the road network may exist at a magnitude smaller than the model timestep.

Both of the storms shown in Figures 7-2 and 7-3 are significantly smaller than the mean annual flood. They were presented here in order to explore the mechanisms of the road network/hillslope interaction. The effect of roads on larger, channel forming events is explored in Section 7.2. Initial interpretation suggests that the forest road network, as represented by DHSVM, does redistribute soil moisture through the road network. This results in drier areas downslope of roads, which might be expected to delay future

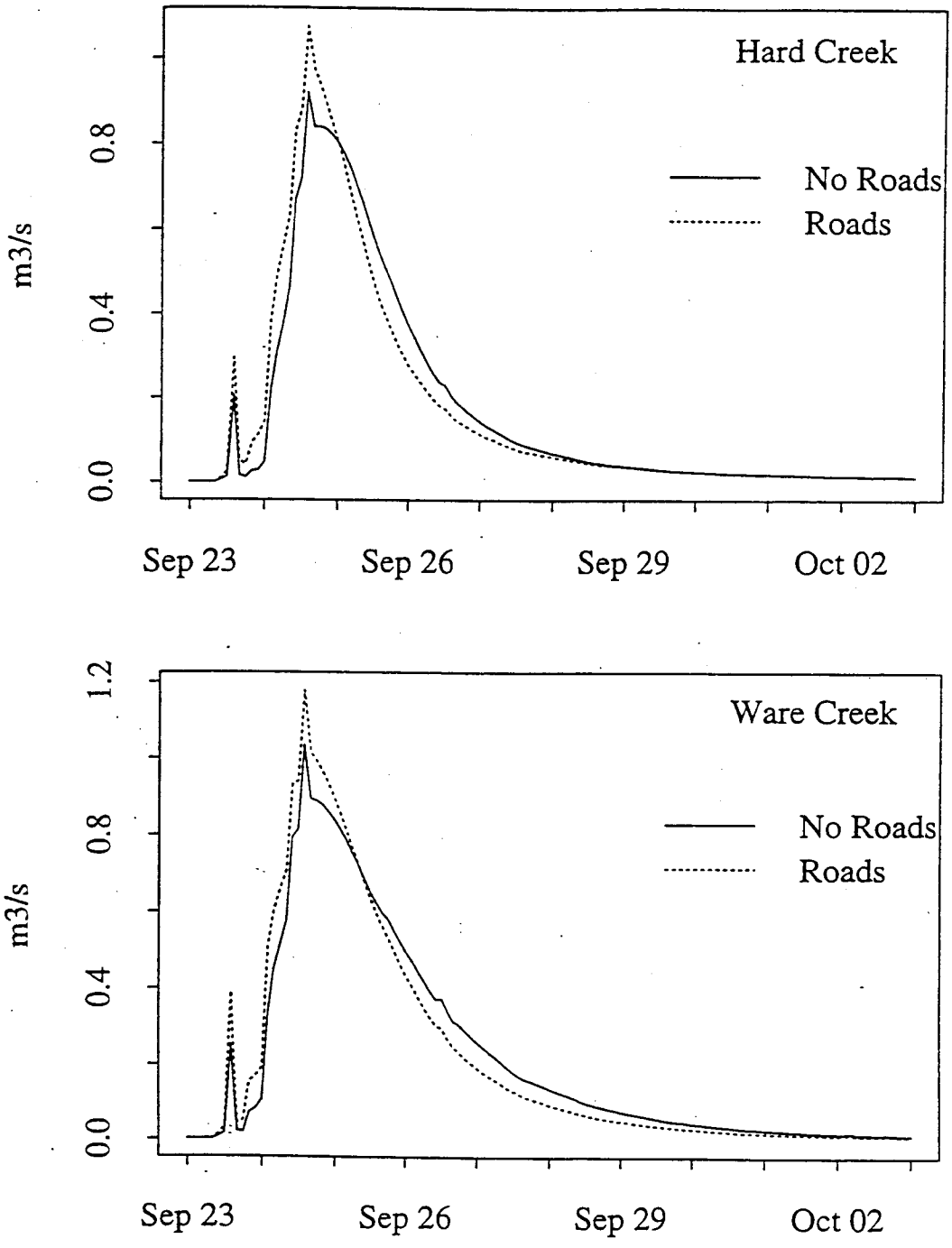

FIGURE 7-2: SIMULATED DISCHARGE WITH AND WITHOUT ROADS FOR DRY ANTECEDENT CONDITIONS, SEPTEMBER 23, 1992 - OCTOBER 3, 1992

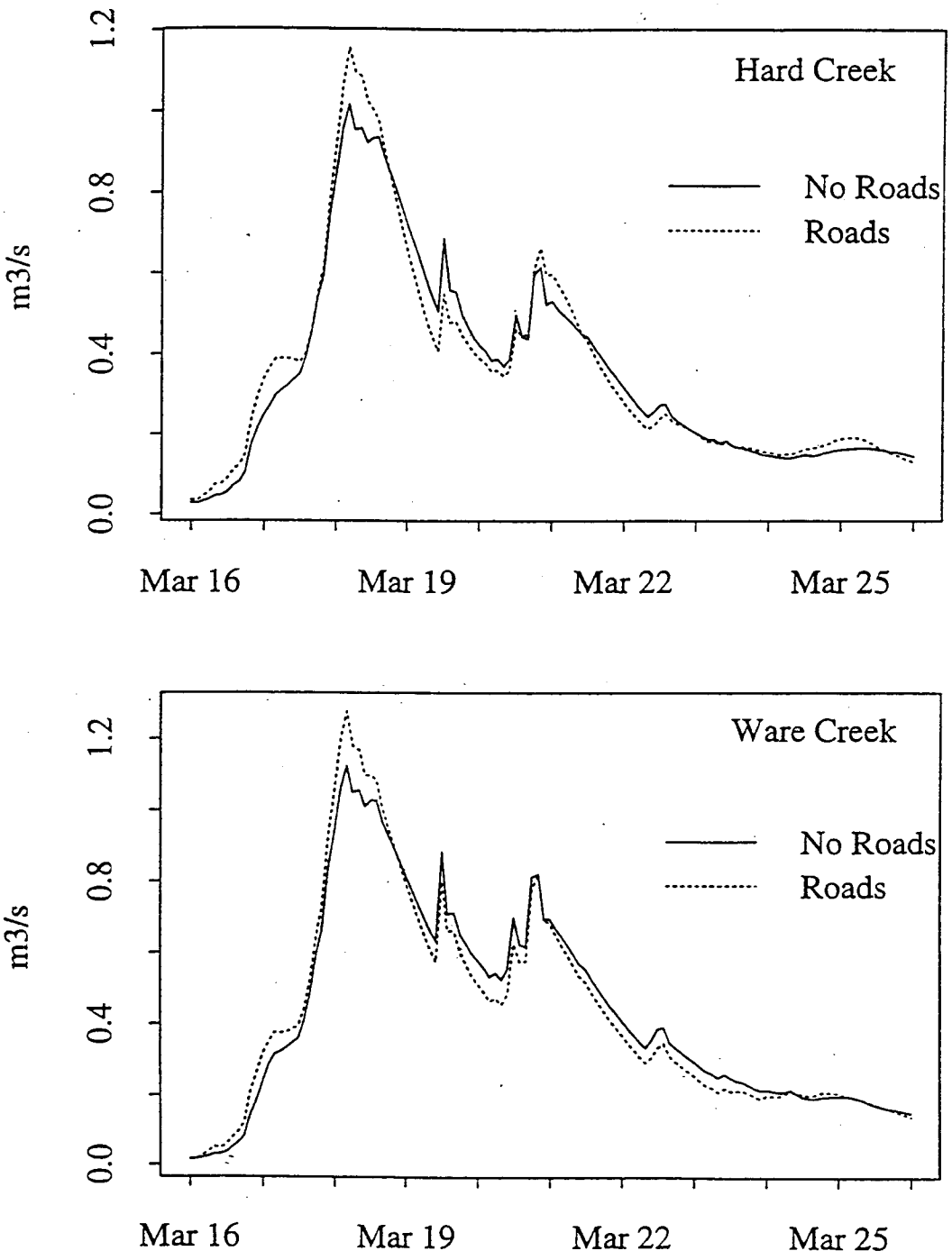

FIGURE 7-3: SIMULATED DISCHARGE WITH AND WITHOUT ROADS FOR WET ANTECEDENT CONDITIONS, MARCH 16, 1994 - MARCH 26, 1994

storm peaks. However, comparison of two similar sized storms under different antecedent moisture conditions suggests that the redistribution of soil moisture does not have much effect on the magnitude of peak discharge increases due to roads.

7.2: ROAD NETWORK EFFECTS ON STREAMFLOW

The cumulative effect of the road network on peak flows was examined based on the POT series and through a frequency analysis. First the annual maxima peak flow rate series was extracted to analyze the effect of roads on the mean annual flood (average of the annual maxima). The base mean annual flood was determined using the annual maxima series from a model simulation from October 1985 - June 1996 with current vegetation and without the imposed road network. Under current vegetation conditions, DHSVM indicates an 11 % increase in both Hard and Ware Creeks' mean annual flood due to the road network. All but one of the annual maxima resulted from the same storm both with and without roads. The annual maximum for water year 1995 for Hard Creek changed from December 20, 1994 to November 30, 1994. Two of the eleven storms in Ware Creek and three in Hard Creek peaked between 2 and 6 hours faster with roads. In addition, two storms in Hard Creek peaked 18 and 20 hours earlier due to the road network.

To investigate road effects for higher magnitude flows, a threshold was next selected which would generate approximately one storm every two years for the 11 year record. A threshold of 3.25 cms for Hard Creek and 3.75 cms for Ware Creek was used to select four storm events based on the simulation without roads. The average peak discharge for these four storms was compared to the average peak discharge for the four largest storms generated for a simulation with roads. For both basins, the largest four storms were the same under both scenarios. This analysis indicated an 8 and 9% increase in the magnitude of the POT series for Hard and Ware Creeks, respectively.

A frequency analysis of the simulated annual flood series was performed by fitting an Extreme Value Type I distribution (EVI) to both the with- and without-road simulations. Parameters of the distribution were found using the method of moments. The fitted distribution is shown in Figure 7-4 for the model simulation without roads. Confidence intervals (95%) were calculated based on the moments of the EVI distribution, following the procedure of Kite (1975). This is based on the assumption that discharge values are normally distributed around a mean value, predicted by the fitted EVI distribution. Goodness of fit was verified using the Kolomogorov-Smirnoff test.

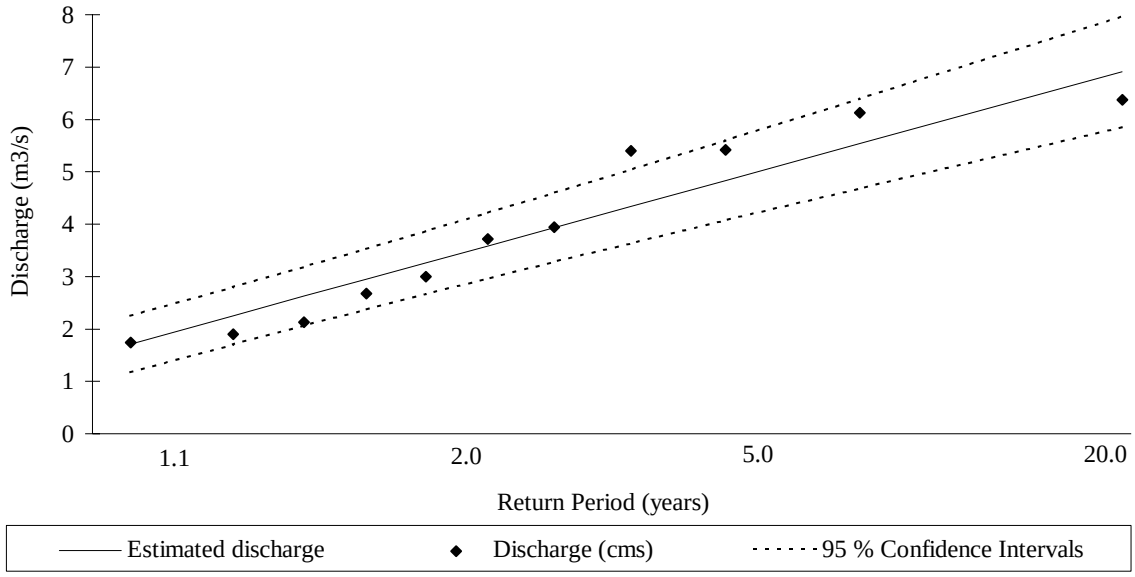

FIGURE 7-4: FITTED EVI DISTRIBUTION FOR WARE CREEK NON-ROADED SCENARIO

Although the length of the simulated discharge record limits analysis of extreme flows, the EVI distribution was used to investigate the effect of roads on events with return intervals of 2, 5 and 10 years. As summarized in Table 7-1, the forest road network as represented by DHSVM results in an increase of the ten year flood of 8 and 10% for Hard and Ware Creeks, respectively. Alternatively, this means that the flood with a ten year return period in a harvested basin without roads would have a return interval of 6.6 or 7 years in Hard or Ware Creeks after road construction (Table 7-2).

Tables 7-1 and 7-2 show a slightly larger increase in discharge due to roads for all but the smallest flows in the Hard Creek catchment as compared to Ware Creek. This is consistent with the degree of change in subsurface flow paths found in Chapter 4. For the two year return interval flow and the mean annual flood, the two catchments show roughly the same change. For these lower return interval flows, it is likely that the greater road network density in Hard Creek is balanced by the larger percentage of harvest in Ware Creek.

TABLE 7-1: EFFECT OF FOREST ROADS ON RETURN PERIOD

RETURN	WITHOUT ROADS			WITH ROADS			%
PERIOD	LOWER LIMIT[1]	DISCHARGE (CMS)	UPPER LIMIT	LOWER LIMIT	DISCHARGE (CMS)	UPPER LIMIT	CHANGE
HARD CREEK							
2	2.5	3.1	3.6	2.8	3.4	4.0	11.4
5	3.5	4.2	5.0	3.9	4.7	5.4	10.3
10	4.1	5.0	6.0	4.6	5.5	6.4	9.9
WARE CREEK							
2	3.0	3.6	4.2	3.4	4.0	4.7	11.8
5	4.3	5.0	5.8	4.7	5.5	6.3	9.4
10	5.1	6.0	6.9	5.6	6.5	7.4	8.4

Notes:
[1] 95% confidence interval

TABLE 7-2: CHANGE IN RETURN INTERVAL DUE TO ROADS

HARD CREEK			WARE CREEK		
DISCHARGE	RETURN INTERVAL W/O ROADS	RETURN INTERVAL W/ ROADS	DISCHARGE	RETURN INTERVAL W/O ROADS	RETURN INTERVAL W/ ROADS
3.1 cms	2 yrs	1.6 yrs	3.6 cms	2	1.6 yrs
4.2 cms	5 yrs	3.6 yrs	5.0 cms	5	3.7 yrs
5.0 cms	10 yrs	6.6 yrs	6.0 cms	10	7.0 yrs

7.3: SENSITIVIY OF PREDICTED INCREASES TO MODEL CALIBRATION

The sensitivity of the estimated increase in peak discharge due to roads to the quality of the model calibration was assessed by varying two calibration parameters: the lateral hydraulic conductivity and the exponent for decrease in lateral hydraulic conductivity with depth. These are two of the most sensitive calibration parameters. Model simulations were made both with and without roads for two values of these parameters, as indicated in Table 7-3.

TABLE 7-3: PARAMETER SETS FOR SENSITIVITY ANALYSIS

	LATERAL HYDRAULIC CONDUCTIVITY, KH	EXPONENT FOR DECREASE IN KH
ORIGINAL CALIBRATION	0.002	1.0
SENSITIVITY CASE 1	0.01	0.75
SENSITIVITY CASE 2	0.0005	2.0

Figure 7-5 shows simulated Hard Creek for sensitivity case 1 during the calibration period. Comparison with observed streamflow indicates that simulated streamflow peaks too early due to the high lateral conductivity. This offset in timing results in a peak error three times larger than in the original calibration. Simulated Hard Creek discharge for the second sensitivity case is shown in Figure 7-6. In this case the low hydraulic conductivity and high exponent tend to keep water in the pixel longer. Therefore, the simulated hydrographs tend to have longer recessions and lower peak flow-rates than the observed. This results in more frequent and larger negative errors for the sensitivity case than for the base calibration.

The increase in mean annual flow and the POT series for the two scenarios are summarized in Table 7-4. These results indicate that the quality of the model calibration does effect the magnitude of the observed road effect. However, the alternative parameter scenarios shown in Figure 7-5 and 7-6 result in noticeably different calibration hydrographs. It is not likely that these parameter sets would be arrived at

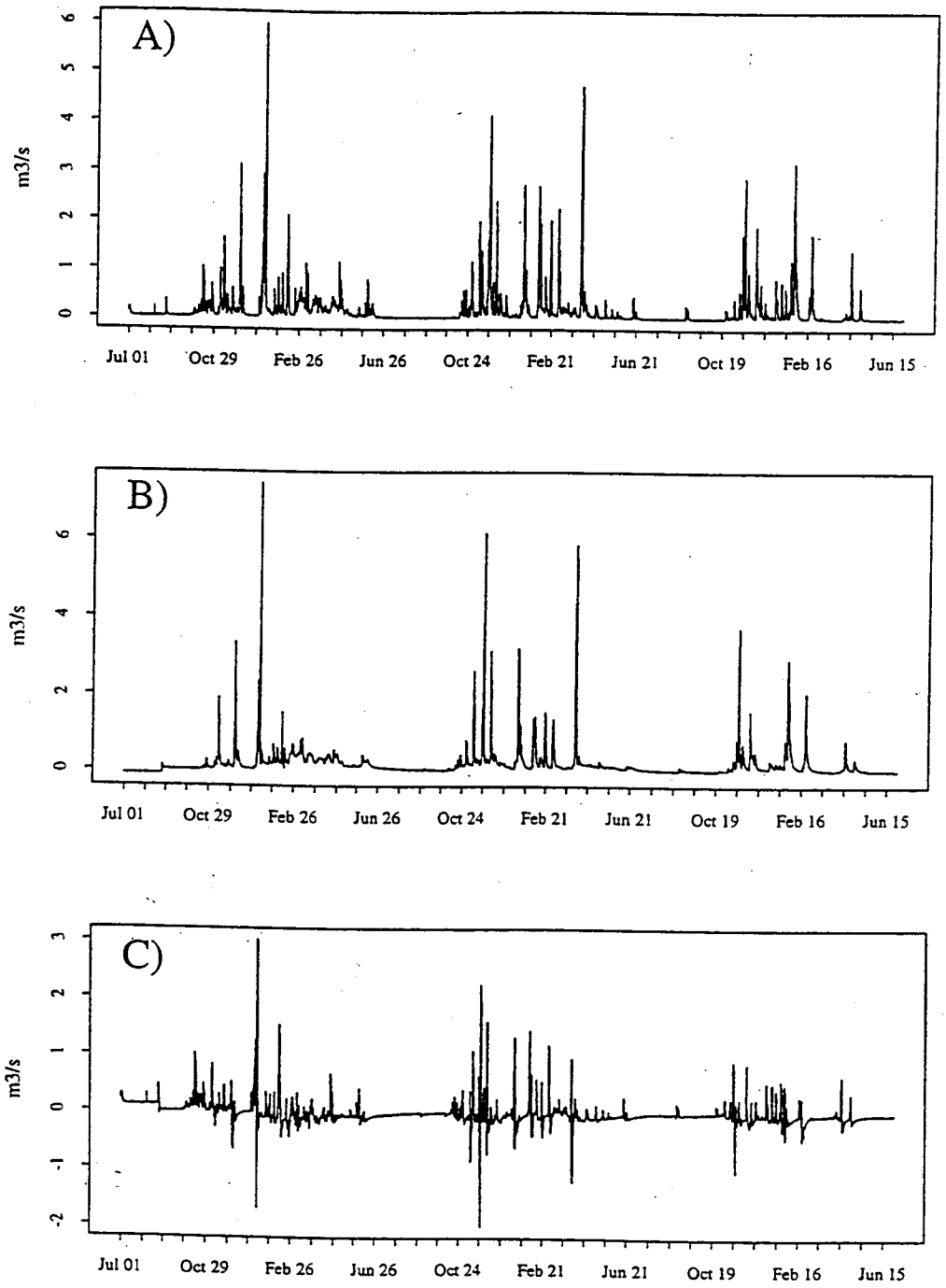

FIGURE 7-5: OBSERVED VS. PREDICTED HARD CREEK DISCHARGE FOR SENSITIVITY CASE I, JULY 1, 1993 - JUNE 30, 1996
A) Average 2hr predicted discharge, B) Average 2 hr observed discharge, C) predicted - observed discharge

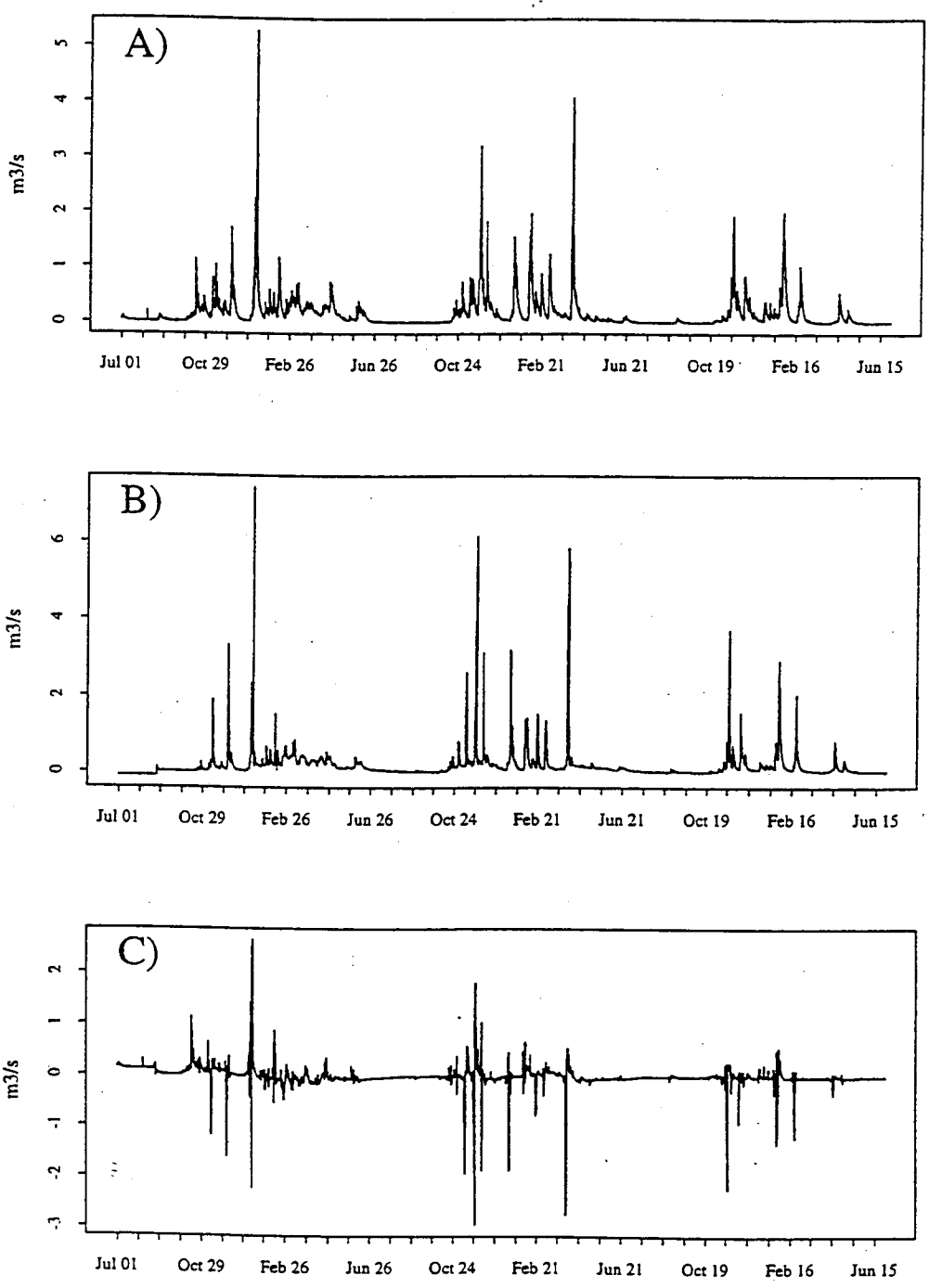

7-6: OBSERVED VS. PREDICTED HARD CREEK DISCHARGE FOR SENSITIVITY CASE 2, JULY 1, 1993 - JUNE 30, 1996
A) Average 2hr predicted discharge, B) Average 2 hr observed discharge, C) predicted - observed discharge

during the calibration process. A more rigorous analysis with more feasible parameter sets is necessary to truly determine the sensitivity of predicted streamflow increases to model calibration.

TABLE 7-4: INCREASE IN DISCHARGE FOR TWO SENSITIVITY CASES

	% INCREASE IN MEAN ANNUAL FLOW		% INCREASE IN MEAN OF POT SERIES	
	WARE CREEK	HARD CREEK	WARE CREEK	HARD CREEK
ORIGINAL CALIBRATION	11.2	11.1	7.6	9.0
SENSITIVITY CASE 1	6.9	6.9	4.4	5.4
SENSITIVITY CASE 2	14.7	14.7	12.9	15.5

7.4: COMBINED FOREST HARVEST AND ROAD CONSTRUCTION EFFECTS

Finally, DHSVM was used to explore the link between forest harvest and road network effects on simulated peak discharge. Comparisons performed up until now have focused on modeled changes due to the imposed road network under harvested conditions. Therefore, the modeled increase in streamflow already reflects the effects of forest harvest. To simulate pre-harvest conditions, both catchments were assumed to be completely covered with the most mature (highest LAI) vegetation class from the original vegetation map described in Chapter 5. Simulations were performed with this mature vegetative cover, both with and without the road network. The changes in mean annual flood and POT were compared with respect to vegetation cover and road network, as summarized in Table 7-5. Several patterns are indicated by this table. Comparison of peak flows before and after timber harvest indicate a larger percent increase for Ware Creek than for Hard Creek. This is consistent with the harvest histories; Ware Creek has been harvested significantly more than Hard Creek, although the exact percentage of harvest difference is unknown. The results in Table 7-5 show the expected result that the relative effects of forest harvest to road construction depend on the total harvested area. Relative to an undisturbed catchment, the increase in streamflow due to roads alone is larger than that for forest harvest alone in Hard Creek. The reverse is true in Ware Creek.

Some previous paired catchment studies have indicated a synergism between forest roads and timber harvest, meaning that the combined effect is greater than the additive effect of the individual components (Jones and Grant 1996, Wright et al. 1990). With respect to mean annual flow and the POT series, DHSVM simulations do not support this theory, although there is some suggestion that the existence of an interaction depends on the quantity of timber harvested. Specifically, the combined effect of forest harvest and roads is slightly larger than the sum of the individual effects in Ware Creek, while the combined effects are approximately equal to the additive effects in the less harvested Hard Creek catchment. But, in both basins there is a smaller relative increase in peak flow due to forest harvest with roads in place, than in forest harvest without roads.

The effect of road construction and forest harvest on discharge return interval is summarized in Table 7-6. For the most part, the changes in mean annual flow and POT are consistent. There is a larger increase in discharge due to roads in Hard Creek relative to Ware Creek and a larger increase in discharge due to forest harvest in Ware Creek. Once again, there is a slightly greater percent increase in discharge due to roads and harvest combined than for the sum of these individual treatments in Ware Creek. This interaction was not present in Hard Creek.

TABLE 7-5: INCREASE IN PEAK DISCHARGE FOR TWO SENSITIVITY CASES

	% INCREASE IN MEAN ANNUAL FLOW		% INCREASE IN POT SERIES	
	WARE CREEK	HARD CREEK	WARE CREEK	HARD CREEK
%CHANGE DUE TO ROADS W/ MATURE COVER	11.7	12.6	8.4	9.7
% CHANGE DUE TO ROADS W/ HARVESTED (1996) COVER	11.2	11.1	7.6	9.0
% CHANGE DUE TO FOREST HARVEST W/O ROADS	14.8	9.7	12.0	7.6
% CHANGE DUE TO FOREST HARVEST W/ ROADS	14.3	8.3	11.2	6.9
% CHANGE DUE TO ROAD CONSTRUCTION AND FOREST HARVEST	27.7	22.0	20.4	17.3

TABLE 7-6: PERCENT INCREASE IN PEAK DISCHARGE FOR VARIOUS RETURN INTERVALS

	WARE CREEK			HARD CREEK		
RETURN INTERVAL:	**2 YR**	**5 YR**	**10 YR**	**2 YR**	**5 YR**	**10 YR**
%CHANGE DUE TO ROADS W/ MATURE COVER	12.3	9.8	8.8	12.9	11.4	10.7
% CHANGE DUE TO ROADS W/ HARVESTED (1996) COVER	11.8	9.4	8.4	11.4	10.3	9.9
% CHANGE DUE TO FOREST HARVEST W/O ROADS	15.4	13.1	12.2	10.1	8.5	7.8
% CHANGE DUE TO FOREST HARVEST W/ ROADS	14.9	12.7	11.8	8.6	7.5	7.0
% CHANGE DUE TO ROAD CONSTRUCTION AND FOREST HARVEST	29.0	23.7	21.7	22.6	20.0	18.5

CHAPTER 8: CONCLUSIONS AND RECOMMENDATIONS

This research has addressed the effect of forest roads on streamflow in a Pacific Northwest maritime mountainous catchment. The central hypothesis of this research has been that forested road networks in mountainous forest catchments increase streamflow by replacing subsurface flow paths with surface flow paths. Road networks can capture runoff in two ways:

By intercepting subsurface flow through the cutbank when the water table is above the depth of the road cut; and

By capturing infiltration excess precipitation when the rainfall intensity exceeds the infiltration capacity through the compacted road surface.

Once in the road drainage network, runoff may reach the natural drainage network as surface flow through direct entry at stream crossing culverts or indirectly through gullies eroded beneath ditch relief culverts. This hypothesis was explored using a combination of field investigation and distributed hydrologic modeling.

The quantity of runoff intercepted by the road network was monitored in Hard and Ware Creeks, both of which are tributaries to the Deschutes River , Western Washington. These observations showed that the magnitude of the observed culvert discharge was controlled by subsurface flow interception rather than road surface runoff. The most consistent pattern in the field results was that the quantity of intercepted subsurface flow is higher beneath harvested hillslopes. Medium or bottom hillslope positions and medium to deep soils also tended to increase the quantity of intercepted subsurface flow. The limited field study also indicated that some road segments do not generate surface runoff, because of infiltration from the ditch above the culvert.

The effect of roads on the spatial distribution of surface and subsurface flow paths in Hard and Ware Creeks was estimated using field observations of culvert drainage paths and road surface slopes. Nearly 39 % of roads in Hard Creek and 46 % of roads in Ware Creek drain directly to streams or gullies. As a result, the average length of subsurface flow was decreased 43 % in Hard Creek and 36 % in Ware Creek.

Finally, the cumulative effect of the forest road network on Hard and Creek streamflow was explored using the Distributed Hydrology-Soils-Vegetation Model (DHSVM) (Wigmosta et al. 1994, Storck et al. 1995, 1997). A recent modification of DHSVM that represents interception of subsurface flow by the road network explicitly was used. In this new model version, surface flow in roadside ditches and stream channels is routed to the basin outlet using a Muskingum-Cunge scheme. The model was calibrated for the period July 1, 1993 through June 30, 1996. Comparison with basin discharge and point observations of peak culvert discharge indicated that the model approximately represented the hydrological processes of Hard and Ware Creeks.

An 11 year simulation (1985-1996) of Hard and Ware Creeks was performed using DHSVM with 1996 vegetation conditions and compared with simulations made without the road network. The comparisons indicated that the roads redistribute soil moisture throughout the basin, resulting in drier areas beneath the road right-of-way and localized saturated areas as a result of culvert discharge. The road network tends to increase peak flows. With current vegetation, the road network was estimated to increase the ten year return period flood by 8% in Ware Creek and 10 % in Hard Creek. Comparison of the current condition simulation with results of a simulated undisturbed basin (mature vegetation and no roads) indicated that the ten-year return peak flow rate might be increased by 22 % and 18% in Ware and Hard Creeks respectively, due to road building and clear cut logging.

A sensitivity analysis of the observed streamflow increase using three different estimates of lateral hydraulic conductivity was performed to determine the extent to which the observed changes were

dependent on the quality of the model calibration. These results indicate that the simulated increase in streamflow due to roads depends strongly on the choice of calibration parameters for the range of parameters tested. Further analysis with more feasible parameter sets is necessary.

Difficulties in calibrating the model included the inability to match the water balance and the peaks for both catchments simultaneously. This is most likely due to an inadequate representation of orographic controls on precipitation. A simple precipitation lapse rate does not seem appropriate. For some storms Ware Creek discharge exceeds Hard Creek discharge, but not consistently. An algorithm which takes into account the storm path might better represent precipitation differences within the basins.

The ability of roads to intercept both precipitation and subsurface flow depends on the water table depth above the road cut. Therefore, model performance is quite sensitive to the soil depth and lateral hydraulic conductivity which control, respectively, the quantity and duration of soil moisture storage within a pixel. Calibration versus observed culvert hydrographs may be improved with a more realistic representation of infiltration through the road bed. Correct representation of the basin hydrographs required a high rate of hydraulic conductivity. As a result, the simulated soil moisture is often near field capacity. The water table responds quickly to storms and returns to near the bottom of the soil column within a few days. Such behavior has been observed at other research basins (see e.g. Montgomery 1997). A field study designed to verify the realism of this behavior in Hard and Ware Creeks, for instance via a piezometer network, would be useful in evaluating model behavior.

REFERENCES:

Anderson, M.G. and Burt, T.P. (1978). The role of topography in controlling throughflow generation. *Earth Surface Processes,* 3, pp. 331-344.

Anderson, M.G. and Burt, T.P. (1990), Subsurface Runoff, in *Process Studies in Hillslope Hydrology*, M.G. Anderson and T.P. Burt, *Ed.*, John Wiley & Sons Ltd.

Arola, A. (1993). Effects of subgrid spatial heterogeneity on mesoscale snow modeling, Master's Thesis, Department of Civil Engineering, University of Washington.

Barnard, J. (1996), "Forest activists: Logging, roads caused flooding", in *The Mail Tribune,* February 15, 1996.

Beadles, J.T. (1995). Positioning with GPS, http://andromeda.einet.net/editors/john-beadles/sum_pos.htm.

Bernton, H. (1996). "Damages in forests extensive", in *The Oregonian*, February 14, 1996.

Berris, S.N. and R.D. Harr (1987), Comparative snow accumulation and melt during rainfall in forested and clear-cut plots in the western Cascades of Oregon, *Water Resurces Research,* 23 (1), pp. 135-142.

Bilby, R.E., K. Sullivan and S.H. Duncan (1989). The generation and fate of road-surface sediment in forested watersheds in southwestern Washington. *Forest Science,* 35 (2), 453-468.

Bosch, J.M. and J.D. Hewlett (1982). A review of catchment experiments to determine the effects of vegetation changes on water yield and evepotranspiration, *Journal of Hydrology*, 55, pp. 3- 23.

Bras, R. L. (1990), *Hydrology, An Introduction to Hydrologic Science*, Addison-Westley Publishing Company, Reading, 1995.

Bristow K. L. and G. S. Campbell, On the Relationship between Solar Radiation and Daily Maximum and Minimum Temperature. *Agricultural and Forest Meteorology,* v. 31, p. 159-166, 1984.

Bunnel, F.L., R.S. McNay, C.C. Shank (1985). Trees and snow: the deposition of snow on the ground - a review and quantitative synthesis, Research Branch, Ministries of Environment and Forests, IWIFR-17, Victoria, B.C. Canada.

Burt, T.P. , Butcher, D.P., Coles, N. and Thomas, A.D. (1983). The natural history of Slapton Ley Natural Reserve.XV.Hydrological processes in the Slapton Wood catchment. *Field Studies* 5, 731-752.

Calder, I.R. (1990). *Evaporation in the Uplands*. John Wiley and Sons, Chichester, 148 pp.

Cederholm, C.J., l.M. Reid and E.O. Salo (1981), Cumulative effects of logging road sediment on salmonid populations in the Clearwater River, Jefferson County, Washington, *Proceedings from the Conference, Salmon-Spawning Gravel: A Renewable Rresource in the Pacific Northwest?,* Report No. 39, State of Washington Water Research Center.

Dubayah, R., J. Dozier and F.W. Davis (1990), Topographic distribution of clear-sky radiation over the Konza prairie, Kansas, *Water Resources Research*, 26, 679-690.

Duncan, S. H. (1986). Peak stream discharge during thirty years of sustained yield timber management in two fifth order watersheds in Washington State, *Northwest Science*, 60 (4), 258-264.

Duncan, S.H., R.E. Bilby and J.T. Heffner (1987). Transport of road-surface sediment through ephemeral stream channels, *Water Resources Bulletin*, 23 (1), 113-119.

Dunn, S.M and R. Mackay (1996). Modelling the hydrological impacts of open ditch drainage, *Journal of Hydrology*, 179 (1-4), May 1.

Dunne, T. and R.D. Black (1970a). An experimental investigation of runoff production in permeable soils, *Water Resources Research*, 6 (2), April.

Dunne, T. and R.D. Black (1970b). Partial area contributions to storm runoff in a small New England watershed, *Water Resources Research*, 6 (5), October.

Entekhabi, D. and P.S. Eagleson (1989). "Land surface hydrology parameterization for atmospheric general circulation models including subgrid scale spatial variability", Journal of Climate, 2, 816-831.

Fahey, B.D. and R.J. Coker (1989). Forest road erosion in the granite terrain of southwest Nelson, New Zealand, *Journal of Hydrology* (NZ), 28 (2).

Foltz, R.B. (1996). Roughness coefficients on forest road-side ditches, supplement to Eos, Transactions, AGU, 77 (46), November 12, 1996.

Foltz, R.B. and E.R. Burroughs (1990). Sediment production from forest roads with wheel ruts. *Watershed Planning and Analysis in Action*. Syposium Proceedings of IR Conference, ASCE, 266-275.

Freeze, R.A. (1974). Streamflow Generation, *Reviews of Geophysics and Space Physics*, 12 (4), pp. 627-647.

Frew, J.E. (1991). "The Image Processing Workbench", PhD Thesis, Department of GEography, University of California, Santa Barbara, CA.

Gandolfi, C. and G.B. Bischetti (1997). Influence of the drainage network identification method on geomorphological properties and hydrological response, *Hydrological Processes*, 11 (4), 353-375.

Garbrecht, J. (1991). Effects of spatial accumulation of runoff on watershed response. *Journal of Environmental Quality*, 120, 31-35.

Gates, D.M. (1980). *Biophysical Ecology*, New York: Springer-Verlag.

Harr, R.D. (1977). Water flux in soil and subsoil in a steep forested, *Journal of Hydrology*, 33, pp. 37-58.

Harr, R.D. (1981). Some characteristics and consequences of snowmelt during rainfall in western Oregon, *Journal of Hydrology*, 53, pp. 277-304.

Harr, R.D. (1986). Effects of clear-cut logging on rain-on-snow runoff in western Oregon: A new look at old studies, *Water Resources Research*, 22(7), 1095-1100.

Harr, R.D. and F.M. McCorison (1979). Initial effects of clearcut logging on size and timing of peak flows in a small watershed in western Oregon, *Water Resources Research*, 15 (1), 90 - 94.

Harr, R.D., A. Levno and R. Mersereau (1982). Streamflow changes after logging 130-year-old Douglas fir in two small watersheds, *Water Resources Research*, 18, 637 - 644.

Harr, R.D., W.C. Harper, J.T. Krygier and F.S. Hsieh (1975). Changes in storm hydrographs after road building and clear-cutting in the Oregon Coast Range. *Water Resources Research* 11 (3), 436-444.

Harris, D.D. (1977). Hydrologic changes after logging in two small Oregon coastal watersheds, Geol. Survey Water Supply Pap. U.S., 2037, 31 pp.

Haupt, H.F., H.C. Rickard and L.E. Finn, (1963). Effect of severe rainstorms in insloped and outsloped roads, USFS Res. Note INT-1, 6 pp.

Hershfield, D.M. (1961). Rainfall frequency atlas of the United States for rainfall durations from 30 minutes to 24 hours and return periods from 1 to 100 years. Washington D.C., Department of Commerce, Weather Bureau.

Hewlett, J.D. and A.R. Hibbert (1967). Factors affecting the response of small watersheds to precipitation in humid areas. In: Sopper, W.E. and Lull, H.W. (eds.), *International Symposium on Forest Hydrology*, Pergamon Press, New York, 275-290.

Horton, R.E. (1945). Erosional development of streams and their drainage basins: hydrophysical approach to quantitative morphology, Bulletin of the Geological Society of America, 56, 265-370.

Jenson, S.K. and J.O. Domingue (1988). Extracting topographic structure from digital elevation data for geographic information system analyses, *Photogrammetric Engineering and Remote Sensing*, Vol. 54, No. 11, November 1988, pp. 1593-1600.

Jones, J.A. and G.E. Grant (1996). Peak flow responses to clearcutting and roads in small and large basins, western Cascades, Oregon, *Water Resources Research*, 32 (4), 959-974.

Jones, J.A.A. and F.G. Crane (1984). Pipeflow and pipe erosion in the Maesnant experimental catchment, *Catchment Experiments in Fluvial Geomorphology*, ed. by T.P. Burt and D.E. Walling, 55-85, Geo Books, Exeter.

Kattelmann, R. (1990). Effects of forest cover on a snowpack in the Sierra Nevada, in *Watershed Planning and Analysis in Action*, ASCE, New York: New York, pp. 276-284.

Keppeler, E.T. and R.R. Ziemer (1990). Logging effects on streamflow: water yield and summer low flows at Caspar Creek in nortwestern California, *Water Resources Research*, 26 (7), pp. 1669-79.

King, J.G. and L.C. Tennyson (1984). Alteration of streamflow characteristics following road construction in north central Idaho, *Water Resources Research*, 20 (8), 1159-1163.

Kitada, T., A. Kaki, H. Ueda and L.K. Peters (1983). Estimation of vertical air motion from limited horizontal wind data - a numerical experiment, *Atmos. Environ.*, 17, pp. 2181-2192.

Leupold and Stevens, Inc, *Ed.* (1978). *Stevens Water Resources Data Book, 3rd Edition*, leupold and Stevens, Beaverton, Oregon.

Linsley, R.K. Jr., M.A. Kohler, J.L.H. Paulhus (1982). *Hydrology for Engineers, 3rd Edition*, McGraw-Hill, Inc.

Luce, C.H. and T.W. Cundy (1994). Parameter identification for a runoff model for forest roads, *Water Resources Research*, 30, 1057-1069.

Maidment, D.R. (1983). *Handbook of Hydrology*, McGraw-Hill Inc., New York.

McCashion, J.D. and R.M. Rice (1983), Erosion on logging roads in northwestern California, *Journal of Forestry*, 81, pp. 23-26.

Megahan, W.F. (1972). Subsurface flow interception by a logging road in mountains of central Idaho, paper presented at Syposium on watersheds in transition, American Water Resources Association, Ft. Collins, Colorada, June 1972.

Megahan, W.F. (1983). Hydrologic effects of clearcutting and wildfire on steep granitic slopes on idaho, *Water Resources Research*, 19 (3), pp. 811-819.

Montgomery, D.R. (1994). Road surface drainage, channel initiation and slope stability, *Water Resources Research*, 30, pp. 1925-1932.

Montgomery, D.R. and E. Fofoula-Georgiou (1993). Channel network source representation using digital elevation models, *Water Resources Research* 29, pp. 3925-3934.

Montgomery, D.R., W.E. Dietrich, T. Torres, S. Prestrud Anderson, J.T. Heffner and K. Loague (1997). Hydrologic response of a steep, unchanneled valley to natural and applied rainfall, *Water Resources Research*, 33 (1), pp. 91-109.

Normann, J.M., R.J. Houghtalen and W.J. Johnston (1985). Hydraulic Design of Highway Culverts, Federal Highway Administration Technical Report No. FHWA-IP-85-15.

NUATMOS (1992). Draft User Manual, NUATMOS Version 6, Centre for Applied Mathematical Modeling, Monash University, Victoria, Australia.

Perkins, W.A., M. S. Wigmosta and B. Nijssen, Development and Testing of Road and Stream Drainage Network Simulation within a Distributed Hydrologic Model, poster presented at the fall meeting of the American Geophysical Union, December 1996.

Piehl, B.T., R.L. Beschta and M.R. Pyles (1988). Ditch relief culverts and low-volume forest roads in the Oregon Coast Range, *Northwest Science*, 62 (3), pp. 91-98.

Ried, L.M. (1981). Sediment production from gravel-surfaced forest roads, Clearwater Basin, Washington, Master's Thesis, Department of Geological Sciences, University of Washington.

Ried, L.M. and T. Dunne (1984). Sediment production from forest road surfaces, *Water Resources Research*, 20 (11), pp. 1753-1761.

Robertson, L. (1996a). "Clear-cuts blamed for recent landslides", in *The Register-Guard*, Eugene, Oregon, February 14, 1996.

Robertson, L. (1996b). "Forest damage may not be fixed", in *The Register-Guard*, Eugene, Oregon, February 15, 1996.

Rosencrantz, S.D., P. Storck and D.P. Lettenmaier (1995). Statistical analysis of logging effects on flooding in the Snoqualmie River basin, Washington, poster presented at the fall meeting of the American Geophysical Union, San Francisco, CA.

Ross, D.G., I.N. Smith, P.C. Manins, D.G. Fox (1988). Diagnostic wind field modeling for complex terrain: model development and testing, *Journal of Applied Meteorology*, 27, pp. 785 - 796.

Rothacher, J. (1965). Streamflow from small watersheds on the western slope of the Cascade Range of Oregon, *Water Resources Research*, 1, pp. 125 - 134.

Rothacher, J. (1970). Increases in water yield following clear-cut logging in the Pacific Northwest, *Water Resources Research*, 6(2), 653-658.

Rothacher, J. (1973). Does harvest in west slope Douglas-fir increase peak flow in small forest streams? USDA Forest Service Research Paper PNW-163, 13 pp., Washington D.C.

Schmidt, R.A. and C.A. Troendle (1992). Sublimation of intercepted snow as a global source of water vapor, Proceedings, 60th Western Snow Conference.

Smart, P.L. and C.M.Wilson (1984). Two methods for the tracing of pipe flow on hillslopes, *Catena*, 11, pp. 159-168.

Storck, P., D.P. Lettenmaier, B.A. Connelly and T.W. Cundy (1995), Implications of forest practices on downstream flooding, Phase II final report.

Storck, P., T. Kern and S. Bolton (1997) Measurement of differences in snow accumulation , melt and micrometeorology between clear-cut and mature forest stands, Proceedings of the Western Snow Conference, Banff, Alberta, Canada.

Sullivan, K.O. and S.H. Duncan (1981). Sediment yield from road surfaces in response to truck traffic and rainfall. Weyerhaeuser Co. technical Report No. 042-4402/81/04.

Sullivan, K., S.H. Duncan, P.A. Bisson, J.T. Heffner, J.W. Ward, R.E. Bilby and J.L.Nielsen (1987), A Summary Report of the Deschutes River Basin, Sediment, Flow, Temperature and Fish Habitat, Weyerhaeuser Company, Technical Report, Paper No.044-5002/87/1.

Swanson, F.J. and C.T. Dyrness (1975). Impact of clearcutting and road construction on soil erosion by landslides in the western Cascade Range, Oregon. *Geology*, 3, pp. 392-396.

Tarboton, D.G., R.L. Bras, I. Rodriguez-Iturbe (1991). On the extraction of channel netwroks from digital elevation data, *Hydrological Processes*, 5, pp. 81-100.

Tsukamoto, Y., T. Ohta and H. Nogucji (1982). Hydrological and geomorphological studies of debris sldies on forested hillslopes in Japan, *Recent Developments in the Explanation and Predication of Erosion and Sediment Yield (Proceedings of the Exeter Symposium),* IAHS Publ. no. 182.

USDA (1994). *State Soil Geographic Data Base, Data use information*, Soil Conservation Service, Miscellaneous Publication Number 1492

USDA Forest Service (1987). *Road Preconstruction Handbook,* FSH 7709.56B.

Wemple, B.C. (1994). Hydrologic Integration of Forest Roads with Stream Networks in Two Basins, Western Cascades, Oregon, M.S. Thesis, Oregon State University.

Wemple, B.C., J.A. Jones and G.E. Grant, (1996). Channel network extension by logging roads in two basins, Western Cascades, Oregon, *Water Resources Bulletin*, 32 (6), pp. 1195 - 1207.

Whipkey, R.Z. (1969). Storm runoff from forested catchments by subsurface routes, *Int. Assoc. Sci. Hydrol.,* 85, pp. 773-779.

Wilson, C.M. and P.L. Smart (1984). Pipes and pipe flow processes in an upland catchment, Wales, *Catena,* 11, pp. 145-158.

Wigmosta, M.S., L.W. Vail and D.P. Lettenmaier (1994), A Distributed Hydrology-Vegetation Model for Complex Terrain. *Water Resources Research,* Vol. 30, No. 6, pp. 1665-1679.

Woods and Rowe (1996). The changing spatial variability of subsurface flow across a hillside. *Journal of Hydrology (NZ),* 35 (1): pp. 51-86.

Wright, K.A., K.H. Sendek, R.M. Rice and R.B. Thomas (1990). Logging effects on streamflow: storm runoff at Caspar Creek in northwestern California, *Water Resources Research*, 26 (7), pp. 1657-1667.

Ziemer, R.R. (1981). Storm flow response to road building and partial cutting in small streams in northern California, *Water Resources Research*, 17, 907-917.

Ziemer, R.R. (1992). Effect of logging on subsurface pipeflow and erosion: coastal northern California, USA, *Erosion, Debris Flows and Environment in Mountain Regions (Proceedings of the Chengdy Symposium),* IAHS Publ. no. 209.

Ziemer, R.R. and J.S. Albright (1987). Subsurface pipeflow dynamics of north-coastal California swale systems, *Erosion and Sedimentation in the Pacific Rim (Proceedings of the Corvallis Symposium),* IAHS Publ. no. 165.

APPENDIX A: EXAMPLE NEWSPAPER ARTICLES FROM THE FEBRUARY 1996 FLOOD IN WESTERN WASHINGTON AND OREGON

Flooding? Don't blame logging

BY JAMES E. BROWN
Oregon State Forester

Over the past few weeks, there have been various news stories and editorials that speculated and made claims regarding forest practices and forest management effects on landslides and elevated stream flow resulting from the February storm.

This has left readers with the impression that poor forest practices caused most of the flooding and flood damage on forest land, and that most of the slides were caused by harvest activities. Many of the claims have had little basis in fact or reality, while some others do merit serious consideration.

It is important to understand that the February storm was an extremely rare natural event with four-day precipitation and snow melt runoff totals varying from 20 to 40 inches at the higher elevations. In many places, stream flows exceeded levels reached during the famous 1964 flood. In one case, a river (the Deschutes River at Moody), with a gauging system in place for nearly 100 years, shattered all records.

During events of this size, there are going to be landslides and road culvert failures no matter what precautions have been taken. Initial observations indicate that slides occurred both in areas that were actively managed and where no harvesting or road building was present.

Some people have claimed that an intact, pristine forest "acts like a sponge" while harvested areas are more like "parking lots." This is simply a myth.

Based on decades of scientific study, generally during extreme storm events, harvested forest ground receives and routes water in a manner similar to unharvested areas.

Forest soils generally have the ability to infiltrate water into the ground at an extremely high rate regardless of harvest activity. In some isolated cases, where there is severe soil compaction or fire effects on soil infiltration, the water may run over-

> ***Some people have claimed that an intact, pristine forest 'acts like a sponge' while harvested areas are more like 'parking lots.' This is simply a myth.***
>
> James E. Brown

land instead subsurface, but this is rare in Western Oregon. During the recent storm, water was generally routed underground to streams from both harvested and unharvested areas.

Another claim we've heard in recent weeks, especially in the Salem area, was that if it were not for forest management activities, the lower North Santiam River would have cleared rapidly after the storm or even run relatively clear during the storm.

In a watershed the size of the North Santiam above Detroit Reservoir, some landslides would be expected, even in unharvested forests, that would cloud the water in the reservoir. Often it takes fine suspended sediment weeks to months to settle in a reservoir.

In addition, the reservoir was filling at two feet per hour during the height of the flood, which also stirred up the sediment. During the weeks following the flooding, the river below the reservoir was running extremely high, and the shifting of the riverbed creates additional turbidity.

It should also be noted that many smaller stream basins nearby with intensive forest management, like Sardine Creek and the Little North Fork Santiam River, cleared considerably within a few days after the crest of the flood.

Some have tallied landslides from the air and said that since a larger percentage come from harvested units, the landslid must be related to forest harvesting.

Such quick conclusions are inappropriate because it is very difficult to see landslides under the cover of forest trees. For example, initial examinations in the Tillamook State Forest, where there has been little or no clear-cutting, show the vast majority of slides occurred in mature forests.

While there is no question that forest roads can increase the likelihood of landslides, road design and maintenance history also need to be considered in discussing factors that cause landslides.

In 1983, the Oregon Board of Forestry adopted new rules regarding road locations, design, construction and maintenance for private and state-owned land to address landslide prevention. It will be interesting to evaluate how the newer roads fared. Roads constructed prior to 1983 were not often designed to these high standards and appear to be a major source of the current landslide activity associated with the recent storm.

Some issues merit further study, to determine what effects they had and what actions can be taken in the future to help minimize damage from future storms.

That's why the Oregon Department of Forestry is already doing a major study on landslides and their effects, downstream effects of road culvert failures on fish habitat and possible management-related changes to peak stream flow on small streams due to road drainage problems and rain-on-snow dynamics. The study will be highly credible, with a number of technical experts in areas of hydrology, riparian function, slope stability, geomorphology and aquatic biology playing key roles.

As state forester, James E. Brown is responsible for the protection of forest lands and conservation of forest resources in Oregon. He can be reached at Department of Forestry, 2600 State St., Salem, 97310.

THE OREGONIAN, FRIDAY, MARCH 8, 1996

The legacy of clear-cutting and road-building

Swollen streams tied to logging

By PETER D. SLEETH and HAL BERNTON
of The Oregonian staff

The effects of past logging practices on mountain streams are far more extensive and enduring than previously thought, federal researchers have declared in a study that reviews more than four decades' worth of data gathered in the Willamette National Forest.

Clear-cutting forests and building roads were found to increase peak flows in mountain streams by as much as 50 percent, a finding that establishes a long-disputed link between logging and swollen streams.

While the findings might seem trussed in common sense, the bulk of past studies has not supported such a conclusion. Extensive clear-cutting and road-building have been a staple of timber harvests in the Northwest for 50 years.

Should the research be widely accepted, it could accelerate a movement in place within the U.S. Forest Service that calls for the obliteration of many old logging roads and a move away from clear-cutting.

The researchers' work found that in some cases streamflows increased by as much as 20 percent to 50 percent after a watershed was logged. The effects diminished gradually but were apparent 25 years after clear-cutting.

Perhaps the most significant finding is the apparent synergy between logging roads and clear-cutting. The logging roads appear to act something like a pipeline — rapidly injecting flows of rain and snowmelt running off clear-cuts into streams.

The study by Gordon E. Grant, a Forest Service hydrologist at the Pacific Northwest Research Station, and Julia A. Jones of Oregon State University is to be published in the April issue of Water Resources Research, the journal of the American Geophysical Union.

The study does not speak to what happens in major events such as the February floods, because of a lack of sufficient records on large floods to allow a valid study.

"What we're looking at is a legacy of clear-cutting and roads over the past 40 years," Grant said. "There is a strong component of history here, and we are noting there are long-term legacies from

Please turn to STUDY, Page C4

Study: Findings contradict earlier works

■ **Continued from Page C1**

past practices that continue into the future."

The authors work at two of the nation's most prestigious centers of forestry research. They have compiled one of the most exhaustive studies on the subject yet, taking in more than 40 years of data. It has been "extensively" reviewed by other scientists who checked for flaws in methodology, Grant said.

But it already is proving controversial.

Its findings contradict some previous studies that showed logging and road-building had little or no effect on peak flood flows in large drainages. And critics, both from industry and the Oregon Department of Forestry, say that the new study is badly flawed.

"I felt that the conclusions in this study far overreach the data that is presented," said Kate Sullivan, a hydrologist with Weyerhaeuser.

Sullivan said that none of her studies of about 60 drainages showed that logging had any major effects in big floods. She said she thought that the information cited in the new report did not show significant effects in big floods.

"She has never published any of her data," Grant said of Sullivan's comment. "So it is impossible for me to react."

The question of the relationship between logging and major floods became a political hot potato after February's high waters. Environmentalists tried to condemn all logging because of its contribution to the floods, while the timber industry pooh-poohed those claims.

"We don't know," Grant said. "I don't know of anyone that can answer that question, no matter what they're political persuasion is."

Increasingly, scientists and others are pointing to land management practices in forests as the culprit for damage to stream beds and fish habitat, as well as increased runoff and flooding. But little definitive science has been available.

To get at the question, Grant and Jones studied stream-flow data from three small basins — those less than 250 acres — and three large basins up to 250 square miles in size.

The three small basins were monitored beginning in the 1950s, before any logging was done, and then afterward. One valley was left alone, a second was 25 percent clear-cut with roads and a third was logged completely with no roads in it.

What the study showed was that for five years after clear-cutting, peak flows in streams in the basins were 50 percent higher than before logging. Twenty-five years after the logging, the flows are 25 percent higher than they were before logging took place.

In the larger valleys, Jones and Grant relied on records of past timber harvesting and streamflows to do their study. But the results were virtually the same as in small basins. Past studies found that large basins didn't have the same impacts from logging.

"Previously, we had thought the effects of small basins would cancel out downstream" as they flowed into large basins, Jones said.

But large basins showed the same effects from logging, the study showed.

Clear-cut logging is down to a fraction of post-World War II levels in federal forests in the Pacific Northwest. Road-building also has declined as environmental restrictions have eased the pressure to log forests.

But extensive networks of old roads and clear-cuts may pose problems for flood management in the future.

The Register-Guard

EUGENE, OREGON • WEDNESDAY, FEBRUARY 14, 1996

Clear-cuts blamed for recent landslides

■ Logging: Environmentalists attribute hundreds of slides last week to timber industry practices.

By LANCE ROBERTSON
The Register-Guard

Environmentalists and many ecologists have been warning for years that there's a time bomb waiting to go off in the woods the next time a major storm hits the Northwest.

It happened last week, they say.

All across Oregon, heavy rains and rapidly melting snow triggered hundreds — perhaps thousands — of landslides on logging roads and in clear-cuts, sending mud and debris shooting down rivers and wiping out fish habitat, conservationists say.

It may be weeks or months before the extent of the damage is fully known, but environmentalists say some quick weekend surveys of selected river valleys uncovered massive levels of road washouts and landslides caused by logging.

"We've been saying for years that we have these loaded guns all over these watersheds," says Bob Doppelt, director of the Pacific Rivers Council in Eugene. "Well, those guns went off. Road systems have blown out all over the region. . . . The damage in the forests is severe, significant and widespread."

Timber companies and public land managers acknowledge that the heavy rain and snowmelt washed out numerous logging roads, but they say the damage may not be as devastating as conservationists say.

"The majority of our lands, surprisingly, were not affected," said Paul Barnum, a spokesman in Springfield for Weyerhaeuser, which has at least 100 roads damaged in its Eugene-Springfield area timberlands.

Improperly built roads — constructed largely before new standards were put in place during the 1980s — are blamed for most of the logging-related landslides.

The warm, heavy rain that came on top of heavy snowfall last week usually causes many of those roads to collapse because they either were built on unstable soils, are on slopes that are too steep, have drainage culverts that are too small, or are not maintained properly.

"This kind of event (storm) produces failures (landslides) on a broad scale," adds Marvin Pyles, a forest engineering professor and landslide expert at Oregon State University.

Pyles estimates that there are about 180,000 miles of logging roads in Oregon and Washington, or about 2½ times the length of the nation's interstate highway system.

Most of those roads were built under old construction standards, Pyles said. For example, soil carved out of a hillside during construction often was used to build the outer half of the roadway, a method called "side-casting." That loose soil often collapses when it becomes super-saturated with water, he added.

Barnum said the timber industry recognizes the problem.

"More likely it is road-building practices, and more specifically past road-building practices, that were at fault," he said.

But Barnum said the industry is dealing with the problem. New road-building rules and methods have been adopted over the years to reduce the number of washouts. New state Department of Forestry standards also require timber companies to install much larger culverts to allow water to drain under roadways.

About three years ago, Weyerhaeuser launched an effort to "storm proof" logging roads in several river drainages, including the Mohawk area that was flooded in last week's storm.

Some environmentalists also claim that excessive clear-cutting in the region contributed to the widespread flooding, but Barnum rejected that notion.

"It's preposterous for anyone to say clear-cutting caused the flooding," Barnum says. "Now if you want to talk about slides and roads, that's a different issue. Flooding is caused by too much water for the earth to absorb."

Pyles agreed, to a point.

He said studies have shown there is a slight increase in the amount of water runoff from clear-cuts when compared to forested areas, but only when soils are relatively dry.

When soils are saturated during winter, there's virtually no difference in runoff volumes, he said. Plus, any extra water coming from clear-cuts would pale in comparison to the vast volume of water tumbling out of the mountains from last week's rainfall and snowmelt, he added.

Environmentalists and the timber industry also have haggled over whether clear-cuts lead to a higher rate of landslides.

Barnum said there's no definitive proof that more landslides occur in clear-cuts than in forested areas.

But Pyles said a landmark OSU study of U.S. Forest Service land in the Mapleton area during the late 1970s showed much higher levels of landslides from roads and clear-cuts.

Landslides in clear-cuts tend to be larger and travel downhill much farther than naturally occurring slides in forested areas, he added.

The Oregon Department of Fish & Wildlife also has surveyed some heavily logged areas of the state to document landslides after big storms.

Pyles said, however, that most of the studies and surveys are somewhat suspect because it is difficult to compare landslide rates in naturally occurring forested areas.

And while studies point to a higher level of slides caused by logging, there's almost no way to say for sure that a specific slide wouldn't have occurred anyway, clear-cut or road notwithstanding.

"Can I state unequivocably that it was a clear-cut that caused this particular slide? No, I can't," Doppelt said. "But I just saw this huge slide on the McKenzie. I walked up to where it started and what do you know? It started at a clear-cut."

Andy Stahl, an environmentalist who used results from the landslide study to win a 1983 lawsuit against the Forest Service over logging in the Mapleton area, said "it is clear that logging and road construction accelerate landslides."

Many are known as "debris torrents."

That's when a small slide begins at the very top of a small drainage, building speed and gathering more rocks, mud and logging slash as it cascades downstream.

Some debris torrents have been known to rocket for miles down streams, wiping out everything in their path and scouring creekbeds needed by salmon to spawn.

Stahl, who now heads the Forest Service Employees for Environmental Ethics in Eugene, is doing a survey of the Mapleton area to see how many slides were created by last week's storm.

Preliminary results show 185 landslides in the Mapleton area. All but three were in clear-cuts or along roads, Stahl said.

Doppelt said his group also will be doing an analysis of certain watersheds to gauge the impact of logging-related landslides.

The floods provide a "perfect opportunity" to start restoring many watersheds by repairing poorly built roads, or closing them altogether, he said.

But private forest crews already are back in the woods, repairing logging roads that have been washed out, said Doppelt.

"We're just loading the gun again."

APPENDIX B: SOIL PARAMETER CALCULATIONS

The variables which were extracted from the STATSGO database are summarized in Table B-1. Percent sand (PS) and percent silt (PSi) were derived from the STATSGO variables as follows:

$$PS = (NO10_H + NO10_L)/2 - (NO200_H + NO200_L)/2 \quad \textbf{B-8-1}$$

$$PSI = (NO200_H + NO200_L)/2 - PC \quad \textbf{B-8-2}$$

The sources used for calculation of the DHSVM soil parameters based on the available STATSGO data are summarized in Table B-2.

TABLE B-8-1: STATSGO VARIABLES

STATSGO VARIABLE	VARIABLE NAME	DESCRIPTION
bd	bulk density	Minimum value for range in moist bulk density (g/cc)
bdh	bulk density	Maximum value for range in moist bulk density (g/cc)
clayh	clay	Maximum value for range in clay content (%)
clayl	clay	Minimum value for range in clay content (%)
laydeph	layer depth	Depth to the lower boundary of the soil layer (in)
laydepl	layer depth	Depth to the upper boundary of the soil layer (in)
no4h	% passing sieve no. 4	Max. value for range in percent by weight which is less than 3 inches and passes a no. 4 sieve
no4l	% passing sieve no. 4	Min. value for range in percent by weight which is less than 3 inches and passes a no. 4 sieve
no10h	% passing sieve no. 10	Max. value for range in percent by weight which is less than 3 inches and passes a no. 10 sieve
no10l	% passing sieve no. 10	Min. value for range in percent by weight which is less than 3 inches and passes a no. 10 sieve
no200l	% passing sieve no. 200	Max. value for range in percent by weight which is less than 3 inches and passes a no. 200 sieve
no200h	% passing sieve no. 200	Min. value for range in percent by weight which is less than 3 inches and passes a no. 200 sieve
permh	permeability rate	Maximum value for permeability (in/hr)
perml	permeability rate	Minimum value for permeability (in/hr)
texture	soil texture class	USDA texture of the specified layer

TABLE B-8-2: SOURCE OF DERIVED SOIL PARAMETERS

PARAMETER NAME	VARIABLES NEEDED	SOURCE
Porosity (%)	texture	Estimated from Table 5.3.2 in Maidment (1993)
Pore size distribution	PS, PC & porosity	Brooks-Corey pore-size distribution index calculated from Table 5.3.3 in Maidment (1993)
Air bubbling pressure	PS, PC & porosity	Brooks-Corey bubbling pressure calculated from Table 5.3.3 in Maidment (1993)
Field Capacity	texture	Estimated from Table 5.3.2 in Maidment (1993) as moisture retained at a suction pressure of -33 kPa in cm^3/cm^3
Wilting point	texture	Estimated from Table 5.3.2 in Maidment (1993) as moisture retained at a suction pressure of 1500 kPa in cm^3/cm^3
Density (kg/m^3)	bd, bdh	(bd+bdh)/2 * 1000 kg m^{-3}/g cm^{-3}
Vertical saturated hydraulic cond. (m/s)	perml, permh	(perml+permh)/2 * (2.54/360,000) m s^{-1}/in hr^{-1}
Effective solids thermal conductivity (W/mK)	PS, PC	$TC = \left(S \cdot TC_{quartz} + C \cdot TC_{clay}\right) / S + C$
Maximum infiltration rate (m/s)	texture	Interpolated from Figure 5.4.2. (a) in Maidment (1993)

Notes:

TC_{quartz}= 8.8 W/m*K is the thermal conductivity of quartz
TC_{clay}=2.9 W/m*K is the thermal conductivity of clay (Elements of Soil Physics)

APPENDIX C: ROAD CLASS PARAMETERS

TABLE C-3: ROAD CLASS PARAMETERS

ROAD CLASS	ROAD WIDTH (METERS)	CUTBANK SLOPE (M/M)	DITCH DEPTH (METERS)	DITCH WIDTH (METERS)	ROAD SLOPE
1	3.1	0.5	0.09	0.22	outsloped
2	3.1	0.5	0.32	1.22	crowned
3	3.1	7.5	0.09	0.92	crowned
4	3.1	7.5	0.09	0.92	outsloped
5	3.1	7.5	0.32	1.22	crowned
6	3.1	7.5	0.32	1.22	outsloped
7	3.1	23.3	0.09	0.22	crowned
8	3.1	23.3	0.09	0.22	insloped
9	3.1	23.3	0.09	0.22	outsloped
10	3.1	23.3	0.09	0.92	crowned
11	3.1	23.3	0.20	0.92	crowned
12	3.1	23.3	0.20	0.92	insloped
13	3.1	23.3	0.20	1.22	outsloped
14	4.9	0.5	0.09	0.22	crowned
15	4.9	0.5	0.20	1.22	crowned
16	4.9	0.5	0.20	1.22	insloped
17	4.9	0.5	0.45	1.22	crowned
18	4.9	0.5	0.45	1.22	insloped
19	4.9	0.5	0.45	1.22	outsloped
20	4.9	7.5	0.09	0.92	crowned
21	4.9	7.5	0.09	0.92	insloped
22	4.9	7.5	0.09	0.92	outsloped
23	4.9	7.5	0.20	0.92	crowned
24	4.9	7.5	0.20	0.92	insloped
25	4.9	7.5	0.20	0.92	outsloped
26	4.9	7.5	0.20	1.22	crowned
27	4.9	7.5	0.20	1.22	insloped
28	4.9	7.5	0.20	1.22	outsloped
29	4.9	7.5	0.32	1.22	crowned
30	4.9	7.5	0.32	1.22	insloped
31	4.9	7.5	0.32	1.22	outsloped
32	4.9	7.5	0.32	1.66	crowned
33	4.9	7.5	0.32	1.66	insloped
34	4.9	7.5	0.32	1.66	outsloped
35	4.9	7.5	0.45	1.22	crowned

TABLE C-3: ROAD CLASS PARAMETERS

ROAD CLASS	ROAD WIDTH (METERS)	CUTBANK SLOPE (M/M)	DITCH DEPTH (METERS)	DITCH WIDTH (METERS)	ROAD SLOPE
36	4.9	7.5	0.45	1.22	insloped
37	4.9	7.5	0.45	1.22	outsloped
38	4.9	7.5	0.45	1.66	crowned
39	4.9	7.5	0.45	1.66	insloped
40	4.9	7.5	0.45	1.66	outsloped
41	4.9	23.3	0.09	0.22	crowned
42	4.9	23.3	0.09	0.22	insloped
43	4.9	23.3	0.09	0.22	outsloped
44	4.9	23.3	0.09	0.92	crowned
45	4.9	23.3	0.09	0.92	insloped
46	4.9	23.3	0.09	0.92	outsloped
47	4.9	23.3	0.20	0.22	crowned
48	4.9	23.3	0.20	0.22	insloped
49	4.9	23.3	0.20	0.22	outsloped
50	4.9	23.3	0.20	0.92	crowned
51	4.9	23.3	0.20	0.92	insloped
52	4.9	23.3	0.20	0.92	outsloped
53	4.9	23.3	0.20	1.22	crowned
54	4.9	23.3	0.20	1.22	insloped
55	4.9	23.3	0.20	1.22	outsloped
56	4.9	23.3	0.32	1.22	crowned
57	4.9	23.3	0.32	1.22	insloped
58	4.9	23.3	0.32	1.22	outsloped
59	4.9	23.3	0.45	1.22	crowned
60	4.9	23.3	0.45	1.22	insloped
61	4.9	23.3	0.45	1.22	outsloped
62	4.9	23.3	0.45	1.66	crowned
63	4.9	23.3	0.45	1.66	insloped
64	4.9	23.3	0.45	1.66	outsloped
65	6.6	0.5	0.20	1.22	crowned
66	6.6	0.5	0.20	1.22	insloped
67	6.6	0.5	0.20	1.22	outsloped
68	6.6	7.5	0.20	0.92	crowned
69	6.6	7.5	0.20	0.92	insloped
70	6.6	7.5	0.20	0.92	outsloped
71	6.6	7.5	0.32	1.22	crowned
72	6.6	7.5	0.32	1.22	insloped
73	6.6	7.5	0.32	1.22	outsloped
74	6.6	23.3	0.09	0.22	crowned
75	6.6	23.3	0.09	0.22	insloped

TABLE C-3: ROAD CLASS PARAMETERS

ROAD CLASS	ROAD WIDTH (METERS)	CUTBANK SLOPE (M/M)	DITCH DEPTH (METERS)	DITCH WIDTH (METERS)	ROAD SLOPE
76	6.6	23.3	0.09	0.22	outsloped
77	6.6	23.3	0.09	0.92	crowned
78	6.6	23.3	0.09	0.92	insloped
79	6.6	23.3	0.09	0.92	outsloped
80	6.6	23.3	0.20	0.92	crowned
81	6.6	23.3	0.20	0.92	insloped
82	6.6	23.3	0.20	0.92	outsloped
83	6.6	23.3	0.20	1.22	crowned
84	6.6	23.3	0.20	1.22	insloped
85	6.6	23.3	0.20	1.22	outsloped
86	6.6	23.3	0.32	1.22	crowned
87	6.6	23.3	0.32	1.22	insloped
88	6.6	23.3	0.32	1.22	outsloped
89	6.6	23.3	0.32	1.66	crowned
90	6.6	23.3	0.32	1.66	insloped
91	6.6	23.3	0.32	1.66	outsloped
92	6.6	23.3	0.45	1.22	crowned
93	6.6	23.3	0.45	1.22	insloped
94	6.6	23.3	0.45	1.22	outsloped
95	6.6	23.3	0.45	1.66	crowned
96	6.6	23.3	0.45	1.66	insloped
97	6.6	23.3	0.45	1.66	outsloped
98	8.5	7.5	0.20	0.92	crowned
99	8.5	7.5	0.20	0.92	insloped
100	8.5	7.5	0.20	0.92	outsloped
101	8.5	7.5	0.20	1.22	crowned
102	8.5	7.5	0.20	1.22	insloped
103	8.5	7.5	0.20	1.22	outsloped
104	8.5	7.5	0.32	1.22	crowned
105	8.5	7.5	0.32	1.22	insloped
106	8.5	7.5	0.32	1.22	outsloped
107	8.5	23.3	0.09	0.22	crowned
108	8.5	23.3	0.09	0.22	insloped
109	8.5	23.3	0.09	0.22	outsloped
110	8.5	23.3	0.20	0.92	crowned
111	8.5	23.3	0.20	0.92	insloped
112	8.5	23.3	0.20	0.92	outsloped
113	8.5	23.3	0.20	1.22	crowned
114	8.5	23.3	0.20	1.22	insloped
115	8.5	23.3	0.20	1.22	outsloped

TABLE C-3: ROAD CLASS PARAMETERS

ROAD CLASS	ROAD WIDTH (METERS)	CUTBANK SLOPE (M/M)	DITCH DEPTH (METERS)	DITCH WIDTH (METERS)	ROAD SLOPE
116	8.5	23.3	0.32	1.22	crowned
117	8.5	23.3	0.32	1.22	insloped
118	8.5	23.3	0.32	1.22	outsloped

APPENDIX D: DESCHUTES BASIN SURFACE WIND FIELDS

The following figures represented wind fields simulated using the NUATMOS distributed model for the eight primary wind directions. The vectors represent average wind fields for the surface layer which varies between 0 and 6 meters above the bottom boundary. Since NUATMOS does not recognize vegetation, the boundary is taken as the top of the overstory. A reference height of 90 m is used within DHSVM as the origin for wind speed 'observations'.

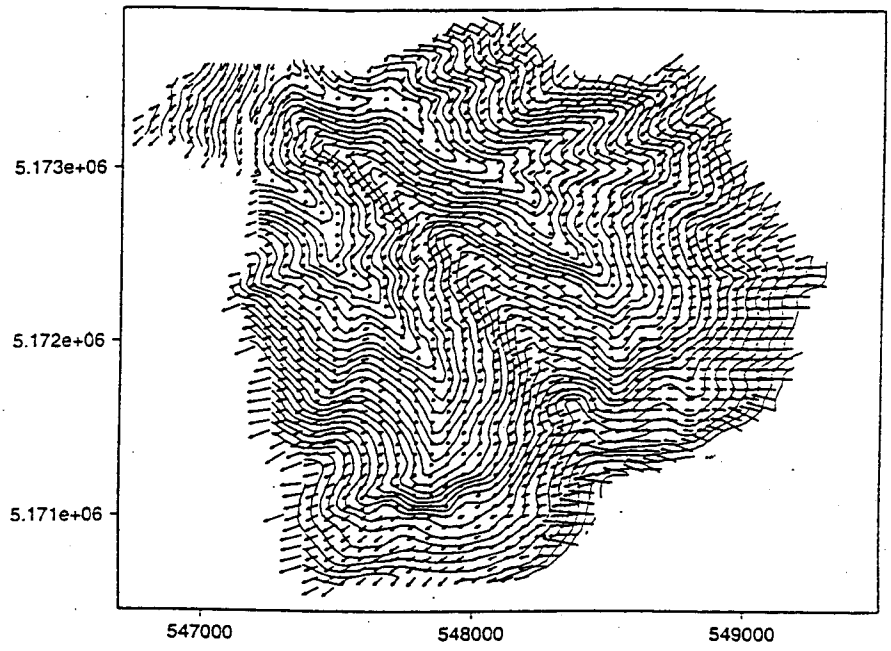

FIGURE D-1: SURFACE WINDS ORIGINATING FROM ENE

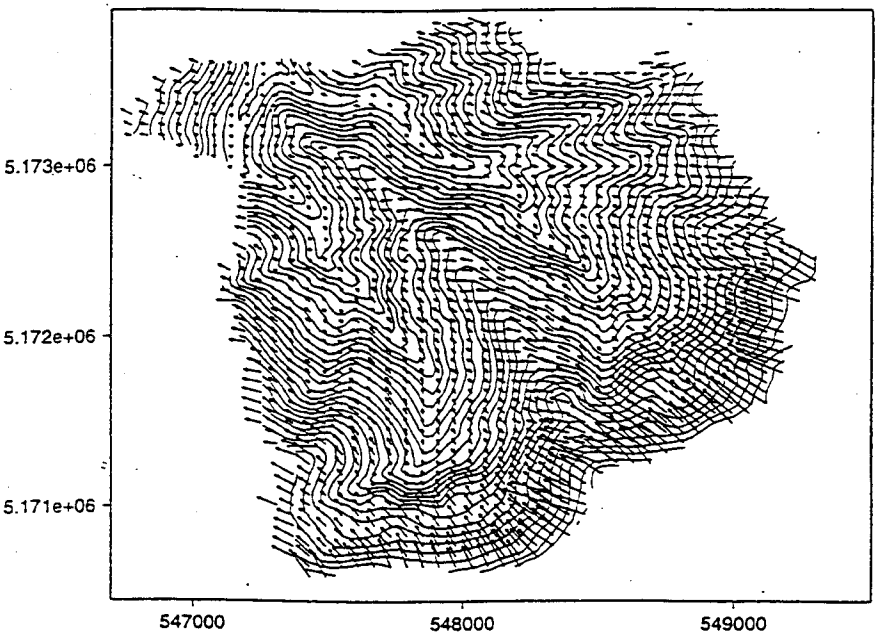

FIGURE D-2: SURFACE WINDS ORIGINATING FROM ESE

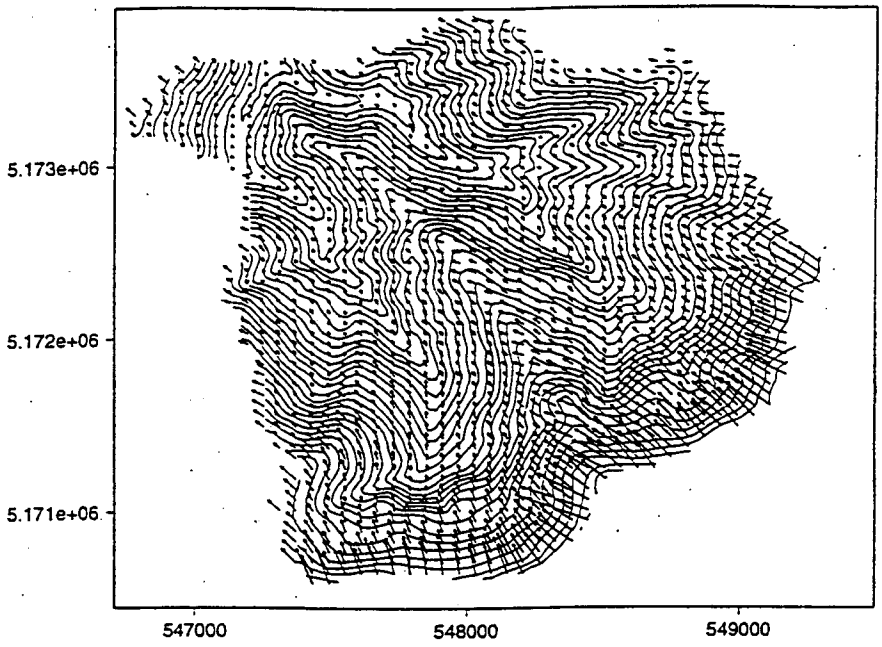

FIGURE D-3: SURFACE WINDS ORIGINATING FROM SSE

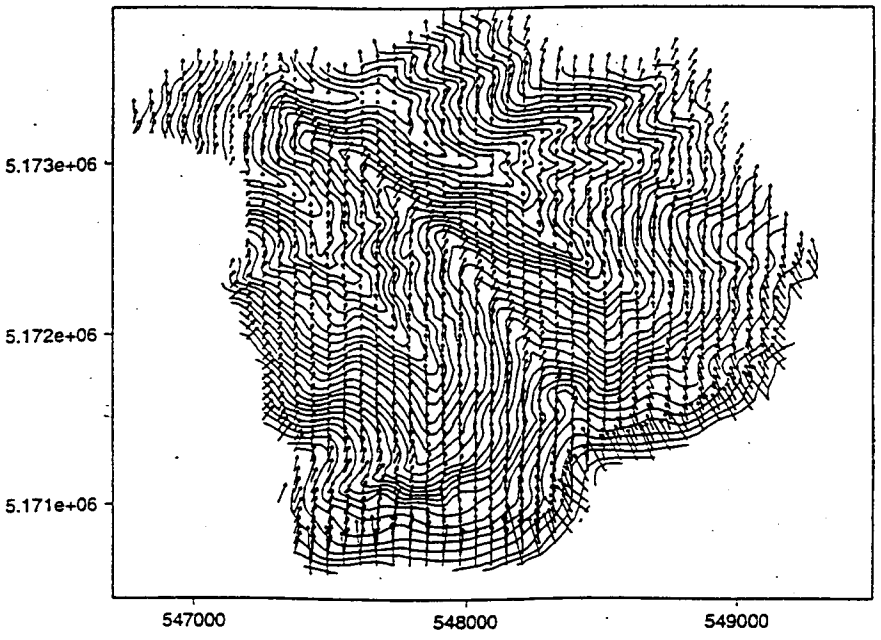

FIGURE D-4: SURFACE WINDS ORIGINATING FROM SSW

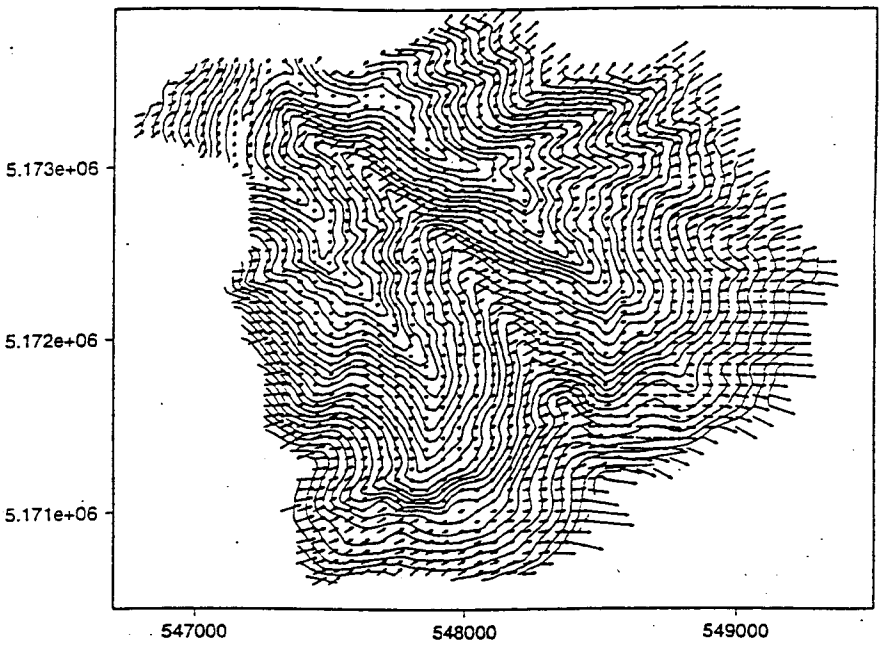

FIGURE D-5: SURFACE WINDS ORIGINATING FROM WSW

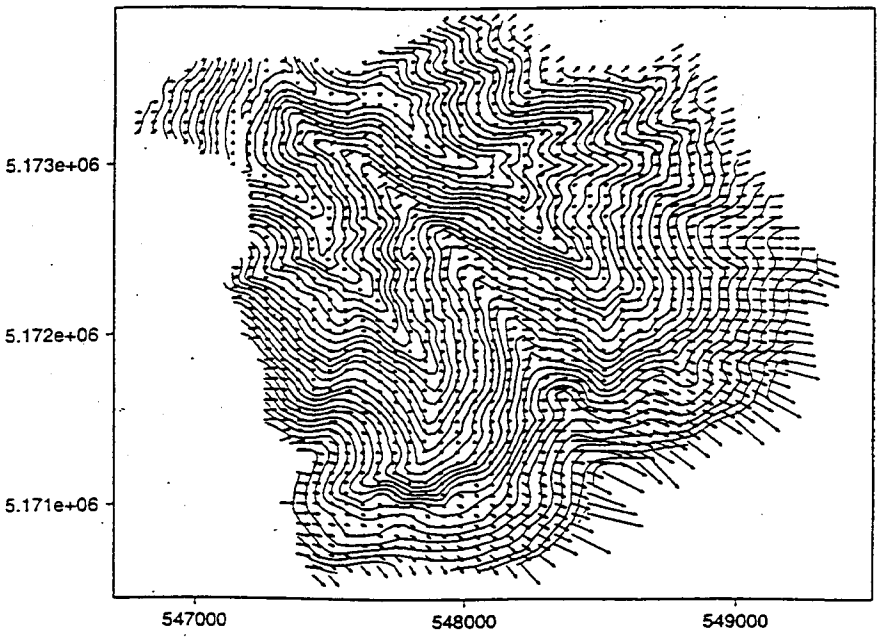

FIGURE D-6: SURFACE WINDS ORIGINATING FROM WNW

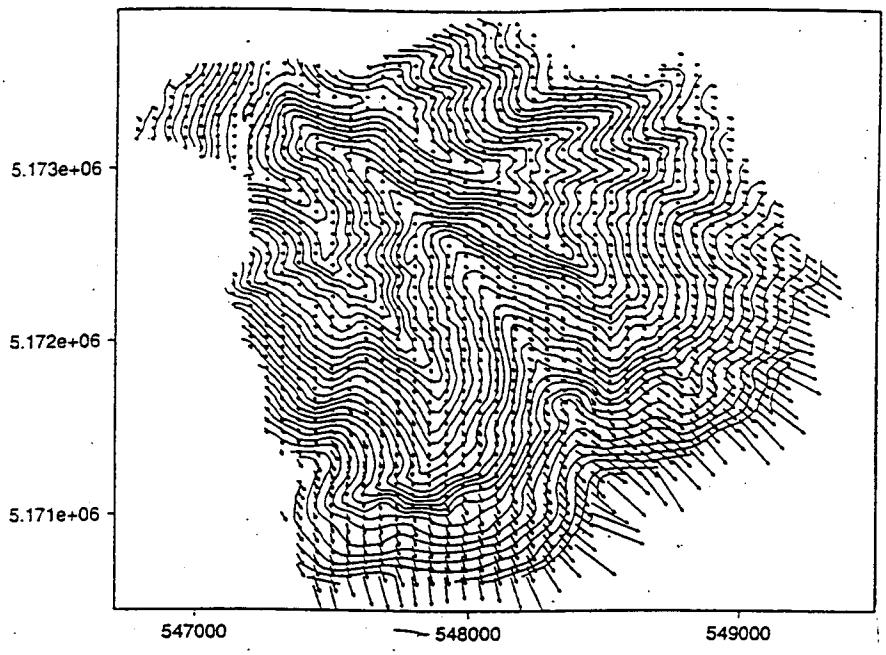

FIGURE D-7: SURFACE WINDS ORIGINATING FROM NNW

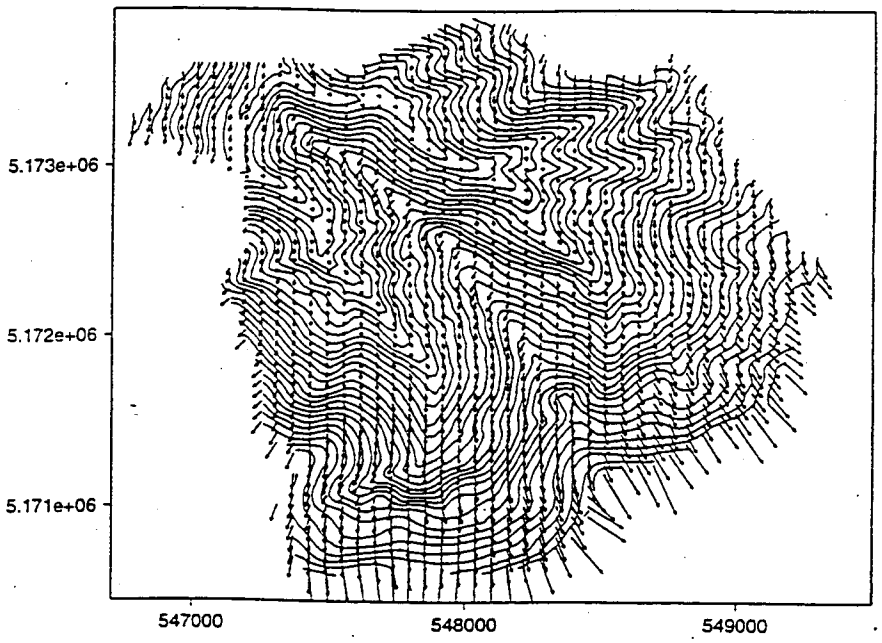

FIGURE D-8: SURFACE WINDS ORIGINATING FROM NNE

APPENDIX E: DHSVM EVALUATION HYDROGRAPHS

Following calibration for the period July 1, 1993 through June 30, 1996, the model was run for the remaining length of record. This includes the period from July 1, 1989 through June 30, 1993 for Ware Creek (Figure E-1) and from October 25, 1985 through June 30, 1992 for Hard Creek (Figure E-2). These hydrographs indicate that no consistent bias develops in the model over time.

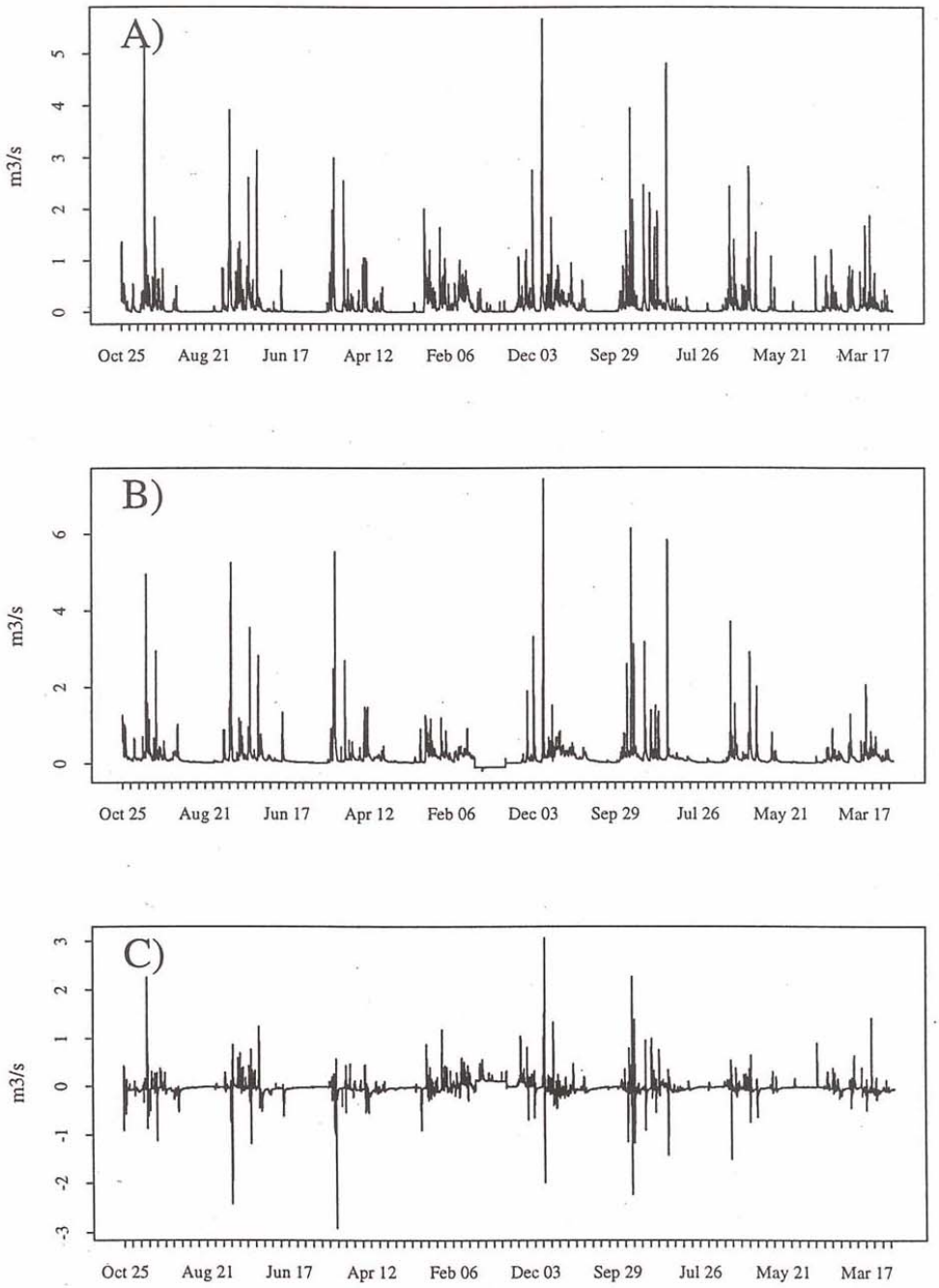

FIGURE E-1: OBSERVED VS. PREDICTED HARD CREEK DISCHARGE, OCTOBER 25, 1985 - JUNE 30, 1993

A) Average 2hr predicted discharge, B) Average 2 hr observed discharge, C) predicted - observed discharge

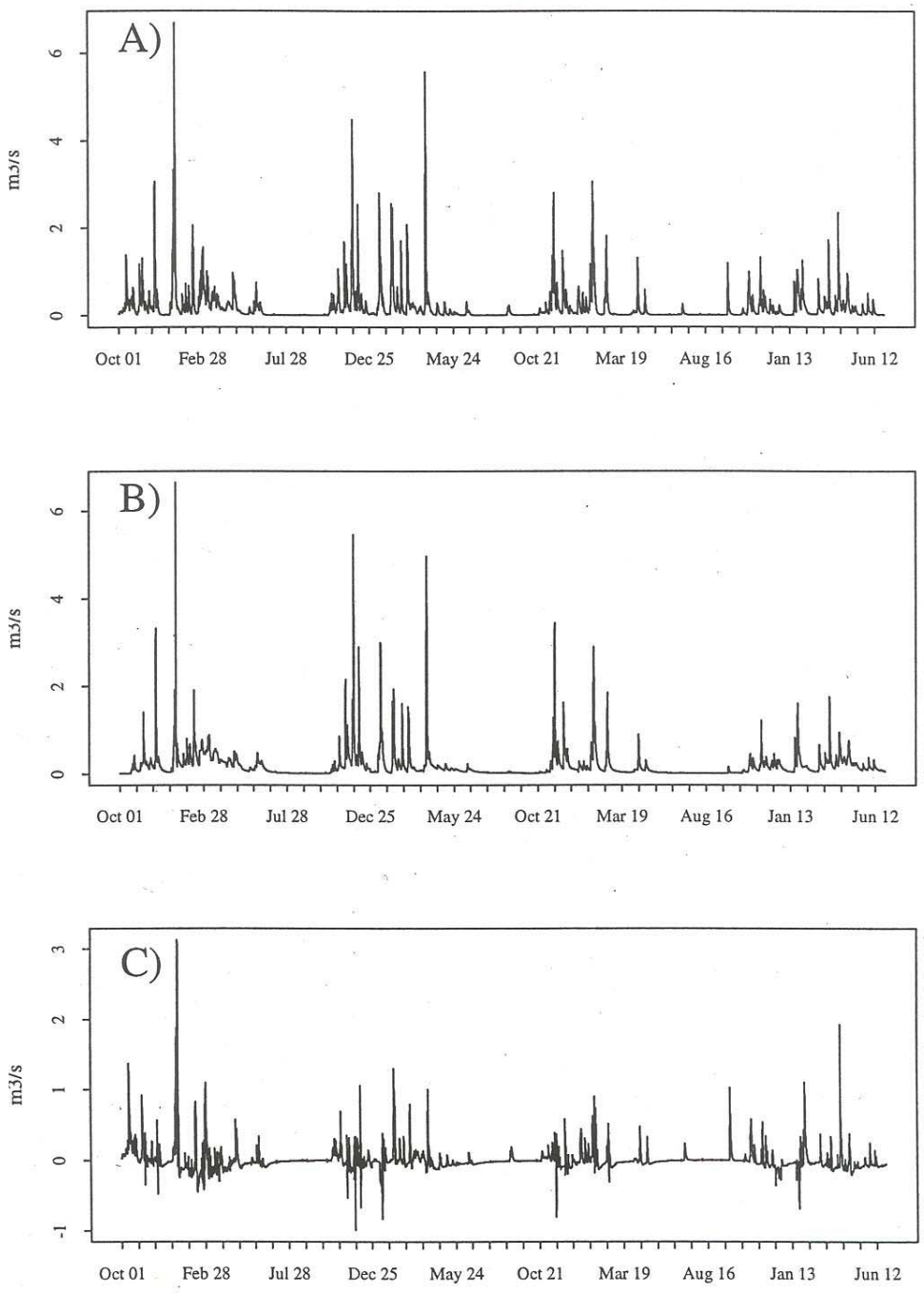

FIGURE E-2: WARE CREEK SIMULATED VS. OBSERVED DISCHARGE, OCTOBER 1, 1989 - JUNE 30, 1993

A) Average 2hr predicted discharge, B) Average 2 hr observed discharge, C) predicted - observed discharge